CRUCIAL ROLE OF PANCREATIC DUCTS IN THE INITIATION AND PROGRESSION OF PANCREATITIS

József Maléth, M.D.

Ph.D. Thesis

Supervisor: Péter Hegyi, M.D., Ph.D., D.Sc

Zoltán Rakonczay Jr., M.D., Ph.D., D.Sc

First Department of Medicine

University of Szeged

Szeged, Hungary

2014

Articles closely related to the subject of the thesis and cited in the thesis

I. **Maléth J**, Venglovecz V, Rázga Zs, Tiszlavicz L, Rakonczay Z, Hegyi P. The non-conjugated chenodeoxycholate induces severe mitochondrial damage and inhibits bicarbonate transport in pancreatic duct cells. *Gut* 2011; 60(1):136-8. **[IF: 10.111]**

II. **Maléth J,** Balla Z, Kui B, Balázs A, Katona M, Judák L, Németh I, Pallagi P, Kemény LV, Rakonczay Jr. Z, Venglovecz V, Földesi I, Pető Z, Somorácz Á, Borka K, Perdomo D, Lukacs GL, Gray MA, Monterisi S, Zaccolo M, Sendler M, Mayerle J, Kühn JP, Lerch MM, Sahin-Tóth M, Hegyi P. Alcohol Disrupts Levels and Function of the Cystic Fibrosis Transmembrane Conductance Regulator to Promote Development of Pancreatitis. *Gastroenterology accepted* **[IF_{2013}: 13.926]**

III. Pallagi-Kunstár E, Farkas K, **Maléth J,** Rakonczay Z Jr, Nagy F, Molnár T, Szepes Z, Venglovecz V, Lonovics J, Rázga Z, Wittmann T, Hegyi P. Bile acids inhibit Na^+/H^+ exchanger and Cl^-/HCO_3^- exchanger activities via cellular energy breakdown and Ca^{2+} overload in human colonic crypts. *Pflugers Arch* 2014 Jul 13. [Epub ahead of print] **[IF_{2013}: 3.073]**

Articles related to the subject of the thesis and cited in the thesis

IV. Pallagi P, Venglovecz V, Rakonczay Z Jr, Borka K, Korompay A, Ózsvári B, Judák L, Sahin-Tóth M, Geisz A, Schnúr A, **Maléth J,** Takács T, Gray MA, Argent BE, Mayerle J, Lerch MM, Wittman T, Hegyi P. Trypsin reduces pancreatic ductal bicarbonate secretion by inhibiting CFTR Cl^- channels and luminal anion exchangers. *Gastroenterology* 2011;141, 2228–2239.e6. **[IF: 11.675]**

V. Hegyi P, **Maléth J,** Venglovecz V, Rakonczay Z Jr. Pancreatic ductal bicarbonate secretion: challenge of the acinar acid load. *Front Physiol.* 2011 14;2:36. **[IF: -]**

VI. Takács T, Rosztóczy A, **Maléth J,** Rakonczay Z Jr, Hegyi P. Intraductal acidosis in acute biliary pancreatitis. *Pancreatology* 2013;13(4):333-5. **[IF: 2.504]**

VII. **Maléth J,** Rakonczay Z Jr, Venglovecz V, Dolman NJ, Hegyi P. Central role of mitochondrial injury in the pathogenesis of acute pancreatitis. *Acta Physiol (Oxf).* 2013;207:226-35. **[IF: 4.251]**

VIII. Judák L, Hegyi P, Rakonczay Z Jr, **Maléth J,** Gray MA, Venglovecz V. Ethanol and its non-oxidative metabolites profoundly inhibit CFTR function in pancreatic epithelial cells which is prevented by ATP supplementation. *Pflugers Arch.* 2014 466(3):549-62. **[IF_{2013}: 3.073]**

IX. Pallagi P, Balla Z, Singh AK, Dósa S, Iványi B, Kukor Z, Tóth A, Riederer B, Liu Y, Engelhardt R, Jármay K, Szabó A, Janovszky A, Perides G, Venglovecz V, **Maléth J,** Wittmann T, Takács T, Gray MA, Gácser A, Hegyi P, Seidler U, Rakonczay Z Jr. The role of pancreatic ductal secretion in protection against acute pancreatitis in mice*. *Crit Care Med.* 2014;42(3):e177-88. **[IF_{2013}: 6.147]**

X. **Maléth J,** Hegyi P. Calcium signaling in pancreatic ductal epithelial cells: an old friend and a nasty enemy. *Cell Calcium.* 2014;55(6):337-45. **[IF_{2013}: 4.21]**

XI. Ahuja M, Jha A, **Maléth J,** Park S, Muallem S. cAMP and Ca^{2+} signaling in secretory epithelia: crosstalk and synergism. *Cell Calcium.* 2014;55(6):385-93. **[IF_{2013}: 4.21]**

Article not related to the subject of the thesis

XII. Kemény LV, Schnúr A, Czepán M, Rakonczay Z Jr, Gál E, Lonovics J, Lázár G, Simonka Z, Venglovecz V, **Maléth J,** Judák L, Németh IB, Szabó K, Almássy J, Virág L, Geisz A, Tiszlavicz L, Yule DI, Wittmann T, Varró A, Hegyi P. Na^{+}/Ca^{2+} exchangers regulate the migration and proliferation of human gastric myofibroblasts. *Am J Physiol Gastrointest Liver Physiol.* 2013 15;305(8):G552-63. **[IF: 3.737]**

XIII. Jha A, Ahuja M, **Maléth J,** Moreno CM, Yuan JP, Kim MS, Muallem S. The STIM1 CTID domain determines access of SARAF to SOAR to regulate Orai1 channel function. *J Cell Biol.* 2013 8;202(1):71-9 **[IF: 9.688]**

XIV. Pajenda G, Hercher D, Márton G, Pajer K, Feichtinger GA, **Maléth J,** Redl H, Nógrádi A. Spatiotemporally limited BDNF and GDNF overexpression rescues motoneurons destined to die and induces elongative axon growth. *Exp Neurol.* 2014 27. pii: S0014-4886(14)00161-7. **[IF_{2013}: 4.617]**

XV. Choi S, **Maleth J,** Jha A, Lee KP, Kim MS, So I, Ahuja M, Muallem S. The TRPCs-STIM1-Orai Interaction. *Handb Exp Pharmacol.* 2014;223:1035-54.

XVI. **Maléth J,** Choi S, Muallem S, Ahuja M. Translocation Between PI(4,5)P2-Poor and PI(4,5)P2-Rich Microdomains During Store Depletion Determines STIM1 Conformation and Orai1 Gating. *Nature Communications accepted* **[IF_{2013}: 10.742]**

Number of full publications:	16 (5 first author)
Cumulative impact factor:	**91.964**

TABLE OF CONTENTS

LIST OF ABBREVIATIONS 7
1. INTRODUCTION 8
1.1. The physiology of the pancreatic ductal HCO_3^- secretion 8
1.2. Pathophysiological role of pancreatic HCO_3^- secretion 10
1.3. The effects of etiological factors of pancreatitis on the exocrine pancreas 11
1.3.1. Ethanol 11
1.3.2. Bile acids 12
1.3.3. Viral infections 13
1.3.4. Other etiological factors 13
2. AIMS OF THE STUDY 14
3. MATERIALS AND METHODS 15
3.1. Solutions and chemicals 15
3.2. Culturing of Capan-1 pancreatic ductal adenocarcinoma cell line 16
3.3. Isolation and culture of guinea pig pancreatic ducts 16
3.4. Maintenance of CFTR knockout mice 16
3.5. *In vitro* measurement of pH_i, $[Ca^{2+}]_i$, $(ATP)_i$ and $(\Delta\Psi)_m$ 17
3.6. *In vitro* measurement of pancreatic fluid secretion 18
3.7. Magnetic resonance imaging of the exocrine pancreatic fluid secretion 18
3.8. Electrophysiology 19
3.9. Electron microscopy 19
3.10. Quantitative real-time reverse transcription polymerase chain reaction 20
3.11. Immunofluorescence 21
3.12. Statistical Analysis 22
3.13. Ethical Approvals 22
4. RESULTS 23
4.1. Low concentration of ethanol stimulates, whereas high concentration of ethanol and fatty acids inhibit the HCO_3^- secretion in pancreatic ductal epithelial cells 23
4.2. High concentration of ethanol and fatty acids inhibit the CFTR Cl^- current in pancreatic ductal epithelial cells 25
4.3. High concentration of ethanol and fatty acids inhibit the HCO_3^- secretion 26

and the CFTR Cl^- current in guinea pig pancreatic ductal epithelial cells
4.4. Ethanol and fatty acids inhibit the pancreatic ductal ductal fluid secretion 28
4.5. Low concentration of ethanol stimulates both the apical Cl^-/HCO_3^- exchanger and CFTR via intracellular Ca^{2+} signalling in PDEC 29
4.6. High concentration of ethanol and fatty acids inhibit both the apical Cl^-/HCO_3^- exchanger and CFTR in PDEC 32
4.7. High concentration of ethanol and fatty acids induce sustained Ca^{2+} release in PDEC 33
4.8. High concentration of ethanol and fatty acids induce $(ATP)_i$ depletion and decrease mitochondrial membrane potential in PDEC 35
4.9. The inhibitory effects of ethanol and fatty acids on HCO_3^- secretion are mediated by sustained $[Ca^{2+}]_i$ elevation and $(ATP)_i$ depletion 36
4.10. Ethanol and non-oxidative ethanol metabolites cause translocation and expression defect of CFTR in PDEC 37
4.11. The effects of bile acids on the mitochondrial morphology and $(ATP)_i$ level in pancreatic ductal and colonic epithelial cells 39
4.12. The effect of $(ATP)_i$ depletion on the bicarbonate secretion of pancreatic ductal epithelial cells 41
5. DISCUSSION 43
5.1. The effects of ethanol and non-oxidative ethanol metabolites on the pancreatic fluid and HCO_3^- secretion 43
5.2. The effects of high concentration of chenodeoxycholate on the pancreatic fluid and HCO_3^- secretion 46
6. SUMMARY 48
7. ACKNOWLEDGEMENTS 49
8. REFERENCES 50
9. ANNEX 58

LIST OF ABBREVIATIONS

$(ATP)_i$	intracellular ATP level
BAPTA-AM	1,2-bis(o-aminophenoxy)ethane-N,N,N',N'-tetraacetic acid
BCECF-AM	2'7'-bis(carboxyethyl)-5(6)-carboxyfluorescein acetoxymethyl ester
$[Ca^{2+}]_i$	intracellular Ca^{2+} concentration
cAMP	cyclic adenosine monophosphate
CBE	Cl^-/HCO_3^- exchanger
CFTR	cystic fibrosis transmembrane conductance regulator Cl^- channel
CFTRinh-172	CFTR inhibitor-172
FA	fatty acid
FAEE	fatty acid ethyl ester
FURA-2-AM	5-Oxazolecarboxylic acid, 2-(6-(bis(carboxymethyl)amino)-5-(2-(2-(bis(carboxymethyl)amino)-5-methylphenoxy)ethoxy)-2-benzofuranyl)-5-oxazolecarboxylic acetoxymethyl ester
H_2DIDS	dihydro-4,4'-diisothiocyanostilbene-2,2'-disulfonic acid
J(*B*-)	transmembrane base flux
KO	knockout
NBCe1-B	Na^+/HCO_3^- contransporter
NHE	Na^+/H^+ exchanger
NBD	nucleotide binding domain
PDEC	pancreatic ductal epithelial cells
PA	palmitic acid
POA	palmitoleic acid
POAEE	palmitoleic acid ethyl ester
pH_i	intracellular pH
pH_L	intraluminal pH
PKA	protein kinase A
RT-PCR	real-time reverse transcription polymerase chain reaction
SLC26	solute carrier family 26
WT	wild-type

1. INTRODUCTION

The exocrine pancreas consists of two different cell types. The pancreatic acinar cells produce and secrete the digestive enzymes, whereas the pancreatic ductal epithelial cells (PDEC) secrete high quantity of HCO_3^--rich low viscosity fluid (Bolender, 1974). The final HCO_3^- concentration of the pancreatic juice varies among species (human PDEC can produce a maximal intraluminal HCO_3^- concentration of 140mM). The alkaline pancreatic fluid secretion, in response to meal washes the digestive enzymes out of the pancreatic ductal tree and neutralises the acidic chyme entering the duodenum. The function of the pancreatic ductal fluid and HCO_3^- secretion used to be underestimated; however recent findings suggest that it plays a central role in the physiology and pathophysiology of the pancreas. Importantly, HCO_3^- neutralises protons secreted by the acinar cells and keeps trypsinogen and most probably other proteases in an inactive form (Pallagi et al., 2011). Pallagi et al. have recently demonstrated that the autoactivation of trypsinogen is a pH dependent process, with increased activity in acidic environment meaning that HCO_3^- secretion prevents the premature trypsinogen activation (Pallagi et al., 2011). We also have to highlight that one of the most common pathogenic factors for acute pancreatitis (bile acids) impair ductal HCO_3^- secretion which likely contributes in a major manner to the pancreatic damage (Venglovecz et al., 2008, Hegyi and Rakonczay, 2010, Hegyi et al., 2011). However the exact mechanism of the inhibitory effects of bile acids has not been revealed yet, moreover we have no information about the effects of the other most common pathogenetic factor (ethanol) on the pancreatic ductal secretion.

1.1. The physiology of the pancreatic ductal HCO_3^- secretion

Pancreatic ductal HCO_3^- secretion can be divided to two separate steps, first the accumulation of the HCO_3^- ions in the cells via the basolateral membrane and second the secretion into the ductal lumen across the apical membrane (Figure 1.). The basolateral accumulation is carried out by a Na^+/HCO_3^- cotransporter (NBCe1-B), which transports 1 Na^+ and 2 HCO_3^- into the cells, driven by the high intracellular Na^+ gradient (Ishiguro et al., 1996). Another possible mechanism for the HCO_3^- accumulation is the passive diffusion of CO_2 trough the cell membrane, followed by the carbonic anydrase mediated conversion of CO_2 to HCO_3^- (Dyck et al., 1972). The electroneutral Na^+/H^+ exchanger (NHE1) might also contribute to the HCO_3^- accumulation, although its role differs among

species (Wizemann and Schulz, 1973, Veel et al., 1992), it is essential for intracellular pH (pH_i) homeostasis. On the luminal membrane PDEC express electrogenic Cl^-/HCO_3^- exchangers (SLC26A6, which operates with a 1 Cl^- : 2 HCO_3^- stoichiometry and possibly SLC26A3, which transports 2 Cl^- : 1 HCO_3^-) (Shcheynikov et al., 2006) and the cystic fibrosis transmembrane conductance regulator (CFTR) Cl^- channel (Zeng et al., 1997). The electrogenic Cl^-/HCO_3^- exchange allows the pancreatic ductal cells to transport HCO_3^- into the ductal lumen and establish the very high (140mM) maximal intraluminal HCO_3^- concentration during stimulated secretion, resulting in an intraluminal HCO_3^- level which is ~5-6 fold higher compared to the cell interior (Lee et al., 2012, Barry E. Argent, 2012). It is important to note that CFTR mutations, which are associated with exocrine pancreatic insufficiency, also establish a major deficiency in the apical CFTR-dependent Cl^-/HCO_3^- exchange activity (Choi et al., 2001). Recent improvements in the field help to understand the puzzling role of CFTR in HCO_3^- secretion. In the proximal pancreatic ducts, where the luminal Cl^- concentration ($[Cl^-]_L$) is high, CFTR functions as a Cl^- channel, providing the necessary substrate (luminal Cl^-) for the Cl^-/HCO_3^- exchange of the SLC26A6 and A3 transporters. In the distal pancreatic ducts however, where the $[Cl^-]_L$ and intracellular Cl^- concentration ($[Cl^-]_i$) is low, HCO_3^- secretion through CFTR can play an important role. Under these conditions the CFTR Cl^- permeability is switched by the With-No-Lysine (WNK)/STE20/SPS1-related proline/alanine-rich kinase (SPAK) kinase pathway (which is regulated by $[Cl^-]_i$), changing CFTR into a HCO_3^- permeable channel (Park et al., 2010). Another recently described regulatory protein, named IRBIT, seems to play a crucial role in the regulation of HCO_3^- secretion as well. Under resting conditions WNK/SPAK constitutively inhibit the activity of CFTR and NBCe1-B, which is antagonised by IRBIT upon stimulation. Moreover IRBIT promotes the insertion of CFTR into the apical membrane (Yang et al., 2009) and mediate synergism between Ca^{2+} and cAMP signalling pathways (Park et al., 2013, Ahuja et al., 2014).

Pancreatic ductal HCO_3^- secretion is a strongly ATP dependent processes. CFTR, also called ABCC7, a member of the ATP-binding cassette transporter superfamily, has two nucleotide binding domain (NBD1 and NBD2). During the activation of CFTR, protein kinase A (PKA) uses ATP to phosphorylate and activate the R domain of CFTR (Chappe et al., 2005). This phosphorylation step is followed by the binding of two Mg-ATP molecules on the inter-NBD interface of the NBD domains, leading to the channel gating (Anderson et al., 1991, Hunt et al., 2013). PKA-dependent phosphorylation of the CFTR R domain is also required for the interaction of the R domain with the STAS domain of

the SLC26 Cl^-/HCO_3^- exchangers, which increases the overall open probability and therefore the activity of CFTR (Ko et al., 2004). Moreover, evidence suggests that NHE1 acts as an ATP-binding transporter; thus, ATP may directly activate NHE1, however its activity does not require ATP hydrolysis (Shimada-Shimizu et al., 2013).

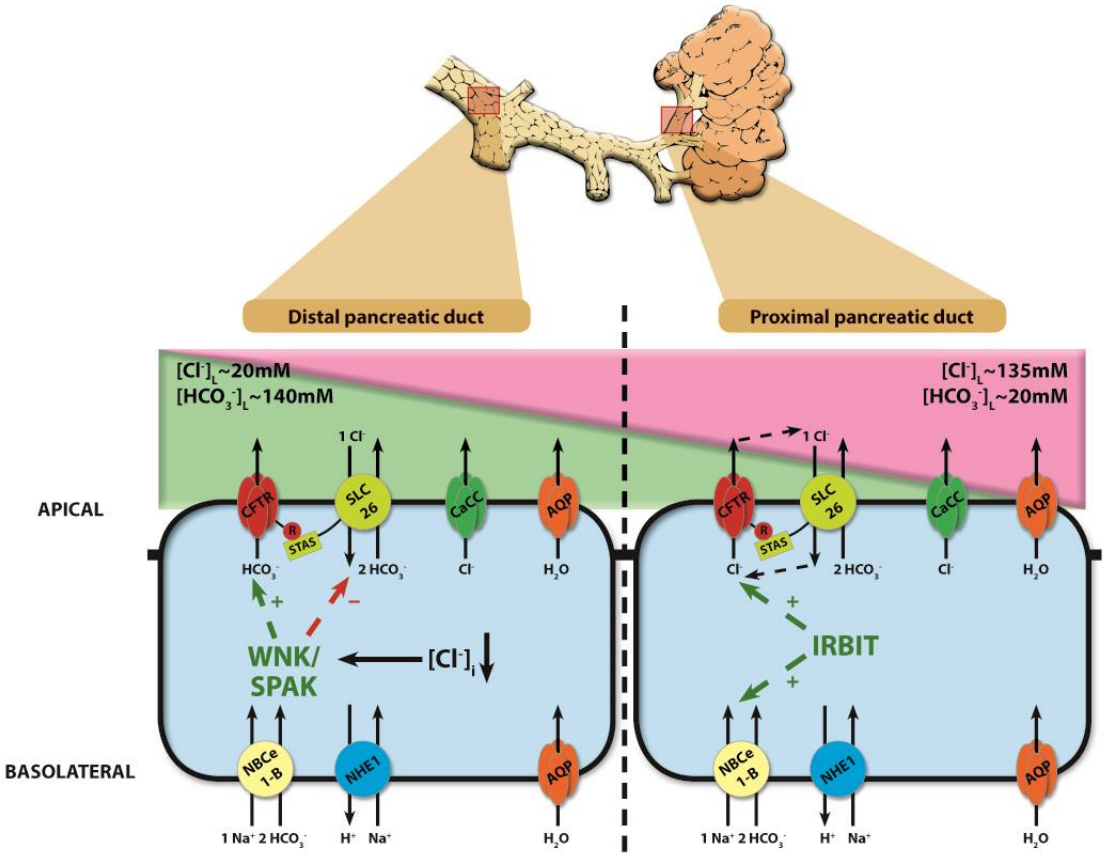

Fig.1. Mechanism of pancreatic ductal HCO_3^- secretion. Pancreatic ductal cells accumulate HCO_3^- across the basolateral membrane via the electrogenic Na^+/HCO_3^- cotransporter NBCe1-B. On the luminal membrane PDEC express electrogenic Cl^-/HCO_3^- exchangers (SLC26A6 and possibly A3) and cystic fibrosis transmembrane conductance regulator (CFTR) Cl^- channel. The operation of these transporters allows the pancreatic ductal cells to create 140 mM maximal HCO_3^- concentration during stimulated secretion. The R domain of CFTR interact with the STAS domain of the SLC26 Cl^-/HCO_3^- exchanger, which increases overall open probability of CFTR. In the proximal ducts, where the intraluminal Cl^- concentration ($[Cl^-]_L$)is high, HCO_3^- is secreted via the electrogenic Cl^-/HCO_3^- exchange, driven by the high $[Cl^-]_L$. Under these conditions CFTR functions as a Cl^- channel. In the distal ducts, where the $[Cl^-]_L$ is low, the low intracellular Cl^- concentration ($[Cl^-]_i$) activates the WNK/SPAK kinases, which phosphorylate CFTR, switching the ion selectivity to HCO_3^-. The SLC26 mediated HCO_3^- transport is inhibited under these conditions. ***(Origin:** Maleth et al. Cell Calcium. 2014;55(6):337-45)*

1.2. Pathophysiological role of pancreatic HCO_3^- secretion

The physiological role of pancreatic ductal HCO_3^- secretion has been investigated in details, however recent evidences suggest that this process is playing a curtail role in the pathophysiology of the pancreas as well. The impaired pancreatic ductal secretion can influence the pancreatic acinar cells. Earlier Freedman et al. showed that impaired ductal electrolyte and fluid secretion in CFTR knockout mice leads to acinar cell damage and to primary defect in membrane trafficking at the apical plasma membrane of acinar cells (Freedman et al., 2001). They also showed that correction of the luminal pH reverses this membrane trafficking defect. In an elegant study Ooi et al. demonstrated that the risk of developing pancreatitis was much higher in CF patients, who had milder CFTR mutations (type IV and V) and were pancreatic sufficient compared to those who had severe mutations and were pancreatic insufficient (Ooi et al., 2011). In the pathogenetic model proposed in this study, the risk of developing pancreatitis inversely correlates with CFTR function. The importance of the intraluminal pH was further confirmed by showing that protons co-realsed during exocytosis cause significant acidosis in the lumen of the acini (Behrendorff et al., 2010). Physiological stimulation of exocytosis causes a decrease in the extracellular pH of up to 1 pH unit. Pathophysiological stimuli using supramaximal concentration of cerulein evokes more enhanced and prolonged acidification of the lumen. Importantly, the high proton concentration of luminal fluid can disrupt junctional links which may be involved in the initiation or development of pancreatitis. In addition acidosis may elevate the risk of developing acute pancreatitis. Bhoomagoud et al. showed that lowering the extracellular pH from 7.6 to 6.8 enhanced secretagogue induced zymogen activation and injury in acinar cells in vitro, however the low extracellular pH itself had no effect on the acinar cells (Bhoomagoud et al., 2009). They also showed that an acute acid load given in vivo enhanced cerulein-induced trypsinogen activation and pancreatic oedema. These findings also suggest that low pH environments might play an important role in the pathogenesis of acute pancreatitis.

1.3. The effects of etiological factors of pancreatitis on the exocrine pancreas

1.3.1. Ethanol

One of the most common causes of acute pancreatitis is excessive ethanol consumption (Yadav and Lowenfels, 2013), although the pathogenesis of alcohol-induced acute pancreatitis remained elusive. Ethanol alone had no detectable effect on pancreatic

acinar cells, however non-oxidative ethanol metabolites (fatty acid ethyl esters; FAEE and fatty acids; FA) induced a sustained $[Ca^{2+}]_i$ elevation leading to necrosis (Criddle et al., 2007, Criddle et al., 2006, Criddle et al., 2004) and depolarized the mitochondria, which was abolished by BAPTA-AM preincubation. Importantly, ATP supplementation via a patch pipette prevented the formation of sustained $[Ca^{2+}]_c$ elevation during the administration of palmitoleic acid (POA) (Criddle et al., 2006). There are less information available about the effects of ethanol, or ethanol metabolites on pancreatic ductal cells. Earlier Yamamoto et al. showed that a low concentration (1mM) of ethanol induced a $[Ca^{2+}]_i$ elevation and augmented secretin-stimulated fluid secretion in guinea pig pancreatic ducts (Yamamoto et al., 2003). They also observed a weak inhibition of the stimulated fluid secretion during the administration of 100mM ethanol. The stimulatory effect of 1mM ethanol was abolished by BAPTA-AM preincubation, suggesting that it was mediated by the $[Ca^{2+}]_i$ elevation. Using isolated guinea pig PDEC Judák et al. showed that high concentration of ethanol, or fatty acids inhibit the CFTR Cl^- current (Judak et al., 2014), however the mechanism of the inhibition and the effects of ethanol, or ethanol metabolites on pancreatic ductal fluid and HCO_3^- secretion was not investigated in details.

1.3.2. Bile acids

Similarly to non-oxidative ethanol metabolites, bile acids induced Ca^{2+} release from both the ER and acidic intracellular Ca^{2+} stores through activation of IP_3R and ryanodine receptors in isolated pancreatic acinar cells (Gerasimenko et al., 2006b). Moreover, Voronina *et al*. showed that taurolithocholicacid 3-sulfate (TLC-S) decreased $(ATP)_i$ in pancreatic acinar cells (Voronina et al., 2010) and caused the loss of $(\Delta\Psi)_m$, which was not influenced by BAPTA-AM pretreatment (Voronina et al., 2004). Using isolated guinea pig pancreatic ducts Venglovecz et al. demonstrated that the non-conjugated bile acid chenodeoxycholate (CDC) a has dose-dependent dual effects on pancreatic HCO_3^- secretion, which might be explained by the type of Ca^{2+} signals evoked by CDC (Venglovecz et al., 2008). Low concentrations (100µM) of CDC induced repetitive, short-lasting Ca^{2+} oscillations, which stimulated HCO_3^- secretion from the luminal membrane of PDEC. The oscillations were abolished by the IP_3R inhibitor caffeine, or xestospongin C and the phospholipase C (PLC) inhibitor U73122. Preincubation of the PDEC with the intracellular Ca^{2+} chelator BAPTA-AM prevented

the Ca^{2+} signals and also abolished the stimulatory effect of 100µM CDC on HCO_3^- secretion. In contrast, high concentrations (1mM) of CDC induced a toxic sustained Ca^{2+} elevation, which inhibited the acid/base transporters including the basolateral NHE, NBCe1-B and the luminal Cl^-/HCO_3^- exchanger (CBE) (Venglovecz et al., 2008). Notably, BAPTA-AM preincubation failed to prevent the inhibitory effect of CDC on the HCO_3^- secretion, suggesting a Ca^{2+}-independent cellular toxicity which has not been clarified yet.

1.3.3. Other etiological factors

Viral infection. Transfection of pancreatic ducts with a virulent strain of pseudorabies virus (PRV), which is able to initiate a lytic viral cycle, stimulated HCO_3^- secretion in guinea pig pancreatic ductal epithelial cells by about four- to fivefold, 24 h after the infection. However, the non-virulent strain of PRV, which can infect, but fails to replicate, has no effect on HCO_3^- secretion. These observations suggest that this response of pancreatic ducts to virulent PRV infection may represent a defence mechanism against invasive pathogens to avoid pancreatic injury (Hegyi et al., 2005)

Smoking. Smoking also increases the risk of acute pancreatitis (Sadr-Azodi et al., 2012, Tolstrup et al., 2009). A Swedish study found that smoking increased the risk of nongallstone-related (by approximately 2-fold) but not gallstone-related acute pancreatitis (Sadr-Azodi et al., 2012). The risk was especially high in patients who consumed alcohol (defined as ≥400 g/mo), current smokers, and those with ≥20 pack-years of smoking. The risk was highest in subjects who had all of these characteristics (relative risk, 4.12); these patients had to stop smoking for 2 decades to reduce their risk level to that of never-smokers. Our preliminary result showed that cigarette smoke extract dose dependently inhibits pancreatic ductal fluid secretion and CFTR Cl^- current in isolated guinea pig pancreatic ductal cells. Taking into account that impaired pancreatic fluid and HCO_3^- secretion directly increases the severity of acute pancreatitis (Pallagi et al., 2014) this could play an important role in the harmful effects of smoking on pancreatitis.

2. AIMS OF THE STUDY

I. Excessive ethanol consumption is one of the most common cause of acute pancreatitis, but it is not know in details how ethanol, or ethanol metabolites influence the pancreatic ductal secretion. Therefore the aim of this study was to characterize the effects of ethanol and ethanol metabolites on the pancreatic ductal epithelial cells.

Our specific aims were:

- *to characterize the effects of ethanol and ethanol metabolites on the pancreatic ductal HCO_3^- and fluid secretion in vivo and in vitro*
- *to characterize the effects of ethanol and ethanol metabolites on the CFTR Cl^- current of PDEC*
- *to investigate the effects of ethanol and ethanol metabolites on the intracellular Ca^{2+} and ATP levels of PDEC*
- *to assess the effects of ethanol and ethanol metabolites on the expression of CFTR Cl^- channel in PDEC*

II. Earlier we showed that the non-conjugated bile acids can inhibit the pancreatic ductal HCO_3^- secretion in high concentration, but the mechanism of inhibition remained elusive.

Our specific aims were:

- *to characterize the effects of chenodeoxycholate on the mitochondrial morphology and function*
- *to assess the effect of intracellular ATP depletion on the pancreatic HCO_3^- secretion*

3. MATERIALS AND METHODS

3.1. Solutions and chemicals

Table 1. summarizes the composition of the solutions used in these series of experiments. The pH of the Hepes-buffered solutions was set to 7.4 with HCl, whereas, the HCO_3^--buffered solutions were gassed with 95%O_2/5%CO_2 to set pH. For patch clamp studies the standard extracellular solution contained (in mM): 145NaCl, 4.5KCl, 2$CaCl_2$, 1$MgCl_2$, 10HEPES, and 5glucose (pH 7.4). The osmolarity of the external solutions were 300mOsm/L. The standard pipette solution contained (in mM): 120CsCl, 2$MgCl_2$, 0.2ethylene glycol-bis(b-aminoethyl ether)-N,N,N8,N8-tetraacetic acid (EGTA), 10HEPES, and 1Na_2ATP (pH 7.2). 2.7-bis-(2-carboxyethyl)-5-(and-6-)carboxyfluorescein-acetoxymethylester (BCECF-AM), 2-(6-(bis(carboxymethyl)amino)-5-(2-(2-(bis(carboxymethyl)amino)-5-methylphenoxy)ethoxy)-2-benzofuranyl)-5-oxazolecarboxylic-acetoxymethylester (Fura2-AM), MagnesiumGreen-AM, Tetramethylrhodamine-methylester (TMRM), H_2DIDS and 1,2-bis(o-aminophenoxy)ethane-N,N,N',N'-tetraaceticacid (BAPTA-AM) were from Invitrogen (Carlsbad, CA, USA). Forskolin was purchased from Tocris (Ellisville, Missouri, USA) and Thapsigargin from Merck (Darmstadt, Germany). All other chemicals were obtained from Sigma-Aldrich (Budapest, Hungary), unless stated otherwise. To solubilise fatty acids in water-based solution first we made 1M stock solution of palmitoleic acid and palmitoleic acid ethyl ester in 100% ethanol. After that 10µL stock solution was added carefully to 1mL HEPES, or HCO_3^-/CO_2 buffered solution at 37°C, which was gently sonicated. Then this was added dropwise and diluted to the concentration we used during

	Standard HEPES	Standard HCO_3^-	Cl^--free HCO_3^-	Ca^{2+}-free HEPES
NaCl	130	115		132
KCl	5	5		5
$MgCl_2$	1	1		1
$CaCl_2$	1	1		
Na-HEPES	10			10
Glucose	10	10	10	10
$NaHCO_3$		25	25	
Na-gluconate			115	
Mg-gluconate			1	
Ca-gluconate			6	
K_2-sulfate			2.5	
EGTA				0.1

Table 1. Composition of solutions for *in vitro* studies. Values are concentrations in mmol/L.

the experiments again at 37°C. This way we were able to avoid using the high ethanol concentration.

3.2. Culturing of Capan-1 pancreatic ductal adenocarcinoma cell line

Capan-1 cells were obtained from the American Type Culture Collection (HTB-79, ATCC, Manassas, VA) and were used for experiments between 20-60 passages. Cells were cultured according to the distributors' instruction. The culture media consisted of RPMI-1640 supplemented with 15% fetal calf serum, 1% L-Glutamine and 1% Penicillin-Streptomycin For the intracellular pH (pH_i) measurements, $5x10^5$ cells were seeded onto polyester permeable supports (12mm-diameter, 0.4mm pore size Transwells; Corning, NY, USA). Cell confluence was checked by light microscopy and determination of transepithelial electrical resistance (TER) using EVOM-G Volt-Ohm-Meter (World Precision Instruments, Sarasota, FL). Experiments were performed after the TER of the monolayer had increased to at least 50 Ωcm^2 (after subtraction of the filter resistance). For intracellular Ca^{2+} concentration ($[Ca^{2+}]_i$) or intracellular ATP level ($(ATP)_i$) measurements $5x10^5$ cells were seeded onto 24mm-diameter cover glasses and for confocal imaging to assess mitochondrial membrane potential ($(\Delta\Psi)_m$) $2.5x10^5$ cells were seeded onto glass bottom dishes (Mattek, Ashland, USA) and were grown until ~60-80% confluency.

3.3. Isolation and culture of guinea pig pancreatic ducts

4-8 week-old guinea pigs were sacrificed by cervical dislocation and intra/interlobular ducts were isolated by enzymatic digestion and microdissection from the pancreas and cultured overnight as previously described (Argent et al., 1986). Single pancreatic ductal cells were isolated as described previously (Venglovecz et al., 2011).

3.4. Maintenance of CFTR knockout mice

CFTR knockout mice were originally generated by Ratcliff et al. (Ratcliff et al., 1993) and was a kind gift of Ursula Seidler (Xiao et al., 2012). The mice were congenic on the FVB/N background. No wild-type CFTR protein is made by the null CF mice, since the hypoxanthine phosphoribosyl transferase (HPRT) cassette disrupts the *cftr* coding sequence and introduces a termination codon, and none of the possible RNA transcripts from the disrupted locus can encode a functional CFTR protein. Genotyping was performed by RT-PCR. The animals were kept at a constant room temperature of

24°C with a 12 h light–dark cycle and were allowed free access to specific CFTR chow and drinking solution in the Animal Facility of the First Department of Medicine, University of Szeged. The mice received electrolyte drinking solution containing polyethylene glycol (PEG) and high HCO_3^- (in mM: 40 Na_2SO_4, 75 $NaHCO_3$, 10 NaCl, 10 KCl, 23 g l^{-1} PEG 4000), and a fibre-free diet (Altromin, C1013) to allow survival beyond weaning. All mice were genotyped prior to the experiments. Wild type (WT) refers to the +/+ littermates of the CFTR knockout mice. The mice used in this study were 6-8 weeks old and weighted 20-25 grams, the gender ratio was 1:1 for all groups.

3.5. In vitro measurement of pH_i, $[Ca^{2+}]_i$, $(ATP)_i$ and $(\Delta\Psi)_m$

Isolated guinea pig pancreatic ducts, or Capan-1 cells were incubated in standard HEPES solution and loaded with BCECF-AM (1.5μmol/L), Fura2-AM (2.5μmol/L), MgGreen-AM (5μmol/L), or TMRM (100nmol/L) respectively for 30 min at 37°C. The Transwells or cover glasses were then transferred to a perfusion chamber mounted on an IX71 inverted microscope (Olympus, Budapest, Hungary). The measurements were carried out as described previously (Pallagi et al., 2011, Venglovecz et al., 2008). In situ calibration of pH_i in Capan-1 cells (measured with BCECF) was performed using the high K^+-nigericin technique (Hegyi et al., 2004). The initial pH_i of Capan-1 cells was 7.31±0.02. During the experiments the apical and the basolateral membrane of the Capan-1 PDEC were perfused separately, which allowed us to selectively change the composition of the apical or basolateral solutions. The HCO_3^- efflux across the luminal membrane was determined as described previously (Hegyi et al., 2003). Briefly, cells were exposed to 20mM NH_4Cl in HCO_3^-/CO_2-buffered solution from the basolateral and luminal side, which produced an immediate increase in pH_i due to the rapid influx of NH_3 across the membrane. After the alkalisation, there was a recovery in pH_i toward the basal value, which depends on the HCO_3^- efflux (ie, secretion) from the duct cells via SLC26 Cl^-/HCO_3^- anion exchanger and CFTR. In this study, the initial rate of recovery from alkalosis (dpH/dt) over the first 30s from the highest pH_i value obtained in the presence of 20mM NH_4Cl was calculated as described previously (Hegyi et al., 2003). The apical Cl^-/HCO_3^- exchange activity was also measured using the luminal Cl^- withdrawal technique. The removal of Cl^- from the apical extracellular solution induced pH_i increase in PDEC by driving HCO_3^- via the basolateral NBCe1-B and the apical SLC26 CBE into the cells, whereas, re-addition of Cl^- decreased pH_i inducing secretion of HCO_3^- via the CBE and

the CFTR Cl^- channel. In this study the rate of pH_i decrease (acidification) after luminal Cl^--readdition was calculated by linear regression analysis of pH_i measurements made over the first 30 s after exposure to the Cl^--containing solution (Stewart et al., 2009). The total buffering capacity ($ß_{total}$) of Capan-1 cells was estimated according to the NH_4^+ pulse technique as described previously (Hegyi et al., 2003).

For $(\Delta\Psi)_m$ measurements confocal imaging was performed using Fluoview 10i-W system (Olympus, Budapest, Hungary). Glass bottom petri dishes were perfused continuously with solutions containing 100nmol/L TMRM at 37^{o}C at a rate of 2-2.5ml/min. 5-10 ROIs (mitochondria) of 5-10 cells were excited with light at a given wavelengths. Excitation of TMRM was 543nm and the emitted light was captured between 560–650nm to follow the changes of $(\Delta\Psi)_m$ (Baumgartner et al., 2009).

3.6. *In vitro* measurement of pancreatic fluid secretion

Fluid secretion into the closed luminal space of the cultured guinea pig pancreatic ducts was analysed using a swelling method developed by Fernandez-Salazar et al. (Fernandez-Salazar et al., 2004). Briefly, the ducts were transferred to a perfusion chamber (0.45ml) and were attached to a coverslip precoated with poly-L-lysine in the base of the chamber. Bright-field images were acquired at 1 min intervals using a CCD camera (CFW 1308C, Scion Corporation, Frederick, MD, USA). The integrity of the duct wall was checked at the end of each experiment by perfusing the chamber with a hypotonic solution (standard HEPES-buffered solution diluted 1:1 with distilled water). Digital images of the ducts were analysed using Scion Image software (Scion Corporation, Frederick, MD, USA) to obtain values for the area corresponding to the luminal space in each image.

3.7. Magnetic resonance imaging of the exocrine pancreatic fluid secretion

Magnetic resonance imaging (MRI) was performed to measure the pancreatic exocrine function as described previously (Cendrowski et al., 2014, Mensel et al., 2014). Quantification of duodenal filling after secretin stimulation was observed in 6 wild type and 6 CFTR knockout mice before and 24 hours after intraperitonal injection with the mixture of 1.75 g/kg ethanol and 750 mg/kg palmitic acid (PA). Animals were allowed free access to pineapple juice instead of water 12 hours before the MRI examination. MRI was performed in a 7.1 Tesla animal scanner (Bruker, Ettlingen, Germany). Strong T2-

weighted series of the complete abdomen were acquired before and after retroorbital injection of secretin (ChiroStim, ChiRhoClin, Burtonville MD, USA) in a dose of 10 IU units/kg/body. The time between injection and MRI was six minutes. The sequences were acquired using the image parameters: TR/TE 4400/83ms; flip angle: 180°; matrix 256x256; field of view 40x40mm; bandwidth 315hz/pixel; slice thickness 1mm; 20 slices. All image analyses were performed using Osirix (version 5; Pixameo, Bernex, Switzerland). First, we reduced image noise to minimize artefacts in images. Second, fluid excretion into the small intestine was segmented in each slice. Care was taken to avoid artefacts caused by magnetic inhomogeneity and motion especially bowel motion. The volume of intestinal fluid was assessed before and after secretin stimulation. From these data total extracted volume (TEV) was assessed.

3.8. Electrophysiology

Single PDEC and Capan-1 cells were prepared as described above. Few drops of cell suspension were placed into a perfusion chamber mounted on an inverted microscope (TMS; Nikon, Tokyo, Japan) and allowed to settle for 30 min. Patch clamp micropipettes were fabricated from borosilicate glass capillaries (Clark, Reading, UK) by using a P-97 Flaming/Brown micropipette puller (Sutter Co, Novato, CA). The resistances of the pipettes were between 2.5-4MΩ. Membrane currents were recorded with an Axopatch1D amplifier (Axon Instruments, Union City, CA) using whole cell at 37°C. After establishing a high-resistance seal (1–10GΩ) by gentle suction, the cell membrane beneath the tip of the pipette was disrupted. The series resistance was typically 4-8MΩ before compensation (50%–80%, depending on the voltage protocol). Current-voltage (I/V) relationships were obtained by holding Vm at 0mV and clamping to ±100mV in 20mV increments. Membrane currents were digitized by using a 333-kHz analog-to-digital converter (Digidata1200; Axon Instruments) under software control (pClamp6; Axon Instruments). Analyses were performed by using pClamp6 software after low-pass filtering at 1kHz (Pallagi et al., 2011).

3.9. Electron microscopy

Morphological changes of the different cell organelles of in pancreatic ductal cells and human colon biopsy samples were evaluated by transmission electron microscopy (TEM). Isolated guinea pig pancreatic ducts and colon biopsy samples were fixed in 2%

glutarldehyde (in PBS) overnight at 4°C degree. Samples were infiltrated with 2% gelatin (PBS) and the small cubes were made, which were than embedded to Embed 812 (EMS, USA) using a routine TEM embedding protocol. After the semithin sections (1µm), the ultrathin (70nm) sections were cut for TEM examination.

3.10. Quantitative real-time reverse transcription polymerase chain reaction

Total RNA was purified from individual cell culture samples (from 10^6 cells) using the RNA isolation kit of Macherey-Nagel (Macherey-Nagel, Düren, Germany). All the preparation steps were carried out according the manufacturer's instructions. RNA samples were stored at –80°C in the presence 30U of Prime RNAse inhibitor (Thermo Scientific, Szeged, Hungary) for further analysis. The quantity of isolated RNA samples was evaluated by spectrophotometry (NanoDrop 3.1.0, Rockland, DE, USA). In order to monitor gene expression, qPCR was performed on a RotorGene 3000 instrument (Corbett Research, Sydney, Australia) using the TaqMan probe sets of CFTR gene (Applied Biosystems Foster City, CA, USA). 3µg of total RNA was reverse transcribed using the High-Capacity cDNA Archive Kit (Applied Biosystems Foster City, CA, USA) according to the manufacturer's instructions in a final volume of 30µl. The temperature profile of the reverse transcription was as follows: 10min at RT, 2 h at 37°C, 5min on ice, 10min at 75°C for enzyme inactivation in a Thermal Cycler machine (MJ Research Waltham, MA, USA). After dilution with 30µl of water, 1µl of the diluted reaction mix was used as template in the qPCR. For all the reactions TaqMan Universal Master Mix (Applied Biosystems Foster City, CA, USA) were used according to the manufacturer's instructions. Each reaction mixture (final volume 20µl) contained 1µl of primer-TaqMan probe mix. Gene expression assay identification No for CFTR: Hs00357011_m1 and HPRT: Hs03929098_m1. The qPCR reactions were carried out under the following conditions: 15min at 95°C and 45 cycles of 95°C for 15sec, 60°C for 1min. Fluorescein dye intensity was detected after each cycle. Relative expression ratios were calculated as normalized ratios to human Hypoxanthine-guanine phosphoribosyltransferase (HPRT) internal control gene. Non-template control sample was used for each PCR run to check the primer-dimer formation. The final relative gene expression ratios were calculated as ΔCt values (Ct values of gene of interest versus Ct values of the control gene).

3.11. Immunofluorescence

Cultured cells. For CFTR immunostaining Capan-1 cells were rinsed twice with phosphate buffered saline (PBS) and fixed in 4% paraformaldehyde (PFA) for 5 min at RT, followed by 20 min permeabilisation in 0.1%Triton X-100. Nonspecific antibody binding was blocked with 10% goat serum and 1% BSA for 60min at RT. For CFTR detection cells were incubated with anti-NBD2 monoclonal primary CFTR antibody obtained from CF Foundation (Coding No.: 596) (Kreda et al., 2005) (1:100) overnight on 4°C. After this the cells were washed and incubated with anti-mouse FITC conjugated secondary antibody (Dako, Denmark) for 2 h at RT. The nuclei of the cells were stained with Hoechst 33342 (5µg/ml) for 20 min. The images were captured using Olympus Fluoview10i-W system.

Guinea pig pancreatic tissue. To detect the effects of ethanol and FA on CFTR expression and localisation we used guinea pig as an *in vivo* model. The animals were kept at a constant room temperature of 24°C with a 12 h light–dark cycle and were allowed free access to chow and water. Guinea pigs were treated with a mixture of 0.8g/kg ethanol (Reanal; Budapest, Hungary) and 300mg/kg palmitic acid (PA) intraperitoneally (*i.p.*). Before the ethanol and PA treatment the animals were injected with 1.2ml physiological saline to avoid ethanol-induced peritoneal irritation. The control animals were treated with 2x1.2ml physiological saline *i.p.* The animals were sacrificed 3, 6, 12 and 24 h after the injection in pentobarbital (37mg/kg *i.p.*) anaesthesia. From frozen samples of guinea pig pancreas 5µm thick sections were cut and placed on silanized slides and fixed in 2% paraformaldehyde solution for 15 min. After washing in 1% TBS solutions slides were stored in 1% BSA-TBS for non-specific antigen blocking. Primary antibody „Mr Pink" (rabbit polyclonal antibody against human CFTR, CFTR Folding Consortium (Peters et al., 2011, Pallagi et al., 2014)) was applied in a dilution of 1:100 in 1%BSA TBS for overnight in 4°C then secondary anti rabbit antibody (Alexa Fluor 488; host: goat; Invitrogen Eugene, Oregon USA – A11034) was used in a dilution of 1:400 for 3 h. at RT. DAPI nuclear staining was performed in a dilution of 1:100 for 20 min. at RT. Between steps careful TBS washings were applied. Finally, slides were coverslipped by DAKO Fluoromount (Glostrup, Denmark). RO-density was calculated as described above.

3.12. Statistical Analysis

All data are expressed as means±SEM. Significant differences between groups were determined by analysis of variance. Statistical analysis of the immunohistochemical data was performed using the Mann–Whitney U test. $P<0.05$ was accepted as statistically significant.

3.13. Ethical Approvals

All experiments were conducted in compliance with the Guide for the Care and Use of Laboratory Animals (National Academies Press, Eight Edition, 2011), and were approved by Committees on investigations involving animals at the University of Szeged and also by independent committees assembled by local authorities.

4. RESULTS

4.1. Low concentration of ethanol stimulates, whereas high concentration of ethanol and fatty acids inhibit the HCO_3^- secretion in pancreatic ductal epithelial cells

To investigate the effects of ethanol and ethanol metabolites on the pancreatic ductal epithelial HCO_3^- secretion we used Capan-1 human polarized pancreatic cell line. During the experiments the apical and the basolateral side of the Capan-1 PDEC were perfused separately, which allowed us to selectively change the composition of the apical or basolateral solutions. The apical Cl^- removal from the extracellular solution increased the pH_i of PDECs by driving HCO_3^- into the cell via the basolateral NBCe1-B and the apical SLC26 CBE, whereas, re-addition of Cl^- decreased pH_i inducing secretion of HCO_3^- via the CBE and the CFTR Cl^- channel (Figure 2.A,B). In this scenario the initial rate of recovery after the re-addition of luminal Cl^- (base flux; $J(B^-)$) reflects the apical Cl^-/HCO_3^- exchange activity (Stewart et al., 2009). The other method, used in these series of experiments, the NH_4Cl pulse technique, during which the initial rate of recovery of pH_i from an alkali load, induced by exposure to NH_4Cl solution reflects the activity of the CBE and CFTR (Figure 2.C,D) (Hegyi et al., 2003). Experiments using both techniques showed that 15 min administration of low concentration of ethanol (10mM) stimulated, high concentration of ethanol (100mM) significantly inhibited $J(B^-)$, suggesting decreased apical Cl^-/HCO_3^- exchange activity (Figure 2.). In the next step we also tested the effects of oxidative and non-oxidative ethanol metabolites on the pancreatic epithelial secretion. We showed that high concentration of palmitoleic acid (POA) (100, 200µM) significantly inhibited, whereas, acetaldehyde (5mM) and palmitoleic acid ethyl ester (50-200µM) (POAEE) had no effects on $J(B^-)$.

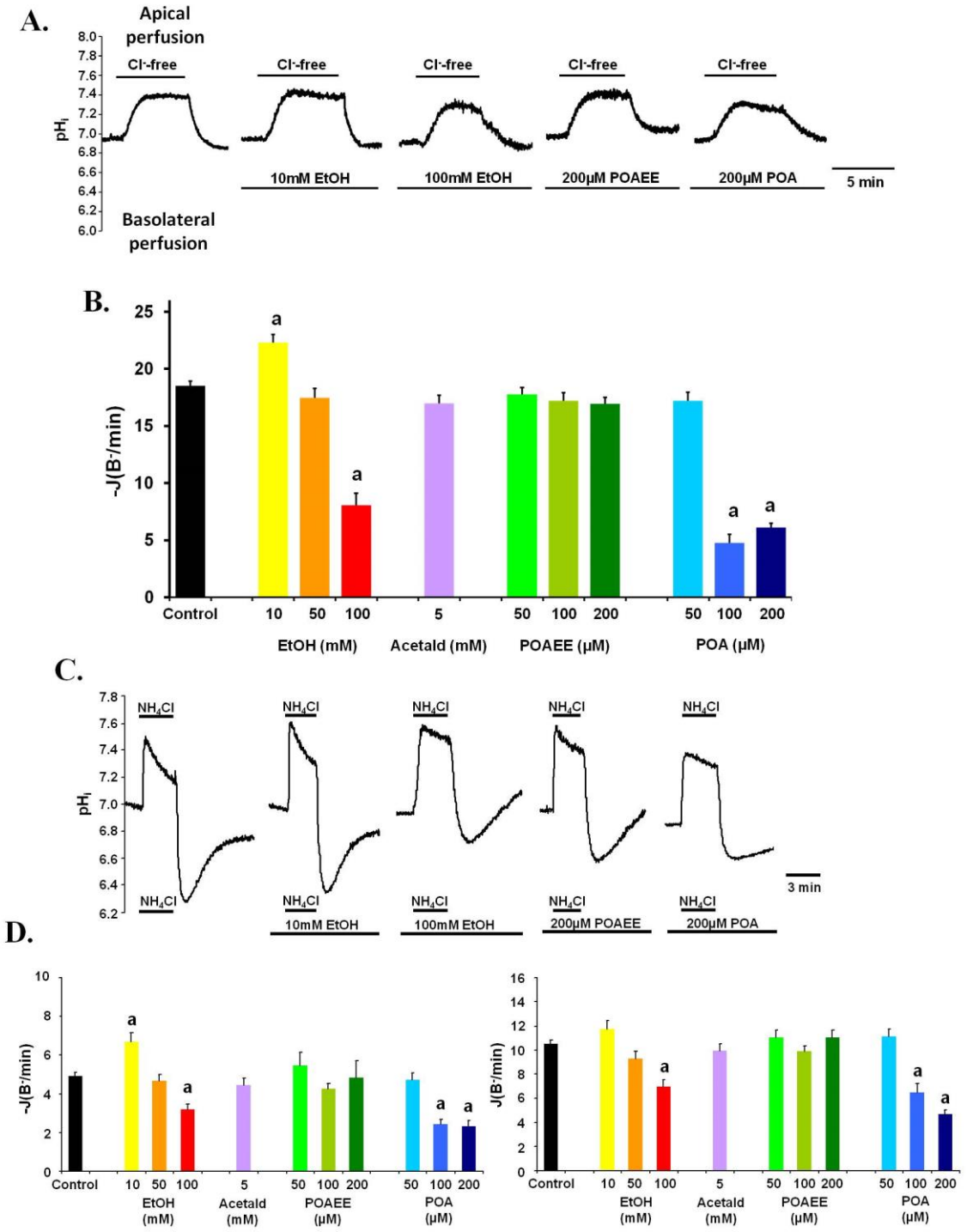

Figure 2. Ethanol and non-oxidative ethanol metabolites inhibit the HCO_3^- secretion in Capan-1 pancreatic epithelial cells. (A) Representative pH_i traces of the initial rate of recovery after Cl^- re-addition showing the effect of basolateral administration of ethanol and ethanol metabolites for 15 min on the pH_i recovery. Cells were perfused separately from the apical and basolateral side with CO_2/HCO_3^- buffered solution. Labels above the traces indicate the Cl^- composition of the luminal solution and labels below the traces denote compounds added to the basolateral perfusion solution. **(B) Summary data of the effect of ethanol, acetaldehyde, palmitoleic acid ethyl ester (POAEE) and palmitoleic acid (POA) the initial rate of recovery after Cl^- re-addition.** The

administration of low concentration of ethanol (10mM) significantly stimulated the activity of the luminal transporters. On the other hand, high concentration of ethanol (100mM) and POA (100-200µM) significantly inhibited the recovery. Data are shown as means ± SEM. n= 3-5 exp for all groups. a: $p<0.05$ vs control. **(C-D) Representative pH_i traces and summary data of the initial rate of recovery from alkali and acid load in Capan-1 cells**. Alkali and acid load was induced by 20mM NH_4Cl in HCO_3^-/CO_2 buffered solution. 10mM ethanol stimulated, whereas 100mM ethanol and 100-200µM POA significantly inhibited the activity of the luminal (recovery from alkali load; **D left panel**) and basolateral acid/base transporters (recovery from acid load; **D right panel**), respectively. Data are shown as means±SEM. n: 3-5 exp for all groups. a: $p<0.05$ vs Control.

4.2. High concentration of ethanol and fatty acids inhibit the CFTR Cl^- current in pancreatic ductal epithelial cells

Next we directly detected the effects of ethanol and ethanol metabolites on the CFTR Cl^- current. Exposure of Capan-1 cells to 10µM forskolin increased basal whole cell currents from 23.61±2.36 to 89.7±9.84 at +60 mV in 90.71±5.87% of cells (Figure 3.). The forskolin-activated currents were time- and voltage-independent, with a near linear I/V relationship and a reversal potential of -5.15mV±1.12 (Figure 3.). These biophysical characteristics indicate that the currents are carried by CFTR channel. Exposure of Capan-1 cells to 10mM ethanol stimulated the forskolin-stimulated CFTR currents by 30.21±12.28%, whereas the administration of 100mM ethanol or 200µM POA significantly decreased the forskolin-stimulated CFTR currents by 45.4±8.51% and 69.7±3.21%, respectively. In both cases, the inhibition was voltage-independent and irreversible. Administration of 200µM POAEE had no effect on forskolin-stimulated CFTR currents.

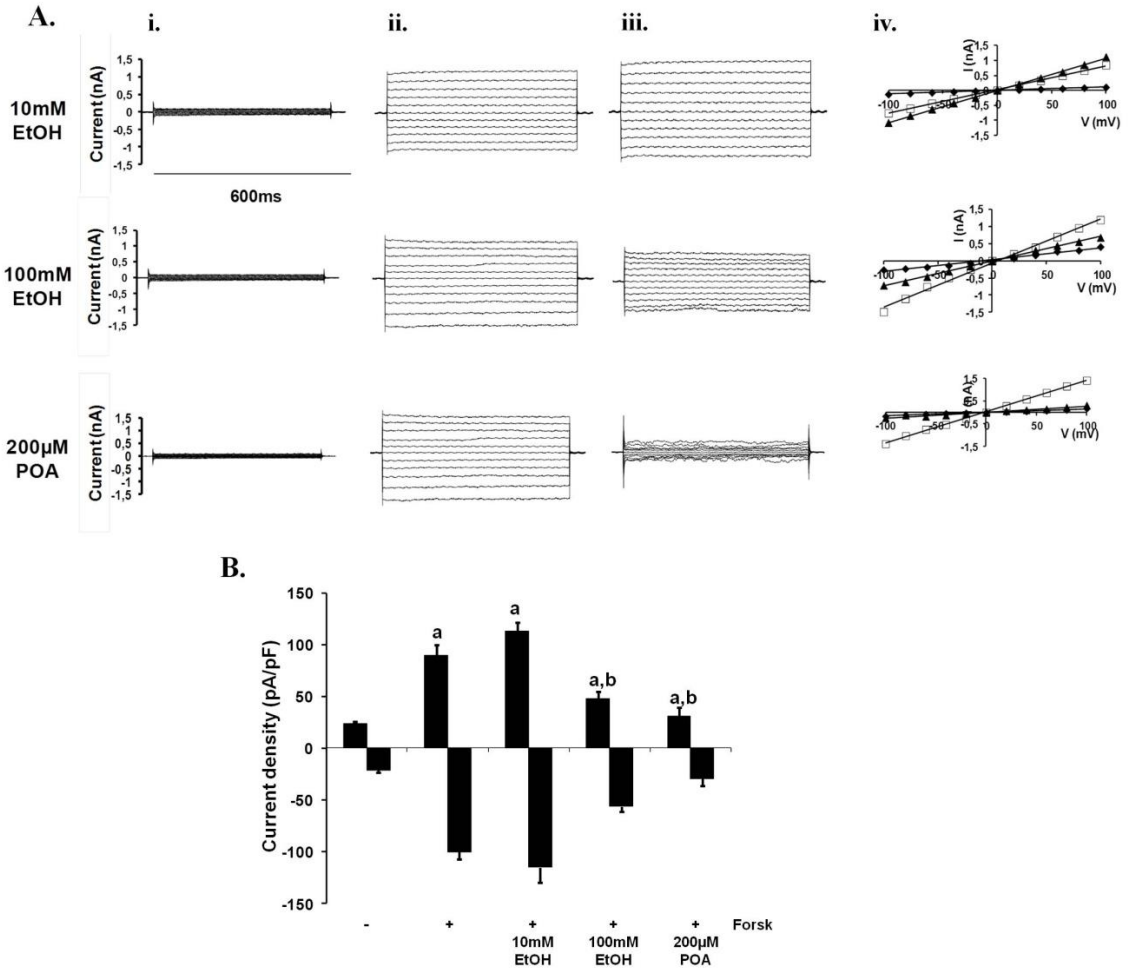

Figure 3. High concentration of ethanol and palmitoleic acid inhibit the CFTR Cl^- current in Capan-1 cells. (A-B) Representative fast whole cell CFTR Cl^- current recordings and summary chart. (i) Unstimulated currents, (ii)) currents after 10 min stimulation with 10μM forskolin (Forsk), and (iii) stimulated currents following 10 min exposure to 10mM or 100mM ethanol and 200μM POA (iv) I/V relationships (diamonds represent unstimulated currents, squares represent forskolin-stimulated currents, and triangles represent forskolin stimulated currents in the presence of the tested agents). Summary of the current density (pA/pF) measured at Erev ±60 mV. Exposure of the Capan-1 cells to 10mM ethanol stimulated, however, 100mM ethanol or 200μM POA blocked the forskolin-stimulated CFTR Cl^- currents. Data are shown as means±SEM. n=5-6 for all groups. a: $p<0.05$ vs basal current; b: $p<0.05$ vs forskolin-stimulated current.

4.3. High concentration of ethanol and fatty acids inhibit the HCO_3^- secretion and the CFTR Cl^- current in guinea pig pancreatic ductal epithelial cells

To confirm our observations we used isolated guinea pig pancreatic ducts, since the guinea pig pancreas secretes a juice containing ~140mM $NaHCO_3$ as does the human

gland (Argent, 2012), making it an attractive animal model to study pancreatic HCO_3^- secretion. Using isolated ducts we showed that administration of 100mM ethanol, or 200µM POA for 30 min markedly reduced the pancreatic HCO_3^- secretion, whereas 200µM POAEE had no effect (Figure 4.A) confirming our observations on Capan-1 cells. The pancreatic ductal HCO_3^- secretion was measured using NH_4Cl pulse, where the initial rate of pH_i recovery from an alkali load (base flux; $J(B^-)$) reflects the activity of the apical SLC26 Cl^-/HCO_3^- exchanger and CFTR (Figure 4.B) (Hegyi et al., 2003).

We detected the effects of ethanol and ethanol metabolites on the CFTR Cl^- current in primary epithelial cells as well (Figure 4.B). Exposure of isolated guinea pig PDEC to 10mM ethanol had no significant effect on the forskolin-stimulated CFTR currents (in Capan-1 significant slight stimulation was observed), whereas 100mM ethanol or 200µM POA significantly decreased it. In this case the inhibition was voltage-independent and irreversible. Administration of 200µM POAEE had no effect on forskolin-stimulated CFTR currents.

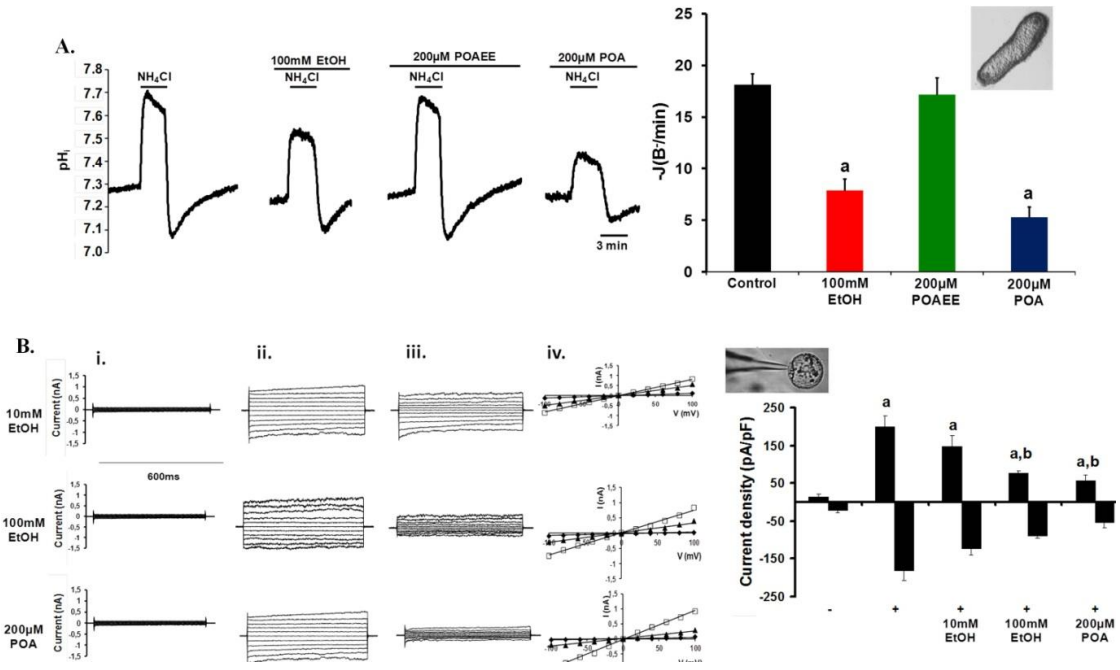

Figure 4. High concentration of ethanol and palmitoleic acid inhibit the HCO_3^- secretion and CFTR Cl^- current in guinea pig pancreatic ductal epithelial cells. (A) Measurements of the luminal Cl^-/HCO_3^- exchange activity shows that basolateral administration of 100mM ethanol and 200µM POA significantly inhibited the activity of the luminal SLC26 Cl^-/HCO_3^- exchanger and CFTR and decreased the recovery from alkali load in isolated guinea pig pancreatic ducts. n=3-5 exp/groups. a:p<0.05vs.Control. **(B) Representative fast whole cell CFTR Cl^- current recordings in guinea pig pacreatic ductal cells.** (i) Unstimulated currents, (ii) currents after forskolin stimulation

(10µM; 10 min; Forsk), and (iii) stimulated currents following 10 min treatment (iv) I/V relationships (diamonds: unstimulated-, squares: forskolin-stimulated-, triangles: forskolin-stimulated currents following treatment). The summary of the current densities (pA/pF; measured at E_{rev}:±60mV) show that 100mM ethanol or 200µM POA blocked the forskolin-stimulated CFTR Cl^- currents (61.5±5.15% and 73.1±4.46%, respectively). n=5-6/groups. a:p<0.05vs.basal current; b:p<0.05vs.forskolin-stimulated current.

4.4. Ethanol and fatty acids inhibit the pancreatic ductal ductal fluid secretion

In addition to the pancreatic HCO_3^- secretion, the pancreatic fluid secretion was also shown to play an important role in the pancreatic physiology and pathophysiology (Pallagi et al., 2014). To detect the pancreatic ductal fluid secretion *in vitro* we used isolated guinea pig pancreatic ducts, an established *in vitro* model to mimic the human situation. Administration of 100mM ethanol, or the non-oxidative ethanol metabolite POA (200µM) for 30 min markedly reduced the pancreatic fluid secretion, whereas 200µM POAEE had no effect (Figure 5.A).

To assess the effects of ethanol and ethanol metabolites to the *in vivo* exocrine pancreatic secretion, we used MRI cholangiopancreatography to measure the total excreted volume (TEV) in anesthetised mice. Upon the retroorbital injection of 10U/bwkg secretin the TEV increased (Figure 5.B-C). We compared the TEV of wild type (WT) animals to CFTR knockout mice, which was significantly lower, highlighting the important role of CFTR in the exocrine pancreatic secretion. We reassessed the secretion 24 h after the *i.p.* injection of 1.75g/kg ethanol and 750mg/kg palmitic acid (PA), which markedly impaired TEV in WT and almost completely abolished in CFTR KO mice.

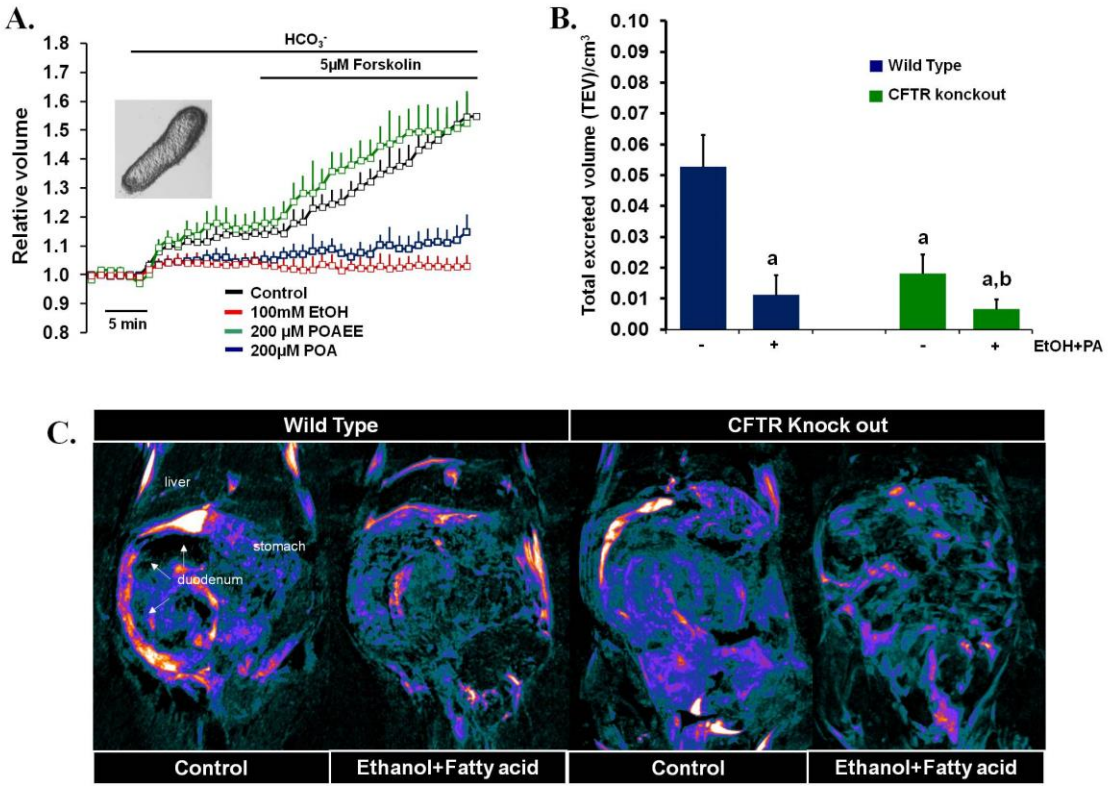

Figure 5. Ethanol and fatty acids inhibit the *in vitro* and *in vivo* pancreatic fluid secretion. (A) Changes of the relative luminal volume of isolated guinea pig pancreatic ducts show that administration of ethanol and palmitoleic acid (POA), but not palmitoleic acid ethyl ester (POAEE) for 30 min diminished the *in vitro* ductal fluid secretion. n=3-4 exp/groups. **(B) Ethanol and fatty acid inhibit the *in vivo* pancreatic exocrine secretion** measured as total excreted volume (TEV) using small animal MRI. Compared to WT, duodenal filling was significantly reduced in CFTR KO mice and it was abolished after *i.p.* injection of ethanol+palmitic acid. Data are shown as means±SEM. n=6/groups. a:p<0.05vs.WT-Control, a:p<0.05vs.KO-Control. **(C) Reconstructed images** of the duodenal filling after secretin stimulation during MRI.

4.5. Low concentration of ethanol stimulates both the apical Cl^-/HCO_3^- exchanger and CFTR via intracellular Ca^{2+} signalling in PDEC

To further confirm our observations, different inhibitors were used to investigate the transport mechanisms involved in the stimulatory effect of low concentration of ethanol on HCO_3^- secretion in Capan-1 PDEC. Using the Cl^- removal technique, we showed, that administration of 10μM CFTR Cl^- channel inhibitor CFTR(inh)-172 or 500μM SLC26A6 inhibitor H_2DIDS for 15 min could not prevent the stimulatory effect of 10mM ethanol alone, however, administration of both inhibitors at the same time totally prevented the stimulatory effect of low concentration of ethanol (Figure 6.A,C).

The NH_4Cl pulse technique resulted in slightly different way. In these series of experiments, not only the co-administration of the two inhibitors, but separate administration alone could prevent the stimulatory effect of ethanol (Figure 6.B,D). However, both techniques confirmed that when the two HCO_3^- transport mechanisms are inhibited, ethanol is unable to stimulate the secretory process.

We went further to identify the intracellular mechanisms, which could lead to the stimulatory effect of 10mM ethanol on HCO_3^- secretion. We found that administration of 10mM ethanol induced short lasting, repetitive Ca^{2+} spikes in 43% of the Capan-1 cells (Figure 7.A.i.). Administration of the inositol-triphosphate receptor (IP_3R) antagonist caffeine (20mM), or the phospholipase C (PLC) inhibitor U73122 (10µM) completely abolished the Ca^{2+} response suggesting that the Ca^{2+} was released from the ER via the IP_3 receptor (Figure 7.A.ii,iii). Next, we examined the connection between the stimulatory effect of ethanol on HCO_3^- secretion and the elevation of the intracellular Ca^{2+} concentration ($[Ca^{2+}]_i$) (Figure 7.B,C) and we showed that pre-treatment of the cells with 20mM caffeine totally inhibited the stimulatory effect of 10mM ethanol during the luminal Cl^- withdrawal or the NH_4Cl pulse technique.

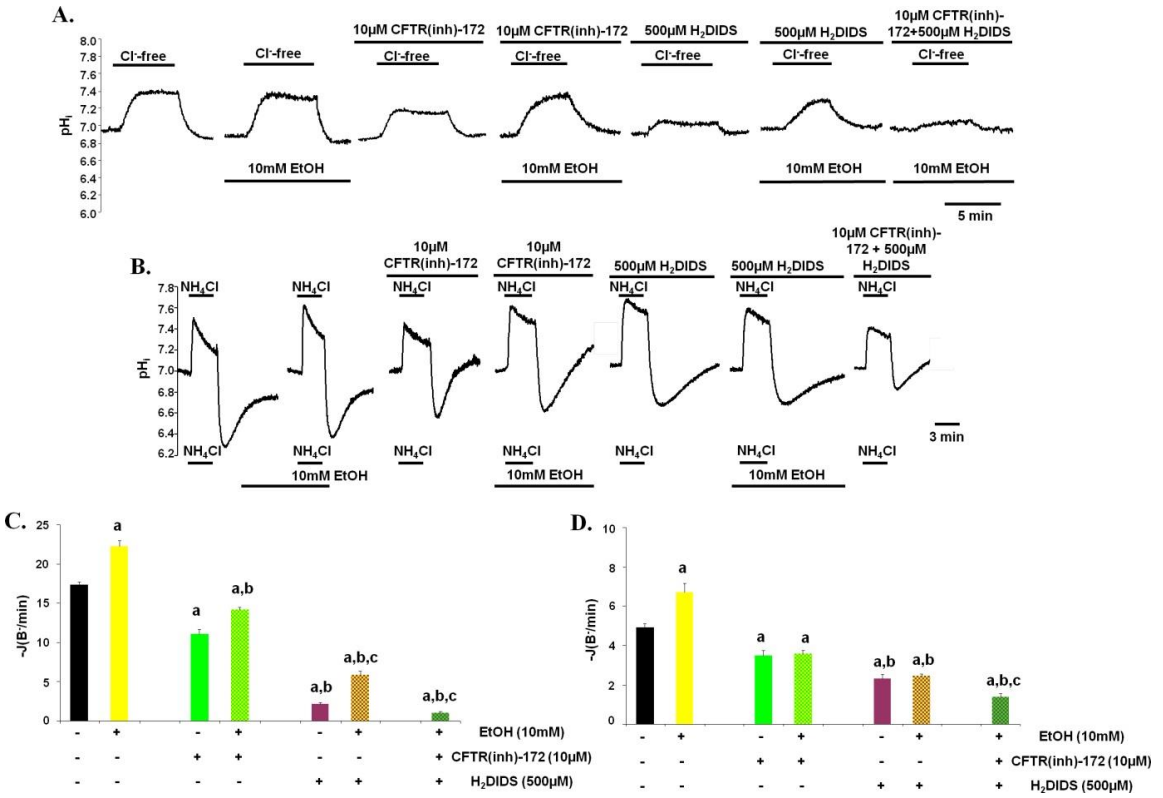

Figure 6. Low concentration of ethanol stimulates the luminal CBE and CFTR in Capan-1 PDEC. Representative pH_i traces showing the effect of luminal

administration of 500µM H_2DIDS and/or 10µM CFTR(inh)-172 in the presence or absence of 10mM ethanol on the pH_i recovery after **(A)** Cl^- re-addition or **(B)** after alkali load. **(C) Summary data of the initial rate of pH_i recovery after chloride re-addition.** The administration of 10µM CFTR(inh)-172 and 500µM H_2DIDS inhibited the recovery. 10mM ethanol stimulated the recovery in both cases. The combined administration of CFTR(inh)-172 and H_2DIDS abolished the stimulatory effect. These data suggest that low concentration of ethanol stimulate the activity of CBE and CFTR on the apical membrane of PDEC. **(D) Summary data of the initial rate of pH_i recovery after alkali load.** The administration of 10µM CFTR(inh)-172 and 500µM H_2DIDS inhibited the recovery. However 10mM ethanol failed to stimulate the recovery under these circumstances. Data are shown as means±SEM. n: 3-5 exp for all groups. a: $p<0.05$ vs Control; b: $p<0.05$ vs 10µM CFTR(inh)-172; c: $p<0.05$ vs 500µM H_2DIDS.

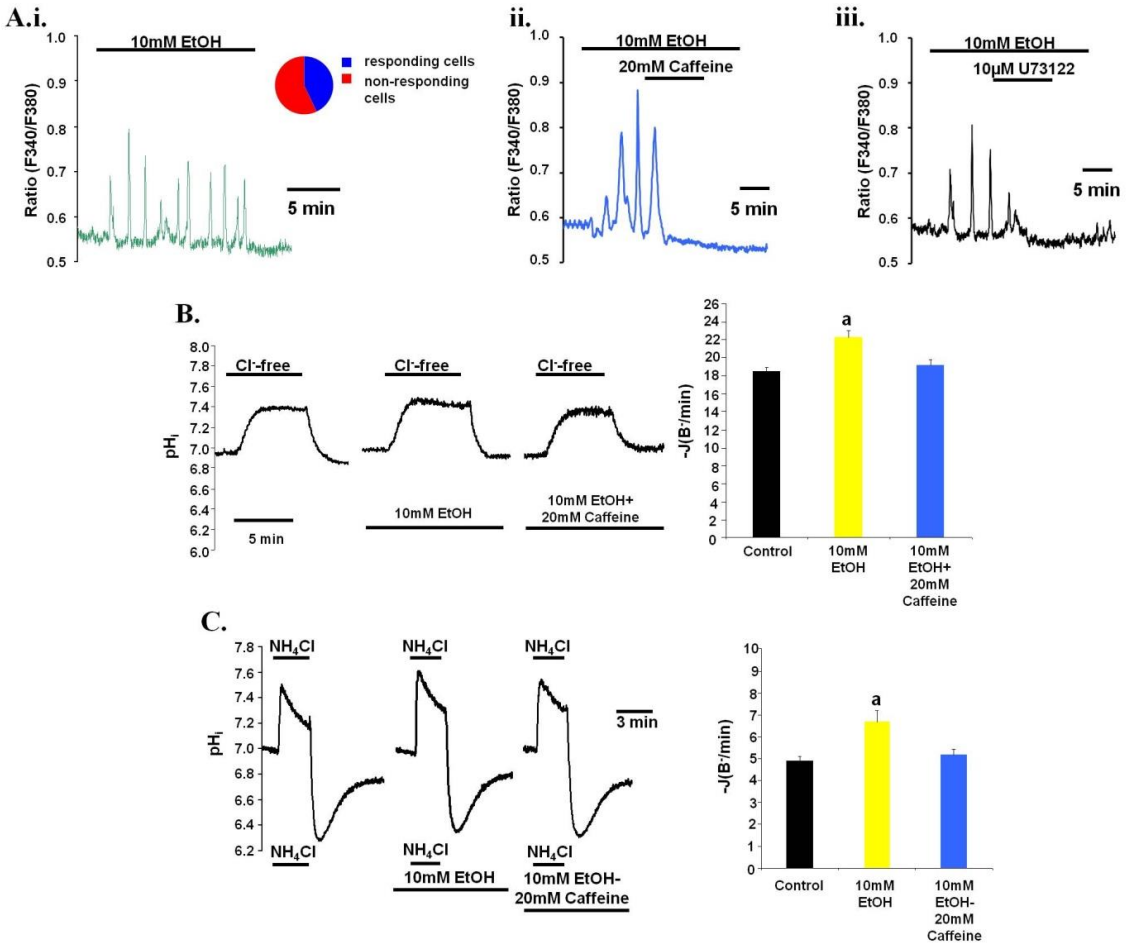

Figure 7. The stimulatory effect of 10mM ethanol is mediated by intracellular Ca^{2+} elevation. (A) Representative curves shows the effect of low concentration of ethanol on the $[Ca^{2+}]_i$ of PDEC. (i) The administration of 10mM ethanol induced short lasting, repetitive Ca^{2+} spikes in the 43% of the cells. The Ca^{2+} oscillation induced by 10mM ethanol was abolished by (ii) 20mM caffeine and (iii) 10µM U73122. **(B) Representative curve and summary data** shows the effect of caffeine pretreatment on the ethanol-stimulated apical Cl^-/HCO_3^- exchange activity. caffeine abolished the stimulatory effect

of low concentration of ethanol. **(C) Representative traces and summary data** showing the effect of the administration of Caffeine on the HCO_3^- secretion of PDEC. caffeine pretreatment abolished the stimulatory effect of 10 min administration of low concentration of ethanol on HCO_3^- secretion. Data are shown as means±SEM n: 3-5 exp for all groups. a: $p<0.05$ vs Control.

4.6. High concentration of ethanol and fatty acids inhibit both the apical Cl^-/HCO_3^- exchanger and CFTR in PDEC

The above mentioned two inhibitors (CFTR(inh)-172; H_2DIDS) were used to evaluate the involvement of CFTR Cl^- channel and SLC26A6 in the inhibitory mechanisms of ethanol and POA as well. Both methods showed that pre-treatment of the cells for 15 min with either 10µM CFTR(inh)-172 or 500µM H_2DIDS strongly decreased the inhibitory effects of ethanol and POA suggesting that both transport mechanisms are inhibited (Figure 7.). Since co-administration of the two inhibitors almost completely blocked the secretory process further inhibition by ethanol or POA was not investigated.

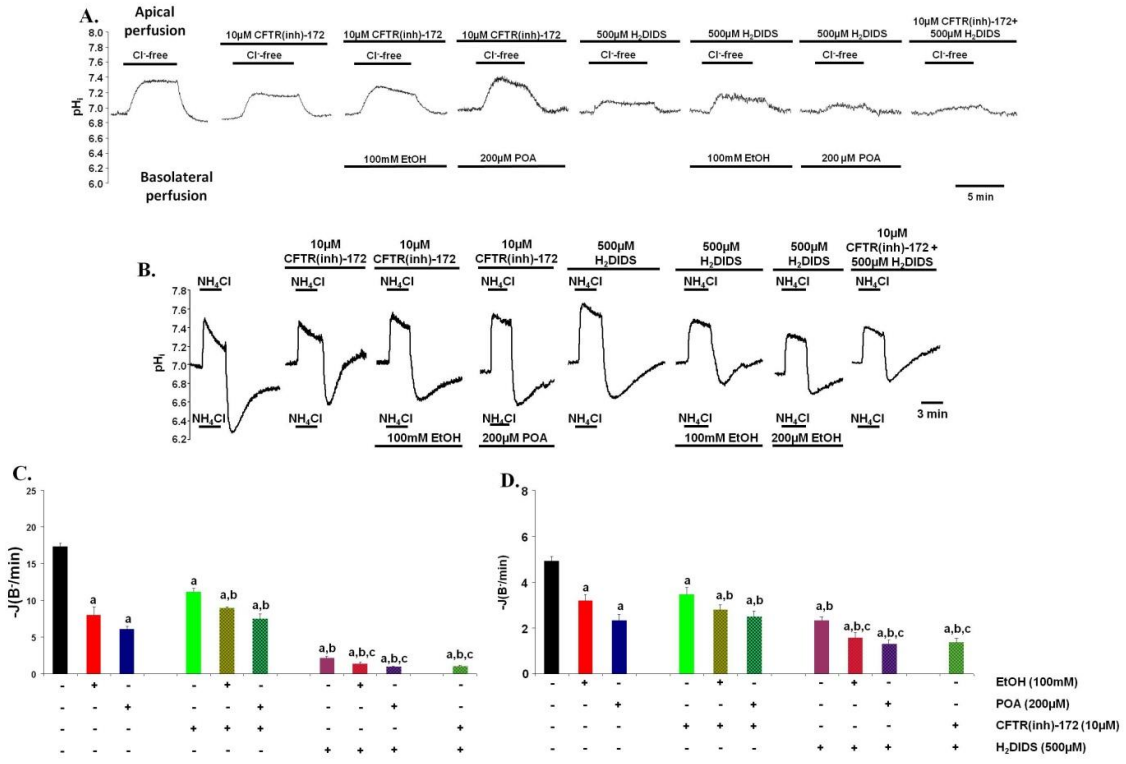

Figure 7. High concentration of ethanol and fatty acids inhibit the luminal CBE and CFTR in Capan-1 pancreatic ductal cells. (A) Representative pH_i traces showing the effects of the basolateral administration of 100mM ethanol or 200µM POA in the presence or absence of 500µM H_2DIDS and/or 10µMCFTR(inh)-172 (luminal

administration) on the pH_i recovery after Cl^- re-addition in HCO_3^-/CO_2-buffered solution. **(B) Representative pH_i traces** of the effects of the basolateral administration of 100mM ethanol or 200µM POA for 10 min in the presence or absence of 500µM H_2DIDS and/or 10µM CFTR(inh)-172 (luminal administration) on the pH_i recovery after alkali load in HCO_3^-/CO_2-buffered solution. **(C) Summary data of the initial rate of pH_i recovery after Cl^- re-addition.** 100mM ethanol and 200µM POA induced further inhibition after the administration of CFTR(inh)-172and/or H_2DIDS. These data suggest that high concentration of ethanol and POA inhibit the activity of CBE and CFTR on the apical membrane of PDEC. Data are shown as means±SEM. n=3-5 exp for all groups. a: $p<0.05$ vs Control; b: $p<0.05$ vs 10µM CFTR(inh)-172; c: $p<0.05$ vs 500µM H_2DIDS. **(D) Summary data of the initial rate of pH_i recovery after alkali load.** Our results further confirmed the inhibitory effect of ethanol and POA on CBE and CFTR. Data are shown as means±SEM.n: 3-5 exp for all groups. a: $p<0.05$ vs Control; b: $p<0.05$ vs 10µM CFTR(inh)-172; c: $p<0.05$ vs 500µM H_2DIDS.

4.7. High concentration of ethanol and fatty acids induce sustained Ca^{2+} release in PDEC

High concentration of ethanol (100mM) induced moderate, but sustained $[Ca^{2+}]_i$ increase in PDEC, whereas POAEE had no effect. POA in low concentration (50µM) evoked small $[Ca^{2+}]_i$ elevation, but in high concentrations (100 and 200µM) induced sustained $[Ca^{2+}]_i$ rise (Figure 8.A). The first phase of the $[Ca^{2+}]_i$ elevation was inhibited by the ryanodin receptor (RyR) inhibitor Ruthenium Red (RR, 10µM)(Gerasimenko et al., 2006c) by 55.5%, whereas, by the IP_3R inhibitor caffeine (20mM) by 86.1% and the PLC inhibitor U73122 (10µM) by 73.5%. Co-administration of the inhibitors almost totally blocked the initial $[Ca^{2+}]_i$ increase by 91.2% (Figure 8.B.i-iv, C), confirming that the initial $[Ca^{2+}]_i$ elevation is due to release from the ER via the activation of IP_3R and RyR.

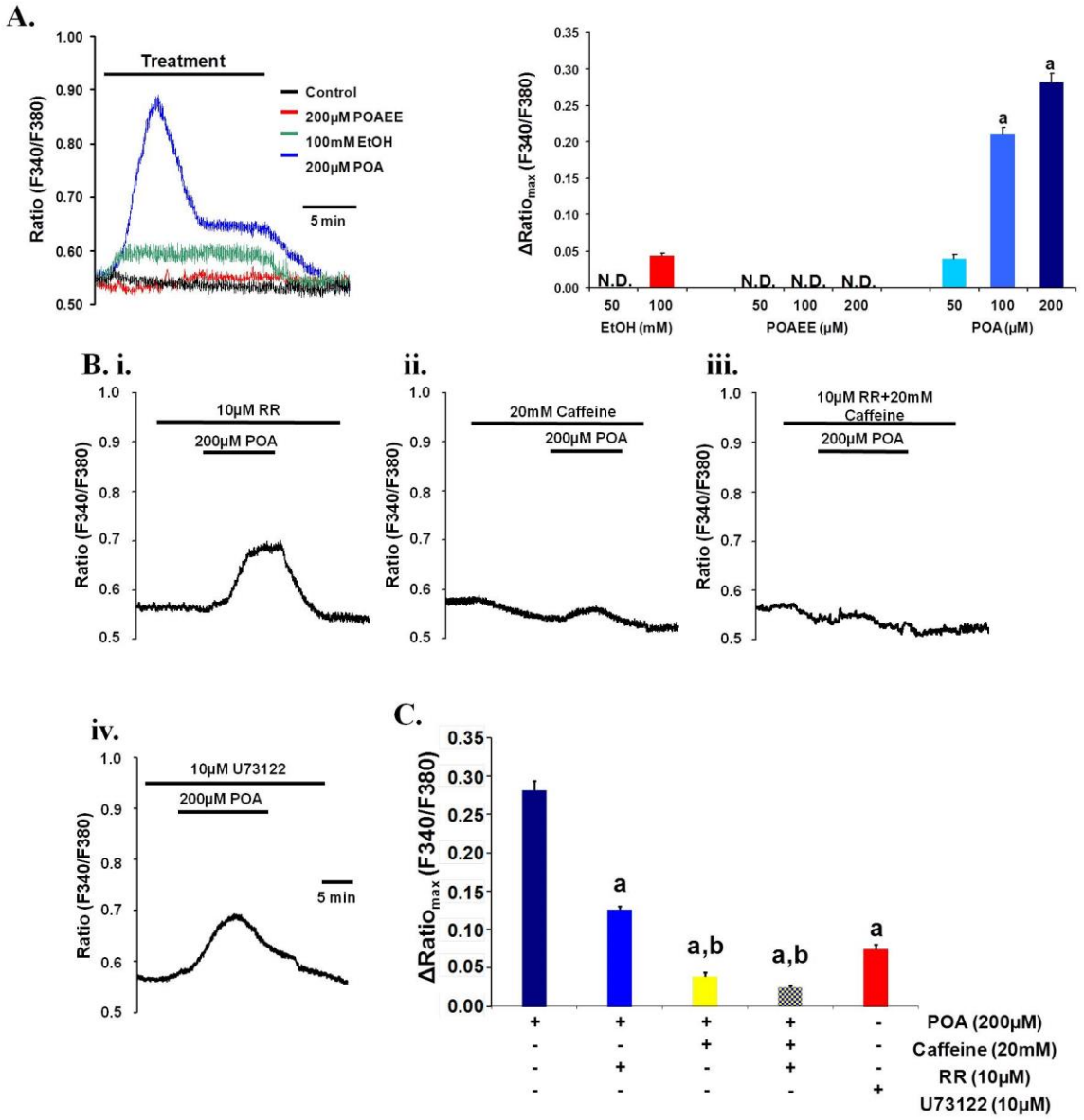

Figure 8. High concentration of ethanol and palmitoleic acid induce sustained $[Ca^{2+}]_i$ elevation in Capan-1 cells. (A) Representative traces and summary data of the $\Delta Ratio_{max}$ show the effect of ethanol, POAEE and POA on $[Ca^{2+}]_i$. 100mM ethanol induced sustained $[Ca^{2+}]_i$ elevation, whereas 100μM-200μM POA induced significantly higher $[Ca^{2+}]_i$ increase. Data are shown as means±SEM. n: 3-5 exp for all groups. a:p<0.05vs.100mM ethanol. **(B) POA releases Ca^{2+} from the ER via IP_3R and RyR activation. Representative curves** show the effect IP_3R and RyR inhibition on the Ca^{2+} release induced by 200μM POA. The administration of (i) 10μM RR significantly decreased the effect of POA on $[Ca^{2+}]_i$ (55.5%), (ii) 20mM caffeine induced significantly higher inhibition (86.1%). (iii) The combined administration of RR and caffeine had no further effects (92.1%). (iv) The PKC inhibitor U73122 decreased the effect of POA similarly to caffeine (73.5%). **(C) Summary data of the $\Delta Ratio_{max}$.** The administration of RR, caffeine and U73122 significantly decreased the effect of POA on $[Ca^{2+}]_i$. Data are shown as means±SEM. n: 3-5 exp for all groups. a: p<0.05 vs Control; b: p<0.05 vs 10μM RR.

4.8. High concentration of ethanol and fatty acids induce $(ATP)_i$ depletion and decrease mitochondrial membrane potential in PDEC

Measurement of $(ATP)_i$ using MgGreen-AM fluorescent Mg^{2+} indictator revealed that low concentration of ethanol, POAEE and POA had no effects on the of PDEC (Figure 9.A-B), however, 100mM ethanol and 100 or 200µM POA markedly and irreversibly decreased $(ATP)_i$. (Please note, that the increase in fluorescent intensity inversely correlates with the cellular ATP levels, since Mg^{2+} has higher affinity to ATP compared to ADP.) In these experiments we used the combination of 10mM deoxyglucose (DOG)/5mM iodoacetate (IAA) and 100µM carbonyl cyanide 3-chlorophenylhydrazone (CCCP) as positive control, to inhibit the cellular glycolysis and the mitochondrial ATP production. To further characterize the effects of ethanol and ethanol metabolites on the mitochondrial function, we showed that 100mM ethanol and 100-200µM POA markedly and irreversibly irreversible decreased $(\Delta\Psi)_m$ (Figure 4.C-D).

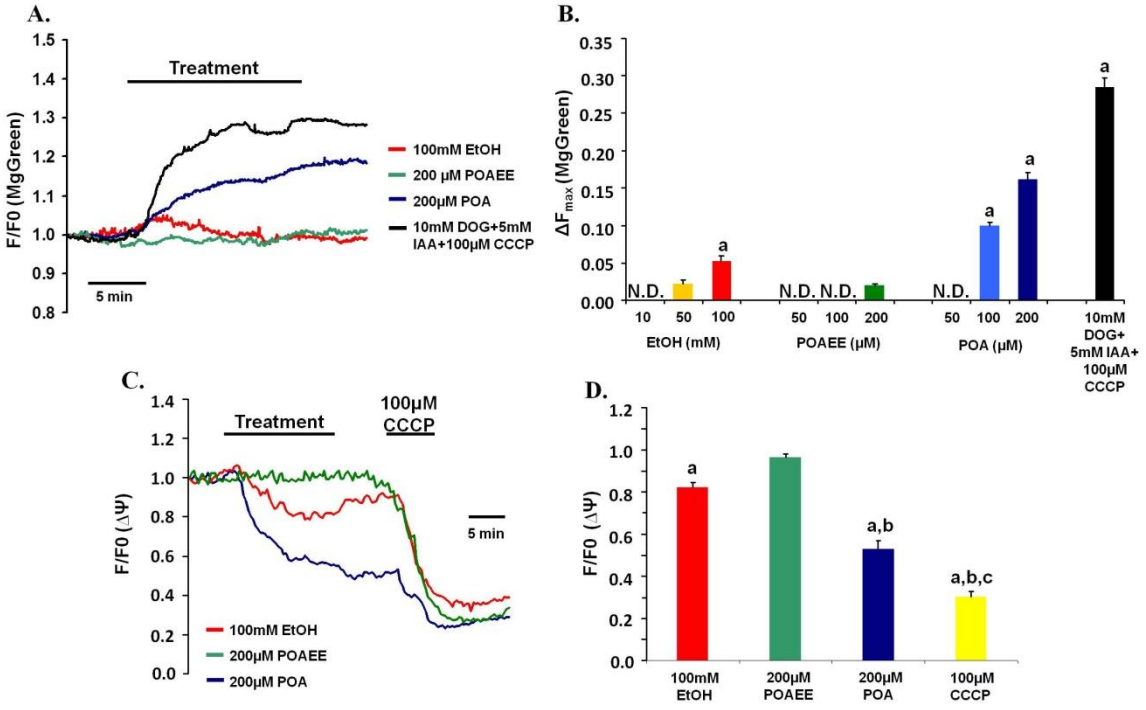

Figure 9. High concentration of ethanol and palmitoleic acid induce irreversible $(ATP)_i$ depletion and decrease the mitochondrial membrane potential in Capan-1 cells. (A-B) Representative traces and summary data of the changes of $(ATP)_i$. High concentration of ethanol and POA induced significant and irreversible $(ATP)_i$ depletion.

Deoxyglucose/iodoacetic acid (DOG/IAA; glycolysis inhibition) and CCCP (inhibition of mitochondrial ATP production) served as control. Data are shown as means±SEM. n=3-5/group; a:p<0.05vs.Control; N.D.: not detected. **(C-D) Representative traces and summary data of the changes of the mitochondrial membrane potential [$(\Delta\Psi)_m$].** 100mM ethanol induced moderate $(\Delta\Psi)_m$ decrease, whereas 200µM POA had more prominent effect. CCCP induced further $(\Delta\Psi)_m$ decrease after POA treatment. Data are shown as means±SEM. n=3-5/group; a:p<0.05vs.Control; b:p<0.05vs.100mM ethanol; c:p<0.05vs.200µM POA.

4.9. The inhibitory effects of ethanol and fatty acids on HCO_3^- secretion are mediated by sustained $[Ca^{2+}]_i$ elevation and $(ATP)_i$ depletion

Sustained elevation of the $[Ca^{2+}]_i$ has been shown to mediate cellular toxicity via intracellular trypsinogen activation (Frick et al., 1997) and damaged mitochondrial ATP production (Criddle et al., 2006) in pancreatic acinar cells. Therefore here we tested the effects of intracellular Ca^{2+} chelation on the inhibitory effects of ethanol and palmitoleic acid using 40µM BAPTA-AM preincubation for 30 min. We detected that the preincubation completely abolished the inhibitory effect of 100mM ethanol and 200µM POA on pancreatic ductal HCO_3^- secretion suggesting that their inhibitory effect was mediated by the sustained elevation of $[Ca^{2+}]_i$ (Figure 10.).

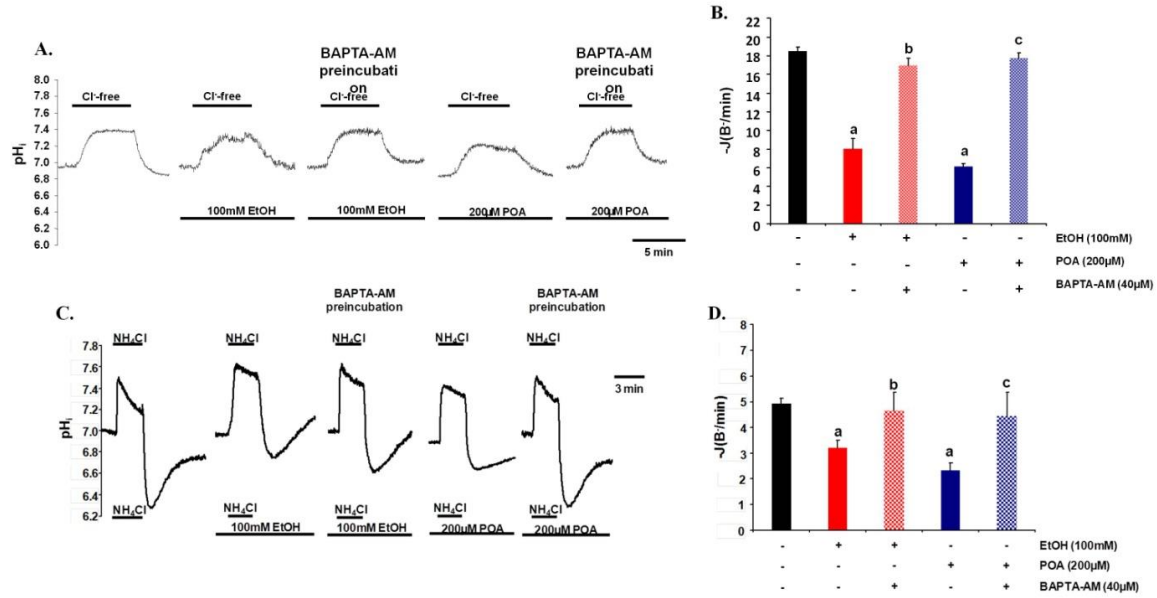

Figure 10. Intracellular Ca^{2+} chelation abolished the inhibitory effect of ethanol and POA on the HCO_3^- secretion in Capan-1 cells. (A-B) Representative traces and summary data of the initial rate of pH_i recovery after luminal Cl^- re-addition. Ca^{2+} chelation abolished the inhibitory effect of ethanol and POA on the pancreatic ductal

epithelial HCO_3^- secretion. Data are shown as means±SEM. n=3-5/group; a:p<0.05vs.Control; b:p<0.05vs.100mM ethanol; c:p<0.05vs.200µM POA. **(C-D) Representative traces and summary data** show that the intracellular Ca^{2+} chelation abolished the inhibitory effect of 100mM ethanol or 200µM POA on the recovery after alkali load. Data are shown as means±SEM. n: 3-5 exp for all groups. a: p<0.05 vs Control; b: p<0.05 vs 100mM ethanol; c: p<0.05 vs 200µM POA.

The final question in these series of experiments was to show that the $(ATP)_i$ depletion is able to inhibit the HCO_3^- secretion directly. To address this question we administrated 10mM DOG/5mM IAA and 100µM CCCP for 10 min to block the glycolysis and the mitochondrial ATP production at the same time. We showed that the administration of DOG/IAA-CCCP significantly decreased HCO_3^- secretion, very similar to the effects of 200µM POA (Figure 11.), or 100mM ethanol (not shown).

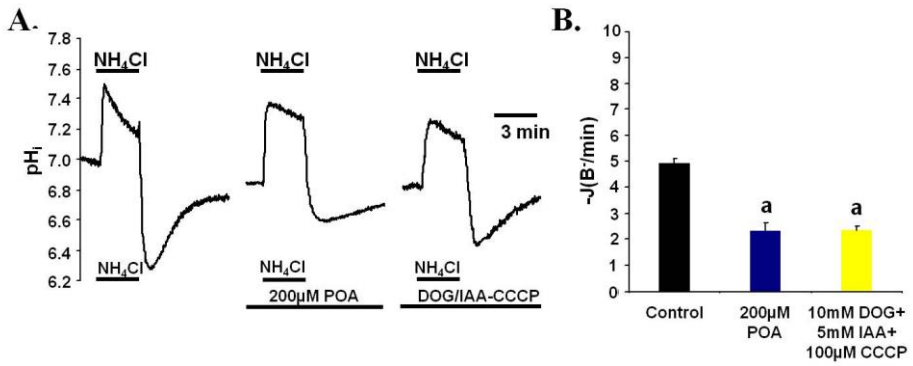

Figure 11. $(ATP)_i$ depletion mimics the inhibitory effect of ethanol and non-oxidative ethanol metabolites on HCO_3^- secretion. (A) Representative traces showing the effect of $(ATP)_i$ depletion on the HCO_3^- secretion. The administration of 10mM DOG/5mM IAA and 100µM CCCP significantly inhibited the recovery after alkali load. **(B) Summary data of the recovery after alkali load.** The recovery after alkali load was significantly reduced by $(ATP)_i$ depletion. Data are shown as means±SEM. n: 3-5 exp for all groups. a: p<0.05 vs Control.

4.10. Ethanol and non-oxidative ethanol metabolites cause translocation and expression defect of CFTR in PDEC

We showed that acute administration of ethanol and non-oxidative ethanol metabolites can inhibit the pancreatic HCO_3^- secretion and the functional activity of the CFTR Cl^- channel. However after heavy ethanol consumption the blood concentration of

ethanol and non-oxidative ethanol metabolites can remain elevated for 24-48 hours (Doyle et al., 1996). To investigate the effects of ethanol and ethanol metabolites on the protein expression levels, Capan-1 cells were incubated with ethanol, POAEE or POA and changes in CFTR expression were measured. We showed that high concentrations of ethanol, POAEE and POA time-dependently decreased both the mRNA and protein expression of CFTR (Figure 12.A-C).

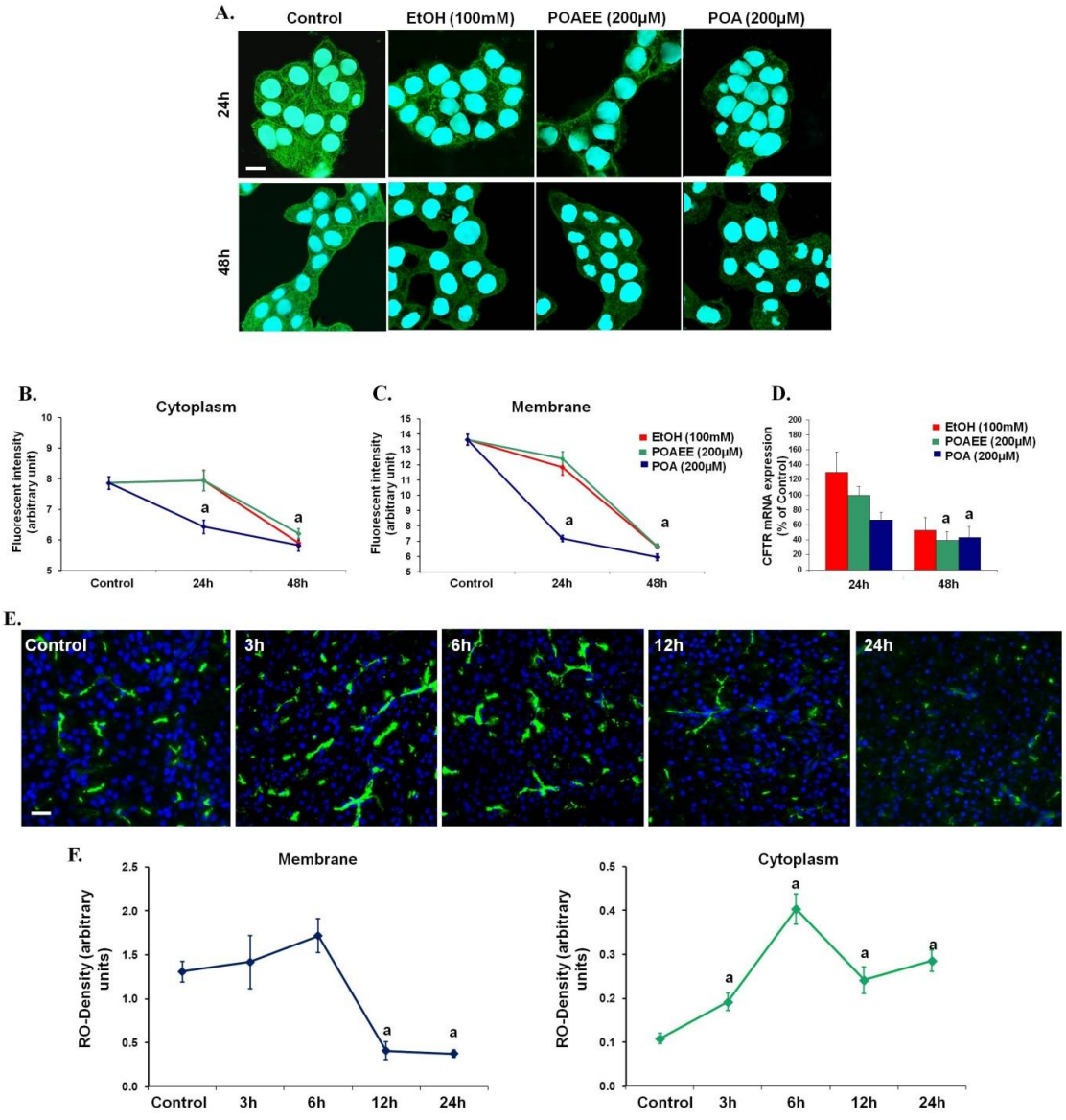

Figure 12. Ethanol, POAEE and POA decrease CFTR expression in Capan-1 cells and in guinea pig pancreatic ducts. (A-C) High concentrations of ethanol, POAEE and POA induced a significant decrease in CFTR membrane and cytoplasmic protein expression. Scale bar=10μm. **(D)** Ethanol, POAEE and POA decreased CFTR mRNA expression after 48 h of exposure. Data were normalized to HPRT mRNA levels and expressed as % of untreated control mRNA levels. **(E-F) CFTR expression in guinea**

pig pancreas. The expression of CFTR on the luminal membrane of guinea pig pancreatic ducts were significantly decreased 12 h following a single *i.p.* injection of 0.8g/kg ethanol and 300mg/kg palmitic acid (PA). Scale bar=100µm n=5/group. a:p<0.05vs.control.

To test whether these effects could be observed *in vivo* as well, guinea pigs were injected *i.p.* with 0.8g/kg ethanol and 300mg/kg palmitic acid (PA). Apical CFTR expression in the pancreatic ducts was not changed at 3 and 6h after injection, however it was significantly decreased 12 and 24 h after the treatment (Figure 12.E,F). Moreover, cytoplasmic CFTR levels were elevated after 3 h, suggesting that a membrane trafficking defect of CFTR was at least partially responsible for this increase.

4.11. The effects of bile acids on the mitochondrial morphology and $(ATP)_i$ level in pancreatic ductal and colonic epithelial cells

Administration of a low dose (0.1mM) of CDC or GCDC for 10 min had no effects on the intracellular organelles (data not shown). In addition, a high dose (1mM) of the conjugated GCDC did not induce morphological changes. Importantly, exposure of 1mM CDC for 10 min strongly damaged all of the mitochondria (Figure 13.A). The mitochondria swelled up and the inner membranes were disrupted. The same mitochondrial damage was observed in colonic epithelial cells isolated from human biopsy samples.

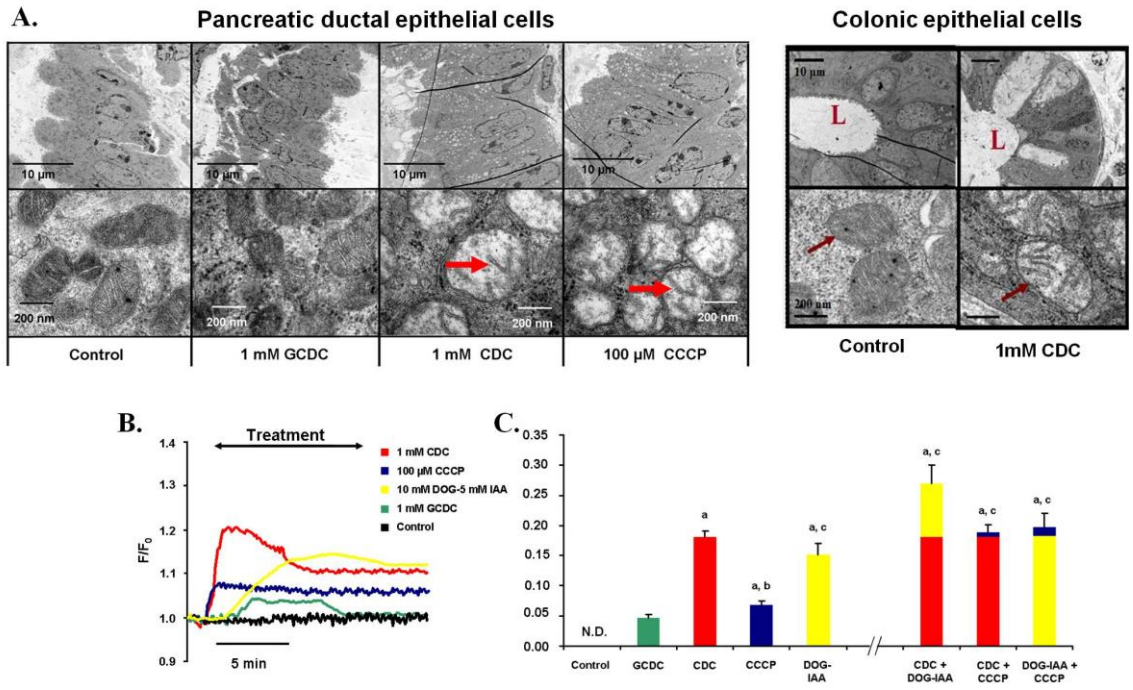

Figure 13. The effects of bile acids on mitochondria and intracellular ATP level of PDEC. (A) Transmission electron microscopy. Intact isolated guinea pig pancreatic ducts were exposed to standard HEPES solution (control), 1mM GCDC, 1mM CDC or 100µM CCCP for 10 min. There were no changes detected in general architecture of the cells in the control and GCDC treated groups. However, all mitochondria were strongly damaged in the 1mM CDC group. The globular shape and the loss of the mitochondrial inner membrane were well visible (red arrows). The same mitochondrial damage was observed in colonic epithelial cells exposed to CDC (right panel). **(B) Representative curves of the Mg-green fluorescence experiments.** Please note that the elevation of fluorescence intensity represents depletion in $(ATP)_i$. 1mM CDC, 100 µM CCCP or 10 mM DOG with 5 mM IAA caused irreversible and high elevation in the fluorescence intensity. 1mM GCDC caused a delayed small and reversible elevation in the fluorescence intensity. **(C) Summary data for the maximal fluorescence intensity changes.** CDC, CCCP and DOG/IAA caused a significantly higher elevation in Mg-green fluorescence intensity. Data are shown as means ± SEM from 25-35 regions of interests (ROIs) in 5-7 ducts. a: $p<0.01$ *vs.* GCDC; b: $p<0.01$ *vs.* CDC, c: $p<0.01$ *vs.* CCCP.

Other intracellular organelles such as nuclei or Golgi apparatus seemed to be unaltered. For positive control experiments we used the mitochondrial toxin CCCP (100µM) which mimicked the effect of CDC on mitochondria. Next we set out to investigate whether $(ATP)_i$ is affected due to the mitochondrial damage. Administration of a low dose of CDC or GCDC for 10 min had no effect on the $(ATP)_i$, however, a high dose of CDC and CCCP markedly and irreversibly reduced it (Figure 13.B, C). Although 1mM GCDC also decreased $(ATP)_i$, this depletion was reversible and significantly less than the depletion

caused by CDC or CCCP. The fact that CDC caused higher depletion of $(ATP)_i$ suggests that bile acids might have additional (non-mitochondria related) effects, which further decrease $(ATP)_i$. Therefore, we used the deoxyglucose (DOG)/idoacetamide (IAA) model which inhibits the intracellular glycolytic metabolism. Administration of 10mM DOG and 5mM IAA decreased $(ATP)_i$ (Figure 13.B-C). Importantly, CCCP or DOG/IAA administered after the high doses of CDC resulted further $(ATP)_i$ depletion, however, their effects were significantly smaller after CDC then administered alone. Exposure of pancreatic ducts to CCCP and DOG/IAA totally mimicked the effect of CDC. These data indicate that CDC inhibits both the oxidative and glycolytic metabolism of PDEC.

4.12. The effect of $(ATP)_i$ depletion on the bicarbonate secretion of pancreatic ductal epithelial cells

To characterize the effects of $(ATP)_i$ depletion on the activities of NHE, NBCe1-B and CBE, we used the NH_4Cl pulse technique in HCO_3^--buffered solution. CCCP strongly inhibited NBCe1-B, NHE (recovery from acid load) and CBE (recovery from alkali load) (Figure 14.A-C). Administration of 10mM DOG and 5mM IAA inhibited the ion transporters as well (Figure 14.A-C). However, significantly higher inhibition was evoked by parallel administration of CCCP and DOG/IAA. These observations suggest that depletion of $(ATP)_i$ is the key element which inhibits the activity of NBCe1-B, NHE and CBE.

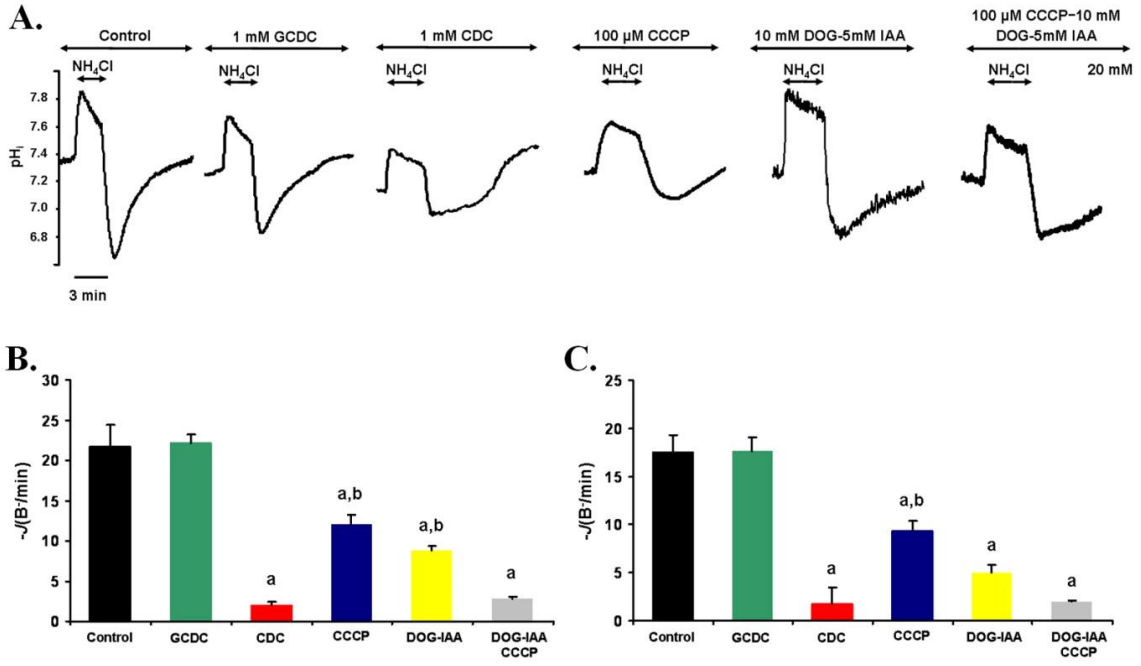

Figure 14. Effect of bile acids and $(ATP)_i$ depletion on the rate of pH_i recovery from an alkali and an acid load. (A) Representative experimental tracings showing the effects of 1mM GCDC, 1mM CDC, 100µM CCCP or 10 mM DOG with 5 mM IAA administered from the basolateral membrane of PDEC in the presence of 25 HCO_3^-/CO_2. CDC, the mitochondrial toxin CCCP and DOG/IAA markedly inhibited both recoveries. **(B) Summary data for the initial rate of recovery from alkali load.** CDC, CCCP and DOG/IAA decreased the recovery from alkali load. **(C) Summary data for the initial rate of recovery from acid load.** CDC, CCCP and DOG/IAA decreased the recovery from acid load. Data are shown as means ± SEM from 25-35 regions of interests (ROIs) in 5-7 ducts. a: $p<0.01$ *vs.* control, b: $p<0.01$ *vs.* CDC

5. DISCUSSION

In this present work we have demonstrated that ethanol, as well as its non-oxidative metabolites cause impairment of pancreatic ductal fluid and HCO_3^- secretion via toxic cellular Ca^{2+} signaling and break down of the mitochondrial ATP production. Very similar mitochondrial damage was found in these cells upon the administration of non-conjugated bile acid. These results highlight the central role of mitochondrial damage in the pathogenesis of acute pancreatitis.

5.1. The effects of ethanol and non-oxidative ethanol metabolites on the pancreatic fluid and HCO_3^- secretion

Pancreatic tissue metabolizes ethanol mainly via the non-oxidative pathway mediated by FAEE synthases (FAEES), which combine ethanol and FA and produce FAEE (Laposata and Lange, 1986). A clinical study showed that blood FAEE concentration was elevated in parallel with ethanol concentration during alcohol consumption; but FAEE remained increased longer in the serum compared to ethanol (Doyle et al., 1996). Moreover, compared with the liver, pancreatic FAEES activity is higher, which creates the possibility for the local accumulation of non-oxidative ethanol metabolites (Gukovskaya et al., 2002). Werner et al. showed that FAEE infusion induced pancreatic edema, intrapancreatic trypsinogen activation, and vacuolization of acinar cells (Werner et al., 1997). Recently Huang et al. developed a novel model of alcohol-induced pancreatitis (Huang et al., 2014) using a combined *i.p.* injection of ethanol and FA, where the pharmacological inhibition of non-oxidative ethanol metabolism decreased the pancreatic damage.

We demonstrated that pancreatic ductal HCO_3^- secretion plays central role in the physiology of the exocrine pancreas, maintaining the intraductal pH (Hegyi and Petersen, 2013, Hegyi et al., 2011), therefore in our experiments we used different *in vivo* and *in vitro* techniques to clarify the acute effects of ethanol and ethanol metabolites on fluid and HCO_3^- secretion and CFTR Cl^- current in human and rodent PDEC. Importantly, our MRI cholangiopancreatography experiments showed that in CFTR KO mice the ductal secretion is remarkably diminished compared to WT, moreover, ethanol and PA strongly impaired ductal secretion in both groups. Besides the fluid transport we characterized the

effects of ethanol and it metabolites on HCO_3^- secretion. Our results showed that ethanol in low concentration stimulates, whereas in high concentrations inhibits HCO_3^- secretion and decreases CFTR activity. Similar dual effects of ethanol on fluid secretion were highlighted earlier (Yamamoto et al., 2003). In our study, the stimulatory effect of 10mM ethanol on HCO_3^- secretion was mediated by IP_3R-dependent Ca^{2+} release from the ER, which is similar to the physiological stimulatory Ca^{2+} signal evoked by acetylcholine, or intraluminal ATP (Maleth and Hegyi, 2014). In contrast, high concentrations of ethanol and POA induced sustained $[Ca^{2+}]_i$ elevation mediated by both the IP_3R and RyR. Notably, similar toxic Ca^{2+} elevation was found in pancreatic acinar cells, and in other cell types leading to premature protease activation and cell death (Criddle et al., 2006, Kouzoukas et al., 2013, Nakayama et al., 2001, Kruger et al., 2000). It is well documented that sustained $[Ca^{2+}]_i$ elevation causes mitochondrial Ca^{2+} overload (Kroemer and Reed, 2000), which impairs $(\Delta\Psi)_m$ and ATP production (Criddle et al., 2006, Walsh et al., 2009). Very recently ethanol was shown to sensitize pancreatic mitochondria to activate the mitochondrial permeability transition pore, leading to mitochondrial failure (Shalbueva et al., 2013). In this study, high concentrations of ethanol and POA also induced $(ATP)_i$ depletion and decreased $(\Delta\Psi)_m$. Although the toxic effects of ethanol and POA were similar to those of high concentration of bile acids, in this study chelation of $[Ca^{2+}]_i$ abolished the inhibitory effect of ethanol and POA on HCO_3^- secretion. This observation indicates, that ethanol and POA, in a similar manner to trypsin (Pallagi et al., 2011), induce a sustained rise in $[Ca^{2+}]_i$, which damage the mitochondria and inhibit the pancreatic fluid and HCO_3^- secretion.

One of the important observations of this study is that upon alcohol and fatty acid administration the expression of CFTR is decreased on the luminal membrane of PDEC. Since decreased CFTR expression under these conditions is very similar to the CFTR mislocalization found in autoimmune pancreatitis (Ko et al., 2010), we wanted to confirm that decreased CFTR expression is caused by alcohol and not by the cellular damage during the inflammatory process. The *in vitro* experiments in human PDEC and the *in vivo* experiments in guinea pig clearly demonstrated that alcohol and its non-oxidative metabolites indeed strongly decrease CFTR expression without damaging PDEC. This effect can be attributed at least partially to the chronic cytoplasmic ATP-depletion, considering that CFTR conformation maturation is an ATP-sensitive process at the ER (Lukacs et al., 1994). These results indicate that chronic exposure of PDEC to ethanol or ethanol metabolites compromise both the biosynthetic processing and peripheral stability

of the channel. It is known that the phosphorylation and dephosphorylation of CFTR mediated by WNK/SPAK and IRBIT/PP1, regulates the PM trafficking of CFTR and other transporters in epithelial cells (Yang et al., 2011, Park et al., 2012), however, the effect of ethanol or ethanol metabolites on these systems is not known. Chronic alcohol consumption dose-dependently increases the risk to develop malignancies, diabetes, hypertension and cardiovascular diseases (Shield et al., 2013). Interestingly Guo et al. showed that CFTR activity plays a crucial role in the insulin secretion of the pancreatic beta cells (Guo et al., 2014), whereas diabetes is a well-known complication of alcoholism (Shield et al., 2013). The decreased CFTR activity induced by alcohol consumption might play an import role in the disease development.

Association between CFTR gene mutations and the risk for the development of acute recurrent (Cavestro et al., 2010) or chronic pancreatitis (Weiss et al., 2005) provides strong evidence that mutations in CFTR and/or insufficiency of electrolyte and fluid secretion by pancreatic ductal cells lead to increased risk for pancreatitis (Hegyi and Rakonczay, 2010). Heterozygous carriers of *CFTR* mutations are at an increased risk of chronic pancreatitis (Sharer et al., 1998), moreover Ooi et al. demonstrated that the risk of developing pancreatitis was much higher in CF patients, who had milder CFTR mutations (type IV and V) and were pancreatic sufficient compared to those who had severe mutations and were pancreatic insufficient (Ooi et al., 2011). In the pathogenetic model proposed in this study, the risk of developing pancreatitis inversely correlates with CFTR function. However, in other studies the association between *CFTR* gene mutation and alcoholic pancreatitis was inconsistent (Maruyama et al., 2010, Pezzilli et al., 2003). Very recently LaRusch et al. elegantly demonstrated that *CFTR* gene mutations that don't cause typical cystic fibrosis, but disrupt the WNK1-SPAK-mediated HCO_3^- permeability of the channel, are associated with pancreatic disorders (LaRusch et al., 2014). In animal model of pancreatitis Dimagno earlier showed that CFTR KO mice developed more severe acute pancreatitis after cerulein hyperstimulation than WT mice (Dimagno et al., 2005) and recently Pallagi et al. had the same observation in mice with genetic deletion of Na^+/H^+ exchanger regulatory factor (NHERF1), which regulates CFTR expression (Pallagi et al., 2014). In our study we have demonstrated using CFTR KO mice that genetic deletion of CFTR leads to more severe pancreatitis after ethanol and fatty acid administration, confirming the crucial role of pancreatic ductal secretion in the pathogenesis of alcohol-induced pancreatitis.

Taken together, our observations provide evidence that ethanol and non-oxidative ethanol metabolites inhibit the pancreatic fluid and HCO_3^- secretion and CFTR Cl^- channel activity and expression via sustained $[Ca^{2+}]_i$ elevation and $(ATP)_i$ depletion. These changes can contribute to the development and progression of the acute alcohol-induced pancreatitis.

5.2. The effects of high concentration of chenodeoxycholate on the pancreatic fluid and HCO_3^- secretion

Besides heavy ethanol consumption bile acids are the other most common etiological factors of pancreatitis. Small bile stones can enter the common bile duct and get stuck at the papilla of Vater, blocking both the outflow of bile and pancreatic juice. Although the exact pathogenesis of biliary pancreatitis is still a matter of debate (Lerch and Aghdassi, 2010), according to the common channel theory bile acids can reach the pancreatic tissue via the pancreatic ductal tree. During biliary reflux the PDEC are the first cell type reached by bile acids, but the earlier studies focused mainly on acinar cells. Taurolithocholic acid 3-sulphate (TLC-S) was shown to induce Ca^{2+} release from the ER and from acidic Ca^{2+} stores in pancreatic acinar cells via IP_3R and RyR activation (Gerasimenko et al., 2006a). In addition, bile acids were shown to inhibit SERCA pump activity (Kim et al., 2002). The depletion of intracellular Ca^{2+} stores activates Ca^{2+} influx from the extracellular space into the cytosol via store-operated Ca^{2+} entry channels (Lur et al., 2009) thereby further contributing to the sustained $[Ca^{2+}]_i$ elevation. Voronina *et al*. showed that TLC-S decreases the $(ATP)_i$ and induced a loss of $(\Delta\Psi)_m$ in pancreatic acinar cells, which was not influenced by BAPTA-AM pretreatment (Voronina et al., 2004, Voronina et al., 2010).

In PDEC the non-conjugated bile acid CDC induced toxic sustained Ca^{2+} signalling and inhibited acid/base transporters including the basolateral NHE, NBCe1-B and the luminal CBE (Venglovecz et al., 2008). In these series of experiments, BAPTA-AM did not prevent the inhibitory effect of CDC on HCO_3^- secretion, suggesting the presence of a Ca^{2+} independent inhibitory mechanism. These experimental data were confirmed in a recent clinical study, where we showed that the intraluminal pH was significantly lower in patients with acute biliary pancreatitis compared to the control group (6.97 ± 0.13 vs. 7.79 ± 0.20) (Takacs et al., 2013). In our current study we provided evidence, that high

concentration of CDC induced severe morphological damage of the mitochondria (mitochondrial swelling and disruption of the inner mitochondrial membrane) and consequent $(ATP)_i$ depletion. Notably, the preincubation of the pancreatic ducts with BAPTA-AM failed to prevent the mitochondrial damage induced by CDC, suggesting a Ca^{2+}-independent mechanism underlying the observed mitochondrial damage in response to CDC in guinea pig PDE. Similar mitochondrial damage was observed in bile epithelial cells upon the administration of non-conjugated bile salts (Benedetti et al., 1997). We also showed that the $(ATP)_i$ depletion directly inhibited pancreatic ductal HCO_3^- secretion. In the mechanism of pancreatic ductal HCO_3^- secretion there are several ATP dependent processes. During the activation of CFTR two Mg-ATP molecules bind on the inter-NBD interface of the NBD domains, leading to the channel gating (Anderson et al., 1991, Hunt et al., 2013). On the other hand, evidence suggests that ATP may directly activate NHE1 as well and the depletion of $(ATP)_i$ inhibited NHEs in different cell types (Dhar-Chowdhury et al., 2007). Importantly, bile acids have been shown to inhibit the function of the acid/base transporters via cellular energy breakdown and Ca^{2+} overload in human colonic epithelial cells, which can reduce fluid and electrolyte absorption in the colon and promote the development of diarrhoea (Pallagi-Kunstar et al., 2014). The mitochondrial damage described in this study was found in *in vivo* models of acute pancreatitis as well (Biczo et al., 2011). In this study L-lysine induced acute pancreatitis and mitochondrial damage in rats, which preceded the activation of trypsinogen or NF-κB activation. In another study Halangk *et al*. showed that, during cerulein-induced acute pancreatitis the mitochondrial oxidative phosphorylation and ATP production are drastically decreased (Halangk et al., 1998). Moreover, they also showed that the opening of the mitochondrial permeability transition pore (MPTP) plays a crucial role in this model of acute pancreatitis (Schild et al., 1999).

Taken together, we provided evidence that the energetic break down, induced by high concentration of the non-conjugated CDC plays a central role in the inhibition of the pancreatic HCO_3^- secretion, therefore the development of pancreatitis. Therefore we suggest that the prevention of the mitochondrial damage during acute pancreatitis should have therapeutic benefits (Maleth et al., 2013).

6. SUMMARY

Background: Alcohol-induced and biliary pancreatitis are the two most common forms of acute pancreatitis. Notably, there is no specific treatment against this inflammatory disease suggesting the lack of knowledge of pathophysiological mechanisms involved in the initiation and progression of the diseases. Although recent evidence suggest that pancreatic ductal epithelial cells (PDEC) play important role in the pathogenesis of pancreatitis the effects of ethanol, fatty acids and their metabolites on PDEC has not been investigated yet. On the other hand bile acid in millimolar concentration has been shown to inhibit the pancreatic ductal HCO_3^- secretion, however the exact mechanism of inhibition remained elusive.

The **aim** of this study was to characterize the effects of ethanol and ethanol metabolites on the pancreatic ductal epithelial HCO_3^- secretion and to dissect the inhibitory effect of non-conjugated bile acids on the pancreatic HCO_3^- secretion.

Methods: We studied the effects of ethanol, fatty acids, and fatty acid ethyl esters on secretion of pancreatic fluid and HCO_3^-, levels and function of CFTR, and exchange of Cl^- for HCO_3^-, in pancreatic cell lines, as well as in tissues from guinea pigs and CFTR-knockout mice following administration of alcohol and fatty acids. We detected the changes of intracellular Ca^{2+} concentration ($[Ca^{2+}]_i$), ATP level ($(ATP)_i$), and mitochondrial membrane potential ($(\Delta\Psi)_m$) upon the administration of ethanol, ethanol metabolites, or chendoxycholate using fluorescent indicators. The mitochondrial morphology was assessed by electron microscopy.

Results: Low concentration of ethanol stimulated the pancreatic HCO_3^- secretion via IP_3 mediated Ca^{2+} release from the endoplasmic reticulum (ER). High concentration of ethanol and fatty acids inhibited secretion of fluid and HCO_3^-, as well as CFTR activity, in pancreatic ductal epithelial cells. These effects were mediated by sustained increases in $[Ca^{2+}]_i$, depletion of $(ATP)_i$, and depolarization of mitochondrial membranes. Moreover in pancreatic cell line and guinea pig pancreatic tissue administration of ethanol, or non-oxidative ethanol metabolites reduced the expression of CFTR. Similarly, high concentration of the non-conjugated bile acid chenodeoxycholate disrupted the mitochondrial structure and consequently depleted $(ATP)_i$ in guinea pig pancreatic ductal cells. The $(ATP)_i$ depletion induced by the inhibition of the cellular ATP production significantly impaired the HCO_3^- secretion.

Conclusions: In this present work we have demonstrated that ethanol, as well as its non-oxidative metabolites cause impairment of pancreatic ductal fluid and HCO_3^- secretion via toxic cellular Ca^{2+} signaling and break down of the mitochondrial ATP production. Very similar mitochondrial damage was found in these cells upon the administration of non-conjugated bile acid. These results highlight the central role of mitochondrial damage in the pathogenesis of acute pancreatitis.

7. ACKNOWLEDGEMENTS

I would like to thank all of the people who have helped and inspired me during my doctoral studies.

I am grateful to **Prof. Dr. György Ábrahám** and **Prof. Dr. Tibor Wittmann**, the current and former head of the First Department of Medicine and to **Prof. Dr. András Varró**, the head of Department of Pharmacology and Pharmacotherapy, who gave me opportunity to work their Departments.

I would like express my deep and sincere gratitude to my supervisors **Prof. Dr. Péter Hegyi** and **Dr. Zoltán Rakonczay Jr**. for their support, guidance and friendship. Their wide knowledge and logical way of thinking have been of great value for me. Without their outstanding supervision, this Ph.D project would not have been possible. In addition, a very special thank goes to **Dr. Viktória Venglovecz** for her help, support, advice and enthusiasm.

I would also like to thank my colleagues and friends, **Dr. Petra Pallagi, Dr. Anita Balázs, Tamara Madácsy, Zsolt Balla, Éva Kunstár, Dr. Andrea Geisz, Dr. Andrea Schnúr, Dr. Balázs Kui, Dr. Dorottya Laczkó, Dr. Eszter Kormányos, Máté Katona, Dr. Eszter Végh** for all the help, entertainment and care they provided.

This work would not have been possible to accomplish without the assistance and work of **Edit Magyarné Pálfi, Tünde Pritz, Zsoltné Árva, Miklósné Árva, Zoltánné Fuksz and Etus Enyinginé**.

I am deeply grateful to **István Németh** (Department of Dermatology and Allergology; University of Szeged) **Gergely L. Lukacs** (McGill University, Canada), **Markus M. Lerch** (University Medicine Greifswald, Germany) and their research teams for the outstanding collaborations.

Our research was supported by the Hungarian National Development Agency grants (TÁMOP-4.2.2.A-11/1/KONV-2012-0035, TÁMOP-4.2.2-A-11/1/KONV-2012-0052; TÁMOP-4.2.2.A-11/1/KONV-2012-0073; TÁMOP-4.2.4.A/2-11-1-2012-0001; TÁMOP-4.2.4.A2-SZJÖ-TOK-13-0017), MTA-SZTE Momentum Grant (LP2014-10/2014) and the Hungarian Scientific Research Fund (K109756, NF105785, NF100677).

Lastly, I owe warm thanks to **my family** for all their love, support, never-ending patience, encouragement and for always being there. I dedicate this thesis to them.

8. REFERENCES

Ahuja, M., Jha, A., Maleth, J., Park, S. & Muallem, S. 2014. cAMP and Ca(2)(+) signaling in secretory epithelia: crosstalk and synergism. *Cell Calcium,* **55,** 385-93.

Anderson, M. P., Berger, H. A., Rich, D. P., Gregory, R. J., Smith, A. E. & Welsh, M. J. 1991. Nucleoside triphosphates are required to open the CFTR chloride channel. *Cell,* **67,** 775-84.

Argent, B. E., Arkle, S., Cullen, M. J. & Green, R. 1986. Morphological, biochemical and secretory studies on rat pancreatic ducts maintained in tissue culture. *Q J Exp Physiol,* **71,** 633-48.

Argent, B. E., GrayM.A., Steward M.C.and Case R.M. 2012. *Cell Physiology of Pancreatic Ducts,* Oxford, Elsevier.

Barry E. Argent, M. A. G., Martin C. Steward, R. Maynard Case 2012. Cell Physiology of Pancreatic Ducts. In: JOHNSON, L. L. (Ed.) *Physiology of the Gastronintestinal Tract.* Oxford, Academic Press.

Baumgartner, H. K., Gerasimenko, J. V., Thorne, C., Ferdek, P., Pozzan, T., Tepikin, A. V., Petersen, O. H., Sutton, R., Watson, A. J. & Gerasimenko, O. V. 2009. Calcium elevation in mitochondria is the main Ca2+ requirement for mitochondrial permeability transition pore (mPTP) opening. *Journal of Biological Chemistry,* **284,** 20796-803.

Behrendorff, N., Floetenmeyer, M., Schwiening, C. & Thorn, P. 2010. Protons released during pancreatic acinar cell secretion acidify the lumen and contribute to pancreatitis in mice. *Gastroenterology,* **139,** 1711-20, 1720 e1-5.

Benedetti, A., Alvaro, D., Bassotti, C., Gigliozzi, A., Ferretti, G., La Rosa, T., Di Sario, A., Baiocchi, L. & Jezequel, A. M. 1997. Cytotoxicity of bile salts against biliary epithelium: a study in isolated bile ductule fragments and isolated perfused rat liver. *Hepatology,* **26,** 9-21.

Bhoomagoud, M., Jung, T., Atladottir, J., Kolodecik, T. R., Shugrue, C., Chaudhuri, A., Thrower, E. C. & Gorelick, F. S. 2009. Reducing extracellular pH sensitizes the acinar cell to secretagogue-induced pancreatitis responses in rats. *Gastroenterology,* **137,** 1083-92.

Biczo, G., Hegyi, P., Dosa, S., Shalbuyeva, N., Berczi, S., Sinervirta, R., Hracsko, Z., Siska, A., Kukor, Z., Jarmay, K., Venglovecz, V., Varga, I. S., Ivanyi, B., Alhonen, L., Wittmann, T., Gukovskaya, A., *et al.* 2011. The crucial role of early mitochondrial injury in L-lysine-induced acute pancreatitis. *Antioxid Redox Signal,* **15,** 2669-81.

Bolender, R. P. 1974. Stereological analysis of the guinea pig pancreas. I. Analytical model and quantitative description of nonstimulated pancreatic exocrine cells. *J Cell Biol,* **61,** 269-87.

Cavestro, G. M., Zuppardo, R. A., Bertolini, S., Sereni, G., Frulloni, L., Okolicsanyi, S., Calzolari, C., Singh, S. K., Sianesi, M., Del Rio, P., Leandro, G., Franze, A. & Di Mario, F. 2010. Connections between genetics and clinical data: Role of MCP-1, CFTR, and SPINK-1 in the setting of acute, acute recurrent, and chronic pancreatitis. *Am J Gastroenterol,* **105,** 199-206.

Cendrowski, J., Sanchez-Arevalo Lobo, V. J., Sendler, M., Salas, A., Kuhn, J. P., Molero, X., Fukunaga, R., Mayerle, J., Lerch, M. M. & Real, F. X. 2014. Mnk1 is a novel acinar cell-specific kinase required for exocrine pancreatic secretion and response to pancreatitis in mice. *Gut*.

Chappe, V., Irvine, T., Liao, J., Evagelidis, A. & Hanrahan, J. W. 2005. Phosphorylation of CFTR by PKA promotes binding of the regulatory domain. *EMBO J,* **24,** 2730-40.

Choi, J. Y., Muallem, D., Kiselyov, K., Lee, M. G., Thomas, P. J. & Muallem, S. 2001. Aberrant CFTR-dependent HCO3- transport in mutations associated with cystic fibrosis. *Nature,* **410,** 94-7.

Criddle, D. N., McLaughlin, E., Murphy, J. A., Petersen, O. H. & Sutton, R. 2007. The pancreas misled: signals to pancreatitis. *Pancreatology,* **7,** 436-46.

Criddle, D. N., Murphy, J., Fistetto, G., Barrow, S., Tepikin, A. V., Neoptolemos, J. P., Sutton, R. & Petersen, O. H. 2006. Fatty acid ethyl esters cause pancreatic calcium toxicity via inositol trisphosphate receptors and loss of ATP synthesis. *Gastroenterology,* **130,** 781-93.

Criddle, D. N., Raraty, M. G., Neoptolemos, J. P., Tepikin, A. V., Petersen, O. H. & Sutton, R. 2004. Ethanol toxicity in pancreatic acinar cells: mediation by nonoxidative fatty acid metabolites. *Proc Natl Acad Sci U S A,* **101,** 10738-43.

Dhar-Chowdhury, P., Malester, B., Rajacic, P. & Coetzee, W. A. 2007. The regulation of ion channels and transporters by glycolytically derived ATP. *Cell Mol Life Sci,* **64,** 3069-83.

Dimagno, M. J., Lee, S. H., Hao, Y., Zhou, S. Y., McKenna, B. J. & Owyang, C. 2005. A proinflammatory, antiapoptotic phenotype underlies the susceptibility to acute pancreatitis in cystic fibrosis transmembrane regulator (-/-) mice. *Gastroenterology,* **129,** 665-81.

Doyle, K. M., Cluette-Brown, J. E., Dube, D. M., Bernhardt, T. G., Morse, C. R. & Laposata, M. 1996. Fatty acid ethyl esters in the blood as markers for ethanol intake. *JAMA,* **276,** 1152-6.

Dyck, W. P., Hightower, N. C. & Janowitz, H. D. 1972. Effect of acetazolamide on human pancreatic secretion. *Gastroenterology,* **62,** 547-52.

Fernandez-Salazar, M. P., Pascua, P., Calvo, J. J., Lopez, M. A., Case, R. M., Steward, M. C. & San Roman, J. I. 2004. Basolateral anion transport mechanisms underlying fluid secretion by mouse, rat and guinea-pig pancreatic ducts. *J Physiol,* **556,** 415-28.

Freedman, S. D., Kern, H. F. & Scheele, G. A. 2001. Pancreatic acinar cell dysfunction in CFTR(-/-) mice is associated with impairments in luminal pH and endocytosis. *Gastroenterology,* **121,** 950-7.

Frick, T. W., Fernandez-del Castillo, C., Bimmler, D. & Warshaw, A. L. 1997. Elevated calcium and activation of trypsinogen in rat pancreatic acini. *Gut,* **41,** 339-43.

Gerasimenko, J. V., Flowerdew, S. E., Voronina, S. G., Sukhomlin, T. K., Tepikin, A. V., Petersen, O. H. & Gerasimenko, O. V. 2006a. Bile acids induce Ca2+ release from both the endoplasmic reticulum and acidic intracellular calcium stores through activation of inositol trisphosphate receptors and ryanodine receptors. *Journal of Biological Chemistry,* **281,** 40154-63.

Gerasimenko, J. V., Flowerdew, S. E., Voronina, S. G., Sukhomlin, T. K., Tepikin, A. V., Petersen, O. H. & Gerasimenko, O. V. 2006b. Bile acids induce Ca2+ release from both the endoplasmic reticulum and acidic intracellular calcium stores through activation of inositol trisphosphate receptors and ryanodine receptors. *J Biol Chem,* **281,** 40154-63.

Gerasimenko, J. V., Sherwood, M., Tepikin, A. V., Petersen, O. H. & Gerasimenko, O. V. 2006c. NAADP, cADPR and IP3 all release Ca2+ from the endoplasmic reticulum and an acidic store in the secretory granule area. *J Cell Sci,* **119,** 226-38.

Gukovskaya, A. S., Mouria, M., Gukovsky, I., Reyes, C. N., Kasho, V. N., Faller, L. D. & Pandol, S. J. 2002. Ethanol metabolism and transcription factor activation in pancreatic acinar cells in rats. *Gastroenterology,* **122,** 106-18.

Guo, J. H., Chen, H., Ruan, Y. C., Zhang, X. L., Zhang, X. H., Fok, K. L., Tsang, L. L., Yu, M. K., Huang, W. Q., Sun, X., Chung, Y. W., Jiang, X., Sohma, Y. & Chan, H. C. 2014. Glucose-induced electrical activities and insulin secretion in pancreatic islet beta-cells are modulated by CFTR. *Nat Commun,* **5,** 4420.

Halangk, W., Matthias, R., Schild, L., Meyer, F., Schulz, H. U. & Lippert, H. 1998. Effect of supramaximal cerulein stimulation on mitochondrial energy metabolism in rat pancreas. *Pancreas,* **16,** 88-95.

Hegyi, P., Gray, M. A. & Argent, B. E. 2003. Substance P inhibits bicarbonate secretion from guinea pig pancreatic ducts by modulating an anion exchanger. *Am J Physiol Cell Physiol,* **285,** C268-76.

Hegyi, P., Maleth, J., Venglovecz, V. & Rakonczay, Z., Jr. 2011. Pancreatic ductal bicarbonate secretion: challenge of the acinar Acid load. *Front Physiol,* **2,** 36.

Hegyi, P., Ordog, B., Rakonczai, Z., Jr., Takacs, T., Lonovics, J., Szabolcs, A., Sari, R., Toth, A., Papp, J. G., Varro, A., Kovacs, M. K., Gray, M. A., Argent, B. E. & Boldogkoi, Z. 2005. Effect of herpesvirus infection on pancreatic duct cell secretion. *World J Gastroenterol,* **11,** 5997-6002.

Hegyi, P. & Petersen, O. H. 2013. The exocrine pancreas: the acinar-ductal tango in physiology and pathophysiology. *Rev Physiol Biochem Pharmacol,* **165,** 1-30.

Hegyi, P. & Rakonczay, Z. 2010. Insufficiency of electrolyte and fluid secretion by pancreatic ductal cells leads to increased patient risk for pancreatitis. *Am J Gastroenterol,* **105,** 2119-20.

Hegyi, P., Rakonczay, Z., Jr., Gray, M. A. & Argent, B. E. 2004. Measurement of intracellular pH in pancreatic duct cells: a new method for calibrating the fluorescence data. *Pancreas,* **28,** 427-34.

Huang, W., Booth, D. M., Cane, M. C., Chvanov, M., Javed, M. A., Elliott, V. L., Armstrong, J. A., Dingsdale, H., Cash, N., Li, Y., Greenhalf, W., Mukherjee, R., Kaphalia, B. S., Jaffar, M., Petersen, O. H., Tepikin, A. V., *et al.* 2014. Fatty acid ethyl ester synthase inhibition ameliorates ethanol-induced Ca2+-dependent mitochondrial dysfunction and acute pancreatitis. *Gut,* **63,** 1313-24.

Hunt, J. F., Wang, C. & Ford, R. C. 2013. Cystic fibrosis transmembrane conductance regulator (ABCC7) structure. *Cold Spring Harb Perspect Med,* **3,** a009514.

Ishiguro, H., Steward, M. C., Lindsay, A. R. & Case, R. M. 1996. Accumulation of intracellular HCO3- by Na(+)-HCO3- cotransport in interlobular ducts from guinea-pig pancreas. *J Physiol,* **495 (Pt 1),** 169-78.

Judak, L., Hegyi, P., Rakonczay, Z., Jr., Maleth, J., Gray, M. A. & Venglovecz, V. 2014. Ethanol and its non-oxidative metabolites profoundly inhibit CFTR function in pancreatic epithelial cells which is prevented by ATP supplementation. *Pflugers Arch,* **466,** 549-62.

Kim, J. Y., Kim, K. H., Lee, J. A., Namkung, W., Sun, A. Q., Ananthanarayanan, M., Suchy, F. J., Shin, D. M., Muallem, S. & Lee, M. G. 2002. Transporter-mediated bile acid uptake causes Ca2+-dependent cell death in rat pancreatic acinar cells. *Gastroenterology,* **122,** 1941-53.

Ko, S. B., Mizuno, N., Yatabe, Y., Yoshikawa, T., Ishiguro, H., Yamamoto, A., Azuma, S., Naruse, S., Yamao, K., Muallem, S. & Goto, H. 2010. Corticosteroids correct aberrant CFTR localization in the duct and regenerate acinar cells in autoimmune pancreatitis. *Gastroenterology,* **138,** 1988-96.

Ko, S. B., Zeng, W., Dorwart, M. R., Luo, X., Kim, K. H., Millen, L., Goto, H., Naruse, S., Soyombo, A., Thomas, P. J. & Muallem, S. 2004. Gating of CFTR by the STAS domain of SLC26 transporters. *Nat Cell Biol,* **6,** 343-50.

Kouzoukas, D. E., Li, G., Takapoo, M., Moninger, T., Bhalla, R. C. & Pantazis, N. J. 2013. Intracellular calcium plays a critical role in the alcohol-mediated death of cerebellar granule neurons. *J Neurochem,* **124,** 323-35.

Kreda, S. M., Mall, M., Mengos, A., Rochelle, L., Yankaskas, J., Riordan, J. R. & Boucher, R. C. 2005. Characterization of wild-type and deltaF508 cystic fibrosis transmembrane regulator in human respiratory epithelia. *Mol Biol Cell,* **16,** 2154-67.

Kroemer, G. & Reed, J. C. 2000. Mitochondrial control of cell death. *Nat Med,* **6,** 513-9.

Kruger, B., Albrecht, E. & Lerch, M. M. 2000. The role of intracellular calcium signaling in premature protease activation and the onset of pancreatitis. *Am J Pathol,* **157,** 43-50.

Laposata, E. A. & Lange, L. G. 1986. Presence of nonoxidative ethanol metabolism in human organs commonly damaged by ethanol abuse. *Science,* **231,** 497-9.

LaRusch, J., Jung, J., General, I. J., Lewis, M. D., Park, H. W., Brand, R. E., Gelrud, A., Anderson, M. A., Banks, P. A., Conwell, D., Lawrence, C., Romagnuolo, J., Baillie, J., Alkaade, S., Cote, G., Gardner, T. B., *et al.* 2014. Mechanisms of CFTR functional variants that impair regulated bicarbonate permeation and increase risk for pancreatitis but not for cystic fibrosis. *PLoS Genet,* **10,** e1004376.

Lee, M. G., Ohana, E., Park, H. W., Yang, D. & Muallem, S. 2012. Molecular mechanism of pancreatic and salivary gland fluid and HCO3 secretion. *Physiol Rev,* **92,** 39-74.

Lerch, M. M. & Aghdassi, A. A. 2010. The role of bile acids in gallstone-induced pancreatitis. *Gastroenterology,* **138,** 429-33.

Lukacs, G. L., Mohamed, A., Kartner, N., Chang, X. B., Riordan, J. R. & Grinstein, S. 1994. Conformational maturation of CFTR but not its mutant counterpart (delta F508) occurs in the endoplasmic reticulum and requires ATP. *EMBO J,* **13,** 6076-86.

Lur, G., Haynes, L. P., Prior, I. A., Gerasimenko, O. V., Feske, S., Petersen, O. H., Burgoyne, R. D. & Tepikin, A. V. 2009. Ribosome-free terminals of rough ER allow formation of STIM1 puncta and segregation of STIM1 from IP(3) receptors. *Curr Biol,* **19,** 1648-53.

Maleth, J. & Hegyi, P. 2014. Calcium signaling in pancreatic ductal epithelial cells: an old friend and a nasty enemy. *Cell Calcium,* **55,** 337-45.

Maleth, J., Rakonczay, Z., Jr., Venglovecz, V., Dolman, N. J. & Hegyi, P. 2013. Central role of mitochondrial injury in the pathogenesis of acute pancreatitis. *Acta Physiol (Oxf),* **207,** 226-35.

Maruyama, K., Harada, S., Yokoyama, A., Mizukami, S., Naruse, S., Hirota, M., Nishimori, I. & Otsuki, M. 2010. Association analyses of genetic polymorphisms of GSTM1, GSTT1, NQO1, NAT2, LPL, PRSS1, PSTI, and CFTR with chronic alcoholic pancreatitis in Japan. *Alcohol Clin Exp Res,* **34 Suppl 1,** S34-8.

Mensel, B., Messner, P., Mayerle, J., Fluhr, G., Volzke, H., Lerch, M. M., Ittermann, T. & Kuhn, J. P. 2014. Secretin-stimulated MRCP in volunteers: assessment of safety, duct visualization, and pancreatic exocrine function. *AJR Am J Roentgenol,* **202,** 102-8.

Nakayama, N., Eichhorst, S. T., Muller, M. & Krammer, P. H. 2001. Ethanol-induced apoptosis in hepatoma cells proceeds via intracellular Ca(2+) elevation, activation of TLCK-sensitive proteases, and cytochrome c release. *Exp Cell Res,* **269,** 202-13.

Ooi, C. Y., Dorfman, R., Cipolli, M., Gonska, T., Castellani, C., Keenan, K., Freedman, S. D., Zielenski, J., Berthiaume, Y., Corey, M., Schibli, S., Tullis, E. & Durie, P. R. 2011. Type of CFTR mutation determines risk of pancreatitis in patients with cystic fibrosis. *Gastroenterology,* **140,** 153-61.

Pallagi-Kunstar, E., Farkas, K., Maleth, J., Rakonczay, Z., Jr., Nagy, F., Molnar, T., Szepes, Z., Venglovecz, V., Lonovics, J., Razga, Z., Wittmann, T. & Hegyi, P. 2014. Bile acids inhibit Na/H exchanger and Cl /HCO exchanger activities via cellular energy breakdown and Ca overload in human colonic crypts. *Pflugers Arch*.

Pallagi, P., Balla, Z., Singh, A. K., Dosa, S., Ivanyi, B., Kukor, Z., Toth, A., Riederer, B., Liu, Y., Engelhardt, R., Jarmay, K., Szabo, A., Janovszky, A., Perides, G., Venglovecz, V., Maleth, J., *et al.* 2014. The role of pancreatic ductal secretion in protection against acute pancreatitis in mice*. *Crit Care Med,* **42,** e177-88.

Pallagi, P., Venglovecz, V., Rakonczay, Z., Jr., Borka, K., Korompay, A., Ozsvari, B., Judak, L., Sahin-Toth, M., Geisz, A., Schnur, A., Maleth, J., Takacs, T., Gray, M. A., Argent, B. E., Mayerle, J., Lerch, M. M., *et al.* 2011. Trypsin reduces pancreatic ductal bicarbonate secretion by inhibiting CFTR Cl(-) channels and luminal anion exchangers. *Gastroenterology,* **141,** 2228-2239 e6.

Park, H. W., Nam, J. H., Kim, J. Y., Namkung, W., Yoon, J. S., Lee, J. S., Kim, K. S., Venglovecz, V., Gray, M. A., Kim, K. H. & Lee, M. G. 2010. Dynamic regulation of CFTR bicarbonate permeability by [Cl-]i and its role in pancreatic bicarbonate secretion. *Gastroenterology,* **139,** 620-31.

Park, S., Hong, J. H., Ohana, E. & Muallem, S. 2012. The WNK/SPAK and IRBIT/PP1 pathways in epithelial fluid and electrolyte transport. *Physiology (Bethesda),* **27,** 291-9.

Park, S., Shcheynikov, N., Hong, J. H., Zheng, C., Suh, S. H., Kawaai, K., Ando, H., Mizutani, A., Abe, T., Kiyonari, H., Seki, G., Yule, D., Mikoshiba, K. & Muallem, S. 2013. Irbit mediates synergy between ca(2+) and cAMP signaling pathways during epithelial transport in mice. *Gastroenterology,* **145,** 232-41.

Peters, K. W., Okiyoneda, T., Balch, W. E., Braakman, I., Brodsky, J. L., Guggino, W. B., Penland, C. M., Pollard, H. B., Sorscher, E. J., Skach, W. R., Thomas, P. J., Lukacs, G. L. & Frizzell, R. A. 2011. CFTR Folding Consortium: methods available for studies of CFTR folding and correction. *Methods Mol Biol,* **742,** 335-53.

Pezzilli, R., Morselli-Labate, A. M., Mantovani, V., Romboli, E., Selva, P., Migliori, M., Corinaldesi, R. & Gullo, L. 2003. Mutations of the CFTR gene in pancreatic disease. *Pancreas,* **27,** 332-6.

Ratcliff, R., Evans, M. J., Cuthbert, A. W., MacVinish, L. J., Foster, D., Anderson, J. R. & Colledge, W. H. 1993. Production of a severe cystic fibrosis mutation in mice by gene targeting. *Nat Genet,* **4,** 35-41.

Sadr-Azodi, O., Andren-Sandberg, A., Orsini, N. & Wolk, A. 2012. Cigarette smoking, smoking cessation and acute pancreatitis: a prospective population-based study. *Gut,* **61,** 262-7.

Schild, L., Matthias, R., Stanarius, A., Wolf, G., Augustin, W. & Halangk, W. 1999. Induction of permeability transition in pancreatic mitochondria by cerulein in rats. *Mol Cell Biochem,* **195,** 191-7.

Shalbueva, N., Mareninova, O. A., Gerloff, A., Yuan, J., Waldron, R. T., Pandol, S. J. & Gukovskaya, A. S. 2013. Effects of oxidative alcohol metabolism on the mitochondrial permeability transition pore and necrosis in a mouse model of alcoholic pancreatitis. *Gastroenterology,* **144,** 437-446 e6.

Sharer, N., Schwarz, M., Malone, G., Howarth, A., Painter, J., Super, M. & Braganza, J. 1998. Mutations of the cystic fibrosis gene in patients with chronic pancreatitis. *N Engl J Med,* **339,** 645-52.

Shcheynikov, N., Wang, Y., Park, M., Ko, S. B., Dorwart, M., Naruse, S., Thomas, P. J. & Muallem, S. 2006. Coupling modes and stoichiometry of Cl-/HCO3- exchange by slc26a3 and slc26a6. *J Gen Physiol,* **127,** 511-24.

Shield, K. D., Parry, C. & Rehm, J. 2013. Chronic diseases and conditions related to alcohol use. *Alcohol Res,* **35,** 155-73.

Shimada-Shimizu, N., Hisamitsu, T., Nakamura, T. Y. & Wakabayashi, S. 2013. Evidence that Na+/H+ exchanger 1 is an ATP-binding protein. *FEBS J,* **280,** 1430-42.

Stewart, A. K., Yamamoto, A., Nakakuki, M., Kondo, T., Alper, S. L. & Ishiguro, H. 2009. Functional coupling of apical Cl-/HCO3- exchange with CFTR in stimulated HCO3- secretion by guinea pig interlobular pancreatic duct. *Am J Physiol Gastrointest Liver Physiol,* **296,** G1307-17.

Takacs, T., Rosztoczy, A., Maleth, J., Rakonczay, Z., Jr. & Hegyi, P. 2013. Intraductal acidosis in acute biliary pancreatitis. *Pancreatology,* **13,** 333-5.

Tolstrup, J. S., Kristiansen, L., Becker, U. & Gronbaek, M. 2009. Smoking and risk of acute and chronic pancreatitis among women and men: a population-based cohort study. *Arch Intern Med,* **169,** 603-9.

Veel, T., Villanger, O., Holthe, M. R., Cragoe, E. J., Jr. & Raeder, M. G. 1992. Na(+)-H+ exchange is not important for pancreatic HCO3- secretion in the pig. *Acta Physiol Scand,* **144,** 239-46.

Venglovecz, V., Hegyi, P., Rakonczay, Z., Jr., Tiszlavicz, L., Nardi, A., Grunnet, M. & Gray, M. A. 2011. Pathophysiological relevance of apical large-conductance Ca(2)+-activated potassium channels in pancreatic duct epithelial cells. *Gut,* **60,** 361-9.

Venglovecz, V., Rakonczay, Z., Jr., Ozsvari, B., Takacs, T., Lonovics, J., Varro, A., Gray, M. A., Argent, B. E. & Hegyi, P. 2008. Effects of bile acids on pancreatic ductal bicarbonate secretion in guinea pig. *Gut,* **57,** 1102-12.

Voronina, S. G., Barrow, S. L., Gerasimenko, O. V., Petersen, O. H. & Tepikin, A. V. 2004. Effects of secretagogues and bile acids on mitochondrial membrane potential of pancreatic acinar cells: comparison of different modes of evaluating DeltaPsim. *Journal of Biological Chemistry,* **279,** 27327-38.

Voronina, S. G., Barrow, S. L., Simpson, A. W., Gerasimenko, O. V., da Silva Xavier, G., Rutter, G. A., Petersen, O. H. & Tepikin, A. V. 2010. Dynamic changes in cytosolic and mitochondrial ATP levels in pancreatic acinar cells. *Gastroenterology,* **138,** 1976-87.

Walsh, C., Barrow, S., Voronina, S., Chvanov, M., Petersen, O. H. & Tepikin, A. 2009. Modulation of calcium signalling by mitochondria. *Biochim Biophys Acta,* **1787,** 1374-82.

Weiss, F. U., Simon, P., Bogdanova, N., Mayerle, J., Dworniczak, B., Horst, J. & Lerch, M. M. 2005. Complete cystic fibrosis transmembrane conductance regulator gene sequencing in patients with idiopathic chronic pancreatitis and controls. *Gut,* **54,** 1456-60.

Werner, J., Laposata, M., Fernandez-del Castillo, C., Saghir, M., Iozzo, R. V., Lewandrowski, K. B. & Warshaw, A. L. 1997. Pancreatic injury in rats induced by fatty acid ethyl ester, a nonoxidative metabolite of alcohol. *Gastroenterology,* **113,** 286-94.

Wizemann, V. & Schulz, I. 1973. Influence of amphotericin, amiloride, ionophores, and 2,4-dinitrophenol on the secretion of the isolated cat's pancreas. *Pflugers Arch,* **339,** 317-38.

Xiao, F., Li, J., Singh, A. K., Riederer, B., Wang, J., Sultan, A., Park, H., Lee, M. G., Lamprecht, G., Scholte, B. J., De Jonge, H. R. & Seidler, U. 2012. Rescue of epithelial HCO3- secretion in murine intestine by apical membrane expression of the cystic fibrosis transmembrane conductance regulator mutant F508del. *J Physiol,* **590,** 5317-34.

Yadav, D. & Lowenfels, A. B. 2013. The epidemiology of pancreatitis and pancreatic cancer. *Gastroenterology,* **144,** 1252-61.

Yamamoto, A., Ishiguro, H., Ko, S. B., Suzuki, A., Wang, Y., Hamada, H., Mizuno, N., Kitagawa, M., Hayakawa, T. & Naruse, S. 2003. Ethanol induces fluid hypersecretion from guinea-pig pancreatic duct cells. *J Physiol,* **551,** 917-26.

Yang, D., Li, Q., So, I., Huang, C. L., Ando, H., Mizutani, A., Seki, G., Mikoshiba, K., Thomas, P. J. & Muallem, S. 2011. IRBIT governs epithelial secretion in mice by antagonizing the WNK/SPAK kinase pathway. *J Clin Invest,* **121,** 956-65.

Yang, D., Shcheynikov, N., Zeng, W., Ohana, E., So, I., Ando, H., Mizutani, A., Mikoshiba, K. & Muallem, S. 2009. IRBIT coordinates epithelial fluid and HCO3- secretion by stimulating the transporters pNBC1 and CFTR in the murine pancreatic duct. *J Clin Invest,* **119,** 193-202.

Zeng, W., Lee, M. G., Yan, M., Diaz, J., Benjamin, I., Marino, C. R., Kopito, R., Freedman, S., Cotton, C., Muallem, S. & Thomas, P. 1997. Immuno and functional characterization of CFTR in submandibular and pancreatic acinar and duct cells. *Am J Physiol,* **273,** C442-55.

9. ANNEX

A hasnyálmirigy duktuszok központi szerepe az akut pankreatitisz kialakulásában és progressziójában

Tézis kivonat

BEVEZETÉS

A pankreasz egyik leggyakrabban előforduló megbetegedése az akut pankreatitisz, melynek leggyakoribb oka az epekövesség mellett a nagy mennyiségű alkohol fogyasztás. Gyakorisága ellenére az akut pankreatitisz terápiája többnyire szupportív jellegű, specifikus terápia a legtöbb típus esetében nem áll rendelkezésre.

A pankreasz duktális epitél sejtek bikarbonátban gazdag alkalikus folyadékot termelnek. A szekretált bikarbonát semlegesíti az acinussejtek enzimszekréciója során felszabaduló protonokat, ezáltal fontos szerepet tölt be a hasnyálmirigy fiziológiai működésében. A bikarbonát szekréció döntően a kisméretű intralobuláris duktuszokban valósul meg, során a sejtek bazolaterális memránja felől a HCO_3^- a Na/HCO_3 ko-transzporteren (NBC) és a Na^+/H^+ cserélőn (NHE) keresztül jut a sejtekbe. Ezt követően a HCO_3^- a duktuszok lumenébe a cisztás fibrozis transmembrán konduktancia regulátor-on (CFTR) és a Cl^-/HCO_3^- cserélőn keresztül jut ki.

Munkacsoportunk korábbi kutatásai során vizsgálta az epesavak duktális epitél sejtekre gyakorolt hatását. Azt tapasztaltuk, hogy a luminálisan alkalmazott kis koncentrációjú (0,1mM) nem-konjugált kenodezoxikólsav (CDC) szignifikánsan növelte a duktális sejtek HCO_3^- szekrécióját. Kimutattuk továbbá, hogy mind a nem-konjugált CDC, mind pedig a konjugált glikokenodezoxikólsav (GCDC) dózisfüggő kálcium emelkedést váltanak ki tengerimalac hasnyálmirigy duktális epitél sejtekben (PDEC). A nagy koncentrációjú (1mM) CDC mind a bazolaterális, mind a luminális membrán felől adva gátolta a sav/bázis transzporterek (NHE, NBC és CBE) aktivitását. Arra azonban, hogy a bikarbonát szekréció gátlása milyen módon valósul meg ezidiág nem kaptunk választ.

Az akut pankreatitsz másik igen gyakori oka a nagy mennyiségű alkohol fogyasztás. Az etanol lebontása in vivo kétféle úton történik. Az oxidatív út a májban, a non-oxidatív az extrahepatikus szervekben (a pankreászban) jelentős. Az utóbbi évtizedben végzett kutatások arra utalnak, hogy az akut alkohol indukált pankreatitisz patogenezisében a non-oxidatív etanol metabolitok fontos szerepet játszhatnak. Azonban jelenleg kevés adat

áll rendelkezésünkre az alkohol és a non-oxidatív etanol metabolitok pankreasz duktális szekrécióra gyakorolt hatására vonatkozóan.

CÉLKITŰZÉS

Kísérleteink fő célja a pankreász vezetéksejtek HCO_3^- szekréciójának vizsgálata patofiziológiás körülmények között.

Specifikus céljaink:

- az etanol és etanol metabolitok hatásának vizsgálata a hasnyálmirigy bikarbonát szekréciójára
- a nem-konjugált kenodezoxykólsav a hasnyálmirigy bikarbonát szekrécióra gyakorolt gátló hatásának vizsgálata

ANYAGOK ÉS MÓDSZEREK

Az etanol, a zsírsavak és a zsírsav etil-észterek hatását a hasnyálmirigy folyadék és HCO_3^- szekrécióra, valamint a CFTR klorid csatorna aktivitására és expressziójára hasnyálmirigy duktális epitél sejtvonalon (Capan-1) és rágcsáló modelleken (tengeri malac, CFTR knockout egér) vizsgáltuk. Az intracelluláris Ca^{2+} koncentráció ($[Ca^{2+}]_i$), ATP szint ($(ATP)_i$), és mitokondrium membrán potenciál ($(\Delta\Psi)_m$) változásait etanol, non-oxidatív etanol metabolitok és epesavak hatására fluoreszcens módszerekkel határoztuk meg. A mitokondriális morfológiát elektron mikroszkóp segítségével vizsgáltuk.

EREDMÉNYEK

I. A kis dózisú etanol (10mM) IP_3-mediálta úton Ca^{2+}-t szabadított fel az endolplazmás retikulumból, amely szignifikáns mértékben serkentette a hasnyálmirigy duktális bikarbonát szekréciót Capan-1 sejtekben. A serkentő hatás létrejöttében az apikális membránon elhelyezkedő CBE és CFTR aktivitásának fokozódása is szerepet játszott.

II. Nagy dózisú etanol (100mM) és palmitoleát (POA; 200µM) gátolta a duktális bikarbonát szekréciót és a CFTR klorid csatorna aktivitását Capan-1 sejtekben, illetve izolált tengerimalac duktuszokban.

III. Nagy dózisú etanol és zsírsav gátolta a pankreász duktális folyadékszekréciót *in vivo* vad típusú és CFTR knock out egerekben, illetve *in vitro* izolált tengerimalac duktuszokban.

IV. Az etanol és a palmitoleát gátolta az apikális membránon elhelyezkedő CBE-t és CFTR klorid csatornát.

V. Nagy dózisú etanol és palmitoleát IP_3 és rianodin receptor mediálta úton Ca^{2+}-t szabadított fel az endolplazmás retikulumból és elhúzódó kalcium szignált váltott ki Capan-1 sejtekben.

VI. Nagy dózisú etanol és palmitoleát csökkentette az intracelluláris ATP szintet és a mitokondriális transzmembrán potenciált. A celluláris ATP depléció, amit a mitokondriális és glikolítikus ATP termelés gátlásával idéztünk elő, az etanolhoz és a palmitoleáthoz hasnonló mértékben gátolta a HCO_3^- szekréciót.

VII. Az intracelluláris Ca^{2+} szint emelkedésének megakadályozása BAPTA-AM preinkubációval kivédte az etanol és a palmitoleát gátló hatását, ami azt sugallja, hogy az elhúzódó Ca^{2+} emelkedés kulcsfontosságú a gátló hatás létrejöttében.

VIII. Az alkohol és a non-oxidatív alkohol metabolitok gátolták a CFTR klorid csatorna expresszióját *in vitro* hasnyálmirigy duktális epitél sejtekben és *in vivo* tengerimalac modellben.

IX. A nagy dózisú (1mM) nem-konjugált kenodezoxikólsav jelentős mértékű mitokondrium károsodást idézett elő tengerimalac pankreász duktális epitél sejtekben, illetve humán kolón epitél sejtekben. A mitkondriumok morfológiai károsodása következményes intracelluláris ATP deplécióval is járt, ami szignifikáns mértékben gátolta a duktális epitél sejtek HCO_3^- szekrécióját.

KÖVETKEZTETÉSEK

Jelen tanulmány során sikeresen demonstráltuk, hogy az akut pankreatitisz két fontos etiologiai tényezőjének (a nem-konjugált epesavak, illetve az alkohol és a non-oxidatív metabolitok) hatására $(ATP)_i$ depélció jön létre a hasnyálmirigy duktális epitél sejtekben, a bikarbonát szekréció pedig gátlás alá kerül. Mind az $(ATP)_i$ csökkenés megakadályozása, mind a bikarbonát szekréció helyreállítása (különös tekintettel a CFTR aktivitásának helyreállására) potenciális terápiás kozekvenciával bírhatnak.

Articles closely related to the subject of the thesis and cited in the thesis

I.

---------- Forwarded message ----------
From: **Gastroenterology** <em@editorialmanager.com>
Date: Tue, Nov 4, 2014 at 5:35 PM
Subject: Gastroenterology - GASTRO-D-14-00547R1
To: Péter Hegyi <hegyi.peter@med.u-szeged.hu>

CC: lflecha@gastro.org, knovak@gastro.org

Nov 04 2014 09:23AM

Dear Dr. Hegyi,

We are pleased to inform you that your manuscript, (GASTRO-D-14-00547R1) "Alcohol Disrupts Levels and Function of the Cystic Fibrosis Transmembrane Conductance Regulator to Promote Development of Pancreatitis" has been accepted for publication in Gastroenterology.

Our medical illustration staff may redraw or reformat line art and graphs for publication quality, or contact you if higher quality versions are needed. Please be sure to carefully review your figures when you receive your publication proofs.

We encourage you to submit photos and/or artwork from your accepted article to be considered for our journal cover. In addition, for clinically oriented papers, we're happy to entertain images that are artistic in nature (i.e., not necessarily showing direct data from the article)and that capture the essence of the article and appeal to a broad audience (See our November 2012 cover as an example). All cover submissions must meet specific standards. Refer to our FAQs document, question "Can I submit artwork for consideration for the Gastro or CGH covers?"

Please ensure that if you have co-authors, each of them has verified co-authorship via our manuscript tracking system, Editorial Manager. Each co-author received an email when you originally submitted your manuscript. The email prompted them to verify authorship; please remind them to open this email and complete the action requested if they haven't already done so.

For a complete list of rights you retain as author, click here.

We will forward your unedited manuscript to our publisher for posting to the Articles in Press section of our Web site and for indexing on PubMed. Your article should be posted within 1-2 weeks of receipt of files.

Once the journal's publisher has processed the article, the uncorrected proof will be indexed on PubMed, to be followed and replaced by the final, printed article.

The publisher will forward page proofs to you for your final review within 4-6 weeks; your paper will be published in print within 8-12 weeks.

AUTHOR SPONSORED ARTICLES: Gastroenterology offers authors the option to sponsor immediate open access to their articles online at www.gastrojournal.org and www.sciencedirect.com. The charge for article sponsorship is $3000, which is used to offset publishing costs of typesetting, tagging, and indexing of articles, hosting articles on dedicated servers, supporting sales and marketing costs to ensure global dissemination via www. gastrojournal.org and www.sciencedirect.com, and permanently preserving the published journal article. The fee excludes taxes and other potential author fees such as submission, page fee, and color charges, which are additional. If you'd like to sponsor your article, please complete and submit the sponsored-article order form. You will need your Elsevier Production Article Number to complete the form. You will receive this number via email once your accepted manuscript has been received and processed by the Elsevier team.

If you choose to sponsor your article, please notify Jason Woodson at ja.woodson@elsevier.com. Please include your manuscript number.

PAGE FEES: Gastroenterology charges authors of original research articles a fee for each printed

page published. Corresponding authors will receive invoices for page charges with payment instructions after the corrected proof of their accepted manuscript has been finalized. Page charges for non-AGA members are $100 per page. AGA members who are first or corresponding author at the time of submission will receive a 15% discount on page charges and pay $85 per page. Page charges apply only to unsolicited original research submitted as one of the following manuscript types: Clinical-Alimentary Tract, Clinical-Liver, Clinical-Pancreas, Clinical-Biliary, Basic and Translational-Alimentary Tract, Basic and Translational-Liver, Basic and Translational-Pancreas, Basic and Translational-Biliary, and Brief Report.Page charges do not apply to solicited content or online supplemental material. PLEASE PAY THE PAGE FEE INVOICE WITHIN 30 DAYS OF RECEIPT to avoid delays in processing future manuscript submissions.

PRESS EMBARGO: There is a press embargo for all studies and articles published in Gastroenterology until they are posted online in our Articles in Press section as a CORRECTED proof. Studies cannot be publicized as accepted manuscripts or uncorrected proofs. In the event a corrected proof is not posted online, the embargo will be lifted on the first day of the scheduled month of publication. Please see our Embargo Policy at http://www.gastrojournal.org/content/embargo for more details.

Please also remember to register for free e-mail table of contents alerts for each issue of Gastroenterology to stay abreast of the latest research.

Thank you for having allowed us to review this interesting work for Gastroenterology.

Congratulations and with best wishes,

John A. Williams, MD, PhD
Associate Editor

Bishr Omary, MD, PhD
Editor-in-Chief
Gastroenterology

Find us on Facebook to discover more about Gastroenterology.

If you are not an AGA member, we urge you to consider joining more than 16,000 of your colleagues who belong to the field's premier organization. The AGA provides valuable member benefits and services, including the latest advances in GI research, educational offerings, and clinical and translational resources. Learn how the AGA can benefit you.
Visit http://www.gastro.org/membership for more information and an application.

Accepted Manuscript

Alcohol Disrupts Levels and Function of the Cystic Fibrosis TransmembraneConductance Regulator to Promote Development of Pancreatitis

József Maléth, Zsolt Balla, Balázs Kui, Anita Balázs, Máté Katona, Linda Judák, István Németh, Petra Pallagi, Lajos V. Kemény, Zoltán Rakonczay Jr., V. Viktória Venglovecz, Imre Földesi, Zoltán Pető, Áron Somorácz, Katalin Borka, Doranda Perdomo, Gergely L. Lukacs, Mike A. Gray, Stefania Monterisi, Manuela Zaccolo, Matthias Sendler, Julia Mayerle, Jens-Peter Kühn, Markus M. Lerch, Miklós Sahin-Tóth, Péter Hegyi

PII: S0016-5085(14)01336-5
DOI: 10.1053/j.gastro.2014.11.002
Reference: YGAST 59421

To appear in: *Gastroenterology*
Accepted Date: 4 November 2014

Please cite this article as: Maléth J, Balla Z, Kui B, Balázs A, Katona M, Judák L, Németh I, Pallagi P, Kemény LV, Rakonczay Jr. Z, Viktória Venglovecz V, Földesi I, Pető Z, Somorácz Á, Borka K, Perdomo D, Lukacs GL, Gray MA, Monterisi S, Zaccolo M, Sendler M, Mayerle J, Kühn J-P, Lerch MM, Sahin-Tóth M, Hegyi P, Alcohol Disrupts Levels and Function of the Cystic Fibrosis TransmembraneConductance Regulator to Promote Development of Pancreatitis, *Gastroenterology* (2014), doi: 10.1053/j.gastro.2014.11.002.

Alcohol Disrupts Levels and Function of the Cystic Fibrosis Transmembrane Conductance Regulator to Promote Development of Pancreatitis

Short title: CFTR impairment in alcoholic pancreatitis

József Maléth[1], Zsolt Balla[1], Balázs Kui[1], Anita Balázs[1], Máté Katona[1], Linda Judák[1,2], István Németh[3], Petra Pallagi[1], Lajos V. Kemény[1], Zoltán Rakonczay Jr.[1], Viktória Venglovecz V.[2], Imre Földesi[4], Zoltán Pető[5], Áron Somorácz[6], Katalin Borka[6], Doranda Perdomo[7], Gergely L. Lukacs[7], Mike A. Gray[8], Stefania Monterisi[9], Manuela Zaccolo[9], Matthias Sendler[10], Julia Mayerle[10], Jens-Peter Kühn[11], Markus M. Lerch[10], Miklós Sahin-Tóth[12] and Péter Hegyi[1]

[1]First Dept. of Medicine, [2]Department of Pharmacology and Pharmacotherapy, [3]Department of Dermatology and Allergology , [4]Department of Laboratory Medicine and [5]Department of Emergency Medicine, University of Szeged, Szeged, Hungary, [6]2nd Department of Pathology, Semmelweis University, Budapest, Hungary, [7]Department of Physiology, McGill University, Montréal, Canada, [8]Institute for Cell & Molecular Biosciences, Newcastle University, Newcastle upon Tyne, UK; [9]Department of Physiology, Anatomy and Genetics, Oxford University, Oxford, UK, [10]Department of Medicine A, University Medicine Greifswald, Greifswald, Germany, [11]Institute of Radiology, University Medicine, Ernst-Moritz-University, Greifswald, Germany, [12]Department of Molecular and Cell Biology, Boston University Henry M. Goldman School of Dental Medicine, Boston, USA

Disclosure statement: The authors have no conflict of interest to disclose.

Corresponding author:

Péter Hegyi, M.D., Ph.D. D.Sc.
University of Szeged
Faculty of Medicine
First Department of Medicine

Korányi fasor 8-10
H-6720, Szeged, Hungary
Phone: (36)(62)545-200
Fax: (36)(62)545-185
Email: hegyi.peter@med.u-szeged.hu

Grant support: Our research was supported by the Hungarian National Development Agency grants (TÁMOP-4.2.2.A-11/1/KONV-2012-0035, TÁMOP-4.2.2-A-11/1/KONV-2012-0052; TÁMOP-4.2.2.A-11/1/KONV-2012-0073; TÁMOP-4.2.4.A/2-11-1-2012-0001; TÁMOP-4.2.4.A2-SZJÖ-TOK-13-0017) and the Hungarian Scientific Research Fund (NF100677). MML was supported by grants from the Alfried-Krupp-von-Bohlen-und-Halbach-Foundation (Graduate Schools Tumour Biology and Free Radical Biology), the Deutsche Krebshilfe/ Dr. Mildred-Scheel-Stiftung (109102), the Deutsche Forschungsgemeinschaft (DFG GRK840-E3/E4, DFG GRK1947, MA 4115/1-2/3), the Federal Ministry of Education and Research (BMBF GANI-MED 03152061A and BMBF 0314107, 01ZZ9603, 01ZZ0103, 01ZZ0403, 03ZIK012) and the European Union (EU-FP-7: EPC-TM and EU-FP7-REGPOT-2010-1, EPC-TM-Net).

Abbreviations used in this paper: AP, acute pancreatitis; BAC, blood alcohol concentration; BAPTA-AM, 1,2-bis(o-aminophenoxy)ethane-N,N,N',N'-tetraacetic acid; $[Ca^{2+}]_i$, intracellular Ca^{2+} concentration; CBE, Cl^-/HCO_3^- exchanger; CFTR, cystic fibrosis transmembrane conductance regulator Cl- channel; CFTRinh-172, CFTR inhibitor-172; CP, chronic pancreatitis; ER, endoplasmic reticulum; IP_3R, inositol-triphosphate receptor; PDEC, pancreatic ductal epithelial cells; pH_i, intracellular pH; PA, palmitic acid; POA, palmitoliec acid; POAEE, palmitoleic acid ethyl ester; RR, ruthenium red; RyR, ryanodin receptor; SERCA, sarcoplasmic/endoplasmic reticulum calcium ATPase; SLC26, solute carrier family

26; H_2DIDS, dihydro-4,4'-diisothiocyanostilbene-2,2'-disulfonic acid; Cl^-_{sw}, sweat Cl^- concentration; Tg, Thapsigargin;

József Maléth, Máté Katona and Petra Pallagi performed the fluorescence measurements. Katalin Borka, Áron Somorácz, Lajos Kemény and István Németh performed PCR and immunohistochemistry. Viktória Venglovecz, Mike Gray and Linda Judák played parts in electrophysiological experiments. Zsolt Balla, Balázs Kui, Marcus M. Lerch, Miklós Sahin-Tóth and Zoltán Rakonczay were involved in the investigation of the severity of alcohol-induced experimental pancreatitis in mice. Anita Balázs, Zoltán Pető and Imre Földesi measured the sweat chloride of volunteers and alcohol intoxicated patients. Doranda Perdomo and Gergely L. Lukacs investigated the effects of alcohol on CFTR folding and expression. Stefania Monterisi and Manuela Zaccolo measured cAMP in cell lines. Matthias Sendler, Julia Mayerle and Jens-Peter Kühn performed and evaluated the MRI based fluid secretion measurements in mice. Péter Hegyi was the supervisor of the study and had full access to all results during this research project. The manuscript was drafted by Péter Hegyi.

ABSTRACT

Background & Aims: Excessive ethanol consumption is one of the most common causes of acute and chronic pancreatitis. Alterations to the gene encoding the cystic fibrosis transmembrane conductance regulator (*CFTR*) also cause pancreatitis. However, little is known about the role of CFTR in the pathogenesis of alcohol-induced pancreatitis.

Methods: We measured CFTR activity based on chloride concentrations in sweat from patients with cystic fibrosis, patients admitted to the emergency department for excessive alcohol consumption, and healthy volunteers. We measured CFTR levels and localization in pancreatic tissues and from patients with acute or chronic pancreatitis induced by alcohol. We studied the effects of ethanol, fatty acids, and fatty acid ethyl esters on secretion of pancreatic fluid and HCO_3^-, levels and function of CFTR, and exchange of Cl^- for HCO_3^-, in pancreatic cell lines, as well as in tissues from guinea pigs and CFTR-knockout mice following administration of alcohol.

Results: Chloride concentrations increased in sweat samples from patients who acutely abuse alcohol but not in samples from healthy volunteers, indicating alcohol affects CFTR function. Pancreatic tissues from patients with acute or chronic pancreatitis had lower levels of CFTR than tissues from healthy volunteers. Alcohol and fatty acids inhibited secretion of fluid and HCO_3-, as well as CFTR activity, in pancreatic ductal epithelial cells. These effects were mediated by sustained increases in intracellular calcium and cAMP, depletion of ATP, and depolarization of mitochondrial membranes. In pancreatic cell lines and pancreatic tissues of mice and guinea pigs, administration of ethanol reduced expression of *CFTR* mRNA, reduced the stability of CFTR at the cell surface, and disrupted folding of CFTR at the endoplasmic reticulum. CFTR-knockout mice given ethanol or fatty acids developed more severe pancreatitis than mice not given ethanol or fatty acids.

Conclusions: Based on studies of human, mouse, and guinea pig pancreata, alcohol disrupts expression and localization of the CFTR. This appears to contribute to development of pancreatitis. Strategies to increase CFTR levels or function might be used to treat alcohol-associated pancreatitis.

KEYWORDS: exocrine pancreas; Cl^- channel, alcoholism, duct

.

INTRODUCTION

Acute pancreatitis (AP) is now the most common cause of hospitalization for non-malignant gastrointestinal diseases in the USA with an estimated annual cost of at least 2.5 billion dollars[1]. The mortality of the disease is unacceptably high, and no specific pharmaceutical therapy is currently available. There is therefore a pressing economic and clinical need for developing new therapies to help treat AP.

Immoderate alcohol consumption is one of the most common causes of acute and chronic pancreatitis[1-3], and therefore the effects of ethanol and ethanol metabolites on the pancreas have been widely investigated[4, 5]. These studies have, however, focused mainly on pancreatic acinar and stellate cells. On the other hand Sarles et al. described that the initial lesion in the course of pancreatic damage during alcohol-induced chronic calcifying pancreatitis was the formation of mucoprotein plugs in the small pancreatic ducts[6]. These changes are very similar to the alterations of the exocrine pancreas in cystic fibrosis (CF), the most common autosomal recessive disease caused by loss-of-function mutations in the *CFTR* gene. Moreover Ooi et al. demonstrated that CF patients with impaired cystic fibrosis transmembrane conductance regulator (CFTR) function are at an increased risk of developing pancreatitis[7]. These data suggest that the changes in the function or expression of the CFTR Cl^- channels in pancreatic ductal epithelial cells (PDEC), which alone express CFTR in the exocrine pancreas[8], might play a central role in the pathogenesis of alcohol induced pancreatitis.

MATERIALS AND METHODS

Detailed protocols and description for volunteers, patients and all methods used in this study can be found in the supplementary documents.

Human studies

Sweat samples from human subjects were collected by pilocarpine iontophoresis and sweat chloride concentration was determined by conductance measurement. The mRNA and protein expression levels of CFTR and Na^+/K^+-ATPase of the pancreatic ductal epithelia in human pancreatic tissue were determined.

Cell and animal studies

A large variety of human cell lines (Capan-1, MDCK and HEK) and animal models (mice and guinea pigs) were used to assess the role of CFTR in alcohol-induced AP.

Statistical Analysis

All data are expressed as means±SEM. Significant differences between groups were determined by analysis of variance. Statistical analysis of the immunohistochemical data was performed using the Mann–Whitney U test. $P<0.05$ was accepted as statistically significant.

Ethical Approvals

The protocols concerning human subjects, or laboratory animals were approved by the relevant agencies.

RESULTS

Alcohol consumption decreases CFTR activity and expression in human subjects

In CF patients sweat Cl^-concentration (Cl^-_{sw}) is elevated due to diminished CFTR absorbtive activity[9]. In our study the Cl^-_{sw} at 0mM blood alcohol concentration (BAC) was 41.08±3.1mM (Figure 1.A). After consuming 1.6g/kg ethanol within 30 min, the average BAC was elevated to 23.3±1.1mM with no elevation of Cl^-_{sw} (47±1mM). However, to test the effects of higher BAC on Cl^-_{sw}, we enrolled patients admitted to emergency unit due to excessive alcohol consumption. The average BAC in this group was 74.2±2.6mM, whereas, the Cl^-_{sw} was 62.7±2.3mM suggesting strong inhibition of CFTR (Figure 1.B, for patient data see Table 2 in the supplementary document). Importantly when BAC returned to 0 the Cl^-_{sw} normalized (Figure 1.C). To assess the effects of chronic alcohol intake we also enrolled alcohol dependent patients from the department of addictology. Those patients had a background of alcohol consumption for at least one year and did not consume alcohol for at least one week prior to the Cl^-_{sw} measurements. The mean Cl^-_{sw} of this group was 49.92±2.8mM suggesting that ethanol has chronic effects on CFTR too (Figure 1.B).

Next, we determined the effects of ethanol on CFTR expression and localization in the pancreas using tissue samples from control pancreatic tissue and from patients suffering from acute (AP) or chronic (CP) alcohol-induced pancreatitis (Figure 1.D-F, for detailed description of tissue samples see the supplementary documents). In alcoholic AP, CFTR expression decreased both at mRNA and protein levels. Similarly, in CP the membrane expression of CFTR in PDEC was significantly lower, however, both the mRNA level and cytoplasmic density of CFTR were strongly elevated suggesting defective endoplasmic reticulum (ER) protein folding and/or translocation of CFTR from the membrane to the cytosol. As control experiment we showed that neither the mRNA, nor the protein expression

levels of another plasma membrane transporter, namely the Na^+/K^+-ATPase were changed in AP and CP (Supplementary Figure 1.).

Ethanol and fatty acid impair the pancreatic fluid and bicarbonate secretion and inhibit CFTR Cl^- channel activity *in vivo* and *in vitro*

In the next step we applied different *in vivo* and *in vitro* techniques to assess the effects of ethanol and ethanol metabolites on the pancreatic fluid and HCO_3^- secretion in animal models and in a human pancreatic cell line. First we used MRI cholangiopancreatography to measure the total excreted volume (TEV) in WT and CFTR KO mice. Upon the retroorbital injection of 10U/bwkg secretin the increase of TEV in tWT animals was significantly higher than in CFTR KO animals (Figure 2.A). The pancreatic secretion was reassessed 24 h after the *i.p.* injection of 1.75g/kg ethanol and 750mg/kg palmitic acid (PA), which markedly decreased TEV in WT and almost completely abolished in CFTR KO mice. In addition, we also showed that *i.p.* injection of ethanol and PA significantly decreases both the basal and the secretin-stimulated pancreatic fluid secretion in anesthetised mice *in vivo* (Supplementary Figure 2.).

To detect the pancreatic ductal fluid secretion *in vitro* we used isolated guinea pig pancreatic ducts which is the best *in vitro* model to mimic the human situation. Administration of 100mM ethanol, or the non-oxidative ethanol metabolite palmitoleic acid (POA; 200µM) for 30 min markedly reduced the pancreatic fluid secretion, whereas 200µM palmitoleic acid ethyl ester (POAEE) had no effect (Figure 2.B). The pancreatic ductal HCO_3^- secretion was measured using NH_4Cl pulse, where the initial rate of pH_i recovery from an alkali load (base flux; $J(B^-)$; for details see the supplementary documents) reflects the activity of the apical SLC26 Cl^-/HCO_3^- exchangers (CBEs) and CFTR (Figure 2.C)[10]. Similarly to the ductal fluid

secretion, 100mM ethanol and 200µM POA significantly diminished the ductal HCO_3^- secretion after 30 min exposure.

We confirmed our results on human polarized pancreatic cell line (Capan-1) too. Applying two independent methods (luminal Cl^- removal and NH_4Cl pulse) showed that 15 min administration of low concentration of ethanol (10mM) stimulated, high concentration of ethanol (100mM) and POA (100, 200µM) significantly impaired the apical Cl^-/HCO_3^- exchange activity (Supplementary Figure 3.A.). Moreover, 100mM ethanol and 100-200µM POA significantly inhibited the recovery from acid load during NH_4Cl pulse experiments under basal conditions and forskolin-stimulation (Supplementary Figure 3.B-D) suggesting, that the activity of the basolateral transporters might be also impaired.

Finally, we directly detected the effects of ethanol and ethanol metabolites on the CFTR Cl^- current in primary epithelial (Figure 2.D) and human Capan-1 cells (Supplementary Figure 3.F). Exposure of guinea pig PDEC to 10mM ethanol had no significant effect on the forskolin-stimulated CFTR currents (in Capan-1 significant slight stimulation was observed), whereas 100mM ethanol or 200µM POA significantly decreased it. In both cases, the inhibition was voltage-independent and irreversible. Administration of 200µM POAEE had no effect on forskolin-stimulated CFTR currents.

Low concentration of ethanol stimulates both the apical SLC26 Cl^-/HCO_3^- exchanger and CFTR via IP_3R mediated Ca^{2+} signalling

Apical Cl^- removal in Capan-1 cells revealed that separate administration of 10µM CFTR(inh)-172 (CFTR Cl^- channel inhibitor) or 500µM H_2DIDS (SLC26A6 inhibitor) for 15 min could not prevent the stimulatory effect of 10mM ethanol, however their combination totally abolished it (Supplementary Figure 4.A,C). In case of NH_4Cl pulse (where the bicarbonate concentration of the cells are higher) not only the co-administration of the two

inhibitors, but separate administrations alone could prevent the stimulatory effect of ethanol (Supplementary Figure 4.B,D). To identify the intracellular mechanisms of the stimulation we showed that 10mM ethanol induced repetitive Ca^{2+} spikes in Capan-1 cells (Supplementary Figure 5.A). Administration of the inositol-triphosphate receptor (IP_3R) antagonist caffeine (20mM), or the phospholipase C (PLC) inhibitor U73122 (10µM) completely abolished the Ca^{2+} response suggesting that the Ca^{2+} was released from the ER via IP_3R activation. Moreover, 20mM caffeine totally inhibited the stimulatory effect ethanol suggesting that elevation of intracellular Ca^{2+} concentration ($[Ca^{2+}]_i$) mediate the stimulatory effect of ethanol on HCO_3^- secretion (Supplementary Figure 5.B,C).

High concentration of ethanol inhibits both the apical SLC26 Cl^-/HCO_3^- exchanger and CFTR

Administration of CFTR(inh)-172 and H_2DIDS showed that pre-treatment of the cells for 15 min with either CFTR(inh)-172 or H_2DIDS further decreased the HCO_3^- secretion when co-administrated with ethanol or POA suggesting that both transport mechanisms are involved in the inhibitory mechanisms (Figure 3.A,B, Supplementary Figure 6.A,B). When the SLC26 inhibitor H_2DIDS was administrated only when the luminal Cl^- was already removed (Figure 3.C) the same effects were observed.

High concentration of ethanol and POA induce sustained $[Ca^{2+}]_i$ elevation, decreased mitochondrial function and cAMP level

100mM ethanol induced moderate, but sustained $[Ca^{2+}]_i$ increase in Capan-1 cells, POAEE had no effect, whereas POA evoked dose-dependent, sustained $[Ca^{2+}]_i$ rise (Figure 4.A,B). The first phase of the Ca^{2+} signal was inhibited by the ryanodin receptor (RyR) inhibitor Ruthenium Red, the IP_3R inhibitor caffeine and the PLC inhibitor U73122

(Supplementary Figure 7.A), whereas, removal of extracellular Ca^{2+} had no effect on the $\Delta Ratio_{max}$ (Supplementary Figure 7.B). The plateau-phase of the signal was totally dependent on the presence of extracellular Ca^{2+} and blocked by gadolinium, suggesting the involvement of the store operated Ca^{2+} channels. To verify that 200µM POA completely depletes the ER Ca^{2+} stores, we administrated POA in Ca^{2+}-free media followed by the administration of 2µM thapsigargin (Tg; sarcoplasmic/endoplasmic reticulum calcium ATPase (SERCA) inhibitor). Under these conditions Tg was not able to induce further Ca^{2+} release (Supplementary Figure 8.A). For control we administered Tg prior to POA administration, where POA had no effect on $[Ca^{2+}]_i$. These data indicate that POA completely depletes the ER Ca^{2+} stores and induces extracellular Ca^{2+} influx.

To further characterize the effects of POA on the extracellular Ca^{2+} influx, we performed the Tg-Ca^{2+} re-addition protocol[11] (Supplementary Figure 8.B,C). Tg treatment depleted ER Ca^{2+} and the re-addition of extracellular Ca^{2+} evoked store operated Ca^{2+} influx, where the steady state is maintained by the plasma membrane Ca^{2+}-ATPase (PMCA) activity. 200µM POA in Ca^{2+}-free extracellular solution mimicked the effect Tg (depleted the ER Ca^{2+} store and induced SOCE). However, after the SOCE mediated Ca^{2+} rise the decrease of $[Ca^{2+}]_i$ was markedly slower than in the case of Tg-treated cells and the plateau was reached on an elevated $[Ca^{2+}]_i$. These results suggest that POA not only depletes ER Ca^{2+}, but also decreases PMCA activity.

Measurement of $(ATP)_i$ using MgGreen-AM revealed that 100mM ethanol and 100-200µM POA markedly and irreversibly decreased $(ATP)_i$ (Figure 4.B). (The increase in fluorescent intensity inversely correlates with the cellular ATP levels.) The combination of deoxyglucose (DOG)/iodoacetate (IAA) and carbonyl cyanide 3-chlorophenylhydrazone (CCCP) was used as control, to inhibit cellular glycolysis and mitochondrial ATP production. We also tested the effect of $(ATP)_i$ depletion on HCO_3^- secretion (Supplementary Figure 9.C,D) and showed that

administration of DOG/IAA/CCCP significantly decreased HCO_3^- secretion, similarly to the effects of 200µM POA.To further characterize the effects of ethanol and ethanol metabolites on the mitochondrial function, we showed that 100mM ethanol and 100-200µM POA markedly and irreversibly decreased mitochondrial membrane potential $(\Delta\Psi)_m$ (Figure 4.C).

FRET-based cAMP measurements using Epac1-camps sensor revealed that 100mM ethanol and 200µM POAEE significantly decreased forskolin-stimulated cAMP production in HEK cells, however interestingly 100µM POA had no inhibitory effect (Figure 4.D).

Finally, we showed that chelation of intracellular Ca^{2+} (with 40µM BAPTA-AM) completely abolished the inhibitory effect of 100mM ethanol and 200µM POA on pancreatic ductal HCO_3^- secretion suggesting that it was mediated by the sustained elevation of $[Ca^{2+}]_i$ (Figure 4.E, Supplementary Figure 9.A,B).

Ethanol and non-oxidative ethanol metabolites cause translocation and expression defect of CFTR

Our experiments showed that high concentrations of ethanol, POAEE and POA time and –dose dependently decreased both the mRNA and protein expression of CFTR in human pancreatic epithelial cells *in vitro* (Figure 5.A-C). To reproduce these observations *in vivo,* an appropriate animal model was used. Guinea pigs were injected *i.p.* with 0.8g/kg ethanol and 300mg/kg PA. Importantly, apical CFTR expression in the pancreatic ducts was not changed at 3 and 6 h, however it was significantly decreased 12 and 24 h after treatment (Figure 5.E,F). Moreover, cytoplasmic CFTR levels were elevated after 3 h, suggesting a membrane trafficking defect of CFTR. As a control experiment, expression of the Na^+/K^+-ATPase was also measured and no changes were observed (Supplementary Figure 10.).

Ethanol and its metabolites decrease CFTR expression and plasma membrane density via accelerated channel plasma membrane turn over and damaged protein folding

To dissect the mechanism of CFTR expression defect upon ethanol, POA or POAEE exposure, we exposed monolayers of MDCK-II cells, expressing WT human CFTR containing a 3HA epitope in the 4th extracellular loop, to ethanol, POAEE or POA for 48 h. Quantitative immunoblot analysis by anti-HA antibody revealed that in contrast to the modest effect of 100mM ethanol, 100-200μM POAEE and POA significantly decreased the mature, complex-glycosylated CFTR expression, as compared to control (Figure 6.A). Importantly, the protein expression of Na^+/K^+-ATPase was not changed during the treatment. The loss of cellular CFTR expression coincided with the reduction of the apical CFTR plasma membrane density, monitored by the cell surface ELISA taking advantage of the extracellular 3HA epitope (Figure 6.B). CFTR apical plasma membrane density was reduced by ~40% in the presence of 200μM POA, while only ~15% and ~30% was evident after ethanol and POAEE exposure, respectively (Figure 6.C). Accelerated channel turnover at the PM and/or impaired biosynthetic secretion can account for the pronounced apical expression defect of CFTR in the treated cells. To assess the first possibility, apical PM stability of CFTR was measured by ELISA, which revealed that ethanol, POAEE and POA provoked increased removal of CFTR from the PM, during a 2 h chase, suggesting that the channel turnover was accelerated (Figure 6.C). The conformational maturation efficiency of CFTR was measured by the conversion efficiency of the metabolically labeled core-glycosylated form into the complex-glycosylated CFTR (Figure 6.D). CFTR folding efficiency was diminished from 24±3% to 17±2% and 20±1% by POA and POAEE, respectively (Figure 6.D), indicating that non-oxidative ethanol metabolites compromise both the biosynthetic processing and peripheral stability of the channel.

Genetic deletion of CFTR increases the severity of alcohol-induced pancreatitis

To further confirm the central role of CFTR in alcohol-induced pancreatic damage, we compared the severity of alcohol and palmitic acid (PA) induced pancreatitis in WT and CFTR KO mice. *i.p.* administration of 1.75g/kg ethanol and 750mg/kg PA induced significant elevation in all investigated pancreatitis severity parameters (pancreatic water content; serum amylase activity; edema score; leukocyte score and necrosis) (Figure 7.A-B) in WT animals. Importantly, these alterations were significantly higher in CFTR KO animals, showing when expression and activity of CFTR is impaired by alcohol abuse, alcohol-induced acute pancreatitis is worsened.

DISCUSSION

In this study we have demonstrated that ethanol, as well as its non-oxidative metabolites cause impairment of CFTR function and expression, which exacerbate alcohol-induced pancreatitis. While a single alcohol binge of healthy volunteers did not impair CFTR function as determined by sweat chloride absorption, excessive alcohol consumption in habitual drinkers did, in fact, markedly reduce the function of CFTR, as evidenced by a rise in Cl^-_{sw}, which returned to the normal range when the measurement was repeated on sobered patients.

Pancreatic tissue metabolizes ethanol mainly via the non-oxidative pathway mediated by FAEE synthases (FAEES), which combine ethanol and FA and produce FAEE[12]. A clinical study showed that blood FAEE concentration was elevated in parallel with ethanol concentration during alcohol consumption; but FAEE remained increased longer in the serum compared to ethanol[13]. Moreover, compared with the liver, pancreatic FAEES activity is higher, which creates the possibility for the local accumulation of non-oxidative ethanol metabolites[14]. Werner et al. showed that FAEE infusion induced pancreatic edema, intrapancreatic trypsinogen activation, and vacuolization of acinar cells[15]. Recently Huang et al. developed a novel model of alcohol-induced pancreatitis[16] using a combined *i.p.* injection of ethanol and FA, where the pharmacological inhibition of non-oxidative ethanol metabolism decreased the pancreatic damage.

We demonstrated that pancreatic ductal HCO_3^- secretion plays central role in the physiology of the exocrine pancreas, maintaining the intraductal pH[17, 18], therefore in our experiments we used different *in vivo* and *in vitro* techniques to clarify the acute effects of ethanol and ethanol metabolites on fluid and HCO_3^- secretion and CFTR Cl^- current in PDEC. Importantly, our MRI cholangiopancreatography experiments showed that in CFTR KO mice the ductal secretion is remarkably diminished compared to WT, moreover, ethanol and PA

strongly impaired ductal secretion in both groups. The inhibitory effect of ethanol and PA on pancreatic fluid secretion was confirmed *in vivo* using pancreatic duct cannulation in anesthetized mice and *in vitro* using isolated sealed guinea pig pancreatic ducts too. Besides the fluid transport we characterized the effects of ethanol and it metabolites on HCO_3^- secretion. Our results showed that ethanol in low concentration stimulates, whereas in high concentrations inhibits HCO_3^- secretion and decreases CFTR activity. Similar dual effects of ethanol on fluid secretion were highlighted earlier[19]. In our study, the stimulatory effect of 10mM ethanol on HCO_3^- secretion was mediated by IP_3R-dependent Ca^{2+} release from the ER. In contrast, high concentrations of ethanol and POA induced sustained $[Ca^{2+}]_i$ elevation mediated by both the IP_3R and RyR as well as extracellular Ca^{2+} influx (Figure 7.C). Notably, similar toxic Ca^{2+} elevation was found in pancreatic acinar cells, and in other cell types leading to premature protease activation and cell death[20-23]. It is well documented that sustained $[Ca^{2+}]_i$ elevation causes mitochondrial Ca^{2+} overload[24], which impairs $(\Delta\Psi)_m$ and ATP production[20, 25]. Very recently ethanol was shown to sensitize pancreatic mitochondria to activate the mitochondrial permeability transition pore, leading to mitochondrial failure[26]. In this study, high concentrations of ethanol and POA also induced $(ATP)_i$ depletion and decreased $(\Delta\Psi)_m$. Although the toxic effects of ethanol and POA were similar to those of high concentration of bile acids[27, 28], in this study chelation of $[Ca^{2+}]_i$ abolished the inhibitory effect of ethanol and POA on HCO_3^- secretion. This observation indicates, that ethanol and POA, in a similar manner to trypsin[29], inhibit HCO_3^- secretion via a sustained $[Ca^{2+}]_i$ rise. Importantly, CFTR single channel parameters don't change as a result of ethanol application (personal communication; Aleksandrov Andrei and John R. Riordan; UNC School of Medicine, Chapel Hill, NC, USA) suggesting that the effects of high dose of ethanol is not altering the biophysical characteristics of CFTR.

One of the crucial observations of this study is that during alcohol-induced pancreatitis the expression of CFTR is decreased on the luminal membrane of human PDEC. Since decreased CFTR expression during alcoholic-pancreatitis is very similar to the CFTR mislocalization found in autoimmune pancreatitis[30], we wanted to confirm that decreased CFTR expression is caused by alcohol and not by the cellular damage during the inflammatory process. The *in vitro* experiments in human PDEC and the *in vivo* experiments in guinea pig clearly demonstrated that alcohol and its non-oxidative metabolites indeed strongly decrease CFTR expression without panccreatitis. The pronounced apical expression defect of CFTR was caused by accelerated channel turnover at the PM and impaired biosynthetic secretion (Figure 7.C). The latter effect may be attributed, at least in part, to chronic cytoplasmic ATP-depletion, considering that CFTR conformation maturation is an ATP-sensitive process at the ER[31]. These results indicate that chronic exposure of PDEC to ethanol or ethanol metabolites compromise both the biosynthetic processing and peripheral stability of the channel. It is known that the phosphorylation and dephosphorylation of CFTR mediated by WNK/SPAK and IRBIT/PP1, regulates the PM trafficking of CFTR and other transporters in epithelial cells[32, 33], however, the effect of ethanol or ethanol metabolites on these systems is not known. Chronic alcohol consumption dose-dependently increases the risk to develop malignancies, diabetes, hypertension and cardiovascular diseases[34]. Interestingly Guo et al. showed that CFTR activity plays a crucial role in the insulin secretion of the pancreatic beta cells[35], whereas diabetes is a well-known complication of alcoholism[34]. The decreased CFTR activity induced by alcohol consumption might play an import role in the disease development.

Association between CFTR gene mutations and the risk for the development of acute recurrent[36] or chronic pancreatitis[37] provides strong evidence that mutations in CFTR and/or insufficiency of electrolyte and fluid secretion by pancreatic ductal cells lead to increased risk

for pancreatitis[38]. Heterozygous carriers of *CFTR* mutations are at an increased risk of chronic pancreatitis[39], moreover Ooi et al. demonstrated that the risk of developing pancreatitis was much higher in CF patients, who had milder CFTR mutations (type IV and V) and were pancreatic sufficient compared to those who had severe mutations and were pancreatic insufficient[7]. In the pathogenetic model proposed in this study, the risk of developing pancreatitis inversely correlates with CFTR function. However, in other studies the association between *CFTR* gene mutation and alcoholic pancreatitis was inconsistent[40, 41]. Very recently LaRusch et al. elegantly demonstrated that *CFTR* gene mutations that don't cause typical cystic fibrosis, but disrupt the WNK1-SPAK-mediated HCO_3^- permeability of the channel, are associated with pancreatic disorders[42]. In animal model of pancreatitis Dimagno earlier showed that CFTR KO mice developed more severe acute pancreatitis after cerulein hyperstimulation than WT mice[43] and recently Pallagi et al. had the same observation in mice with genetic deletion of Na^+/H^+ exchanger regulatory factor (NHERF1), which regulates CFTR expression[44]. Here we have demonstrated using CFTR KO mice that genetic deletion of CFTR leads to more severe pancreatitis after ethanol and fatty acid administration, confirming the crucial role of CFTR in the pathogenesis of alcohol-induced pancreatitis.

Taken together, our observations provide evidence that the loss of CFTR function not only plays a crucial role in CFTR mutation-related pancreatitis, but it also contributes to the pathogenesis of alcohol-induced pancreatitis. These data indicate that correcting CFTR function should offer therapeutic benefit in alcoholic pancreatitis.

REFERENCES

1. Yadav D,Lowenfels AB.The epidemiology of pancreatitis and pancreatic cancer.Gastroenterology 2013;144:1252-61.
2. Nagar AB,Gorelick FS.Acute pancreatitis.Curr Opin Gastroenterol 2002;18:552-7.
3. Braganza JM,Lee SH,McCloy RF,et al.Chronic pancreatitis.Lancet 2011;377:1184-97.
4. Pandol SJ,Lugea A,Mareninova OA,et al.Investigating the pathobiology of alcoholic pancreatitis.Alcohol Clin Exp Res 2011;35:830-7.
5. Petersen OH,Tepikin AV,Gerasimenko JV,et al.Fatty acids, alcohol and fatty acid ethyl esters: toxic Ca2+ signal generation and pancreatitis.Cell Calcium 2009;45:634-42.
6. Sarles H,Sarles JC,Camatte R,et al.Observations on 205 confirmed cases of acute pancreatitis, recurring pancreatitis, and chronic pancreatitis.Gut 1965;6:545-59.
7. Ooi CY,Dorfman R,Cipolli M,et al.Type of CFTR mutation determines risk of pancreatitis in patients with cystic fibrosis.Gastroenterology 2011;140:153-61.
8. Trezise AE,Buchwald M.In vivo cell-specific expression of the cystic fibrosis transmembrane conductance regulator.Nature 1991;353:434-7.
9. Siegenthaler P,Dehaller R,Dubach UC.Salt Excretion in Sweat in Cystic Fibrosis.JAMA 1963;186:1178.
10. Hegyi P,Gray MA,Argent BE.Substance P inhibits bicarbonate secretion from guinea pig pancreatic ducts by modulating an anion exchanger.Am J Physiol Cell Physiol 2003;285:C268-76.
11. Bird GS,DeHaven WI,Smyth JT,et al.Methods for studying store-operated calcium entry.Methods 2008;46:204-12.
12. Laposata EA,Lange LG.Presence of nonoxidative ethanol metabolism in human organs commonly damaged by ethanol abuse.Science 1986;231:497-9.
13. Doyle KM,Cluette-Brown JE,Dube DM,et al.Fatty acid ethyl esters in the blood as markers for ethanol intake.JAMA 1996;276:1152-6.
14. Gukovskaya AS,Mouria M,Gukovsky I,et al.Ethanol metabolism and transcription factor activation in pancreatic acinar cells in rats.Gastroenterology 2002;122:106-18.
15. Werner J,Laposata M,Fernandez-del Castillo C,et al.Pancreatic injury in rats induced by fatty acid ethyl ester, a nonoxidative metabolite of alcohol.Gastroenterology 1997;113:286-94.
16. **Huang W,Booth DM**,Cane MC,et al.Fatty acid ethyl ester synthase inhibition ameliorates ethanol-induced Ca^{2+}-dependent mitochondrial dysfunction and acute pancreatitis.Gut 2014;63:1313-24.
17. Hegyi P,Petersen OH.The exocrine pancreas: the acinar-ductal tango in physiology and pathophysiology.Rev Physiol Biochem Pharmacol 2013;165:1-30.
18. Hegyi P,Maleth J,Venglovecz V,et al.Pancreatic ductal bicarbonate secretion: challenge of the acinar Acid load.Front Physiol 2011;2:36.
19. Yamamoto A,Ishiguro H,Ko SB,et al.Ethanol induces fluid hypersecretion from guinea-pig pancreatic duct cells.J Physiol 2003;551:917-26.
20. Criddle DN,Murphy J,Fistetto G,et al.Fatty acid ethyl esters cause pancreatic calcium toxicity via inositol trisphosphate receptors and loss of ATP synthesis.Gastroenterology 2006;130:781-93.
21. Kouzoukas DE,Li G,Takapoo M,et al.Intracellular calcium plays a critical role in the alcohol-mediated death of cerebellar granule neurons.J Neurochem 2013;124:323-35.
22. Nakayama N,Eichhorst ST,Muller M,et al.Ethanol-induced apoptosis in hepatoma cells proceeds via intracellular Ca(2+) elevation, activation of TLCK-sensitive proteases, and cytochrome c release.Exp Cell Res 2001;269:202-13.

23. Kruger B,Albrecht E,Lerch MM.The role of intracellular calcium signaling in premature protease activation and the onset of pancreatitis.Am J Pathol 2000;157:43-50.
24. Kroemer G,Reed JC.Mitochondrial control of cell death.Nat Med 2000;6:513-9.
25. Walsh C,Barrow S,Voronina S,et al.Modulation of calcium signalling by mitochondria.Biochim Biophys Acta 2009;1787:1374-82.
26. Shalbueva N,Mareninova OA,Gerloff A,et al.Effects of oxidative alcohol metabolism on the mitochondrial permeability transition pore and necrosis in a mouse model of alcoholic pancreatitis.Gastroenterology 2013;144:437-446 e6.
27. Maleth J,Venglovecz V,Razga Z,et al.Non-conjugated chenodeoxycholate induces severe mitochondrial damage and inhibits bicarbonate transport in pancreatic duct cells.Gut 2011;60:136-8.
28. Maleth J,Rakonczay Z,Jr.,Venglovecz V,et al.Central role of mitochondrial injury in the pathogenesis of acute pancreatitis.Acta Physiol (Oxf) 2013;207:226-35.
29. Pallagi P,Venglovecz V,Rakonczay Z,Jr.,et al.Trypsin reduces pancreatic ductal bicarbonate secretion by inhibiting CFTR Cl(-) channels and luminal anion exchangers.Gastroenterology 2011;141:2228-2239 e6.
30. **Ko SB,Mizuno N,**Yatabe Y,et al.Corticosteroids correct aberrant CFTR localization in the duct and regenerate acinar cells in autoimmune pancreatitis.Gastroenterology 2010;138:1988-96.
31. Lukacs GL,Mohamed A,Kartner N,et al.Conformational maturation of CFTR but not its mutant counterpart (delta F508) occurs in the endoplasmic reticulum and requires ATP.EMBO J 1994;13:6076-86.
32. Yang D,Li Q,So I,et al.IRBIT governs epithelial secretion in mice by antagonizing the WNK/SPAK kinase pathway.J Clin Invest 2011;121:956-65.
33. Park S,Hong JH,Ohana E,et al.The WNK/SPAK and IRBIT/PP1 pathways in epithelial fluid and electrolyte transport.Physiology(Bethesda) 2012;27:291-9.
34. Shield KD,Parry C,Rehm J.Chronic diseases and conditions related to alcohol use.Alcohol Res 2013;35:155-73.
35. Guo JH,Chen H,Ruan YC,et al.Glucose-induced electrical activities and insulin secretion in pancreatic islet beta-cells are modulated by CFTR.Nat Commun 2014;5:4420.
36. Cavestro GM,Zuppardo RA,Bertolini S,et al.Connections between genetics and clinical data: Role of MCP-1, CFTR, and SPINK-1 in the setting of acute, acute recurrent, and chronic pancreatitis.Am J Gastroenterol 2010;105:199-206.
37. **Weiss FU,Simon P,**Bogdanova N,et al.Complete cystic fibrosis transmembrane conductance regulator gene sequencing in patients with idiopathic chronic pancreatitis and controls.Gut 2005;54:1456-60.
38. Hegyi P,Rakonczay Z.Insufficiency of electrolyte and fluid secretion by pancreatic ductal cells leads to increased patient risk for pancreatitis.Am J Gastroenterol 2010;105:2119-20.
39. Sharer N,Schwarz M,Malone G,et al.Mutations of the cystic fibrosis gene in patients with chronic pancreatitis.N Engl J Med 1998;339:645-52.
40. Maruyama K,Harada S,Yokoyama A,et al.Association analyses of genetic polymorphisms of GSTM1, GSTT1, NQO1, NAT2, LPL, PRSS1, PSTI, and CFTR with chronic alcoholic pancreatitis in Japan.Alcohol Clin Exp Res 2010;34 Suppl.1:S34-8.
41. Pezzilli R,Morselli-Labate AM,Mantovani V,et al.Mutations of the CFTR gene in pancreatic disease.Pancreas 2003;27:332-6.

42. **LaRusch J,Jung J,General IJ**,et al.Mechanisms of CFTR functional variants that impair regulated bicarbonate permeation and increase risk for pancreatitis but not for cystic fibrosis.PLoS Genet 2014;10:e1004376.
43. Dimagno MJ,Lee SH,Hao Y,et al.A proinflammatory, antiapoptotic phenotype underlies the susceptibility to acute pancreatitis in cystic fibrosis transmembrane regulator (-/-) mice.Gastroenterology 2005;129:665-81.
44. **Pallagi P,Balla Z,Singh AK,**et al.The role of pancreatic ductal secretion in protection against acute pancreatitis in mice*.Crit Care Med 2014;42:e177-88.

Author names in bold designate shared co-first authors.

ACKNOWLEDGEMENTS

The authors are grateful to John Riordan (University of North Carolina – Chapel Hill) and to the Cystic Fibrosis Foundation Therapeutics for providing us with the CFTR antibody. The CFTR knockout mice were a kind gift from Ursula Seidler (Hannover Medical School, Dept of Gastroenterology). The authors thank Éva Kereszthy (University of Szeged, Department of Forensic Medicine) for the legal advices concerning the investigations on alcoholic patients, to Erzsébet Schneider and the co-workers of the emergency unit of the Second Department of Medicine (University of Szeged) for helping us in the measurements executed on alcohol intoxicated patients and to the volunteers participating in our study. The authors are thankful for the surgical resection samples to the 1st Department of Surgery (Semmelweis University, Budapest).

SUPPLEMENTARY MATERIALS AND METHODS

Abbreviations used in this paper: AP, acute pancreatitis; BAC, blood alcohol concentration; BAPTA-AM, 1,2-bis(o-aminophenoxy)ethane-N,N,N',N'-tetraacetic acid; $[Ca^{2+}]_i$, intracellular Ca^{2+} concentration; CBE, Cl^-/HCO_3^- exchanger; CFTR, cystic fibrosis transmembrane conductance regulator Cl- channel; CFTRinh-172, CFTR inhibitor-172; CP, chronic pancreatitis; ER, endoplasmic reticulum; IP_3R, inositol-triphosphate receptor; PDEC, pancreatic ductal epithelial cells; pH_i, intracellular pH; PA, palmitic acid; POA, palmitoliec acid; POAEE, palmitoleic acid ethyl ester; RR, ruthenium red; RyR, ryanodin receptor; SERCA, sarcoplasmic/endoplasmic reticulum calcium ATPase; SLC26, solute carrier family 26; H_2DIDS, dihydro-4,4'-diisothiocyanostilbene-2,2'-disulfonic acid; Cl^-_{sw}, sweat Cl^- concentration; Tg, Thapsigargin;

Solutions and chemicals

Table 1. summarizes the composition of the solutions used in these series of experiments. The pH of the Hepes-buffered solutions was set to 7.4 with HCl, whereas, the HCO_3^--buffered solutions were gassed with 95%O_2/5%CO_2 to set pH. For patch clamp studies the standard extracellular solution contained (in mM): 145NaCl, 4.5KCl, 2$CaCl_2$, 1$MgCl_2$, 10HEPES, and 5glucose (pH 7.4). The osmolarity of the external solutions were 300mOsm/L. The standard pipette solution contained (in mM): 120CsCl, 2$MgCl_2$, 0.2ethylene glycol-bis(b-aminoethyl ether)-N,N,N8,N8-tetraacetic acid (EGTA), 10HEPES, and 1Na_2ATP (pH 7.2). 2.7-bis-(2-carboxyethyl)-5-(and-6-)carboxyfluorescein-acetoxymethylester (BCECF-AM), 2-(6-(bis(carboxymethyl)amino)-5-(2-(2-(bis(carboxymethyl)amino)-5-methylphenoxy)ethoxy)-2-benzofuranyl)-5-oxazolecarboxylic-acetoxymethylester (Fura2-AM), MagnesiumGreen-AM, Tetramethylrhodamine-methylester (TMRM), H_2DIDS and 1,2-bis(o-aminophenoxy)ethane-N,N,N',N'-tetraaceticacid (BAPTA-AM) were from Invitrogen (Carlsbad, CA, USA). Forskolin was purchased from Tocris (Ellisville, Missouri, USA) and Thapsigargin from

Merck (Darmstadt, Germany). All other chemicals were obtained from Sigma-Aldrich (Budapest, Hungary), unless stated otherwise. To solubilise fatty acids in water-based solution first we made 1M stock solution of palmitoleic acid and palmitoleic acid ethyl ester in 100% ethanol. After that 10µL stock solution was added carefully to 1mL HEPES, or HCO_3^-/CO_2 buffered solution at 37°C, which was gently sonicated. Then this was added dropwise and diluted to the concentration we used during the experiments again at 37°C. This way we were able to avoid using the high ethanol concentration.

Human studies

Characteristics of volunteers and patients. The detailed characteristics of the volunteers and alcohol intoxicated patients enrolled in the study are summarised in Table 2. All volunteers were healthy. Patients were admitted to the emergency department for excessive alcohol consumption, besides this they didn't have any acute or chronic disease. Smokers were not enrolled in this study, since cigarette smoke itself can decrease CFTR function[1]. The laboratory parameters (Table 2., including markers of fluid loss) of the two groups were not significantly different and were within normal range, except the serum sodium level, which was slightly elevated in the alcohol intoxicated patients. It was shown that excessive alcohol consumption could alter the thermoregulatory responses and thermal sensations during mild heat exposure in humans and that it can increase the skin blood flow and sweating[2]. On the other hand chronic alcohol consumption was shown to alter the autonomic nervous system, which might decrease the sweat production[3]. In our experiments we didn't experience any changes in sweat response to pilocarpine stimulation.

Collection of sweat samples. Pilocarpine iontophoresis was conducted according to the method of Gibson and Cooke [4] using Macroduct system (Wescor, Logan, UT). Sweat chloride

concentration (Cl^-_{sw}) was determined by conductance measurement using Wescor Sweat ChekTM 3100.

Collection of serum samples. Simultaneously with the sweat test 5 ml blood was drawn into a native yellow tube. After coagulation the samples were centrifuged (3000 RCF, 10 min, 4°C) and stored at -20°C. Serum alcohol levels were measured by routine laboratory test.

Determination of the effect of ethanol on sweat Cl^- concentration in self-controlled experiment. Studies were conducted on 21 healthy volunteers. Subjects were asked to refrain from ethanol intake 24 h before the experiment. Blood samples were taken before (-45 min) and after (90, 120, 240, 300 min), while sweat samples were taken before and 90 min after alcohol consumption. Ethanol intake was calculated using the updated Widmark's formula [5] for each individual.

Genotyping R117H and deltaF508 variants of CFTR. Genomic DNA was isolated from 300µl EDTA-blood using QIAamp DNA Blood mini kit (Qiagen, Hilden, Germany). Primers were designed according to the genomic sequence of CFTR on chromosome 7 (GenBank: NC_000007.14) (see primer sequences in Table.3.). PCR was performed in a total volume of 30µl, which contained 0.5 U HotStarTaq DNA Polymerase (Qiagen), 1.5mM $MgCl_2$, 0.2mM dNTP, 0.5µM of each primer and 10-50ng genomic DNA. Amplification was performed under the following cycle conditions: 95°C for 5 min to activate the enzyme, followed by 35 cycles of 30 s denaturation at 95°C, 30 s annealing at 60°C and 1 min extension at 72°C, with a final extension of 5 min. R117H variant was genotyped by sequencing. DeltaF508 PCR products were analysed on a 10% native polyacrylamide gel and electrophoresed for 3 h at 80 V. To visualise DNA fragments the gel was stained with ethidium bromide for 10 min. Good resolution of normal (113bp) and mutant allele (110bp) was achieved. None of the patients carried CFTR mutations (ΔF508CFTR, R117H).

Pancreatic tissue samples. Human pancreatic tissue samples were obtained from autopsy and surgical resection from pancreatic surgery. Control pancreatic tissue (n=5) were from tumour free tissue surrounding neuroendocrine pancreatic tumours. Tissue samples from acute pancreatitis patients (n=5) were form autopsy and from surgical resections. The average age of the group was 56±2.8 and male:female ratio 1.5:1. All patients presented elevated serum lipase and liver enzyme levels and a history of alcohol consumption. Tissue samples from chronic pancreatitis patients (n=5) were from surgical resections. The average age of the group was 56.8±2.8 and male:female ratio 4:1. All patients presented elevated serum liver enzyme levels and a history of alcohol consumption.

*Quantitative real time RT-PCR.*CFTR mRNA expression of human pancreatic tissue was investigated using tissue samples from control patients or patients suffering from acute or chronic alcohol-induced pancreatitis. Total RNA was isolated from three 10µm thick sections cut from the formalin fixed, paraffin embedded tissue block applying Qiagen RNeasy FFPE Kit (Qiagen, Hilden, Germany). 1µg total RNA from each sample was submitted to revers transcription applying High Capacity RNA-to-CDNA kit (Applied Biosystems, Foster City, CA) according to the manufacturer's guide. Real-time PCR was performed by ABI PRISM 7000 (Applied Biosystems, Foster City, CA) using duplicates of 100 ng cDNA and TaqMan Gene Expression Assay primers (Applied Biosystems, Foster City, CA, Catalog Number: 4331182) for CFTR (ID: Hs00357011_m1), Na^+/K^+-ATPase (ID: Hs00167556_m1) and the control gene 18S rRNA (ID: Hs99999901_s1). The expression rate was calculated by the 2^{dCT} method.

Immunohistochemistry. Paraffin embedded, 3-4 µm thick sections of surgically removed resection specimens and autopsy tissue samples were used for immunohistochemistry. After deparaffination with EZ Prep Concentrate 10X (Ventana Medical Systems, Tucson, AZ), endogen peroxidase blocking and antigen retrieval (CC1, Ventana Medical Systems, Tucson,

AZ) monoclonal CFTR anti-C-terminal antibody (Millipore MA, USA; 1:300 dilution; incubation at 42°C for 30 min) anti-Na/K ATPase (Clone H3, Santa-Cruz, Dallas, USA; 1:6000; incubation at 42°C for 30 min). The immunohistochemical staining was carried out with HRP multimer based, biotin-free detection technique according to the protocol of automated Ventana system (Ventana Benchmark XT automate, Ventana Medical Systems, Tucson, AZ). For visualisation UltraView™ Universal DAB Detection Kit was applied (Ventana Medical Systems, Tucson, AZ). Sections from human pancreas were used as positive controls. For negative control, primary antibodies were substituted with Antibody diluent (Ventana Medical Systems, Tucson, AZ). The stained slides were digitalized with Mirax Pannoramic MIDI and Mirax Pannoramic SCAN digital slide scanners (3DHistech Ltd, Budapest, Hungary).

Calculation of Relative Optical Density. ImageJ program (National Institutes of Health, Bethesda, MD) was used to calculate Relative optical (RO) density. Pixel values (PV) were normalized to erythrocyte density in all cases. RO-Density value was calculated from the RO-Density = $\log_{10}(255/PV_{Norm})$ equation as described earlier, assuming that the brightest value in the image equals 255 [6].

Cell and animal studies

Animals, pancreatic ductal cell isolation and cell culturing

Mice. CFTR knockout mice were originally generated by Ratcliff et al. [7] and was a kind gift of Ursula Seidler [8]. The mice were congenic on the FVB/N background. No wild-type CFTR protein is made by the null CF mice, since the hypoxanthine phosphoribosyl transferase (HPRT) cassette disrupts the *cftr* coding sequence and introduces a termination codon, and none of the possible RNA transcripts from the disrupted locus can encode a functional CFTR

protein. Genotyping was performed by RT-PCR. The animals were kept at a constant room temperature of 24°C with a 12 h light–dark cycle and were allowed free access to specific CFTR chow and drinking solution in the Animal Facility of the First Department of Medicine, University of Szeged. The mice received electrolyte drinking solution containing polyethylene glycol (PEG) and high HCO_3^- (in mM: 40 Na_2SO_4, 75 $NaHCO_3$, 10 NaCl, 10 KCl, 23 g l^{-1} PEG 4000), and a fibre-free diet (Altromin, C1013) to allow survival beyond weaning. All mice were genotyped prior to the experiments. Wild type (WT) refers to the +/+ littermates of the CFTR knockout mice. The mice used in this study were 6-8 weeks old and weighted 20-25 grams, the gender ratio was 1:1 for all groups.

Guinea pig. 4-8 week-old guinea pigs were sacrificed by cervical dislocation and intra/interlobular ducts were isolated by enzymatic digestion and microdissection from the pancreas and cultured overnight as previously described [9]. Single pancreatic ductal cells were isolated as described previously [10].

Cell cultures. Capan-1 cells were obtained from the American Type Culture Collection (HTB-79, ATCC, Manassas, VA) and were used for experiments between 20-60 passages. Cells were cultured according to the distributors' instruction. For the intracellular pH (pH_i) measurements, $5x10^5$ cells were seeded onto polyester permeable supports (12mm-diameter, 0.4mm pore size Transwells; Corning, NY, USA). Cell confluence was checked by light microscopy and determination of transepithelial electrical resistance (TER) using EVOM-G Volt-Ohm-Meter (World Precision Instruments, Sarasota, FL). Experiments were performed after the TER of the monolayer had increased to at least 50 Ωcm^2 (after subtraction of the filter resistance). For intracellular Ca^{2+} concentration ($[Ca^{2+}]_i$) or intracellular ATP level ($(ATP)_i$) measurements $5x10^5$ cells were seeded onto 24mm-diameter cover glasses and for confocal imaging to assess mitochondrial membrane potential ($(\Delta\Psi)_m$) $2.5x10^5$ cells were

seeded onto glass bottom dishes (Mattek, Ashland, USA) and were grown until ~60-80% confluency.

For FRET based cAMP measurements Human Embryonic Kidney (HEK) 293 cells (ATCC, Manassas, VA) were grown in Dulbecco's Modified Eagle Medium (DMEM) (Invitrogen, Carlsbad, CA) supplemented with 10% fetal bovine serum (Invitrogen, Carlsbad, CA), L-glutamine, penicillin and streptomycin at 37°C under 5% CO_2. Cells were plated on 24mm glass coverslips and at 80–90% confluence were transiently transfected with the FRET-based sensor Epac1-camps [11], using Lipofectamine transfection reagent according to the manufacturer's protocol. FRET imaging was conducted 24 h later. In these series of experiments 100µM POA were used since 200µM induced immediate detachment of HEK cells from the cover glass. At the end of the experiments supraphysiological concentrations of forskolin was added combined with 100µM 3-isobutyl-1-methylxanthine (IBMX) to induce maximal increase in cAMP.

For CFTR cell surface stability and ER folding measurements Madin-Darby canine kidney (MDCK) type II cells stably expressing CFTR-3HA variants under a tetracycline-responsive promoter were generated by lentivirus transduction using the Lenti-X TetON Advanced Inducible Expression System (Clontech, Mountain View, CA) under puromycin (3 µg/ml) and G418 selection (0.2 mg/ml), grown in DMEM (Invitrogen, Carlsbad, CA) supplemented with 10% FBS (FBS), as specified before (6). For all experiments, epithelial cells were cultured at confluence for 4 days in the presence of 500 ng/ml of doxycycline in order to induce expression of CFTR-3HA.

Magnetic resonance imaging of the exocrine pancreatic fluid secretion

Magnetic resonance imaging (MRI) was performed to measure the pancreatic exocrine function as described previously [12, 13]. Quantification of duodenal filling after secretin

stimulation was observed in 6 wild type and 6 CFTR knockout mice before and 24 hours after intraperitonal injection with the mixture of 1.75 g/kg ethanol and 750 mg/kg palmitic acid (PA). Animals were allowed free access to pineapple juice instead of water 12 hours before the MRI examination. MRI was performed in a 7.1 Tesla animal scanner (Bruker, Ettlingen, Germany). Strong T2-weighted series of the complete abdomen were acquired before and after retroorbital injection of secretin (ChiroStim, ChiRhoClin, Burtonville MD, USA) in a dose of 10 IU units/kg/body. The time between injection and MRI was six minutes. The sequences were acquired using the image parameters: TR/TE 4400/83ms; flip angle: 180°; matrix 256x256; field of view 40x40mm; bandwidth 315hz/pixel; slice thickness 1mm; 20 slices. All image analyses were performed using Osirix (version 5; Pixameo, Bernex, Switzerland). First, we reduced image noise to minimize artefacts in images. Second, fluid excretion into the small intestine was segmented in each slice. Care was taken to avoid artefacts caused by magnetic inhomogeneity and motion especially bowel motion. The volume of intestinal fluid was assessed before and after secretin stimulation. From these data total extracted volume (TEV) was assessed.

Measurement of pancreatic fluid secretion

In vitro. Fluid secretion into the closed luminal space of the cultured guinea pig pancreatic ducts was analysed using a swelling method developed by Fernandez-Salazar et al.[14]. Briefly, the ducts were transferred to a perfusion chamber (0.45 ml) and were attached to a coverslip precoated with poly-L-lysine in the base of the chamber. Bright-field images were acquired at 1 min intervals using a CCD camera (CFW 1308C, Scion Corporation, Frederick, MD, USA). The integrity of the duct wall was checked at the end of each experiment by perfusing the chamber with a hypotonic solution (standard HEPES-buffered solution diluted 1:1 with distilled water). Digital images of the ducts were analysed using Scion Image software (Scion

Corporation, Frederick, MD, USA) to obtain values for the area corresponding to the luminal space in each image.

In vivo. In vivo pancreatic fluid secretion was assessed in mice before and 24 hours after intraperitonal injection with the mixture of 1.75 g/kg ethanol and 750 mg/kg palmitic acid (PA). Mice were anesthetized with 1.5 g/kg urethane by i.p. injection. The body temperature of mice was maintained by placing the animals on a warm pad (37°C) during the experiments. The abdomen was opened, and the lumen of the common biliopancreatic duct was cannulated with a blunt-end 31-gauge needle. Then the proximal end of the common duct was occluded with a microvessel clip to prevent contamination with bile, and the pancreatic juice was collected in PE-10 tube for 30 min. Using an operating microscope, the jugular vein was cannulated for i.v. administration of secretin (0.75CU/kg) and the pancreatic juice was collected for an additional 120 min.

In vitro measurement of pH_i, $[Ca^{2+}]_i$, $(ATP)_i$ and $(\Delta\Psi)_m$ and cAMP

Isolated guinea pig pancreatic ducts, or Capan-1 cells were incubated in standard HEPES solution and loaded with BCECF-AM (1.5μmol/L), Fura2-AM (2.5μmol/L), MgGreen-AM (5μmol/L), or TMRM (100nmol/L) respectively for 30 min at 37°C. The Transwells or cover glasses were then transferred to a perfusion chamber mounted on an IX71 inverted microscope (Olympus, Budapest, Hungary). The measurements were carried out as described previously[6, 15, 16]. In situ calibration of pH_i in Capan-1 cells (measured with BCECF) was performed using the high K^+-nigericin technique [17]. The initial pH_i of Capan-1 cells was 7.31±0.02. During the experiments the apical and the basolateral membrane of the Capan-1 PDEC were perfused separately, which allowed us to selectively change the composition of the apical or basolateral solutions. The HCO_3^- efflux across the luminal membrane was determined as described previously[18]. Briefly, cells were exposed to 20mM NH_4Cl in HCO_3^-

/CO_2-buffered solution from the basolateral and luminal side, which produced an immediate increase in pH_i due to the rapid influx of NH_3 across the membrane. After the alkalisation, there was a recovery in pH_i toward the basal value, which depends on the HCO_3^- efflux (ie, secretion) from the duct cells via SLC26 Cl^-/HCO_3^- anion exchanger and CFTR. In this study, the initial rate of recovery from alkalosis (dpH/dt) over the first 30s from the highest pH_i value obtained in the presence of 20mM NH_4Cl was calculated as described previously [18]. The apical Cl^-/HCO_3^- exchange activity was also measured using the luminal Cl^- withdrawal technique. The removal of Cl^- from the apical extracellular solution induced pH_i increase in PDEC by driving HCO_3^- via the basolateral pNBC1 and the apical SLC26 Cl^-/HCO_3^- exchangers (CBE) into the cells, whereas, re-addition of Cl^- decreased pH_i inducing secretion of HCO_3^- via the CBE and the CFTR Cl^- channel. In this study the rate of pH_i decrease (acidification) after luminal Cl^--readdition was calculated by linear regression analysis of pH_i measurements made over the first 30 s after exposure to the Cl^--containing solution [19]. The total buffering capacity ($ß_{total}$) of Capan-1 cells was estimated according to the NH_4^+ pulse technique as described previously [18].

For $(\Delta\Psi)_m$ measurements confocal imaging was performed using Fluoview 10i-W system (Olympus, Budapest, Hungary). Glass bottom petri dishes were perfused continuously with solutions containing 100nmol/L TMRM at 37^{o}C at a rate of 2-2.5ml/min. 5-10 ROIs (mitochondria) of 5-10 cells were excited with light at a given wavelengths. Excitation of TMRM was 543nm and the emitted light was captured between 560–650nm to follow the changes of $(\Delta\Psi)_m$ [20].

FRET imaging experiments were performed 24h after HEK293 cells transfection with Epac1-camps sensor. Cells were maintained at room temperature in the Ringer saline and imaged on an inverted microscope (Olympus IX71) with a 60xNA1.3 oil-immersion objective (Olympus). The microscope was equipped with a CCD camera (Coolsnap) and a beam-splitter

optical device (Optosplit, CAIRN). Images were acquired using Metaphluor software. FRET changes were measured as changes in the background-subtracted 480/545-nm fluorescence emission intensity on excitation at 430 nm and expressed as either R/R0, where R is the ratio at time t and R0 is the ratio at time = 0 sec, or ΔR/R0, where ΔR = R – R0.

Electrophysiology

Single PDEC and Capan-1 cells were prepared as described above. Few drops of cell suspension were placed into a perfusion chamber mounted on an inverted microscope (TMS; Nikon, Tokyo, Japan) and allowed to settle for 30 min. Patch clamp micropipettes were fabricated from borosilicate glass capillaries (Clark, Reading, UK) by using a P-97 Flaming/Brown micropipette puller (Sutter Co, Novato, CA). The resistances of the pipettes were between 2.5-4MΩ. Membrane currents were recorded with an Axopatch1D amplifier (Axon Instruments, Union City, CA) using whole cell at 37°C. After establishing a high-resistance seal (1–10GΩ) by gentle suction, the cell membrane beneath the tip of the pipette was disrupted. The series resistance was typically 4-8MΩ before compensation (50%–80%, depending on the voltage protocol). Current-voltage (I/V) relationships were obtained by holding Vm at 0mV and clamping to ±100mV in 20mV increments. Membrane currents were digitized by using a 333-kHz analog-to-digital converter (Digidata1200; Axon Instruments) under software control (pClamp6; Axon Instruments). Analyses were performed by using pClamp6 software after low-pass filtering at 1kHz [6].

Quantitative real-time reverse transcription polymerase chain reaction (qPCR)

Total RNA was purified from individual cell culture samples (from 10^6 cells) using the RNA isolation kit of Macherey-Nagel (Macherey-Nagel, Düren, Germany). All the preparation steps were carried out according the manufacturer's instructions. RNA samples were stored at

–80°C in the presence 30U of Prime RNAse inhibitor (Thermo Scientific, Szeged, Hungary) for further analysis. The quantity of isolated RNA samples was evaluated by spectrophotometry (NanoDrop 3.1.0, Rockland, DE, USA). In order to monitor gene expression, qPCR was performed on a RotorGene 3000 instrument (Corbett Research, Sydney, Australia) using the TaqMan probe sets of CFTR gene (Applied Biosystems Foster City, CA, USA). 3µg of total RNA was reverse transcribed using the High-Capacity cDNA Archive Kit (Applied Biosystems Foster City, CA, USA) according to the manufacturer's instructions in a final volume of 30µl. The temperature profile of the reverse transcription was as follows: 10min at RT, 2 h at 37°C, 5min on ice, 10min at 75°C for enzyme inactivation in a Thermal Cycler machine (MJ Research Waltham, MA, USA). After dilution with 30µl of water, 1µl of the diluted reaction mix was used as template in the qPCR. For all the reactions TaqMan Universal Master Mix (Applied Biosystems Foster City, CA, USA) were used according to the manufacturer's instructions. Each reaction mixture (final volume 20µl) contained 1µl of primer-TaqMan probe mix. Gene expression assay identification No for CFTR: Hs00357011_m1 and HPRT: Hs03929098_m1. The qPCR reactions were carried out under the following conditions: 15min at 95°C and 45 cycles of 95°C for 15sec, 60°C for 1min. Fluorescein dye intensity was detected after each cycle. Relative expression ratios were calculated as normalized ratios to human Hypoxanthine-guanine phosphoribosyltransferase (HPRT) internal control gene. Non-template control sample was used for each PCR run to check the primer-dimer formation. The final relative gene expression ratios were calculated as ΔCt values (Ct values of gene of interest versus Ct values of the control gene).

Immunofluorescence

Cultured cells. For CFTR immunostaining Capan-1 cells were rinsed twice with phosphate buffered saline (PBS) and fixed in 4% paraformaldehyde (PFA) for 5 min at RT, followed by

20 min permeabilisation in 0.1%Triton X-100. Nonspecific antibody binding was blocked with 10% goat serum and 1% BSA for 60min at RT. For CFTR detection cells were incubated with anti-NBD2 monoclonal primary CFTR antibody obtained from CF Foundation (Coding No.: 596) [21] (1:100) overnight on 4°C. After this the cells were washed and incubated with anti-mouse FITC conjugated secondary antibody (Dako, Denmark) for 2 h at RT. The nuclei of the cells were stained with Hoechst 33342 (5µg/ml) for 20 min. The images were captured using Olympus Fluoview10i-W system.

Guinea pig pancreatic tissue. To detect the effects of ethanol and FA on CFTR expression and localisation we used guinea pig as an *in vivo* model. The animals were kept at a constant room temperature of 24°C with a 12 h light–dark cycle and were allowed free access to chow and water. Guinea pigs were treated with a mixture of 0.8g/kg ethanol (Reanal; Budapest, Hungary) and 300mg/kg palmitic acid (PA) intraperitoneally (*i.p.*). Before the ethanol and PA treatment the animals were injected with 1.2ml physiological saline to avoid ethanol-induced peritoneal irritation. The control animals were treated with 2x1.2ml physiological saline *i.p.* The animals were sacrificed 3, 6, 12 and 24 h after the injection in pentobarbital (37mg/kg *i.p.*) anaesthesia. From frozen samples of guinea pig pancreas 5µm thick sections were cut and placed on silanized slides and fixed in 2% paraformaldehyde solution for 15 min. After washing in 1% TBS solutions slides were stored in 1% BSA-TBS for non-specific antigen blocking. Primary antibody „Mr Pink" (rabbit polyclonal antibody against human CFTR, CFTR Folding Consortium[22, 23]) was applied in a dilution of 1:100 in 1%BSA TBS for overnight in 4°C then secondary anti rabbit antibody (Alexa Fluor 488; host: goat; Invitrogen Eugene, Oregon USA – A11034) was used in a dilution of 1:400 for 3 h. at RT. DAPI nuclear staining was performed in a dilution of 1:100 for 20 min. at RT. Between steps careful TBS washings were applied. Finally, slides were coverslipped by DAKO Fluoromount (Glostrup, Denmark). RO-density was calculated as described above.

Detection of CFTR cell surface density, stability and ER protein folding

Immunoblotting. MDCK membrane proteins were solubilised in RIPA buffer (150 mM NaCl, 20 mM Tris-HCl, 1% (w/v) Triton X-100, 0.1% (w/v) sodium dodecyl sulfate (SDS) and 0.5% (w/v) sodium deoxycholate, pH 8.0) supplemented with protease inhibitors (10µg/ml leupeptin and pepstatin, 0.5mM PMSF) and loaded on a 7% SDS-PAGE gel. Immunoblotting was done with monoclonal anti-HA (Covance, Montreal, Canada) and anti-Na/K ATPase (Clone H3, Santa-Cruz, Dallas, USA). Densitometry analysis was performed using ImageQuantL software (GE Healthcare).

Cell surface density and stability measurement of CFTR. The cell surface expression of CFTR-3HA was measured by quantifying the specific binding of mouse anti-HA primary antibody to MDCK cells by ELISA as described previously [24]. Cells were seeded in 24-well plates at a density of $8x10^4$ cells/well and induced for CFTR-3HA expression. Treatment with ethanol, POA or POAEE was carried out for 48 h at the indicated concentrations.

Pulse-chase experiments. Experiments were performed as previously described [25]. MDCK cells were cultured as specified and treated previously for 48 h with ethanol, POA or POAEE, as well as during the pulse and chase periods.

Mouse model of acute alcohol-induced pancreatitis

Acute pancreatitis induction. The mouse model of acute alcohol-induced pancreatitis was originally developed by Huang et al [26]. We modified the original protocol and applied one injection, instead of two, since the mice in our hand tolerated this treatment better. WT and CFTR KO mice were treated with a mixture of 1.75 g/kg ethanol and 750 mg/kg PA *i.p.*. Before the ethanol and PA treatment mice were injected with 200µl physiogical saline to avoid ethanol-induced peritoneal irritation. The control mice were treated 2x200µl

physiological saline *i.p.* Using the modified protocol no mortality was observed in the different groups. The mice were sacrificed 24 h after the ethanol and PA treatment by exsanguination through the heart in pentobarbital (85mg/kg *i.p.*) anaesthesia. To determine the serum amylase activity, blood was collected from the heart. All blood samples were centrifuged at 2500g for 15 min and the serum was stored at -20°C. The pancreas was quickly removed, trimmed from fat and lymph nodes, and frozen in liquid nitrogen and stored at -80°C until use.

Pancreatic water content. Pancreata were dried for 24 h at 100 ºC. Dry weight and wet weight ratio (100*(wet weight-dry weight)/wet weight) was calculated.

Immunohistochemistry. Pancreatic injury was evaluated by semiquantitative grading of interstitial oedema, and leukocyte infiltration in a double blinded manner by two independent reviewers. The extent (%) of cell necrosis was confirmed by analysis with ImageJ software (NIH, Bethesda, MD, USA) as described earlier [23].

Amylase activity. Serum amylase activity was measured using a colorimetric kinetic method (Diagnosticum, Budapest, Hungary).

Ethical Approvals

Experiments concerning human subjects. The scheme of the experiments complies with the ethics of research. It agrees with the declaration of the Medical World Federation proclaimed in Helsinki in 1964. Before enrolment each volunteer/patient was given a detailed explanation on the nature, possible consequences and side effects of the study by a physician, after this they signed a written informed consent. Patients who had temporarily impaired judgement due to the effect of alcohol (patients admitted to the ER units) were repeatedly given a detailed briefing after they sobered and then gave an informed consent again. Unconscious intoxicated patients were not enrolled in the study.

REFERENCES

1. Raju SV, Jackson PL, Courville CA, et al. Cigarette Smoke Induces Systemic Defects in Cystic Fibrosis Transmembrane Conductance Regulator (CFTR) Function. Am J Respir Crit Care Med 2013. 88(11):1321-30
2. Yoda T, Crawshaw LI, Nakamura M, et al. Effects of alcohol on thermoregulation during mild heat exposure in humans. Alcohol 2005;36:195-200.
3. Chida K, Takasu T, Kawamura H. Changes in sympathetic and parasympathetic function in alcoholic neuropathy. Nihon Arukoru Yakubutsu Igakkai Zasshi 1998;33:45-55.
4. Gibson LE, Cooke RE. A test for concentration of electrolytes in sweat in cystic fibrosis of the pancreas utilizing pilocarpine by iontophoresis. Pediatrics 1959;23:545-9.
5. Watson PE, Watson ID, Batt RD. Prediction of blood alcohol concentrations in human subjects. Updating the Widmark Equation. J Stud Alcohol 1981;42:547-56.
6. Pallagi P, Venglovecz V, Rakonczay Z, Jr., et al. Trypsin reduces pancreatic ductal bicarbonate secretion by inhibiting CFTR Cl(-) channels and luminal anion exchangers. Gastroenterology 2011;141:2228-2239 e6.
7. Ratcliff R, Evans MJ, Cuthbert AW, et al. Production of a severe cystic fibrosis mutation in mice by gene targeting. Nat Genet 1993;4:35-41.
8. Xiao F, Li J, Singh AK, et al. Rescue of epithelial HCO_3^- secretion in murine intestine by apical membrane expression of the cystic fibrosis transmembrane conductance regulator mutant F508del. J Physiol 2012;590:5317-34.
9. Argent BE, Arkle S, Cullen MJ, et al. Morphological, biochemical and secretory studies on rat pancreatic ducts maintained in tissue culture. Q J Exp Physiol 1986;71:633-48.
10. Venglovecz V, Hegyi P, Rakonczay Z, Jr., et al. Pathophysiological relevance of apical large-conductance Ca(2+)-activated potassium channels in pancreatic duct epithelial cells. Gut 2011;60:361-9.
11. Nikolaev VO, Gambaryan S, Engelhardt S, et al. Real-time monitoring of the PDE2 activity of live cells: hormone-stimulated cAMP hydrolysis is faster than hormone-stimulated cAMP synthesis. J Biol Chem 2005;280:1716-9.
12. Cendrowski J, Sanchez-Arevalo Lobo VJ, et al. Mnk1 is a novel acinar cell-specific kinase required for exocrine pancreatic secretion and response to pancreatitis in mice. Gut 2014. Jul 18. pii: gutjnl-2013-306068. doi: 10.1136/gutjnl-2013-306068. [Epub ahead of print]
13. Mensel B, Messner P, Mayerle J, et al. Secretin-stimulated MRCP in volunteers: assessment of safety, duct visualization, and pancreatic exocrine function. AJR Am J Roentgenol 2014;202:102-8.
14. Fernandez-Salazar MP, Pascua P, Calvo JJ, et al. Basolateral anion transport mechanisms underlying fluid secretion by mouse, rat and guinea-pig pancreatic ducts. J Physiol 2004;556:415-28.
15. Venglovecz V, Rakonczay Z, Jr., Ozsvari B, et al. Effects of bile acids on pancreatic ductal bicarbonate secretion in guinea pig. Gut 2008;57:1102-12.
16. Maleth J, Venglovecz V, Razga Z, et al. Non-conjugated chenodeoxycholate induces severe mitochondrial damage and inhibits bicarbonate transport in pancreatic duct cells. Gut 2011;60:136-8.
17. Hegyi P, Rakonczay Z, Jr., Gray MA, et al. Measurement of intracellular pH in pancreatic duct cells: a new method for calibrating the fluorescence data. Pancreas 2004;28:427-34.

18. Hegyi P, Gray MA, Argent BE. Substance P inhibits bicarbonate secretion from guinea pig pancreatic ducts by modulating an anion exchanger. Am J Physiol Cell Physiol 2003;285:C268-76.
19. Stewart AK, Yamamoto A, Nakakuki M, et al. Functional coupling of apical Cl^- /HCO_3^- exchange with CFTR in stimulated HCO3- secretion by guinea pig interlobular pancreatic duct. Am J Physiol Gastrointest Liver Physiol 2009;296:G1307-17.
20. **Baumgartner HK, Gerasimenko JV**, Thorne C, et al. Calcium elevation in mitochondria is the main Ca^{2+} requirement for mitochondrial permeability transition pore (mPTP) opening. Journal of Biological Chemistry 2009;284:20796-803.
21. Kreda SM, Mall M, Mengos A, et al. Characterization of wild-type and deltaF508 cystic fibrosis transmembrane regulator in human respiratory epithelia. Mol Biol Cell 2005;16:2154-67.
22. **Peters KW, Okiyoneda T,** Balch WE, et al. CFTR Folding Consortium: methods available for studies of CFTR folding and correction. Methods Mol Biol 2011;742:335-53.
23. **Pallagi P, Balla Z, Singh AK,** et al. The role of pancreatic ductal secretion in protection against acute pancreatitis in mice*. Crit Care Med 2014;42:e177-88.
24. Okiyoneda T, Barriere H, Bagdany M, Ret al. Peripheral protein quality control removes unfolded CFTR from the plasma membrane. Science 2010;329:805-10.
25. Rabeh WM, Bossard F, Xu H, et al. Correction of both NBD1 energetics and domain interface is required to restore DeltaF508 CFTR folding and function. Cell 2012;148:150-63.
26. **Huang W, Booth DM,** et al. Fatty acid ethyl ester synthase inhibition ameliorates ethanol-induced Ca^{2+}-dependent mitochondrial dysfunction and acute pancreatitis. Gut 2014;63:1313-24.

Author names in bold designate shared co-first authors.

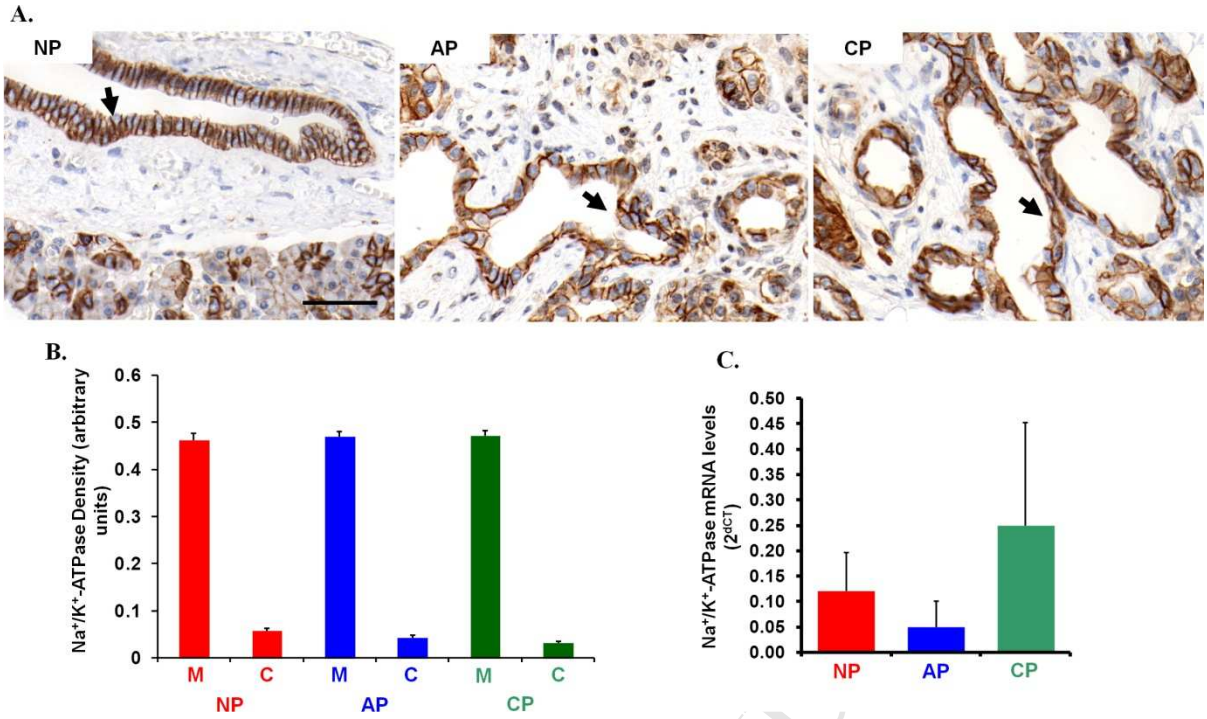

Supplementary Figure 1. The expression of Na^+/K^+-ATPase in human pancreas is not changed in acute or chronic pancreatitis. (A) Na^+/K^+-ATPase expression in human pancreas. Arrowheads point to the pancreatic ducts. NP: normal pancreas, AP: acute pancreatitis, CP: chronic pancreatitis; scale bar: 50µm. **(B) Relative density of Na^+/K^+-ATPase.** The density of Na^+/K^+-ATPase staining was not changed. C: cytoplasm, M: membrane; n: 5. **(C) Quantitative PCR analysis of Na^+/K^+-ATPase mRNA expression in the human pancreas.** Na^+/K^+-ATPase mRNA levels were not changed significantly. Data were normalized to 18rRNA and given as % of NP mRNA levels, n=5.

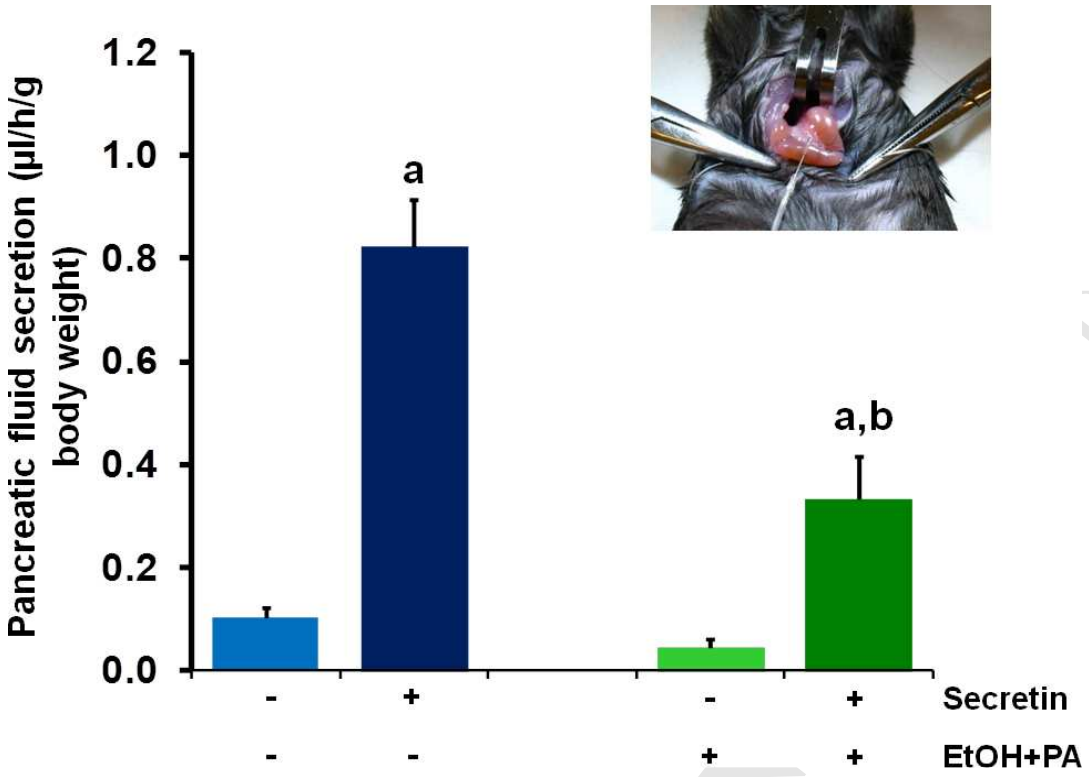

Supplementary Figure 2. Ethanol and fatty acids inhibit the pancreatic fluid secretion. *In vivo* pancreatic fluid secretion was directly measured in anesthetized mice. The i.p. injection of ethanol and palmitic acid (PA) significantly decreased both the basal (0.102±0.02µL/h/bwg vs. 0.045±0.016µL/h/bwg) and the secretin-stimulated (0.824±0.092µL/h/bwg vs. 0.334±0.082µL/h/bwg) pancreatic fluid secretion. n:6/group; a: $p<0.001$ vs control before secretion stimulation; b: $p<0.001$ vs secretin stimulated untreated group.

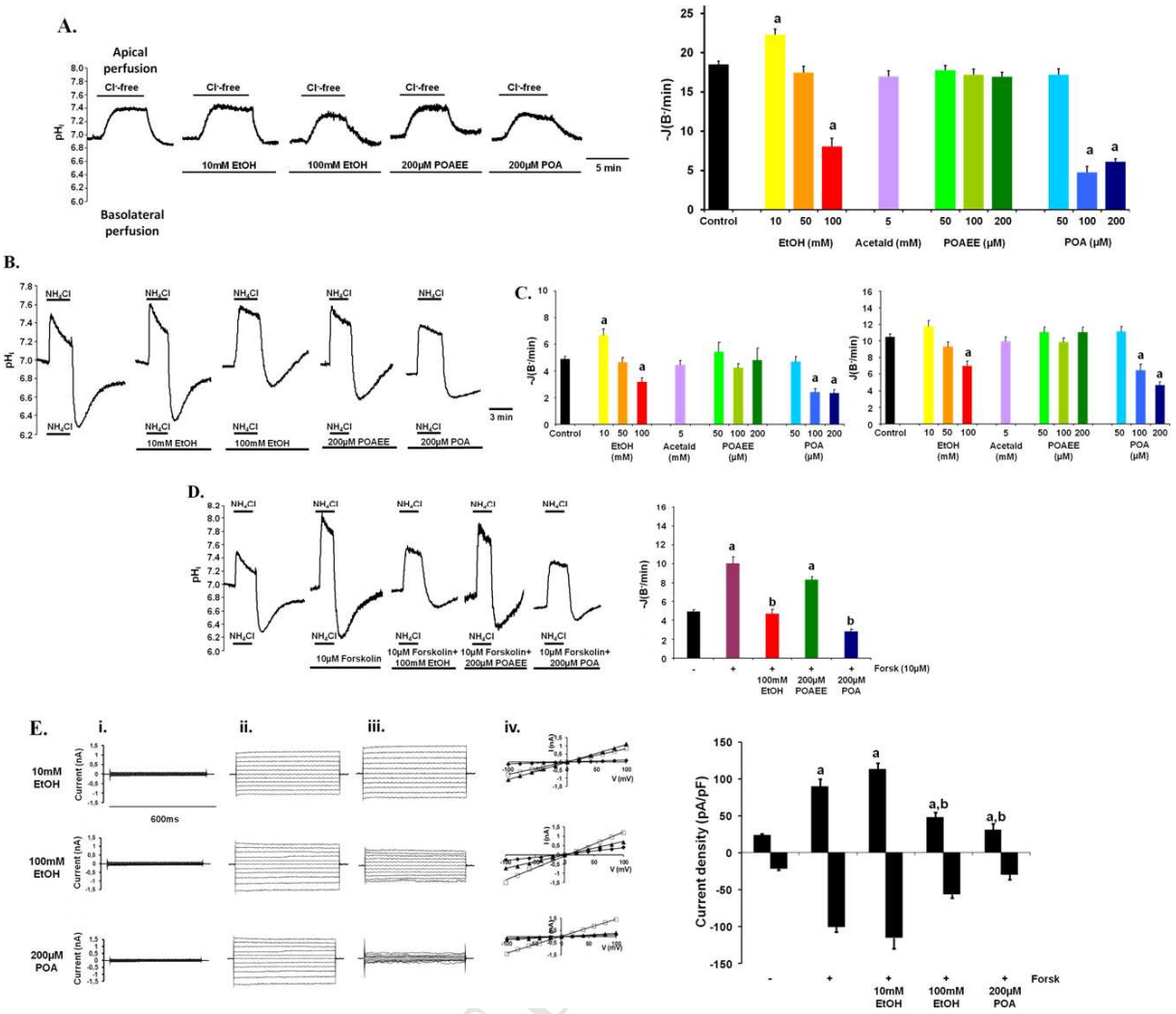

Supplementary Figure 3. (A) Representative pH_i traces and summary data of the initial rate of recovery after Cl^- re-addition showing the effect of basolateral administration of ethanol, acetaldehyde, palmitoleic acid ethyl ester (POAEE) and palmitoleic acid (POA) for 15 min on the pH_i recovery in Capan-1 pancreatic ductal cells. Cells were perfused separately from the apical and basolateral side with CO_2/HCO_3^- buffered solution. Labels above the traces indicate the Cl^- composition of the luminal solution and labels below the traces denote test compounds added to basolateral perfusion solution. The administration of 10mM ethanol significantly stimulated the activity of the luminal transporters. On the other hand, 100mM ethanol and 100-200µM POA significantly inhibited the recovery. Data are shown as means ± SEM. n= 3-5 exp for all groups. a: $p<0.05$ vs control. **(B-D) Representative pH_i traces and summary data of the initial rate of recovery from alkali and acid load under resting and stimulated conditions**. Alkali and acid load was induced by 20mM NH_4Cl in HCO_3^-/CO_2 buffered solution in Capan-1 cells. 10mM ethanol stimulated, whereas 100mM ethanol and high concentrations of POA significantly inhibited the activity of the luminal (recovery from alkali load; **C left panel**) and basolateral transporters (recovery from acid load; **C right panel**), and the forskolin-stimulated secretion **(D)**, respectively. Data are shown as means±SEM. n: 3-5 exp for all groups. a: $p<0.05$ vs Control. **(E) Representative fast whole cell CFTR Cl- current recordings from Capan-1 cells.** (i) Unstimulated currents, (ii)) currents after 10 min stimulation with 10µM forskolin (Forsk), and (iii) stimulated currents following 10 min exposure to 10mM or 100mM ethanol and 200µM POA (iv) I/V relationships (diamonds represent unstimulated currents, squares represent forskolin-

stimulated currents, and triangles represent forskolin stimulated currents in the presence of the tested agents). Summary of the current density (pA/pF) measured at Erev ±60 mV. Exposure of the Capan-1 cells to 10mM ethanol stimulated, however, 100mM ethanol or 200µM POA blocked the forskolin-stimulated CFTR Cl- currents. n=5-6 for all groups. a: $p<0.05$ vs basal current; b: $p<0.05$ vs forskolin-stimulated current.

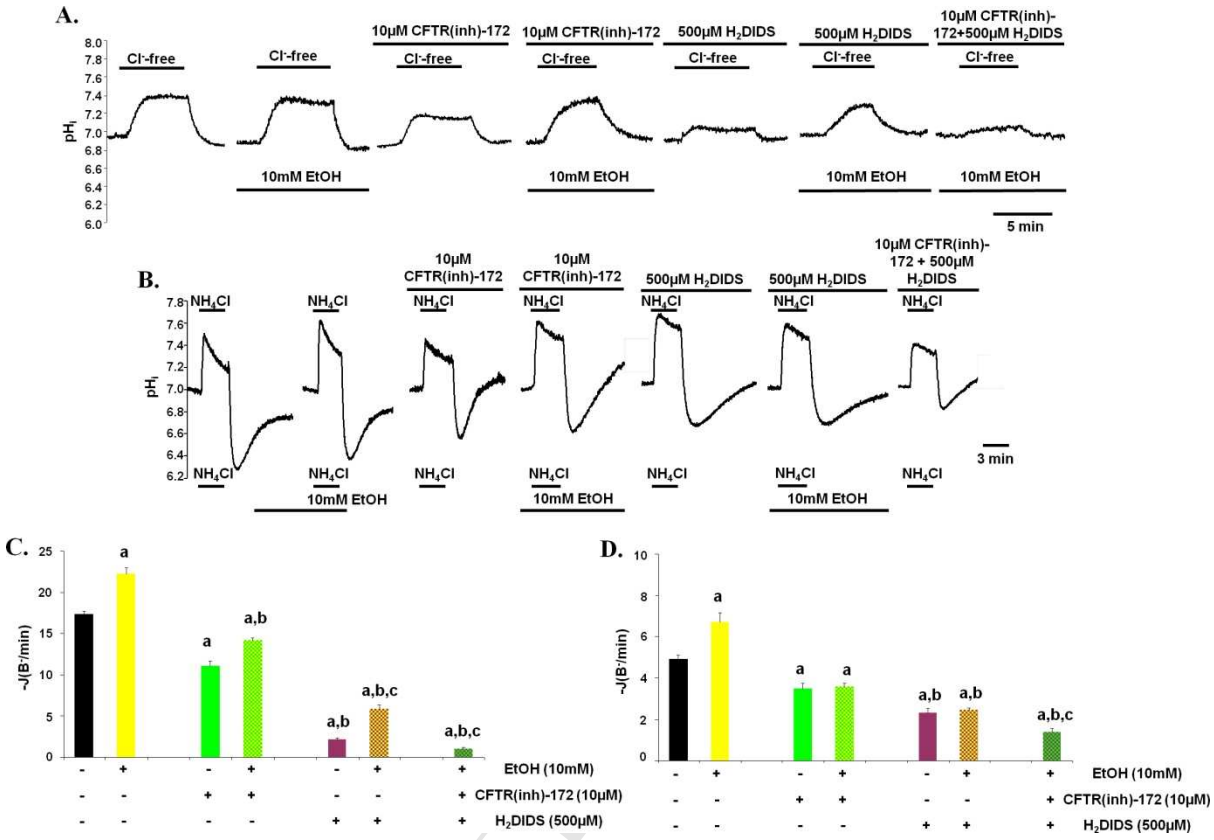

Supplementary Figure 4. Low concentration of ethanol stimulates the luminal CBE and CFTR in Capan-1 PDEC. Representative pH_i traces showing the effect of luminal administration of 500µM H_2DIDS and/or 10µM CFTR(inh)-172 in the presence or absence of 10mM ethanol on the pH_i recovery after **(A)** Cl^- re-addition or **(B)** after alkali load. **(C) Summary data of the initial rate of pH_i recovery after chloride re-addition.** The administration of 10µM CFTR(inh)-172 and 500µM H_2DIDS inhibited the recovery. 10mM ethanol stimulated the recovery in both cases. The combined administration of CFTR(inh)-172 and H_2DIDS abolished the stimulatory effect. These data suggest that low concentration of ethanol stimulate the activity of CBE and CFTR on the apical membrane of PDEC. **(D) Summary data of the initial rate of pH_i recovery after alkali load.** The administration of 10µM CFTR(inh)-172 and 500µM H_2DIDS inhibited the recovery. However 10mM ethanol failed to stimulate the recovery under these circumstances. Data are shown as means±SEM. n: 3-5 exp for all groups. a: $p<0.05$ vs Control; b: $p<0.05$ vs 10µM CFTR(inh)-172; c: $p<0.05$ vs 500µM H_2DIDS.

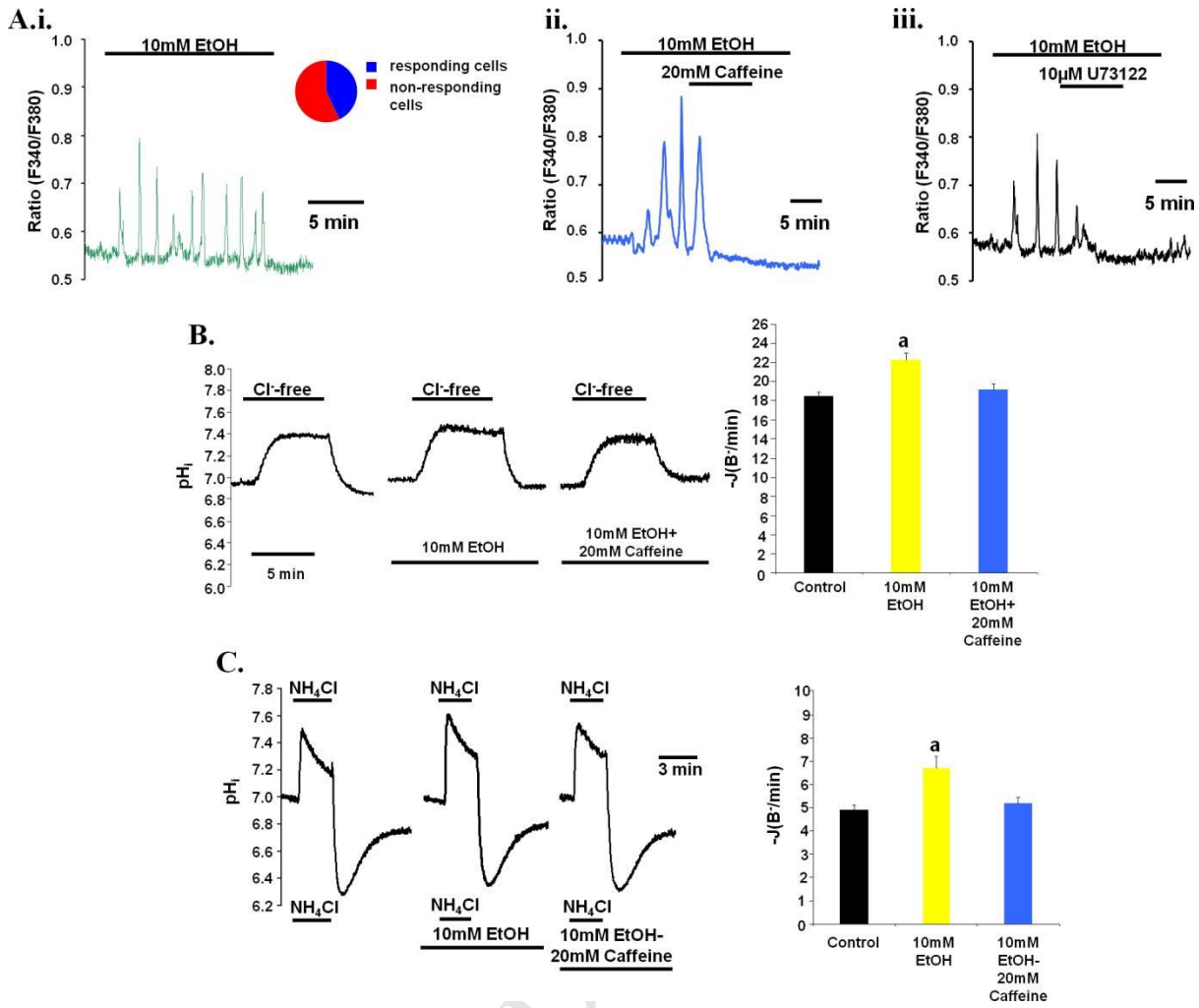

Supplementary Figure 5. The stimulatory effect of 10mM ethanol is mediated by intracellular Ca^{2+} elevation. (A) Representative curves shows the effect of low concentration of ethanol on the $[Ca^{2+}]_i$ of PDEC. (i) The administration of 10mM ethanol induced short lasting, repetitive Ca^{2+} spikes in the 43% of the cells. The Ca^{2+} oscillation induced by 10mM ethanol was abolished by (ii) 20mM caffeine and (iii) 10μM U73122. **(B) Representative curve and summary data** shows the effect of caffeine pretreatment on the ethanol-stimulated apical Cl^-/HCO_3^- exchange activity. caffeine abolished the stimulatory effect of low concentration of ethanol. **(C) Representative traces and summary data** showing the effect of the administration of Caffeine on the HCO_3^- secretion of PDEC. caffeine pretreatment abolished the stimulatory effect of 10 min administration of low concentration of ethanol on HCO_3^- secretion. Data are shown as means±SEM n: 3-5 exp for all groups. a: $p<0.05$ vs Control.

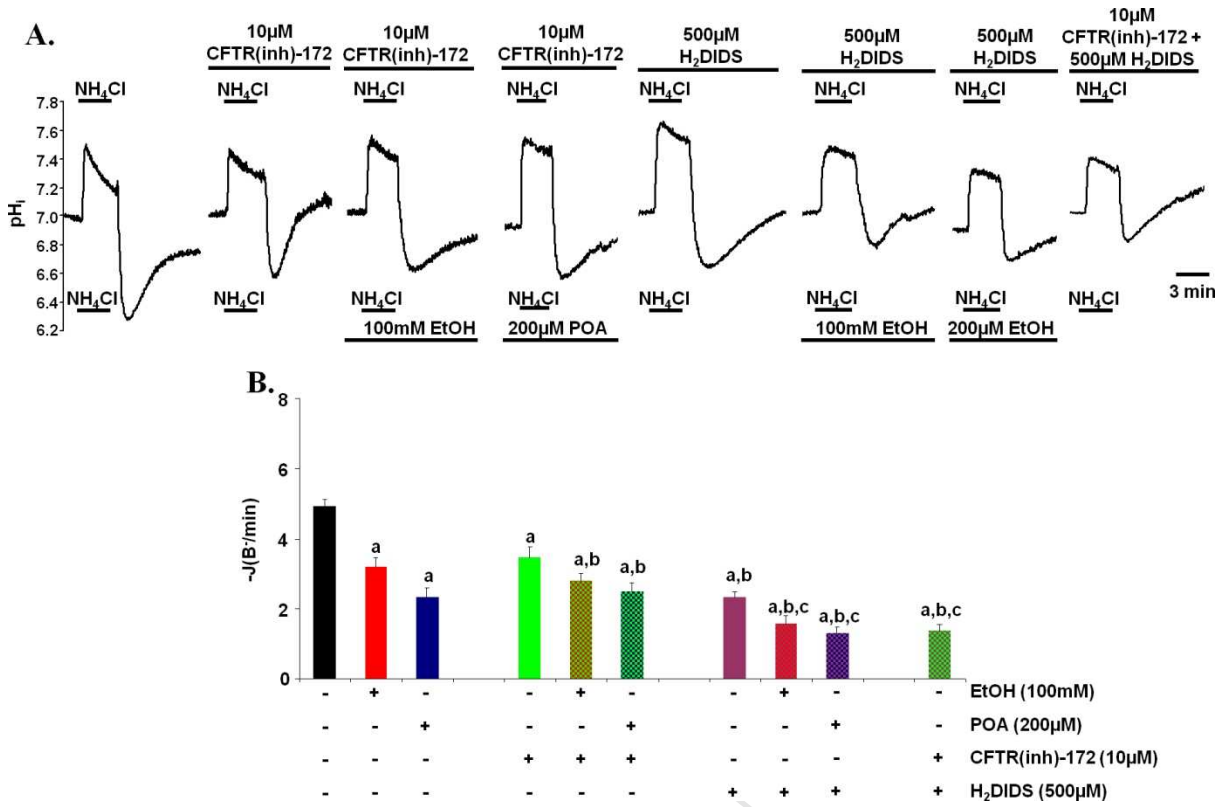

Supplementary Figure 6. High concentration of ethanol and fatty acids inhibit the luminal CBE and CFTR in Capan-1 PDEC. (A) Representative pH_i traces of the effects of the basolateral administration of 100mM ethanol or 200μM POA for 10 min in the presence or absence of 500μM H_2DIDS and/or 10μM CFTR(inh)-172 (luminal administration) on the pH_i recovery after alkali load in HCO_3^-/CO_2-buffered solution. **(B) Summary data of the initial rate of pH_i recovery after alkali load.** Our results further confirmed the inhibitory effect of ethanol and POA on CBE and CFTR. Data are shown as means±SEM.n: 3-5 exp for all groups. a: $p<0.05$ vs Control; b: $p<0.05$ vs 10μM CFTR(inh)-172; c: $p<0.05$ vs 500μM H_2DIDS.

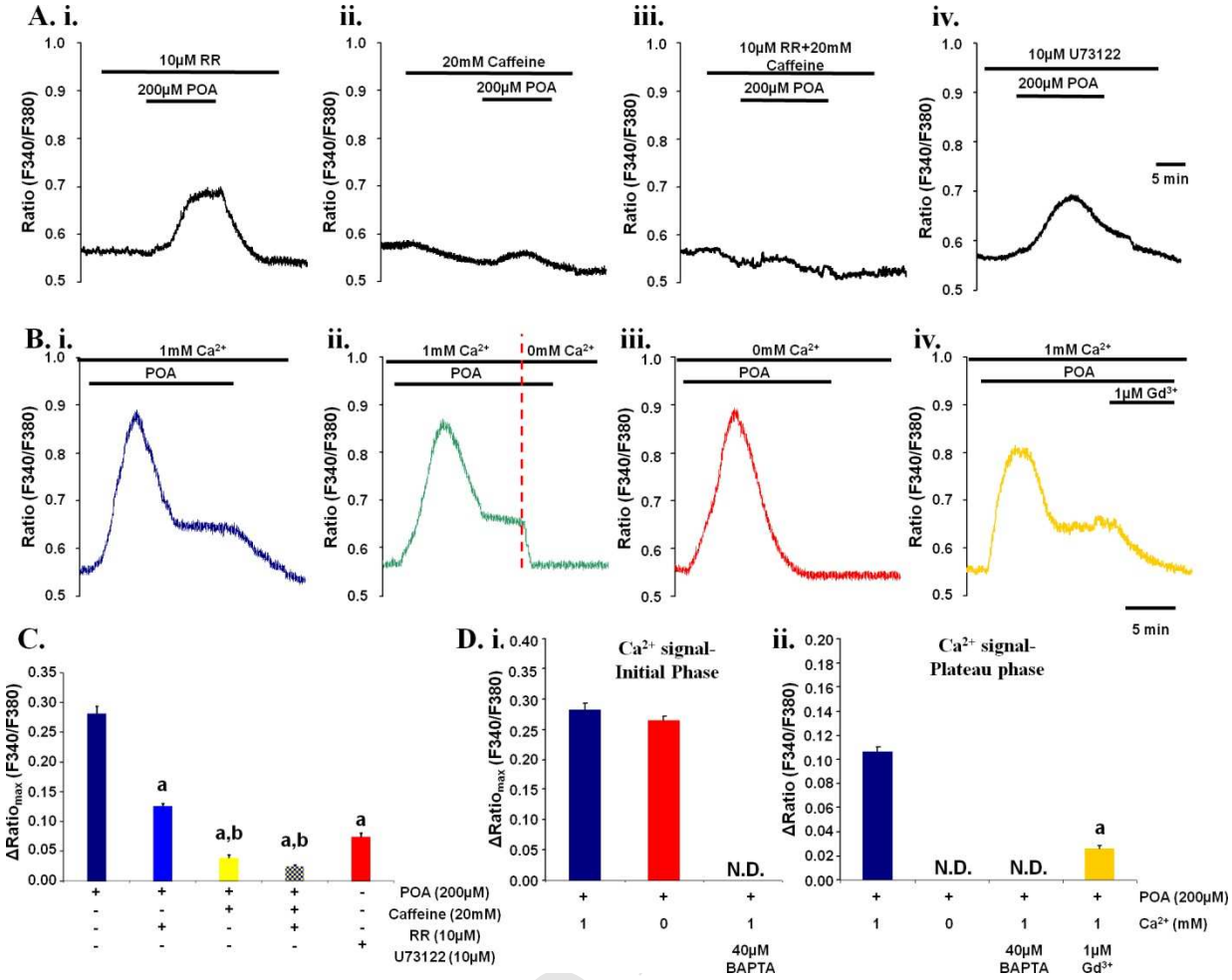

Supplementary Figure 7. (A) POA releases Ca^{2+} from the ER via IP_3R and RyR activation in Capan-1 PDEC. Representative curves show the effect IP_3R and RyR inhibition on the Ca^{2+} release induced by 200μM POA. The administration of (i) 10μM RR significantly decreased the effect of POA on $[Ca^{2+}]_i$ (55.5%), (ii) 20mM caffeine induced significantly higher inhibition (86.1%). (iii) The combined administration of RR and caffeine did not induce further inhibition (92.1%). (iv) The PKC inhibitor U73122 decreased the effect of POA similarly to caffeine (73.5%). **(B) The plateau phase of the POA-induced Ca^{2+} signal depends on extracellular Ca^{2+} influx. Representative curves** show the effect of the administration of **(i)** 200μM POA on $[Ca^{2+}]_i$. **(ii)** The removal of the extracellular Ca^{2+} during the plateau phase of the Ca^{2+} signal abolished the Ca^{2+} elevation. **(iii)** The plateau phase was completely absent in Ca^{2+}-free extracellular solution and **(iv)** was significantly inhibited by the administration of 1μM Gd^{3+}. **(C) Summary data of the $\Delta Ratio_{max}$.** The administration of RR, caffeine and U73122 significantly decreased the effect of POA on $[Ca^{2+}]_i$. Data are shown as means±SEM. n: 3-5 exp for all groups. a: $p<0.05$ vs Control; b: $p<0.05$ vs 10μM RR. **(D) (i) Summary data of the $\Delta Ratio_{max}$ of the initial phase of the POA-induced Ca^{2+} signal.** The effect of POA on the $\Delta Ratio_{max}$ was not affected by extracellular Ca^{2+} withdrawal. Pretreatment with 40μM BAPTA-AM for 30 min completely abolished the Ca^{2+} elevation. **(ii) Summary data of the ΔRatio of the plateau phase of the POA-induced Ca^{2+} signal.** The plateau phase of the POA induced Ca^{2+} signal was completely based on extracellular Ca^{2+} influx. Data are shown as means±SEM. n: 3-5 exp for all groups. N.D.: not detected. a: $p<0.05$ vs Initial phase; b: $p<0.05$ vs Plateau phase.

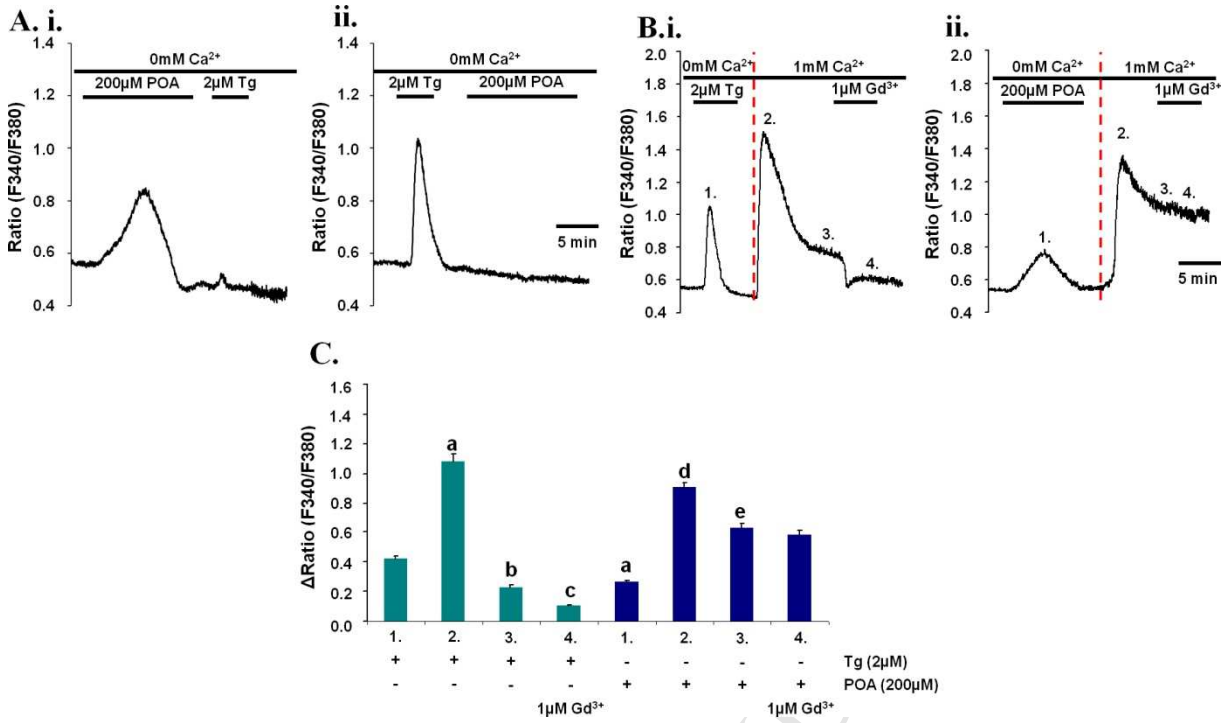

Supplementary Figure 8. (A) The administration of 200μM POA completely depletes the ER Ca^{2+} stores. **(i)** After the administration of 200μM POA the SERCA inhibitor thapsigarin (Tg) was not able to induce further Ca^{2+} release. **(ii)** Similarly, POA was not able to induce further Ca^{2+} release after Tg administration. **(B-C) The administration of 200μM POA induces store operated extracellular Ca^{2+} influx. (i)** The administration of 2μM Tg in Ca^{2+}-free extracellular solution depleted the ER Ca^{2+} store (1.). The re-addition of the extracellular Ca^{2+} induced rapid $[Ca^{2+}]_i$ elevation (2.) which was followed by a decrease and an equilibrium (3.). Gd^{3+} significantly decreased the Ca^{2+} influx (4.). **(ii)** The administration of 200μM POA in Ca^{2+}-free extracellular solution also depleted the ER Ca^{2+} store (1.) which was followed by $[Ca^{2+}]_i$ elevation after the re-addition of the extracellular Ca^{2+} (2.). The decrease after the maximal Ca^{2+} elevation was slower than in the case of the Tg treated cells and the equilibrium was reached on an elevated $[Ca^{2+}]_i$ level (3.) which suggest the failure of the PMCA. Gd^{3+} had no effect on the Ca^{2+} influx in this case (4.). a: $p<0.05$ vs 2μM Tg 1.; b: $p<0.05$ vs 2μM Tg 2.; c: $p<0.05$ vs 2μM Tg 3.; d: $p<0.05$ vs 200μM POA 1.; e: $p<0.05$ vs 200μM POA 2.

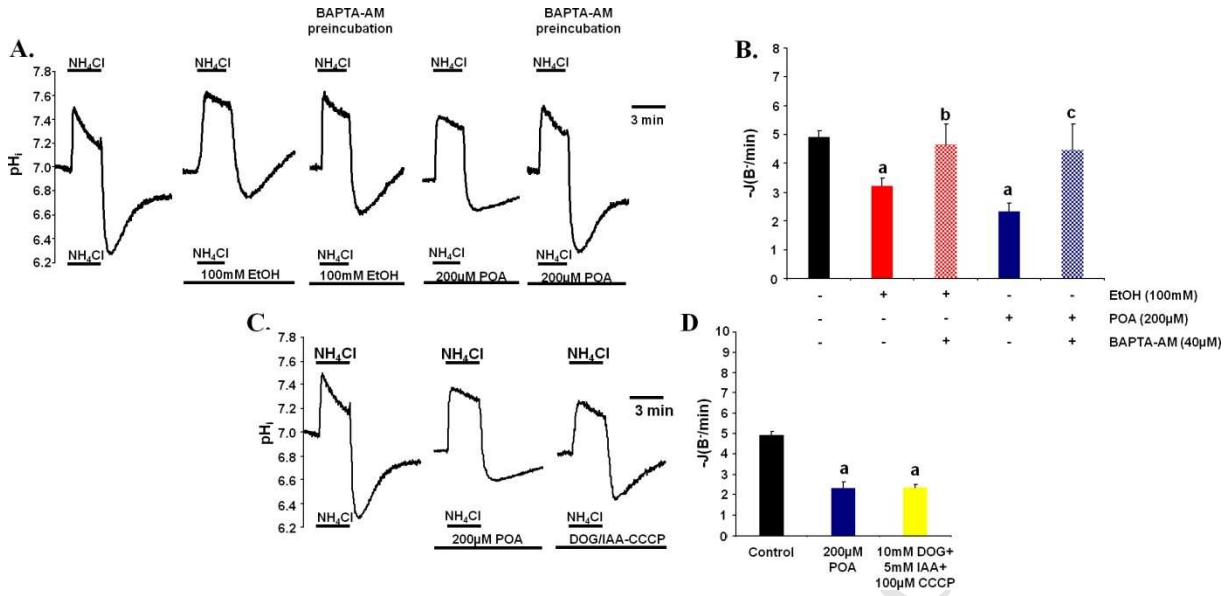

Supplementary Figure 9. (A) $[Ca^{2+}]_i$ chelation abolishes the inhibitory effect of ethanol and POA on the pancraetic HCO_3^- secretion in Capan-1 PDEC. Representative traces showing the effect of Ca^{2+} chelation on inhibitory effect of 100mM ethanol or 200μM POA on the recovery after alkali load. **(B) Summary data of the initial rate of pH_i recovery after alkali load.** The chelation of $[Ca^{2+}]_i$ abolished the inhibitory effect of ethanol and POA on HCO_3^- secretion. Data are shown as means±SEM.n: 3-5 exp for all groups. a: $p<0.05$ vs Control; b: $p<0.05$ vs 100mM ethanol; c: $p<0.05$ vs 200μM POA. **(C) The effect of $(ATP)_i$ depletion on HCO_3^- secretion. Representative traces** showing the effect of $(ATP)_i$ depletion on the HCO_3^- secretion. The administration of 10mM DOG/5mM IAA and 100μM CCCP significantly inhibited the recovery after alkali load. **(D) Summary data of the recovery after alkali load.** The recovery after alkali load was significantly reduced by $(ATP)_i$ depletion. Data are shown as means±SEM. n: 3-5 exp for all groups. a: $p<0.05$ vs Control.

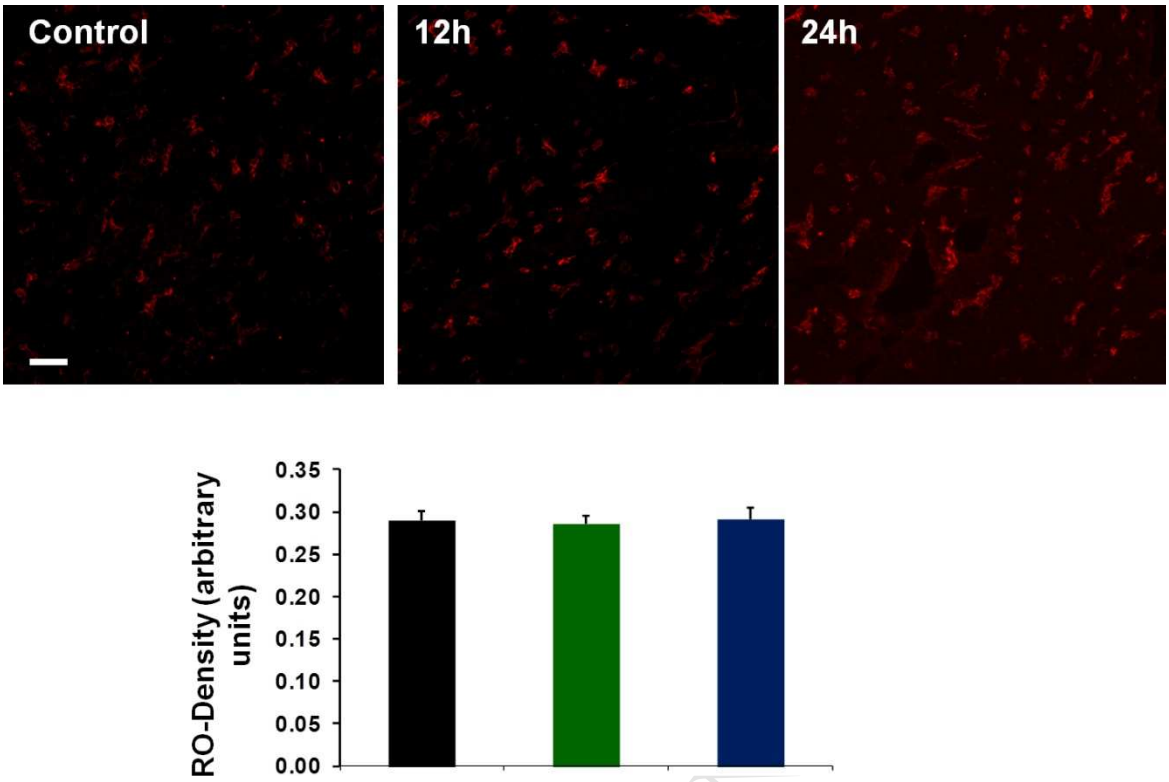

Supplementary Figure 10. (A) Na^+/K^+-ATPase expression in guinea pig pancreas. The expression of Na^+/K^+-ATPase of guinea pig pancreatic ducts were not changed following a single *i.p.* injection of 0.8g/kg ethanol and 300mg/kg palmitate (PA). n=5/each group. a: $p<0.05$ vs control. Scale bar=100μm. Data are shown as means±SEM.

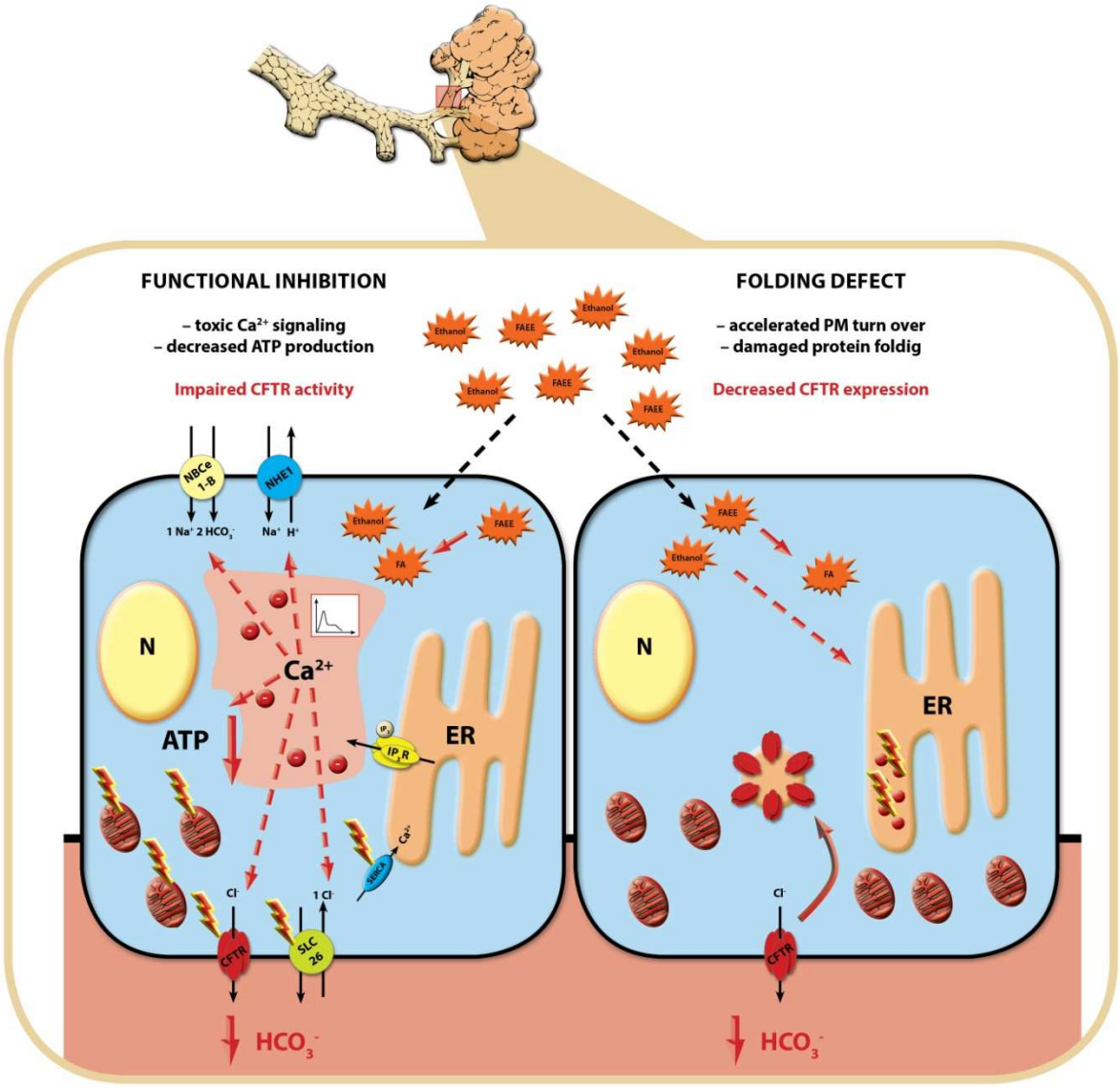

Supplementary Figure 11. Ethanol and non oxidative ethanol metabolites induce sustained intracellular calcium overload, cellular cAMP and ATP depletion and mitochondrial membrane depolarization in pancreatic ductal epithelial cells. These events inhibit the CFTR activity and decrease the pancreatic HCO_3^- secretion. On the other hand ethanol and non oxidative ethanol metabolites severely reduce CFTR expression via a combination of reduced CFTR mRNA levels, decreased cell surface stability and endoplasmic reticulum folding defect of CFTR. The decreased pancreatic fluid and HCO_3^- secretion will increase the severity of alcohol-induced acute pancreatitis.

	Standard HEPES	Standard HCO_3^-	Cl^--free HCO_3^-	Ca^{2+}-free HEPES
NaCl	130	115		132
KCl	5	5		5
$MgCl_2$	1	1		1
$CaCl_2$	1	1		
Na-HEPES	10			10
Glucose	10	10	10	10
$NaHCO_3$		25	25	
Na-gluconate			115	
Mg-gluconate			1	
Ca-gluconate			6	
K_2-sulfate			2.5	
EGTA				0.1

Table 1. Composition of solutions for *in vitro* studies. Values are concentrations in mmol/L.

	Control n=26	Alcohol intoxicated n=49
Age (years)	46.42±2.55	47.65±1.86
Male:female ratio	3.33:1	3.45:1
se Na^+ (mM)	141±0.8	147.2±2.2
se K^+ (mM)	4.3±0.1	4.4±0.1
se Cl^- (mM)	103.8±0.7	103±6.4
Carbamide (mM)	5.2±0.2	4±0.3

Table 2. Charactreistics of patients enrolled in the study to determine the effect of ethanol on sweat Cl^- concentration.

R117H	forward	*5'- GGAAGTCACCAAAGCAGTACA -3'*
	reverse	*5'- GGCCTGTGCAAGGAAGTATTA -3'*
delta F508	forward	*5'- GGAAGAATTTCATTCTGTTCTCAGT -3'*
	reverse	*5'- GCTTTGATGACGCTTCTGTATC -3'*

Table 3. Oligonucleotide primers used for human genotyping in this study.

Figure 1. Alcohol consumption decreases activity and expression of CFTR Cl^- channel. **(A)** No significant change of sweat Cl^- concentration (Cl^-_{sw}) was observed in healthy volunteers (n=21) before and after ethanol consumption. **(B)** The Cl^-_{sw} was significantly higher in patients after excessive alcohol consumption (EAC) compared to the age and sex matched controls, whereas in alcoholics with 0mM blood ethanol (Addict) it was elevated compared to the control group, but significantly lower than the alcohol abusing group. Control n=26; EAC n=49; Addict n=15; a:p<0.001vs.control; b:p<0.001vsEAC. **(C)** The Cl^-_{sw} of patients returned to the normal level, when measured several days after EAC at 0mM blood ethanol concentration. n=8; a:p<0.001vsEAC values. **(D-E) CFTR expression in human pancreas.** Arrowheads point to the luminal membrane of the intralobular pancreatic ducts. NP: normal pancreas, AP: acute, CP: chronic pancreatitis; scale bar:50µm. CFTR staining density at the luminal membrane was decreased both in AP and CP, whereas cytoplasmic density was markedly increased in CP. C: cytoplasm, M: membrane; n=5/group; a:p<0.05vs.NP-M, b:p<0.05vs.NP-C. **(F) Quantitative PCR analysis** of CFTR mRNA expression in the human pancreas. CFTR mRNA levels were decreased in AP and highly increased in CP (normalized to 18rRNA; given as % of NP mRNA). n=5/group; a:p<0.05vs.NP.

Figure 2. Ethanol and fatty acids inhibit the pancreatic fluid and HCO_3^- secretion and CFTR Cl^- current. (A) Reconstructed images of the duodenal filling after secretin stimulation. Compared to WT, duodenal filling was significantly reduced in CFTR KO mice and it was abolished after *i.p.* injection of ethanol+palmitic acid. n=6/groups. a:p<0.05vs.WT-Control, a:p<0.05vs.KO-Control. **(B) Changes of the relative luminal volume of isolated guinea pig pancreatic ducts** show that administration of ethanol and palmitoleic acid (POA), but not palmitoleic acid ethyl ester (POAEE) for 30 min diminished the *in vitro* ductal fluid

secretion. n=3-4 exp/groups. **(C) Measurements of the luminal Cl^-/HCO_3^- exchange activity** shows that basolateral administration of 100mM ethanol and 200µM POA significantly inhibited the activity of the luminal SLC26 Cl^-/HCO_3^- exchanger and CFTR and decreased the recovery from alkali load in isolated guinea pig pancreatic ducts. n=3-5 exp/groups. a:p<0.05vs.Control. **(D) Representative fast whole cell CFTR Cl^- current recordings in guinea pig pacreatic ductal cells.** (i) Unstimulated currents, (ii) currents after forskolin stimulation (10µM; 10 min; Forsk), and (iii) stimulated currents following 10 min treatment (iv) I/V relationships (diamonds: unstimulated-, squares: forskolin-stimulated-, triangles: forskolin-stimulated currents following treatment). The summary of the current densities (pA/pF; measured at E_{rev}:±60mV) show that 100mM ethanol or 200µM POA blocked the forskolin-stimulated CFTR Cl^- currents (61.5±5.15% and 73.1±4.46%, respectively). n=5-6/groups. a:p<0.05vs.basal current; b:p<0.05vs.forskolin-stimulated current.

Figure 3. Ethanol and palmitoleic acid inhibit both the luminal Cl^-/HCO_3^- exchanger and CFTR in Capan-1 cells. (A-B) The initial rate of pH_i recovery after luminal Cl^- re-addition shows the effects of the basolateral administration of 100mM ethanol or 200µM POA in the presence or absence of 500µM H_2DIDS and/or 10µM CFTR(inh)-172 (luminal administration). (Labels above the traces: composition of the luminal solution; below: composition of the basolateral solution.) 100mM ethanol and 200µM POA induced further inhibition after the administration of CFTR(inh)-172 and/or H_2DIDS, suggesting that high concentration of ethanol and POA inhibit the activity of CBE and CFTR on the apical membrane of PDEC. a:p<0.05vs.Control; b:p<0.05vs.10µM CFTR(inh)-172; c:p<0.05vs.500µM H_2DIDS. **(C) Representative pH_i traces and summary data of the**

initial rate of pH_i recovery after Cl^- re-addition using a different protocol confirmed our results. a:p<0.05vs.Control. n=3-5 exp/all groups.

Figure 4. High concentration of ethanol and palmitoleic acid induce sustained $[Ca^{2+}]_i$ elevation, impaired mitochondrial function and decrease cAMP levels in Capan-1 PDEC. (A) Representative traces and summary data of the $\Delta Ratio_{max}$ show the effect of ethanol, POAEE and POA on $[Ca^{2+}]_i$. 100mM ethanol induced a small, sustained $[Ca^{2+}]_i$ elevation, whereas 100µM-200µM POA induced significantly higher $[Ca^{2+}]_i$ increase. a:p<0.05vs.100mM ethanol. **(B) Ethanol and POA induced significant and irreversible $(ATP)_i$ depletion.** Deoxyglucose/iodoacetic acid (DOG/IAA; glycolysis inhibition) and CCCP (inhibition of mitochondrial ATP production) served as control. **(C) Representative traces and summary data of the changes of the mitochondrial membrane potential $[(\Delta\Psi)_m]$.** 100mM ethanol induced moderate $(\Delta\Psi)_m$ decrease, whereas 200µM POA had more prominent effect. CCCP induced further $(\Delta\Psi)_m$ decrease after POA treatment. **(D) Summary data for the cAMP measurements.** 100mM ethanol and 200µM POAEE significantly decreased the forskolin-stimulated cAMP production. **(E) Ca^{2+} chelation abolished the inhibitory effect of ethanol and POA on the pH_i recovery after luminal Cl^- re-addition.** For all conditions n=3-5/group; a:p<0.05vs.Control; b:p<0.05vs.100mM ethanol; c:p<0.05vs.200µM POA. N.D.: not detected.

Figure 5. Ethanol, POAEE and POA decrease CFTR expression in Capan-1 cells and in guinea pig pancreatic ducts. (A-C) High concentrations of ethanol, POAEE and POA induced a significant decrease in CFTR membrane and cytoplasmic protein expression. Scale bar=10µm. **(D)** Ethanol, POAEE and POA decreased CFTR mRNA expression after 48 h of exposure. Data were normalized to HPRT mRNA levels and expressed as % of untreated

control mRNA levels. **(E-F) CFTR expression in guinea pig pancreas.** The expression of CFTR on the luminal membrane of guinea pig pancreatic ducts were significantly decreased 12 h following a single *i.p.* injection of 0.8g/kg ethanol and 300mg/kg palmitic acid (PA). Scale bar=100µm n=5/group. a:p<0.05vs.control.

Figure 6. Effect of ethanol and its metabolites on CFTR and Na^+/K^+-ATPase expression. (A) Immunoblotting and densitometry of CFTR and Na^+/K^+-ATPase expression levels in transfected MDCK monolayers after 48 h treatment with ethanol, POA or POAEE (right panel). Results are expressed as % of the complex-glycosylated CFTR (band C), or Na^+/K^+-ATPase expression in untreated cells (control). (First column: CFTR; second column: Na^+/K^+-ATPase for each condition.) **(B) ELISA measurement** of the apical plasma membrane (PM) density of CFTR revealed that ethanol, POA and POAEE decreased this parameter after 48 h incubation. Results are presented as % of CFTR cell surface density of the untreated cells. **(C) Ethanol, POAEE and POA reduce the PM stability of CFTR** determined by cell surface ELISA. Cell surface resident CFTR was labeled with anti-HA antibody and chased for 1h or 2h in the presence of the indicated compounds at 37°C. Results are presented as % of the initial CFTR surface density. (1 and 2 indicate 1h and 2h chase, respectively). **(D) CFTR folding efficiency** was reduced by 100mM ethanol and diminished by 200µM POA or POAEE after 48h. CFTR folding efficiency was calculated as the percentage of the pulse-labeled, core-glycosylated form conversion into the mature complex-glycosylated form during 3h chase. n=3/each conditions; a:p<0.05vs.Control.

Figure 7. Acute pancreatitis induced by ethanol and fatty acids is more severe in CFTR knock-out mice. (A) Acute pancreatitis induction by a single *i.p.* injection of ethanol and palmitic acid (PA) induced significant elevation of pancreatic water content as measured by

100*(wet weight-dry weight)/wet weight; serum amylase activity; edema and leukocyte scores; and necrosis. The severity of pancreatitis was significantly higher in the CFTR KO mice. **(B)** Representative H&E stained light micrographs of pancreas sections from WT control and ethanol+PA treated WT or CFTR KO mice. Note the massive necrosis in the treated animals. Scale bar=100μm. Data are shown as means±SEM. a:$p<0.05$ vs. control, b:$p<0.05$ vs. WT ethanol+PA treated group. n=6/group; N.D. not detected.

Figure 1.

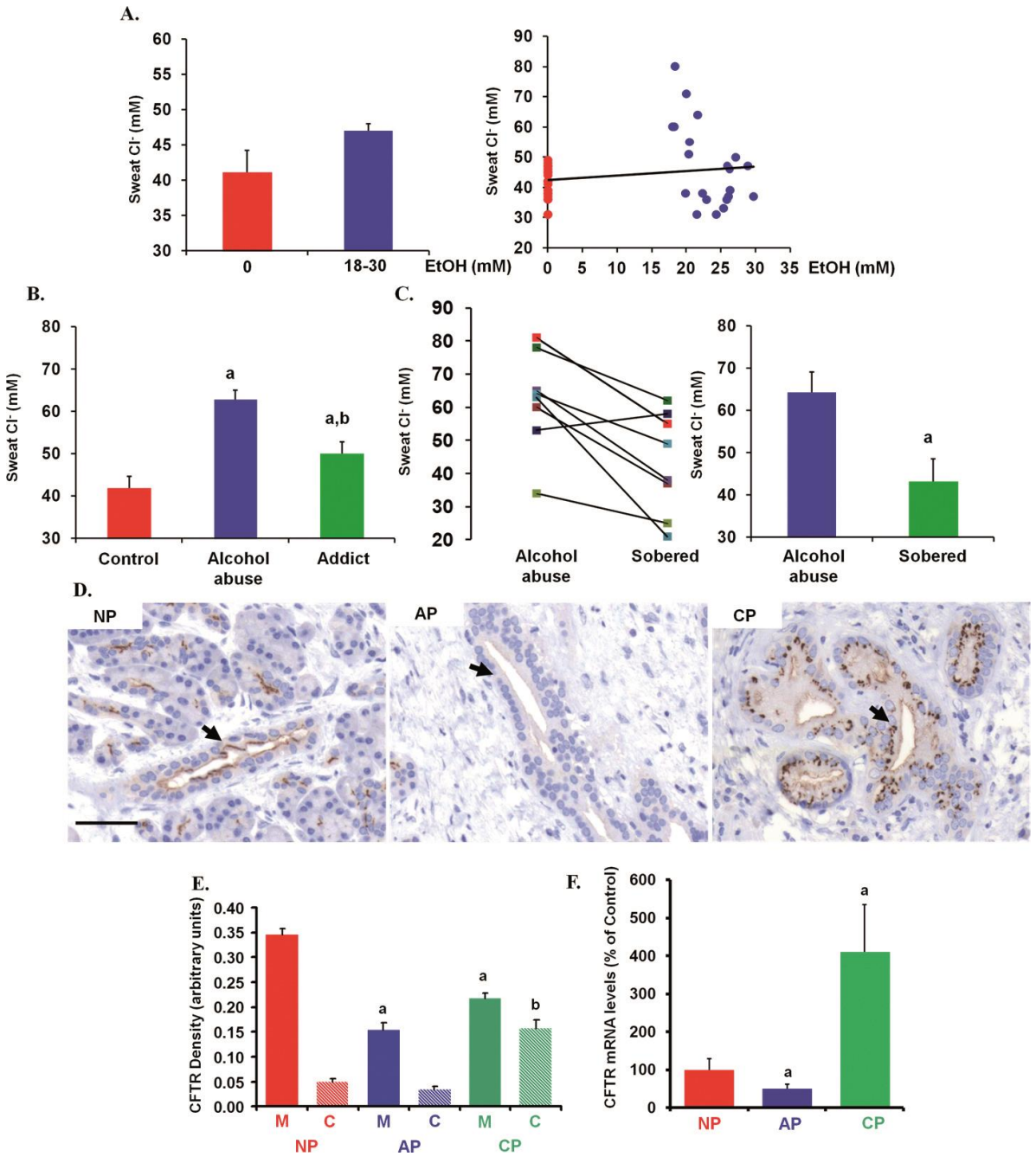

Figure 2.

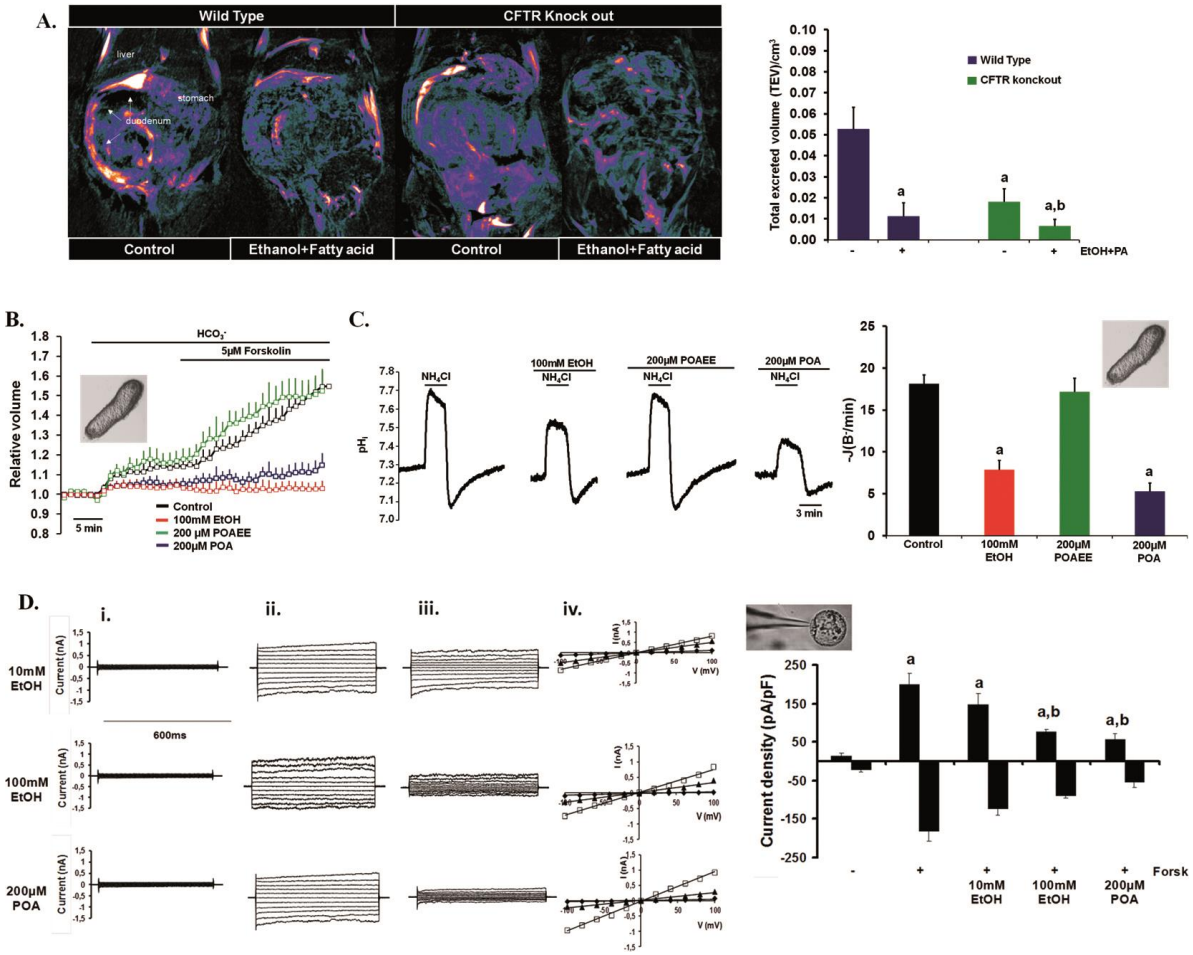
A.
Wild Type
CFTR Knock out
liver
stomach
duodenum
Control
Ethanol+Fatty acid
Control
Ethanol+Fatty acid
Total excreted volume (TEV)/cm³
Wild Type
CFTR konckout
a
a
a,b
EtOH+PA
B.
HCO3-
5μM Forskolin
Relative volume
5 min
Control
100mM EtOH
200 μM POAEE
200μM POA
C.
NH4Cl
100mM EtOH
200μM POAEE
200μM POA
pHi
3 min
-J(B-/min)
Control
100mM EtOH
200μM POAEE
200μM POA
D.
i.
ii.
iii.
iv.
10mM EtOH
100mM EtOH
200μM POA
Current (nA)
600ms
I (nA)
V (mV)
Current density (pA/pF)
Forsk
10mM EtOH
100mM EtOH
200μM POA

Figure 3.

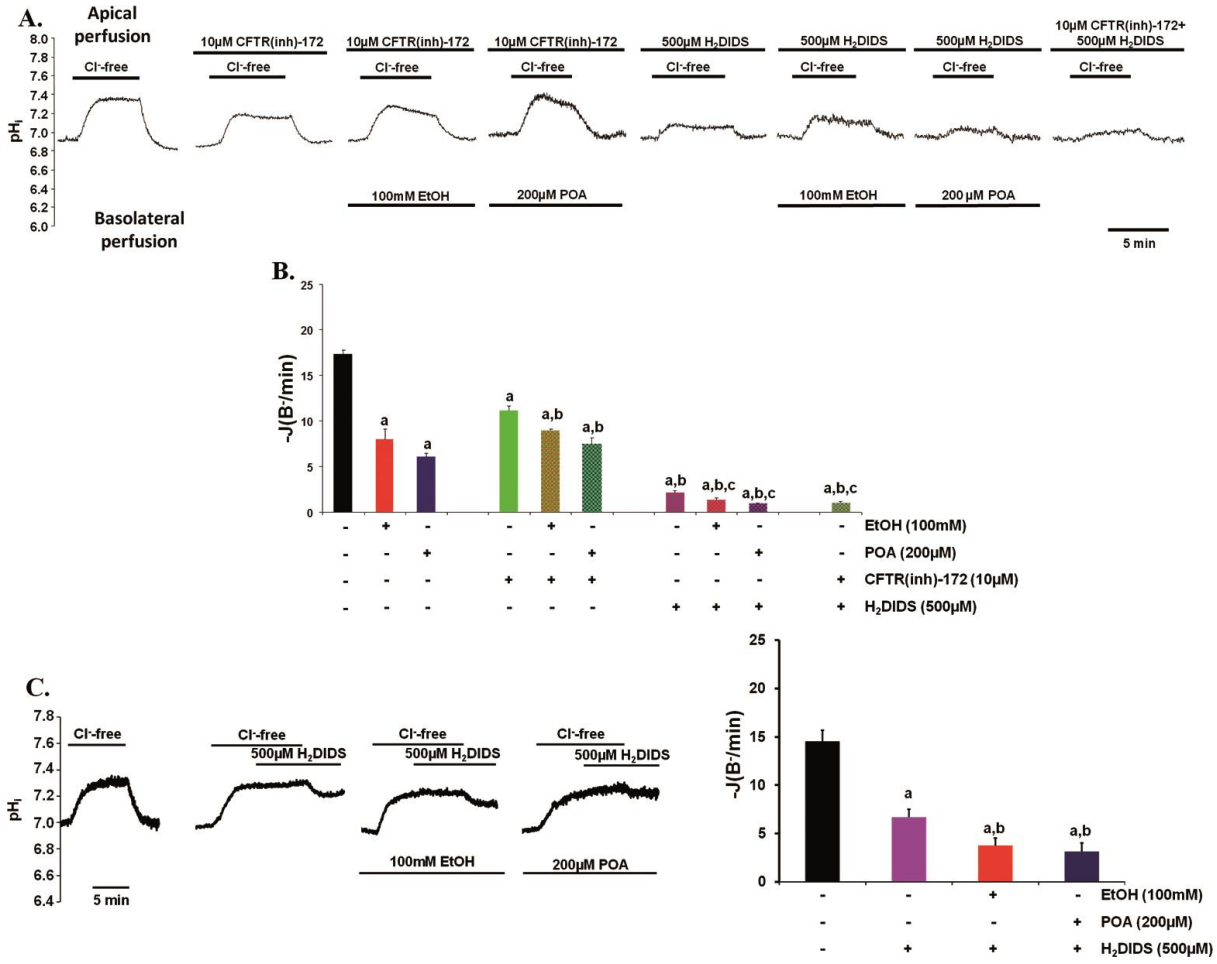
A.
Apical perfusion
Basolateral perfusion
pHi
Cl-free
10μM CFTR(inh)-172
500μM H2DIDS
10μM CFTR(inh)-172+ 500μM H2DIDS
100mM EtOH
200μM POA
5 min
B.
-J(B-/min)
EtOH (100mM)
POA (200μM)
CFTR(inh)-172 (10μM)
H2DIDS (500μM)
C.
Cl-free
500μM H2DIDS
100mM EtOH
200μM POA
5 min
-J(B-/min)
EtOH (100mM)
POA (200μM)
H2DIDS (500μM)

Figure 4.

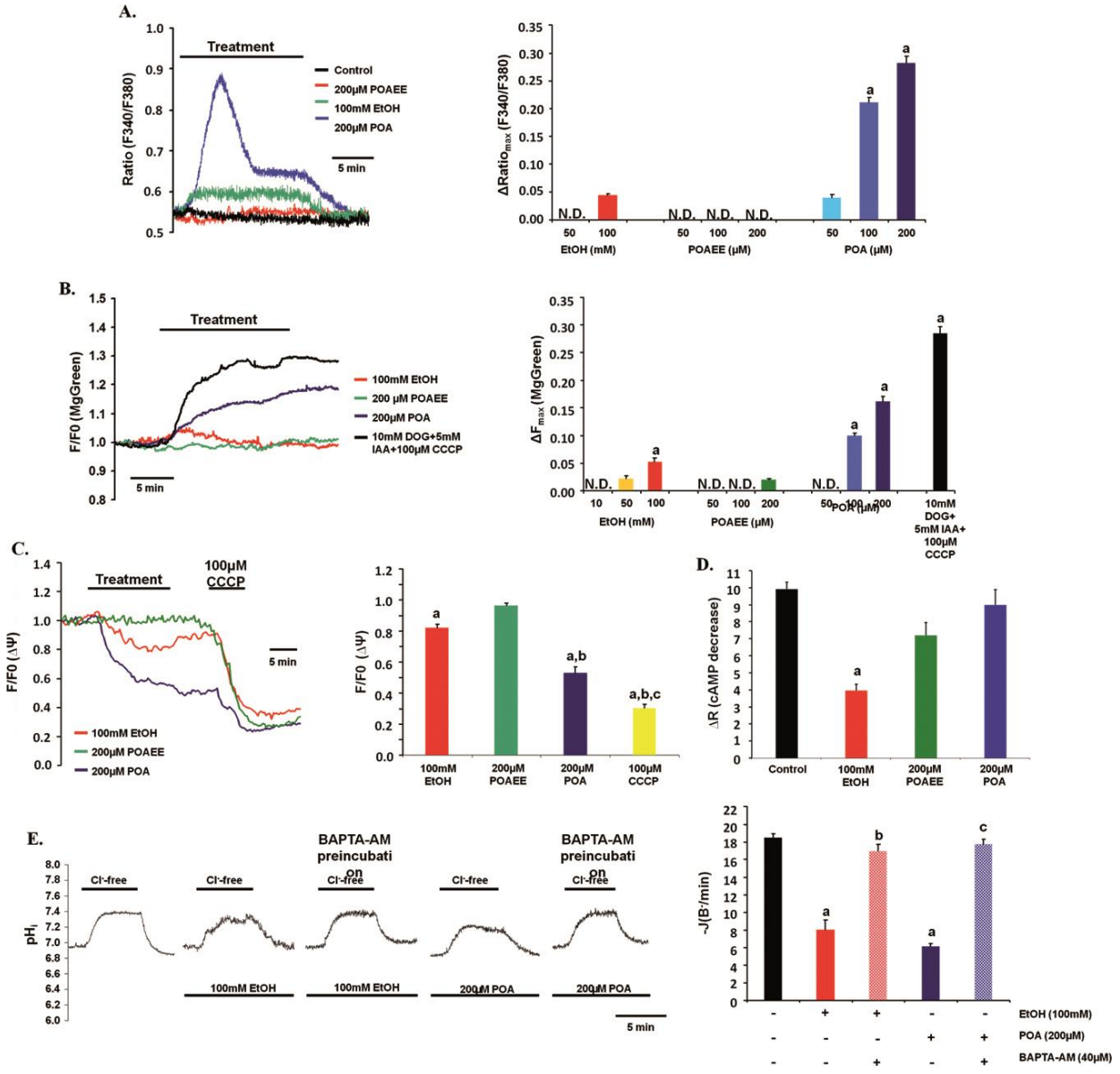
A.
Treatment
Control
200μM POAEE
100mM EtOH
200μM POA
5 min
Ratio (F340/F380)
ΔRatio_max (F340/F380)
N.D.
EtOH (mM)
POAEE (μM)
POA (μM)
B.
Treatment
100mM EtOH
200 μM POAEE
200μM POA
10mM DOG+5mM IAA+100μM CCCP
F/F0 (MgGreen)
ΔF_max (MgGreen)
10mM DOG+ 5mM IAA+ 100μM CCCP
C.
Treatment
100μM CCCP
F/F0 (ΔΨ)
100mM EtOH
200μM POAEE
200μM POA
100μM CCCP
D.
ΔR (cAMP decrease)
Control
E.
BAPTA-AM preincubation
Cl-free
pH_i
EtOH (100mM)
POA (200μM)
BAPTA-AM (40μM)

Figure 5.

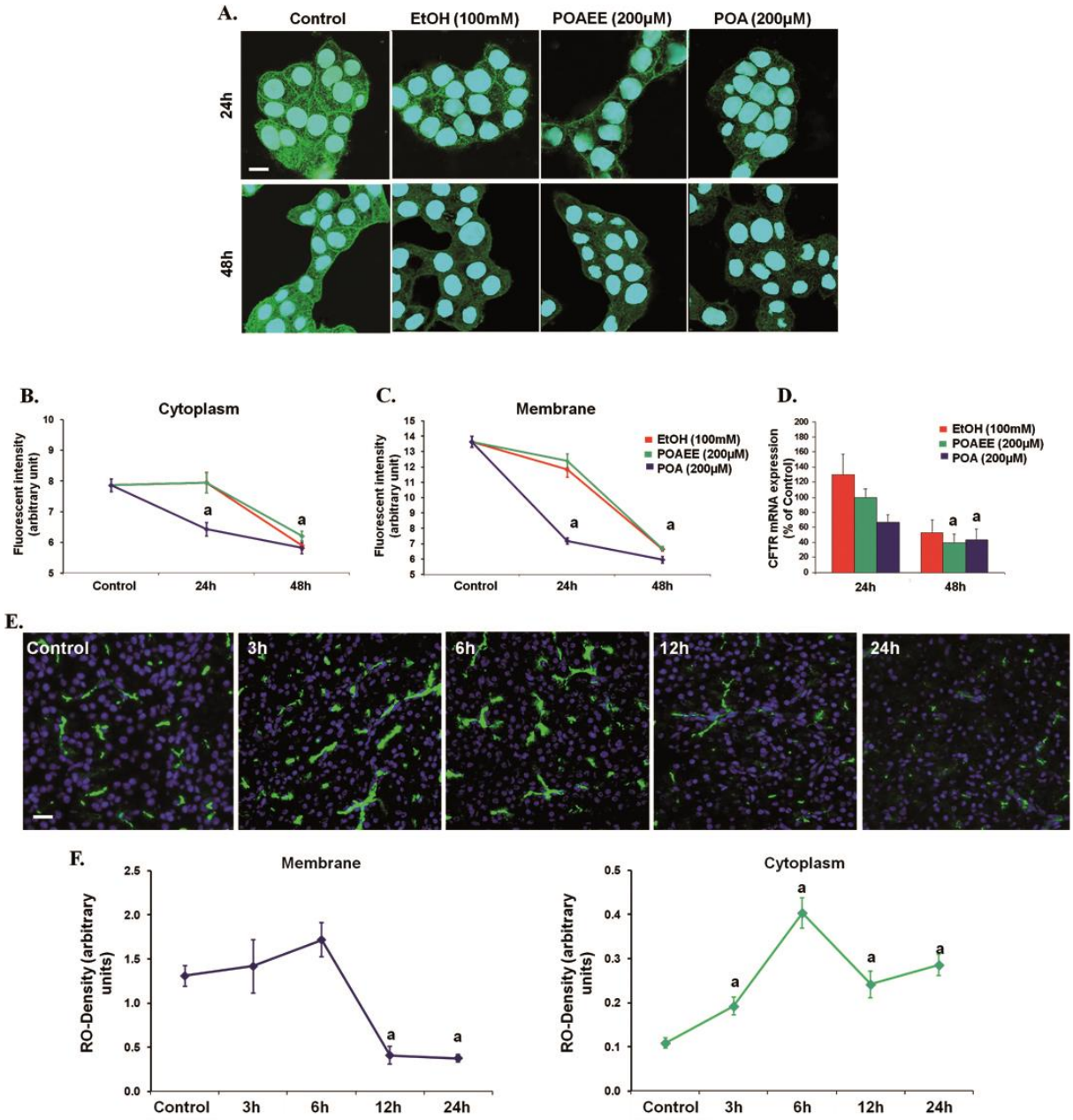
A.
Control
EtOH (100mM)
POAEE (200μM)
POA (200μM)
24h
48h
B.
Cytoplasm
Fluorescent intensity (arbitrary unit)
Control
24h
48h
C.
Membrane
EtOH (100mM)
POAEE (200μM)
POA (200μM)
D.
CFTR mRNA expression (% of Control)
E.
Control
3h
6h
12h
24h
F.
Membrane
RO-Density (arbitrary units)
Cytoplasm

Figure 6.

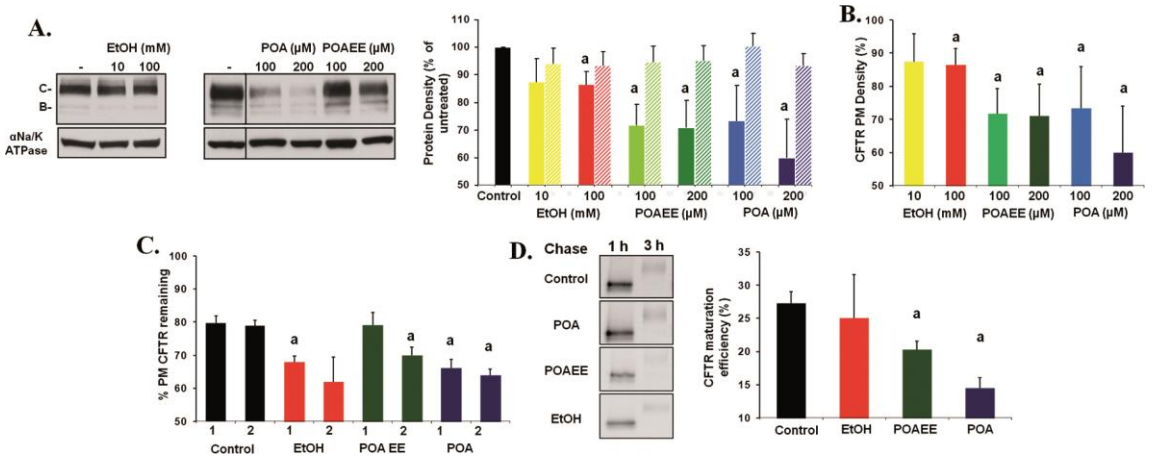
A.
EtOH (mM)
POA (μM) POAEE (μM)
C-
B-
αNa/K ATPase
Protein Density (% of untreated)
Control
EtOH (mM)
POAEE (μM)
POA (μM)
B.
CFTR PM Density (%)
C.
% PM CFTR remaining
Control
EtOH
POA EE
POA
D.
Chase
1 h
3 h
Control
POA
POAEE
EtOH
CFTR maturation efficiency (%)

Figure 7.

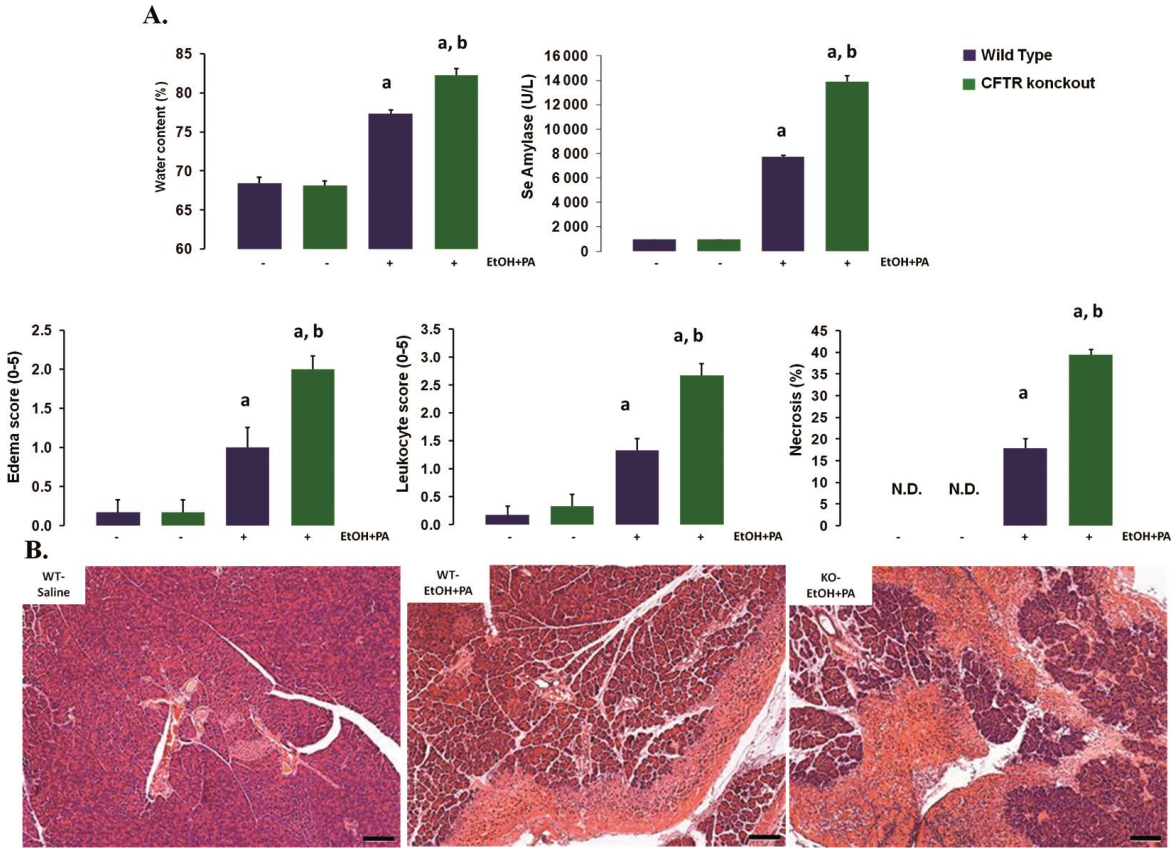
A.
Water content (%)
Se Amylase (U/L)
Wild Type
CFTR konckout
EtOH+PA
Edema score (0-5)
Leukocyte score (0-5)
Necrosis (%)
N.D.
B.
WT-
Saline
WT-
EtOH+PA
KO-
EtOH+PA

II.

Non-conjugated chenodeoxycholate induces severe mitochondrial damage and inhibits bicarbonate transport in pancreatic duct cells

J Maléth, V Venglovecz, Zs Rázga, et al.

Gut 2011 60: 136-138 originally published online August 23, 2010
doi: 10.1136/gut.2009.192153

LETTERS

Non-conjugated chenodeoxycholate induces severe mitochondrial damage and inhibits bicarbonate transport in pancreatic duct cells

We read the manuscripts by Lee and Muallem[1] and Venglovecz *et al*[2] recently published in *Gut* with great interest. In both articles the authors highlighted the role of pancreatic ducts in maintaining the integrity of the pancreas. Venglovecz *et al* showed that a high concentration of the non-conjugated chenodeoxycholate (CDC) inhibits pancreatic ductal bicarbonate secretion; however, the mechanisms of the inhibition were not clarified. This is a follow-up study in which we show that this reduction of ductal bicarbonate secretion by CDC is evoked by inhibition of glycolytic and oxidative (caused by severe mitochondrial damage) metabolism with a consequent depletion of intracellular ATP levels.

Physiologically, pancreatic ductal fluid and HCO_3^- secretion are necessary to wash out the digestive enzymes from the acinar cells into the duodenum. Under pathophysiological conditions toxic factors (such as bile acids and ethanol) involved in the pathogenesis of acute pancreatitis have dual effects on ductal HCO_3^- secretion.[1] Low doses of CDC and ethanol were found to stimulate fluid and HCO_3^- secretion. However, these toxic agents in high concentrations inhibit the secretion. These data suggest that an elevation in pancreatic ductal fluid and HCO_3^- secretion may have protective roles. However, since under physiological conditions the pressure in the main pancreatic duct is higher than in the bile ducts, it is still controversial as to whether bile acids enter the pancreatic ductal tree.

We have recently shown that a high concentration (1 mM) of the non-conjugated bile acid CDC has strong inhibitory effects on the activities of acid/base transporters (Na^+/H^+ exchanger (NHE), Na^+/HCO_3^- cotransporter (NBC) and Cl^-/HCO_3^- exchanger (CBE)) in pancreatic ductal epithelial cells (PDECs). Although the

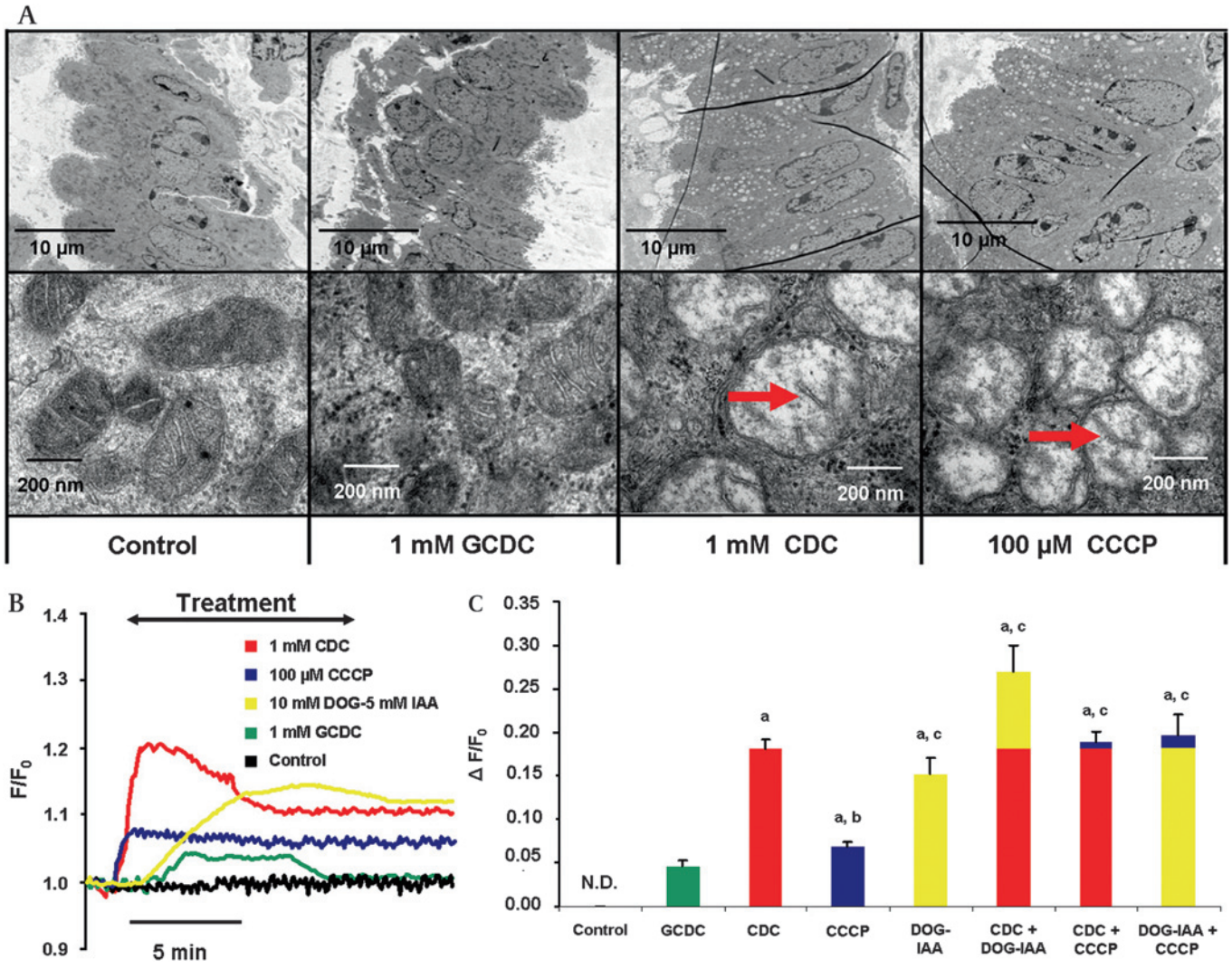

Figure 1 The effects of bile acids on mitochondria and the intracellular ATP (ATP_i) level of pancreatic ductal epithelial cells (PDECs). (A) Transmission electron microscopy. Intact isolated guinea pig pancreatic ducts were exposed to standard HEPES solution (control), 1 mM glycochenodeoxycholate (GCDC), 1 mM chenodeoxycholate (CDC) or 100 µM carbonyl cyanide *m*-chlorophenyl hydrazone (CCCP) for 10 min. There were no changes detected in the general architecture of the cells in the control and GCDC-treated groups. However, all mitochondria were highly damaged in the 1 mM CDC group. The globular shape and the loss of the intramitochondrial inner membrane were clearly visible (red arrows). (B) Representative curves of the Mg-green fluorescence experiments. Please note that the elevation of fluorescence intensity represents depletion of ATP_i. CDC (1 mM), CCCP (100 µM) or deoxyglucose (DOG; 10 mM) with iodoacetamide (IAA; 5 mM) caused irreversible and high elevation of the fluorescence intensity. GCDC (1 mM) caused a delayed small and reversible elevation in the fluorescence intensity. (C) Summary data for the maximal fluorescence intensity changes. CDC, CCCP and DOG/IAA caused a significantly higher elevation in Mg-green fluorescence intensity. Data are shown as the mean±SEM from 25–35 regions of interests (ROIs) in 5–7 ducts. a, $p<0.01$ vs GCDC; b, $p<0.01$ vs CDC, c, $p<0.01$ vs CCCP.

conjugated bile acid glycochenodeoxycholate (GCDC) also enters the cell, it has no effect on the ion transporters.[2]

In this study intra/interlobular pancreatic ducts were isolated from the pancreas of guinea pigs. CDC or GCDC (0.1–1 mM) was administered basolaterally for 1–10 min. The intracellular pH (pH_i) of PDECs was measured by microfluorometry using BCECF (2',7'-bis-(2-carboxyethyl)-5-(and-6)-carboxyfluorescein). The intracellular ATP level (ATP_i) was determined using Mg-Green which has been shown indirectly to reflect the changes in ATP_i. It is well described that an elevation in fluorescence intensity caused by the increase in free intracellular Mg^{2+} concentration suggests a reduction of ATP_i.[3] The ATP_i measurement was performed in standard HEPES-buffered solution whereas the pH_i measurements were performed in 25 mM HCO_3^-/CO_2-buffered solution. Morphological changes of PDECs were evaluated by transmission electron microscopy.

Administration of a low concentration (0.1 mM) of CDC or GCDC for 1–10 min had no effects on the intracellular organelles (data not shown). In addition, a high concentration (1 mM) of the conjugated GCDC did not induce morphological changes. Importantly, exposure to 1 mM CDC for 10 min greatly damaged all of the mitochondria (figure 1A). The mitochondria swelled up and their inner membranes were disrupted. Other intracellular organelles such as nuclei or Golgi apparatus seemed to be unaltered. In agreement with this, Benedetti *et al*[4] have shown that non-conjugated bile salts induce mitochondrial damage in bile epithelial cells.

For positive control experiments we used the mitochondrial toxin carbonyl cyanide *m*-chlorophenyl hydrazone (CCCP, 100 µM) which mimicked the effect of CDC on mitochondria. Next we set out to investigate whether ATP_i is affected due to the mitochondrial damage. Administration of a low concentration of CDC or GCDC for 10 min had no effect on the ATP_i; however, a high concentration of CDC and/or CCCP markedly and irreversibly reduced the ATP_i (figure 1B, C). Although 1 mM GCDC also decreased ATP_i, this depletion was reversible and significantly less than the depletion caused by CDC or CCCP. The fact that CDC caused a greater depletion of ATP_i suggests that bile acids have additional effects which further decrease ATP_i. Therefore, we used the deoxy-glucose (DOG)/iodoacetamide (IAA) model which inhibits intracellular glycolytic metabolism. Administration of 10 mM DOG and 5 mM IAA decreased ATP_i (figure 1B,C). Importantly, CCCP or DOG/IAA administered after high concentrations of CDC resulted in further ATP_i depletion; however, their effects were significantly smaller after CDC than when administered alone. Exposure of pancreatic ducts to CCCP and DOG/IAA totally mimicked the effect of CDC. These data indicate that CDC inhibits both the oxidative and glycolytic metabolism of PDECs.

Finally, we provided evidence that ATP_i depletion is crucial in the toxic inhibitory effect of CDC on the ion transporters. To characterise the effects of ATP_i depletion on the activities of NHE, NBC and CBE, we used the NH_4Cl pulse technique in HCO_3^-/CO_2-buffered solution. CCCP strongly inhibited NBC, NHE (recovery from acid load) and CBE (recovery from alkali load) (figure 2A–C). Administration of 10 mM DOG and 5 mM IAA also inhibited the ion transporters (figure 2A–C). Significantly higher inhibition was evoked by parallel administration of CCCP and DOG/IAA. These observations suggest that depletion of ATP_i is the key factor which inhibits NBC, NHE and CBE. Our findings are in accordance with the results of other authors who showed that depletion of ATP_i inhibits many of the ion transporters such as the NHEs in different cell types.[5]

In conclusion, our results clearly show that (1) a high concentration of the non-conjugated bile acid CDC, but not the conjugated bile acid GCDC, causes mitochondrial damage followed by ATP_i depletion; (2) CDC inhibits the glycolytic metabolism of

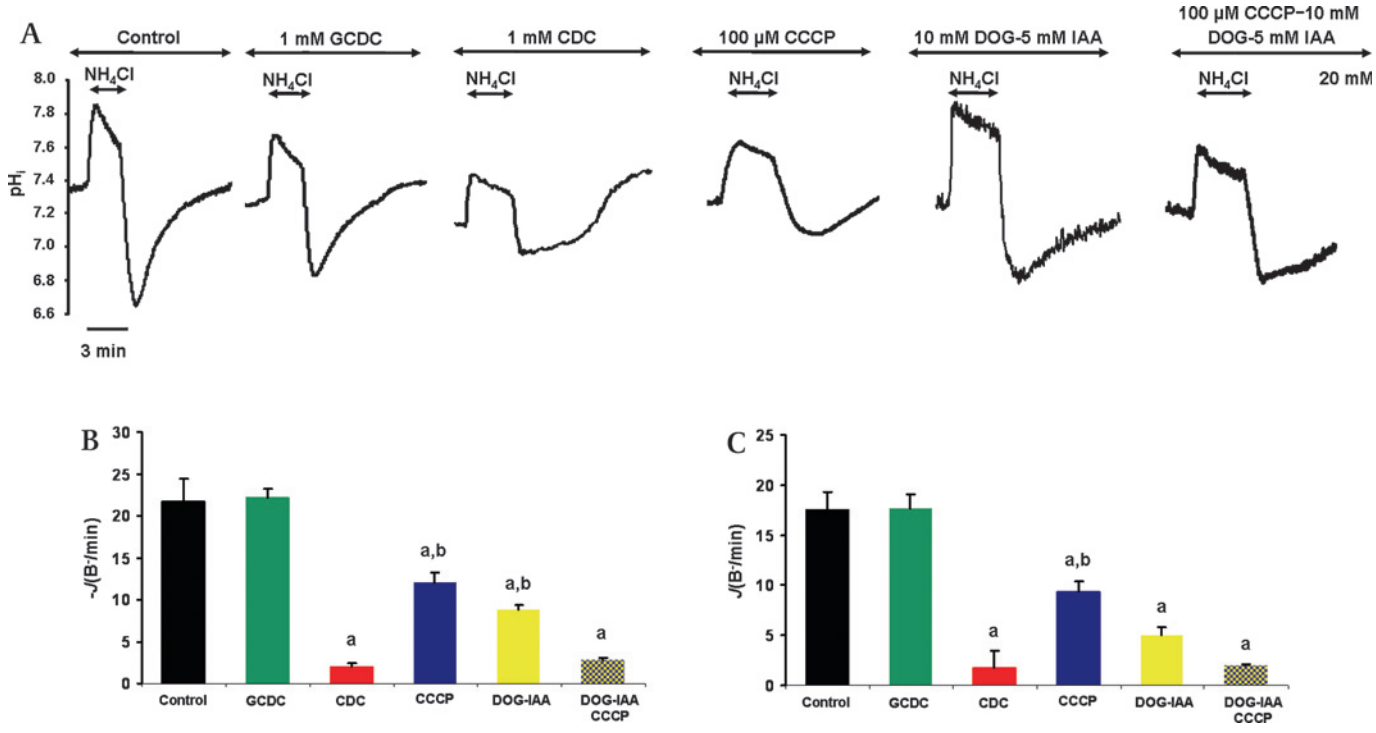

Figure 2 Effect of bile acids on the rate of intracellular pH (pH_i) recovery from an alkali and an acid load. (A) Representative pH_i traces showing the effects of 1 mM glycochenodeoxycholate (GCDC), 1 mM chenodeoxycholate (CDC), 100 µM carbonyl cyanide *m*-chlorophenyl hydrazone (CCCP) or 10 mM deoxyglucose (DOG) with 5 mM iodoacetamide (IAA) administered from the basolateral membrane of pancreatic ductal epithelial cells (PDECs) in the presence of 25 mM HCO_3^-/CO_2. CDC, the mitochondrial toxin CCCP and DOG/IAA markedly inhibited both recoveries. (B) Summary data for the initial rate of recovery from alkali load. CDC, CCCP and DOG/IAA decreased the recovery from alkali load. (C) Summary data for the initial rate of recovery from acid load. CDC, CCCP and DOG/IAA decreased the recovery from acid load. Data are shown as the mean±SEM from 25–35 regions of interests (ROIs) in 5–7 ducts. a, $p<0.01$ vs control, b, $p<0.01$ vs CDC.

PDECs; and (3) ATP_i depletion by itself can be responsible for the impaired fluid and HCO_3^- secretion. The relationship between mitochondrial function and HCO_3^- secretion and the differences between the effects of conjugated and non-conjugated bile acids needs further investigation.

Acknowledgements The authors are greatful to Professor Ole Petersen and co-workers (University of Liverpool, Department of Physiology) for their useful suggestions.

J Maléth,[1] V Venglovecz,[2] Zs Rázga,[3] L Tiszlavicz,[3] Z Rakonczay Jr,[1] P Hegyi[1]

[1]First Department of Medicine; [2]Department of Pharmacology and Pharmacotherapy; [3]Department of Pathology, University of Szeged, Szeged, Hungary

Correspondence to Dr Péter Hegyi, First Department of Medicine, University of Szeged, Faculty of Medicine, PO Box 427, H-6701 Szeged, Hungary; hep@in1st.szote.u-szeged.hu

Funding This work was supported by TÁMOP-4.2.2-08/1/2008-0002 and 0013, K78311 to Z. R., NNF 78851 to P.H., and PD78087 to V.V., BO 00334/08/5 to P.H.

Competing interests None.

Provenance and peer review Not commissioned; externally peer reviewed.

Published Online First 23 August 2010

Gut 2011;**60**:136–138. doi:10.1136/gut.2009.192153

REFERENCES

1. **Lee MG,** Muallem S. Pancreatitis: the neglected duct. *Gut* 2008;**57**:1037–40.
2. **Venglovecz V,** Rakonczay Z Jr, Ózsvári B, *et al*. Effects of bile acids on pancreatic ductal bicarbonate secretion in guinea pig. *Gut* 2008;**57**:1102–12.
3. **Criddle DN,** Murphy J, Fistetto G, *et al*. Fatty acid ethyl esters cause pancreatic calcium toxicity via inositol trisphosphate receptors and loss of ATP synthesis. *Gastroenterology* 2006;**130**:781–93.
4. **Benedetti A,** Alvaro D, Bassotti C, *et al*. Cytotoxicity of bile salts against biliary epithelium: a study in isolated bile ductule fragments and isolated perfused rat liver. *Hepatology* 1997;**26**:9–21.
5. **Dhar-Chowdhury P,** Malester B, Rajacic P, *et al*. The regulation of ion channels and transporters by glycolytically derived ATP. *Cell Mol Life Sci* 2007;**64**:3069–83.

How accurate are the Swansea criteria to diagnose acute fatty liver of pregnancy in predicting hepatic microvesicular steatosis?

We noted that in two recent reports in *Gut*, none of 62 patients diagnosed by the Swansea criteria to have acute fatty liver of pregnancy (AFLP) underwent liver biopsy.[1 2] We retrospectively assessed the accuracy of the Swansea criteria to predict hepatic microvesicular steatosis in 34 patients with suspected pregnancy-related liver disease who underwent liver biopsy at our centre between 1998 and 2006. These patients tested negative for other causes of acute liver dysfunction such as hepatitis viruses (hepatitis B virus surface antigen (HBsAg), hepatitis C virus (HCV) antibody, immunoglobulin (Ig) M hepatitis A virus (HAV) antibody, IgM hepatitis E virus (HEV) antibody), malarial parasite and sepsis (blood culture). No patient gave a history of ingestion of a potentially hepatotoxic drug. We excluded 10 patients (details in figure 1).

The remaining 24 patients included in this study were at 36 (21–40) weeks gestation (median (range)), 23 (17–29) years old and 71% were primigravida. The interval from the first symptom to presentation to our centre was 5 (1–14) days.

Abnormal variables in Swansea criteria for AFLP at presentation in the 24 study patients were: vomiting (11/21 patients), abdominal pain (3/14), polydipsia/polyuria (1/1), encephalopathy (9/24), hyperbilirubinaemia (24/24), hypoglycaemia (8/24), hyperuricaemia (8/10), leucocytosis (20/23), ascites/bright liver on ultrasonogram (16/22), elevated transaminases (23/24), hyperammonaemia (2/2), renal impairment (17/24), coagulopathy (23/24) and hepatic microvesicular steatosis (17/24). Some variables were not recorded/not tested in all 24 patients (eg, vomiting recorded in only 21; uric acid tested in only 10). Baseline laboratory results in study patients were: serum total bilirubin, 12.7±6.2 mg/dl (mean±SD); alanine aminotransferase (ALT), 119±6.2 IU/l; prothrombin time, 39±30 s; serum creatinine, 1.7±0.9 mg/dl; and MELD (Model for End-Stage Liver Disease) score, 30 (range 13–46).

Liver biopsy was done either immediately postmortem (5/24) or postnatally via the transjugular route (19/24). Biopsies were fixed in formalin and routinely stained for H&E and

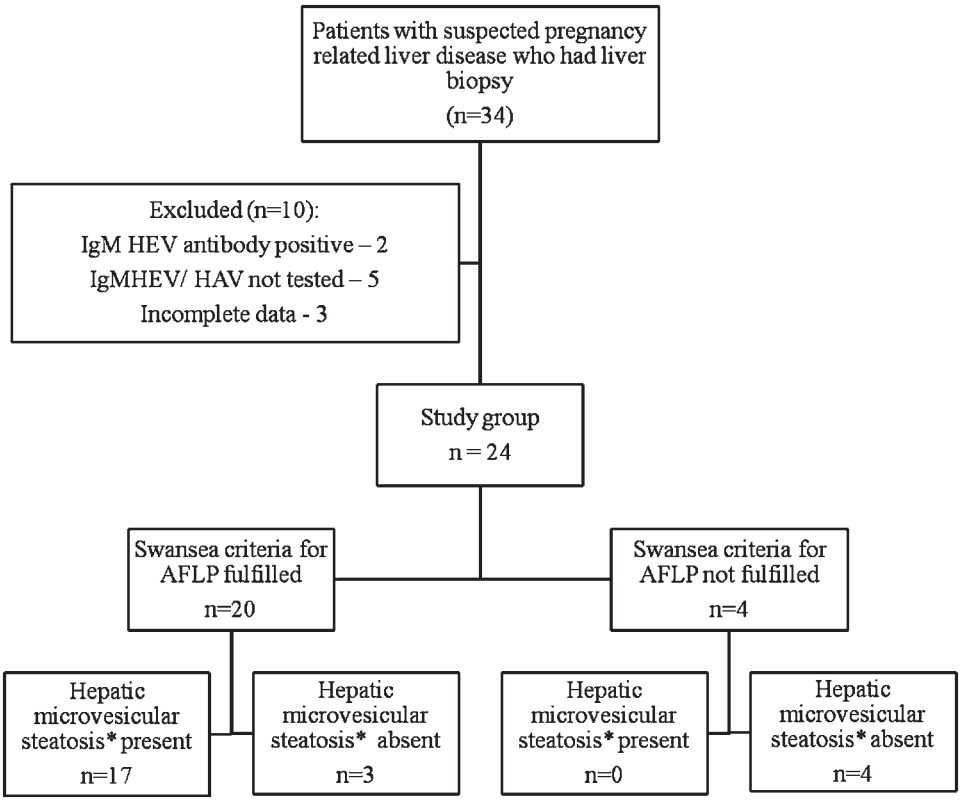

Figure 1 Flowchart of patients with suspected pregnancy-related liver disease who underwent liver biopsy. *Refers to diffuse/perivenular hepatic microvesicular steatosis.

III.

Pflugers Arch - Eur J Physiol
DOI 10.1007/s00424-014-1560-9

Bile acids inhibit Na^+/H^+ exchanger and Cl^-/HCO_3^- exchanger activities via cellular energy breakdown and Ca^{2+} overload in human colonic crypts

É. Pallagi-Kunstár · K. Farkas · J. Maléth · Z. Rakonczay Jr · F. Nagy · T. Molnár · Z. Szepes · V. Venglovecz · J. Lonovics · Z. Rázga · T. Wittmann · P. Hegyi

Received: 22 May 2014 / Accepted: 17 June 2014

Abstract Bile acids play important physiological role in the solubilisation and absorption of dietary lipids. However, under pathophysiological conditions, such as short bowel syndrome, they can reach the colon in high concentrations inducing diarrhoea. In this study, our aim was to characterise the cellular pathomechanism of bile-induced diarrhoea using human samples. Colonic crypts were isolated from biopsies of patients (controls with negative colonoscopic findings) and of cholecystectomised/ileum-resected patients with or without diarrhoea. In vitro measurement of the transporter activities revealed impaired Na^+/H^+ exchanger (NHE) and Cl^-/HCO_3^- exchanger (CBE) activities in cholecystectomised/ileum-resected patients suffering from diarrhoea, compared to control patients. Acute treatment of colonic crypts with 0.3 mM chenodeoxycholate caused dose-dependent intracellular acidosis; moreover, the activities of acid/base transporters (NHE and CBE) were strongly impaired. This concentration of chenodeoxycholate did not cause morphological changes in colonic epithelial cells, although significantly reduced the intracellular ATP level, decreased mitochondrial transmembrane potential and caused sustained intracellular Ca^{2+} elevation. We also showed that chenodeoxycholate induced Ca^{2+} release from the endoplasmic reticulum and extracellular Ca^{2+} influx contributing to the Ca^{2+} elevation. Importantly, our results suggest that the chenodeoxycholate-induced inhibition of NHE activities was ATP-dependent, whereas the inhibition of CBE activity was mediated by the sustained Ca^{2+} elevation. We suggest that bile acids inhibit the function of ion transporters via cellular energy breakdown and Ca^{2+} overload in human colonic epithelial cells, which can reduce fluid and electrolyte absorption in the colon and promote the development of diarrhoea.

Keywords Bile acids · Colonic epithelial cells · Ion transporters · Intracellular Ca^{2+}

Abbreviations

BA	Bile acids
BAM	Bile acid malabsorption
BAPTA-AM	1,2-Bis(*o*-aminophenoxy)ethane -*N*,*N*,*N*′,*N*′-tetraacetic acid
$[Ca^{2+}]_i$	Intracellular Ca^{2+} concentration
CBE	Cl^-/HCO_3^- exchanger
CCCP	Carbonyl cyanide *m*-chlorophenyl hydrazone
CDC	Chenodeoxycholate
ER	Endoplasmic reticulum
GCDC	Glycochenodeoxycholate
H_2DIDS	Dihydro-4,4′-diisothiocyanostilbene-2,2′-disulphonic acid
HOE-642	4-Isopropyl-3-methylsulphonylbenzoyl-guanidin methanesulphonate
IP_3R	Inositol-triphosphate receptor
$(\Delta\Psi)_m$	Mitochondrial transmembrane potential

É. Pallagi-Kunstár · K. Farkas · J. Maléth · Z. Rakonczay Jr · F. Nagy · T. Molnár · Z. Szepes · J. Lonovics · T. Wittmann · P. Hegyi
Faculty of Medicine, First Department of Medicine, University of Szeged, Korányi fasor 8-10, H-6720 Szeged, Hungary

V. Venglovecz
Department of Pharmacology and Pharmacotherapy, University of Szeged, Szeged, Hungary

Z. Rázga
Department of Pathology, University of Szeged, Szeged, Hungary

P. Hegyi (✉)
MTA-SZTE Translational Gastroenterology Research Group, Szeged, Hungary
e-mail: hegyi.peter@med.u-szeged.hu

Published online: 13 July 2014

NHE	Na^+/H^+ exchanger
pH_i	Intracellular pH
RR	Ruthenium red
RyR	Ryanodin receptor
SERCA	Sarcoplasmic/endoplasmic reticulum calcium ATPase
SLC26	Solute carrier family 26
TEM	Transmission electron microscopy
Tg	Thapsigargin

Introduction

One of the main non-motor functions of the colon is to absorb about 90 % of the fluid (~1.5 to 1.9 L) arriving daily from the small intestine [40], which is mediated by the polarised epithelial cell layer. The colonic epithelial cells express numerous ion channels, pumps and transporters located either on the luminal or the basolateral membrane, allowing highly efficient transport of water and ions, especially Na^+ and Cl^- [24]. The adequate activity of these transporters is essential to keep the precise balance between absorption and secretion. The electroneutral NaCl absorption in the colon is most likely mediated via the coupled activity of Na^+/H^+ exchangers (NHEs) and the SLC26 Cl^-/HCO_3^- exchangers (CBE) [29, 44].

Bile acids (BA) are natural detergents excreted into the small intestine, and most of them (90–95 %) are reclaimed in the distal ileum then returned to the liver. If this precisely regulated enterohepatic circulation is impaired, bile acid malabsorption (BAM) occurs, thus BA can enter the colon in higher concentrations and can induce diarrhoea through a yet unidentified mechanism. BAM and diarrhoea are well-known clinical complications following ileal resection or cholecystectomy [1, 10, 36]. The lack of proper diagnostic approaches and limited number of clinical guidelines on the appropriate management of patients with BAM making the disease under-recognized and a great challenge for gastroenterologists [45]. Further complicating the situation that cholestyramine (a bile acid sequestrant) therapy does not solve the problem in every case [3, 9, 33, 47]. Moreover, cholestyramine treatment can reduce the bioavailability of co-administered drugs as well. These observations suggest the necessity of developing new therapeutical approaches, therefore it is crucial to understand the pathogenesis of BA induced diarrhoea.

In this study, we provide strong evidence that BA impair the ion transport mechanisms of human colonic epithelial cells which could play an important role in the development of BAM associated diarrhoea. We demonstrate that chronic exposure of the colon to high concentrations of BA results in decreased activities of acid/base transporters, responsible for NaCl absorption. In addition, the non-conjugated BA chenodeoxycholate (CDC) inhibits the activities of NHEs and CBE via $(ATP)_i$ depletion and sustained intracellular Ca^{2+} elevation in isolated human colonic epithelial cells. These intracellular changes could reduce fluid and electrolyte absorption in the colon and promote the development of diarrhoea. Thus, our results might contribute to the development of new therapeutic approaches in the treatment of bile-induced diarrhoea.

Materials and methods

Human subjects involved in the study

The patients involved in the study were divided into three groups. The first group contained patients having diarrhoea after ileum-resection/cholecystectomy (diarrhoea). In the second group, ileum-resected/cholecystectomised patients were involved who did not develop diarrhoea (non-diarrhoea). The control group included patients without any surgical intervention in the gastrointestinal tract. The patients enrolled in this study were between the ages of 25–55 years. Informed consent was obtained prior to endoscopy. Protocols of the study were approved by the regional ethical committee at the University of Szeged, Szeged, Hungary. Three to six colonic biopsies were obtained from the proximal colon (cecum, colon ascendens) from each patient undergoing colonoscopy at the First Department of Medicine. There were no macroscopic (by endoscopy) or microscopic (by histology) signs of inflammation in the colon of patients. Patients with normal endoscopic findings were examined because of colorectal cancer screening or different abdominal complaints.

Materials and solutions for the experiments

The compositions of the solutions used are shown in Table 1. The pH of HEPES-buffered solutions was set to 7.4 with NaOH at 37 °C. HCO_3^--buffered solutions were gassed with 95 % O_2/5 % CO_2 to set the pH to 7.4 at 37 °C.

General laboratory chemicals were obtained from Sigma-Aldrich. Collagenase A was obtained from Roche Diagnostic (Mannheim, Germany). HOE-642 (4-isopropyl-3-methylsulphonylbenzoyl-guanidin methanesulphonate) was provided by Sanofi Aventis (Frankfurt, Germany) and was dissolved in dimethyl sulphoxide (DMSO). BCECF-AM (2,7-biscarboxyethyl-5(6)-carboxyfluorescein-acetoxymethylester), FURA-2-AM (2-(6-(bis(carboxymethyl)amino)-5-(2-(2-(bis(carboxymethyl)amino)-5-methylphenoxy)-ethoxy)-2-benzofuranyl)-5-oxazolecarboxylic acetoxymethyl ester), BAPTA-AM (1,2-bis(*o*-aminophenoxy)ethane-*N*,*N*,*N*′,*N*′-tetraacetic acid), Magnesium-green-AM and TMRM (tetramethylrhodamine methyl ester) were obtained from

Invitrogen (Eugene, OR); cell and tissue adhesive from Becton Dickinson Bioscience (Cell Tak, Bedford, MA). BCECF-AM, BAPTA-AM, and TMRM were dissolved in DMSO, FURA-2-AM, and Magnesium-green-AM were dissolved in pluronic acid and DMSO. Thapsigargin was obtained from Merck (Darmstadt, Germany) and it was dissolved in DMSO.

Isolation of colonic crypts

Colonic crypts were isolated from three human biopsy specimens obtained from the proximal (cecum or colon ascendens) part of the large intestine. Only one segment of the colon was investigated in each patient. The tissue samples were placed immediately in ice-cold $NaHCO_3$ containing Hank's balanced salt solution (HBSS). The samples were washed three times with HBSS, cut into small pieces with a razor blade and incubated in 1 mM dithiothreitol (DTT) in HBSS for 15 min followed by 2×30 min enzymatic digestion with 0.38 mg/mL collagenase A at 37 °C and continuously gassed with 5 % CO_2/95 % O_2. The small fragments were mixed with a Pasteur pipette, the large fragments were allowed to settle down to the bottom of the flask under gravity for 35–40 s, and the supernatant removed and visualised under a Nikon stereo microscope (Jencons-PLS, Grinstead, UK). The crypts (200–300 crypts/isolation) were aspirated into a micropipette and transferred into a Petri dish. For fluorescent measurements, the crypts were kept in a culture solution for 3 h at 4 °C before the experiments. The culture solution contained Dulbecco's Modified Eagle's Medium (DMEM), 10 % fetal bovine serum (FBS; Sigma-Aldrich, Budapest, Hungary), 2 mM L-glutamine, 100 U/mL penicillin, and 100 μg streptomycin.

Measurement of intracellular pH, Ca^{2+} concentration and ATP level by microfluorometry

Colonic crypts were attached to 24-mm glass coverslips covered with CellTak 3 h after isolation and placed in a perfusion chamber mounted on the stage of an inverted fluorescent microscope linked to an excellence imaging system (Olympus, Budapest, Hungary).

During the microfluorometry experiments, colonic crypts were incubated in standard HEPES solution at 37 °C and loaded with the appropriate fluorescent dye. Crypts were continuously perfused with different solutions at a rate of 9-10 ml/min. Two to three small areas (regions of interest (ROIs)) from the surface of each crypt were investigated (Fig. 1).

Intracellular pH (pH_i) was estimated with the pH-sensitive fluorescent dye BCECF-AM. After incubating with BCECF-AM (2 μmol/l) for 20–30 min, colonic crypts were excited with light at wavelengths of 495 and 440 nm and the 495/440 fluorescence emission ratio were measured at 535 nm [16, 41].

For the measurement of intracellular Ca^{2+} concentration ($[Ca^{2+}]_i$), the cells were loaded with the Ca^{2+} sensitive fluorescent dye FURA-2-AM (5 μmol/L) for 60 min. For excitation, 340 and 380 nm filters were used, and the changes in $[Ca^{2+}]_i$ were calculated from the fluorescence ratio (F340/F380) measured at 510 nm.

To determine changes of intracellular ATP ($(ATP)_i$) concentrations, the fluorescent dye Mg-green-AM was used, which has been shown to indirectly reflect the changes in $(ATP)_i$. Colonic crypts were incubated with Mg-Green (4 μmol/L) for 60 min then were excited with 476 nm light, and emission was detected at 500–550 nm. Because ATP has a 10-fold greater affinity for Mg^{2+} than ADP, and most intracellular Mg^{2+} is present as Mg-ATP [21, 26], the ADP:ATP ratio can be monitored. The elevation of fluorescence intensity caused by the increase in free intracellular Mg^{2+} concentration suggests a reduction of $(ATP)_i$ [7]. The $(ATP)_i$ measurements were performed in standard HEPES-buffered solution.

Measurement of NHE activities

During the measurement of pH_i, in order to characterise NHE activity NH_4Cl pulse technique was used in HEPES-buffered solution. Exposure of colonic crypts for 3 min to 20 mM NH_4Cl induced an immediate rise in pH_i due to the rapid entry of lipophilic base NH_3 into the cells. After the removal of NH_4Cl, pH_i rapidly decreased. This acidification is caused by the dissociation of intracellular NH_4^+ to H^+ and NH_3, followed by the diffusion of NH_3 out of the cell. Under these conditions, the initial rate of pH_i recovery from the acid load reflects the activities of NHEs. $-J(B^-)$ was calculated from the first 60 s of pH_i recovery from acidification.

Further experiments were performed to investigate the activities of the different NHE isoforms. The crypts were acid loaded by exposure to a 3-min pulse of 20 mM NH_4Cl in HEPES solution followed by a 10-min exposure of Na^+-free HEPES solution. Due to the blocked acid/base transporters (neither sodium nor bicarbonate were present in the solution); the pH_i is set to a stable acidic level. NHE activity was switched on by re-addition of extracellular sodium and the activities of NHEs were determined by measuring the initial rate of pH_i recovery over the first 60 s. The activities of the different NHE isoforms are extracted by using the isoform-selective NHE inhibitor HOE-642. The isoform selectivity of HOE-642 is dose-dependent, 1 μM HOE642 inhibits NHE1 whereas 50 μM HOE642 inhibits both NHE1 and 2 but not NHE3 [2, 6]. The activities (A) of NHE isoforms can be calculated from the recoveries (R) as follows:

$$A_{\mathrm{NHE1}} = R_{0\mu\mathrm{M}\,\mathrm{HOE}-642} - R_{1\mu\mathrm{M}\ \mathrm{HOE}-642}$$
$$A_{\mathrm{NHE2}} = R_{1\mu\mathrm{M}\ \mathrm{HOE}-642} - R_{50\mu\mathrm{M}\ \mathrm{HOE}-642}$$
$$A_{\mathrm{NHE3}} = R_{50\mu\mathrm{M}\ \mathrm{HOE}-642}$$

Determination of buffering capacity and base efflux

The total buffering capacity (β_{total}) of colonic epithelial cells was estimated according to the NH_4^+ pre-pulse technique [15, 46]. Colonic epithelial cells were exposed to various concentrations of NH_4Cl in Na^+- and HCO_3^--free solution. β_i (which refers to the ability of intrinsic cellular components to buffer changes of pH_i) was estimated by the Henderson–Hasselbach equation. β_{total} was calculated from: $\beta_{total}=\beta_i+\beta_{HCO3-}=\beta_i+2.3\times[HCO_3^-]_i$, where β_{HCO3-} is the buffering capacity of the HCO_3^-/CO_2 system. The measured rates of pH_i change (dpH/dt) were converted to transmembrane base flux $J(B^-)$ using the equation: $J(B^-)$ = dpH/dtx β_{total}. The β_{total} value at the start point pH_i was used for the calculation of $J(B^-)$. We denote base influx as $J(B^-)$ and base efflux (secretion) as $-J(B^-)$.

Measurement of Cl^-/HCO_3^- exchanger activity

Cl^- withdrawal technique was used to investigate the activity of CBE [42]. Removing Cl^- from the standard HCO_3^-/CO_2 buffered solution caused alkalization due to the reversed activity of the Cl^-/HCO_3^- exchanger. The activity of the exchanger was determined by measuring the initial rate of alkalization over the first 30 s.

Electron microscopy

Morphological changes of the different cell organelles of the colonic epithelial cells were evaluated by transmission electron microscopy (TEM). Biopsy samples were fixed in 2 % glutaraldehyde (in PBS) overnight at 4 °C. Samples were cut into small pieces (1×1 mm) then were infiltrated with 2 % gelatin (PBS) and the small cubes were made, which were then embedded to Embed 812 (EMS, USA) using a routine TEM embedding protocol. After the semithin sections (1 μm), the thin (70 nm) sections were cut for TEM examination.

Measurement of mitochondrial transmembrane potential

Changes of mitochondrial transmembrane potential $(\Delta\psi)_m$ were assessed by loading cells with 100 nmol/L tetramethylrhodamine methyl ester (TMRM) for 30 min at 37 °C to measure fluorescence in the perigranular mitochondrial region. Depolarisation of the mitochondria results in redistribution of TMRM from the mitochondria to the cytosol, causing a decrease in mitochondrial fluorescence [43]. Excitation 488 nm, emission was detected at >550 nm with Olympus Fluoview FV10i confocal system [7].

Statistical analysis

Values are means±SE. Statistical analyses were performed using analysis of variance (ANOVA) with the post-hoc test Dunnett or Bonferroni. $P \leq 0.05$ was accepted as significant.

Results

Chronic exposure of the colon to bile acids impair the activities of NHEs and CBE of isolated human colonic epithelial cells

Colonic crypts were isolated from patients whose colon is probably exposed to high concentrations of BA. Ileum-resected or cholecystectomised patients were divided into two groups depending on the presence (diarrhoea; D) or absence (non-diarrhoea; NON-D) of diarrhoea after the surgical intervention. The calculated acid/base transporter activities were compared to those

Table 1 Composition of solutions for in vitro studies. Values are concentrations in mmol/L

	Standard HEPES	Standard HCO_3^-	Cl^--free HCO_3^-	Ca^{2+}-free HEPES
NaCl	130	115		130
KCl	5	5		5
$MgCl_2$	1	1		1
$CaCl_2$	1	1		
Na-HEPES	10			
Glucose	10	10	10	10
$NaHCO_3$		25	25	
Na-gluconate			115	
Mg-gluconate			1	
Ca-gluconate			6	
K_2-sulfate			2.5	
EGTA				0.1

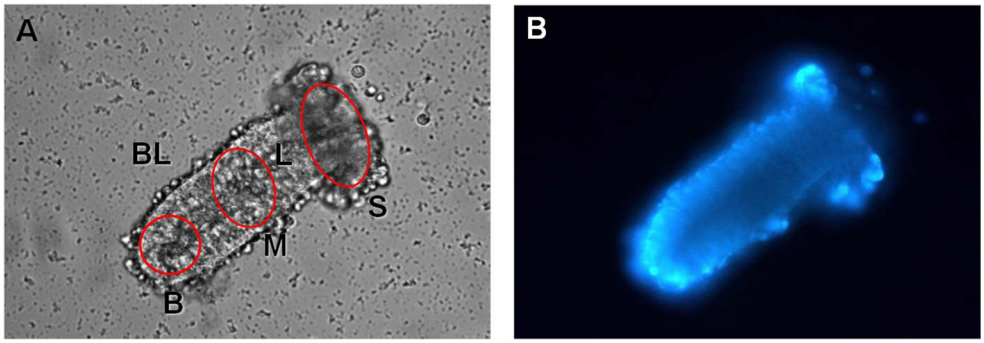

Fig. 1 Phase contrast (**a**) and fluorescent (**b**) pictures of an isolated human colonic crypt. Crypts were fixed on glass coverglass. Three regions of interest (ROIs) of each crypt were excited with lights at different wavelengths and the fluorescence emissions were measured. *B* base, *M* middle, *S* surface, *L* lumen of the crypt, *BL* basolateral membrane

measured in control patients to determine the effects of BA on the epithelial ion transport.

Representative curves of the pH_i traces and the summary data of the calculated NHE activities are shown in Fig. 2a, b. The activities of the different NHE isoforms were extracted by using the isoform-selective NHE inhibitor HOE-642; 1 μM HOE642 inhibits NHE1, whereas 50 μM HOE642 inhibits both NHE1 and 2 but not NHE3 [2, 6]. The functions of all examined NHE isoforms were significantly reduced in patients in group D compared to control patients.

The function of CBE was investigated using the Cl^- withdrawal technique (Fig. 2c). Removal of Cl^- from the standard HCO_3^-/CO_2 bath solution caused a marked alkalization in colonic crypt cells suggesting the presence of a functionally active anion exchange

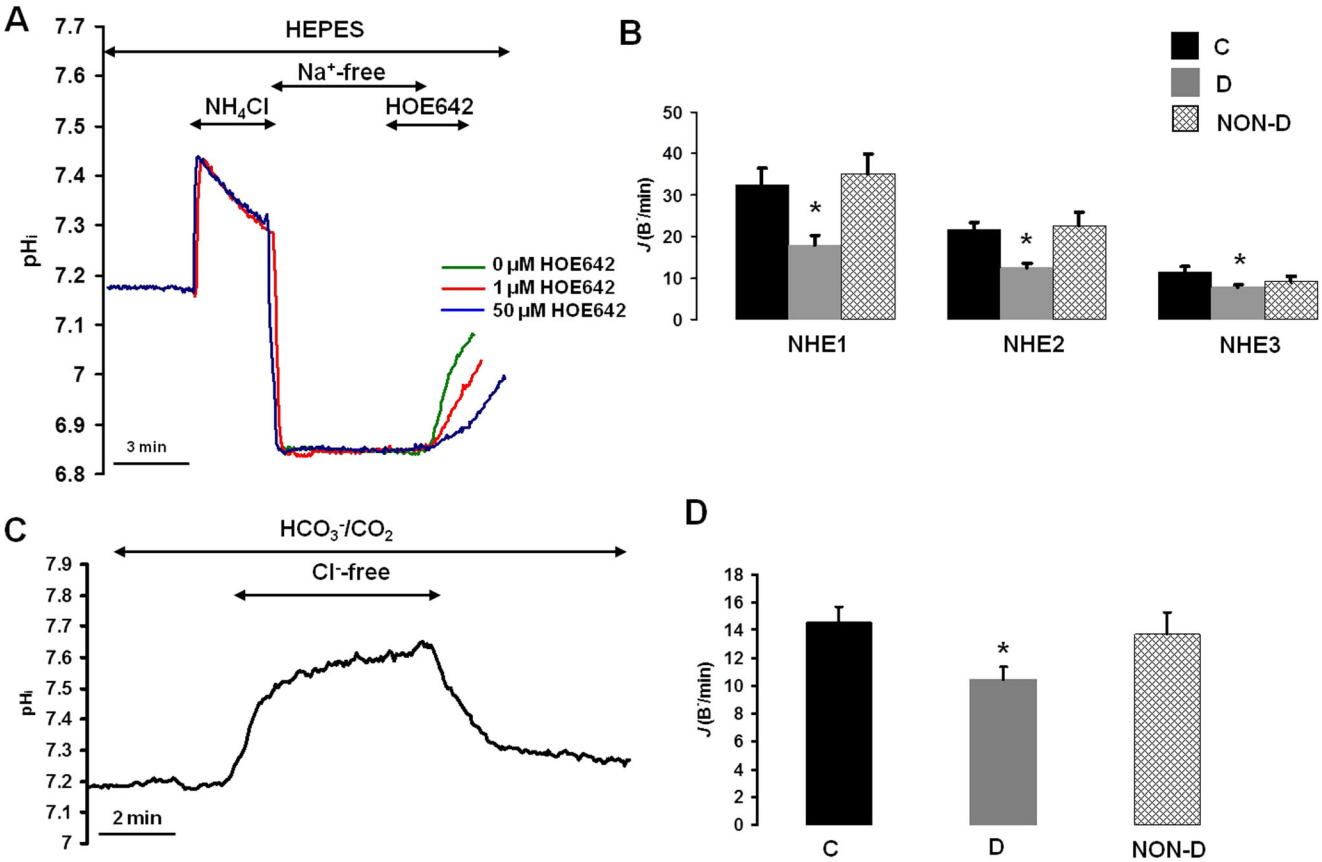

Fig. 2 The activities of NHE and CBE were decreased in colonic epithelial cells isolated from ileum-resected/cholecystectomised patients suffering from diarrhoea. **a** The activities of different NHE isoforms were determined by NH_4Cl pulse technique with the isoform-specific NHE inhibitor HOE-642 as described in the "Materials and methods" section. **b** Summary data of the calculated NHE activities. The activities of NHE1-3 were significantly impaired in patients suffering from diarrhoea. **c** Representative pH_i traces showing the effect of the Cl^- removal on the pH_i of the colonic epithelial cells. **d** Summary data of the calculated CBE activities, which were significantly decreased in patients suffering from diarrhoea. Groups of patients were *C* control, *D* ileum-resected/cholecystectomised with diarrhoea, and *NON-D* ileum-resected/cholecystectomised without diarrhoea. Data are presented as means ± SEM. n=5–6 patients/16–24 crypts/32–48 ROIs, *p<0.05 vs. control

mechanism. The activity of the CBE was significantly impaired in D group compared to control patients (Fig. 2d). In colonic crypt cells, isolated from NON-D patients, the activities of the examined acid/base transporters were not changed significantly compared to the control group, suggesting the significant role of ion transporters in bile-induced diarrhoea.

Bile acid administration dose-dependently reduce the pH_i of isolated human colonic epithelial cells

Our next aim was to characterise the acute effects of BA on colonic epithelial cells. For these experiments, colonic crypts were isolated from control patients. The administration of CDC resulted in a dose-dependent reduction of the pH_i of perfused colonic epithelial cells (Fig. 3). The characteristic response was a rapid decrease in pH_i which then slowly recovered to a variable degree during continuous exposure to BA (Fig. 3a–d). In HEPES-buffered solution, the ΔpH_{max} was more prominent during CDC administration compared to those observed in HCO_3^--containing solution, which can be explained by the increased buffering capacity of the colonic epithelial cells in the presence of HCO_3^-/CO_2.

Acute exposure to bile acid inhibits the activities of acid/base transporters of isolated human colonic epithelial cells

Impaired NHE and CBE activities were observed in patients suffering from diarrhoea, whose colon was probably continuously exposed to an elevated BA concentration, therefore we wanted to characterise the effects of acute BA administration on the ion transport mechanisms of human colonic epithelial cells. Colonic crypts isolated from control patients were used during these series of experiments. In order to investigate the effects of BA on the activities of NHEs, we analysed the pH_i recovery from an acid load induced by the removal of NH_4Cl. The representative pH_i traces (Fig. 4a) and the summary data of the calculated NHE activities (Fig. 4b) show that 10 min treatment with 0.1 mM CDC had no effects on the NHE activities. When the colonic crypts were perfused with 0.3 mM CDC, an inhibition of the activities of NHEs was observed. To identify the exact NHE isoforms, which were inhibited by 0.3 mM CDC, we used the ammonium pulse technique with the isoform-selective NHE inhibitor HOE-642 during the continuously perfusion with 0.3 mM CDC. According to our results, all of the NHE isoforms were significantly inhibited by 0.3 mM CDC (Fig. 4c).

We also tested the effects of higher BA concentrations, although when 20 mM NH_4Cl was applied together with

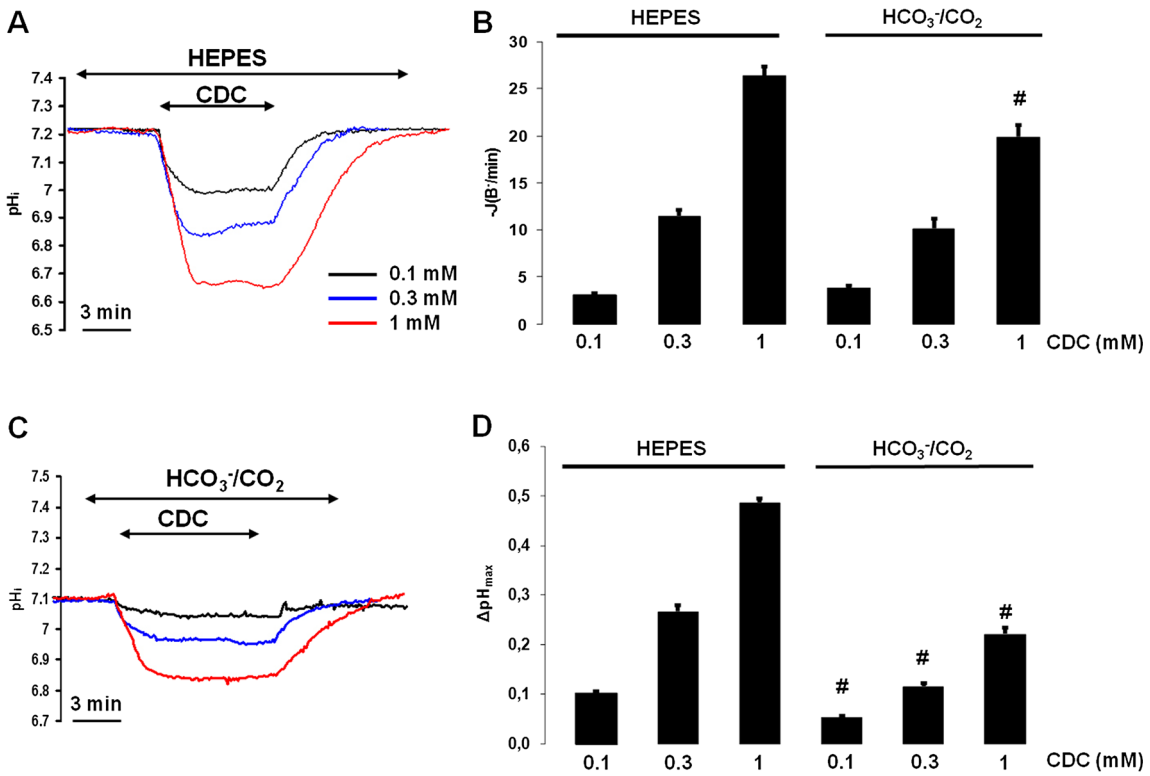

Fig. 3 Bile acids induce dose-dependent acidosis in isolated human colonic epithelial cells. Representative pH_itraces demonstrating the effect of non-conjugated CDC (0.1, 0.3 and 1 mM) administered in HEPES-(**a**)or in HCO_3^-/CO_2-buffered (**c**) solution. Summary data of the calculated base flux ($J(B^-/min)$) (**b**) and the maximal pH_i change (ΔpH_{max}) (**d**) induced by bile acids. Bile acids dose-dependently reduced the pH_i of colonic epithelial cells. Data are presented as means ± SEM. n=4–6 patients/14–18 crypts/28–36 ROIs. *p<0.05 vs. CDC, $^{\#}p$<0.05 vs. HEPES

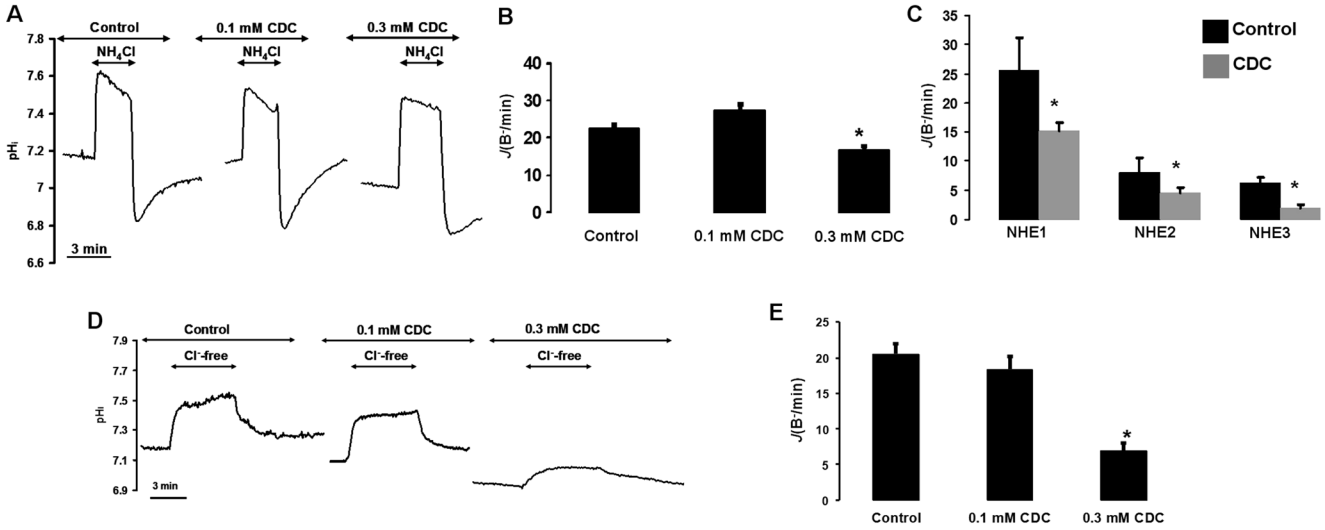

Fig. 4 Administration of 0.3 mM CDC significantly inhibited the activities of acid/base transporters in isolated human colonic crypts. **a** Representative pH_i curves showing the effects of CDC (0.1 and 0.3 mM) on the recovery from an acid load induced by removal of 20 mM NH_4Cl. **b** Summary data of the initial rate of pH_i recovery from acid load. **c** Summary data of the effect of 0.3 mM CDC on the calculated activities of the different NHE isoforms. The isoform-selective NHE inhibitor HOE-642 revealed that all NHE isoforms were inhibited by 0.3 mM CDC. **d** Representative pH_i traces showing the effects of CDC (0.1 and 0.3 mM) during the removal of extracellular Cl^-. **e** Summary data of the initial rate of pH_i elevation after Cl^- withdrawal. **a** and **b** were in HEPES-buffered, **c** and **d** were performed in HCO_3^--buffered solution. High concentration of CDC significantly decreased the activity of CBE. Data are presented as means ± SEM. n=3–6 patients/6–12 crypts/12–40 ROIs, *p<0.05 vs. control

1 mM CDC, the fluorescent intensities at 440 and 495 nm rapidly decreased causing an immediate elevation of the 440/495 ratio. This might be explained by the loss of BCECF and reflects the permeation of the plasma membrane, or by the lysis of the cells.

The Cl^--withdrawal technique was applied to examine the activity of CBE as well. The apical Cl^- removal from the extracellular solution increased the pH_i of the cells by driving HCO_3^- into the cell via the apical CBE, whereas, re-addition of Cl^- decreased pH_i inducing secretion of HCO_3^- via the CBE. Treating the crypts with 0.3 mM CDC resulted in a strong inhibition of CBE activity (Fig. 4d, e).

Besides non-conjugated BA, we also investigated the effects of conjugated BA on the ion transport activities of colonic epithelial cells. We tested the effects of glycochenodeoxycholate in different concentrations (0.1, 0.3, 1 mM) on the activities of NHE and CBE; however, no changes were observed (data not shown).

High concentration of bile acid induces severe mitochondrial damage

Our next aim was to explore the intracellular mechanisms by which BA inhibit acid/base transporters. Since previous studies have reported that BA can disrupt intracellular organelles (mitochondria, or Golgi) [4, 28, 30], we first analysed the structure of the cell compartments of human colonic epithelial cells following incubation with BA. TEM revealed that administration of low concentrations of CDC (0.1 mM or 0.3 mM) for 1–10 min had no effect on the structure of intracellular organelles (Fig. 5a). On the other hand, a 10-min exposure of human colonic epithelial cells to high concentration (1 mM) of CDC strongly damaged all of the mitochondria. The mitochondria swelled up and the inner membrane structures were disrupted. We did not observe such alteration in other intracellular organelles, such as endoplasmic reticulum (ER), Golgi or nuclei. For positive control experiments, the mitochondrial toxin carbonyl cyanide *m*-chlorophenyl hydrazone (CCCP, 100 μM) was applied. The mitochondrial injury was similar to that seen after 1 mM CDC treatment.

Bile acid treatment decreases $(ATP)_i$ and $(\Delta\psi)_m$ of isolated human colonic epithelial cells

Since TEM experiments did not reveal completely the inhibitory mechanism of 0.3 mM CDC, we tried to dissect the mechanism at a functional level. Therefore, in the next step, we aimed to find out whether CDC has any influence on the $(ATP)_i$ of human colonic epithelial cells. Using the Mg-Green fluorescent probe, which is indirectly sensitive to $(ATP)_i$ (see "Materials and methods") we showed that 0.3 mM CDC significantly, but reversibly depleted $(ATP)_i$ of isolated human colonic epithelial cells (Fig. 5b, c). Following administration of 0.1 mM CDC the $(ATP)_i$ was not affected (data not shown). In case of 1 mM CDC, not only was the structural impairment of the mitochondria evident, but a significant and irreversible decrease of the $(ATP)_i$ level was perceptible as well. For

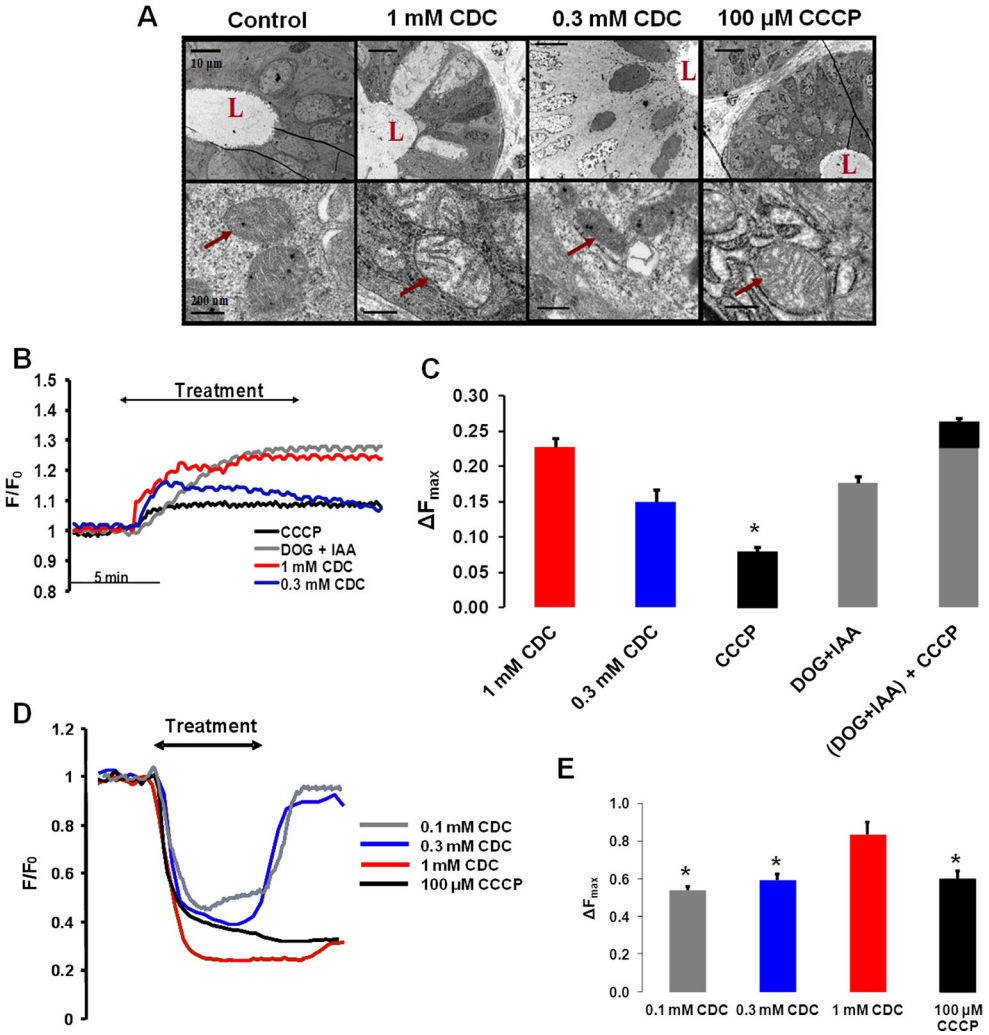

Fig. 5 Treatment with 0.3 mM CDC does not alter the structure of intracellular organelles but it significantly decreases $(ATP)_i$ and disturbs $(\Delta\psi)_m$. **a** Representative transmission electron microscopy pictures showing the effects of CDC (0.3 and 1 mM) on the mitochondria of human colonic epithelial cells. *L* crypt lumen, *arrow* mitochondria; 1 mM but not 0.3 mM CDC induced severe mitochondrial damage. **b** Representative curves of the Mg-green fluorescent experiments. Elevation of fluorescent intensity represents depletion in $(ATP)_i$. **c** Summary data for the maximal fluorescent intensity changes. High concentrations of CDC significantly decreased $(ATP)_i$. **d** Representative traces of the $(\Delta\psi)_m$ measurements. Decrease of fluorescent intensity represents loss of mitochondrial transmembrane potential. **e** Summary data for the maximal fluorescent intensity changes. High concentrations of CDC significantly decreased $(\Delta\psi)_m$. All experiments were performed in HEPES-containing solution. Data are presented as means±SEM. n=3 patients/5–6 crypts/13–15 ROIs. *p<0.05 vs. 1 mM CDC

positive control, the mitochondrial toxin CCCP was applied similarly to the morphological studies. The fact that high concentration of CDC caused more prominent $(ATP)_i$ depletion than CCCP suggests that BA have additional effects, which further decreases $(ATP)_i$. To investigate the effects of BA on glycolytic $(ATP)_i$ production the combination of deoxyglucose (DOG)/iodoacetamide (IAA) was used, which inhibit the glycolytic metabolism of colonic epithelial cells. 10 mM DOG + 5 mM IAA significantly and irreversibly depleted $(ATP)_i$. CCCP and DOG + IAA together mimicked the effect of high concentrations of CDC on the $(ATP)_i$ of isolated human colonic epithelial cells.

Alterations of $(\Delta\psi)_m$ were also examined. Representative traces in Fig. 5d demonstrate that administration of 0.1 mM or 0.3 mM CDC induced a significant decrease in TMRM fluorescence, which indicates the loss of $(\Delta\psi)_m$. This effect was reversible, $(\Delta\psi)_m$ returned to basal level following removal of CDC. Furthermore, 1 mM CDC or 100 µM CCCP caused a marked and irreversible reduction of $(\Delta\psi)_m$.

Bile acid treatment dose-dependently increases $[Ca^{2+}]_i$ via endoplasmic reticulum Ca^{2+} release and extracellular Ca^{2+} influx

To further investigate the intracellular effects of BA, the changes of $[Ca^{2+}]_i$ in isolated human colonic epithelial cells were measured during CDC treatment. In our experiments, administration of CDC caused a dose-dependent increase in

$[Ca^{2+}]_i$ (Fig. 6a–c). The increase in $[Ca^{2+}]_i$ was sustained, plateau-like pathophysiological signal. The removal of Ca^{2+} from the extracellular solution significantly decreased this effect. Pretreatment of the colonic crypts with BAPTA-AM (40 μM), a fast chelator of $[Ca^{2+}]_i$ abolished the effects of 0.1 and 0.3 mM CDC, however, a moderate increase of $[Ca^{2+}]_i$ was still detectable when 1 mM CDC was applied (Fig. 6d).

We made attempts to identify the source of Ca^{2+}, released during CDC-treatment. Caffeine (20 mM) and/or Ruthenium red (RR, 10 μM) were utilised in order to antagonise inositol-triphosphate receptor (IP_3R) and ryanodin receptor (RyR), which can mediate Ca^{2+} release from the ER. Representative curves and the summary bar chart (Fig. 7a, b) demonstrate that the application of caffeine significantly inhibited the increase in $[Ca^{2+}]_i$ generated by 0.3 mM CDC, while the administration of RR had no effect on the Ca^{2+} release. The rate of $[Ca^{2+}]_i$ increase was significantly diminished as well during the administration of caffeine (Fig. 7c). In the next step, gadolinium (Gd^{3+}, 1 μM) was applied to block plasma membrane Ca^{2+} entry channels. Gd^{3+} alone was not able to decrease the elevation of $[Ca^{2+}]_i$ induced by 0.3 mM CDC, while the simultaneous administration of Gd^{3+}, caffeine and RR significantly reduced it. To further characterise the CDC-induced increase of $[Ca^{2+}]_i$ in colonic epithelial cells, thapsigargin (Tg), the sarcoplasmic/endoplasmic reticulum calcium ATPase (SERCA pump) inhibitor was applied. In Ca^{2+}-free solution, Tg (2 μM) induced Ca^{2+} store depletion with consequent $[Ca^{2+}]_i$ elevation (Fig. 7d). This elevation was markedly decreased when Tg was administered after 0.3 mM CDC (Fig. 7e). Tg, when administered during 0.3 mM CDC, further induced a slight increase in $[Ca^{2+}]_i$ (Fig. 7). These observations suggest that beside the extracellular Ca^{2+} influx, CDC depletes ER Ca^{2+}-stores via IP_3R mediated processes.

The BA induced inhibition of Na^+/H^+ exchange activities is ATP-dependent, whereas the inhibition of CBE activity is Ca^{2+}-dependent in isolated human colonic epithelial cells

Next, we examined the potential connection between the intracellular effects of 0.3 mM CDC ($(ATP)_i$ depletion and $[Ca^{2+}]_i$ elevation) and the decreased function of acid/base transporters following treatment with the BA. Ammonium pulse technique (Fig. 8a) showed that chelation of intracellular Ca^{2+} with BAPTA-AM did not influence the inhibitory effect of 0.3 mM CDC on the NHE activity. In contrast, when the glycolysis inhibitors DOG + IAA were applied the same inhibition of NHEs was detectable (Fig. 8b, d), which suggests that CDC inhibits NHE via $(ATP)_i$ depletion. These results confirm the observation of other workgroups that the NHEs are ATP-dependent transporters [5, 37, 38].

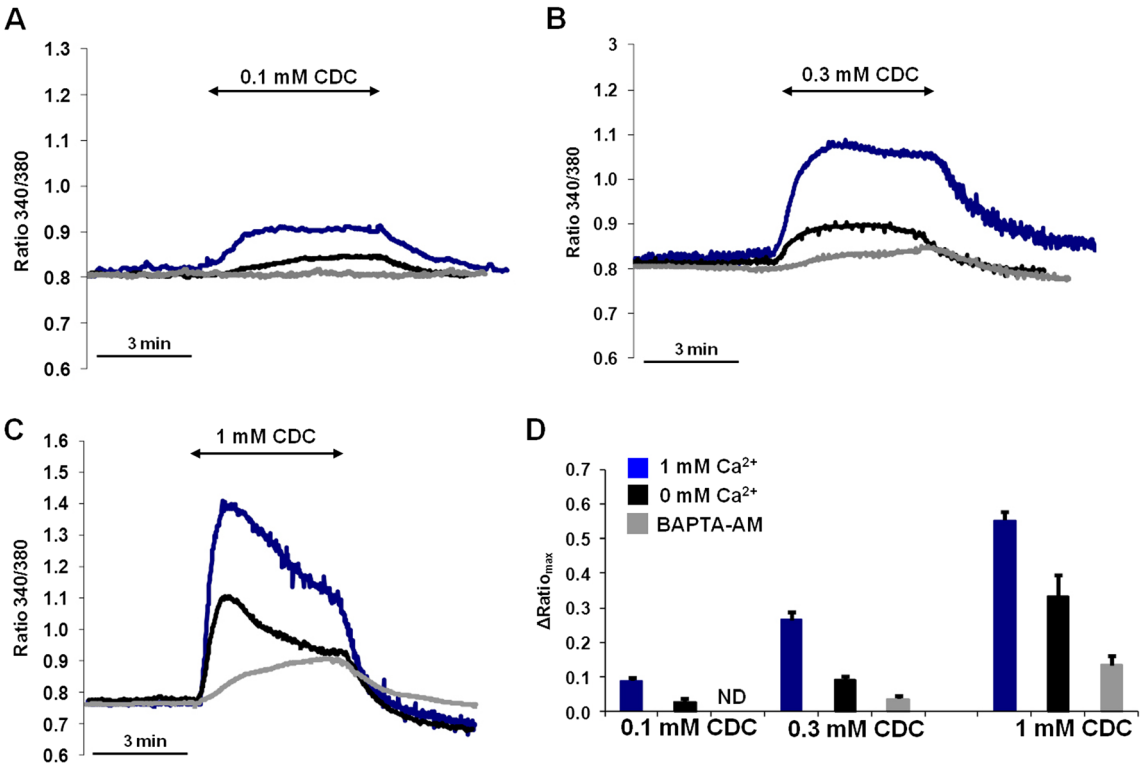

Fig. 6 CDC dose-dependently increased the $[Ca^{2+}]_i$ of isolated human colonic epithelial cells. **a-c** Representative curves showing the effect of CDC (0.1, 0.3 and 1 mM) on $[Ca^{2+}]_i$ of isolated human colonic crypts in Ca^{2+}-free or 1 mM Ca^{2+}-containing solution with/without pretreatment with the $[Ca^{2+}]_i$ chelator BAPTA-AM. **d** Summary data for the maximal fluorescent intensity changes. All experiments were performed in HEPES-buffered solution. Data are presented as means±SEM. n=2–4 patients/5–10 crypts/10–21 ROIs

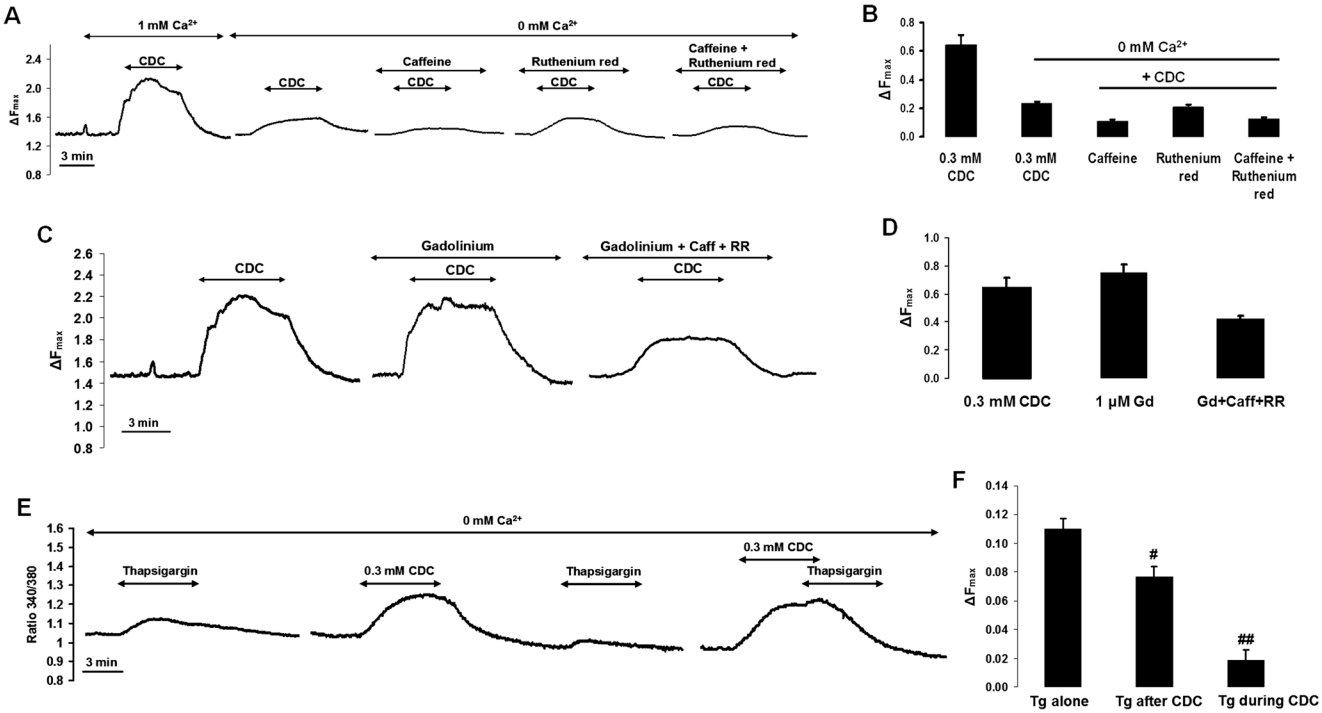

Fig. 7 CDC released Ca^{2+} from the ER and induced extracellular Ca^{2+} influx in isolated human colonic epithelial cells. **a** Representative curves showing the effect of the IP_3R inhibitor caffeine (20 mM) and RyR inhibitor Ruthenium Red (10 μM) on the increase of $[Ca^{2+}]_i$ induced by 0.3 mM CDC. **b** Summary data of the maximal fluorescent intensity changes. The inhibition of IP_3R, but not RyR decreased the CDC-induced Ca^{2+} release. **c** Representative curves showing the effect of the plasma membrane Ca^{2+} channel inhibitor Gd^{3+} (1 μM). **d** Summary data of the maximal fluorescent intensity changes. All experiments were performed in HEPES-buffered solution. Data are presented as means±SEM. n=2–4 patients/5–8 crypts/10–18 ROIs. *p<0.05 vs. CDC in 0 mM Ca^{2+} containing solution, $^{\#}p$<0.05 vs. CDC in 1 mM Ca^{2+} containing solution. **e** Representative traces showing the effects of SERCA inhibitor Tg (2 μM) administered alone and following or during 0.3 mM CDC on the $[Ca^{2+}]_i$. **f** Summary data of the maximal fluorescent intensity changes. All experiments were performed in Ca^{2+}-free HEPES-buffered solution. Data are presented as means±SEM. n=2–3 patients/5–6 crypts/12–14 ROIs. $^{\#}p$<0.05, $^{\#\#}p$<0.01 vs. Tg alone

We also investigated the inhibitory effect of 0.3 mM CDC on CBE in more detail. We tested the effects of $[Ca^{2+}]_i$ chelation and $(ATP)_i$ depletion during the Cl^--removal technique in isolated human colonic epithelial cells. We showed that the intracellular Ca^{2+}-chelator BAPTA-AM completely abolished the inhibitory effect of 0.3 mM CDC on the activity of CBE. In contrast, depletion of $(ATP)_i$ with DOG+IAA was not able to reduce CBE activity. These observations suggest that BA inhibit CBE activity via toxic $[Ca^{2+}]_i$ elevation unlike NHE activity, which is inhibited by $(ATP)_i$ depletion.

Discussion

Bile acids are amphipathic molecules participating in fat solubilisation and lipid digestion [22]. Besides the physiological functions, BAs are also known to cause bile-induced diarrhoea, a common feature of BAM, which often develops after small bowel resection or post-cholecystectomy [1, 36, 39]. Although bile-induced diarrhoea is a frequent complication affecting high number of patients, its pathogenesis is not completely understood yet. In this study, we provide strong evidence that bile acids impair the activity of the acid/base transporters (NHE and CBE) via different mechanisms in human colonic epithelial cells. The impaired activities of NHE and CBE can decrease the fluid and electrolyte absorption in the colon and promote the development of diarrhoea.

The colonic epithelial cells express different ion channels and transporters, which transport ions and water. NHE1 is constitutively expressed on the basolateral membrane of the epithelial cells. Although it does not play a role in the Na^+ absorption, it fulfils housekeeping functions, regulating cell volume and pH_i [23]. In addition, the presence of NHE2 and NHE3 on the apical membrane of colonic epithelial cells has been confirmed [19]. NHE3 knock-out mice develop diarrhoea, which supports the idea that this might be the dominant NHE isoform, responsible for Na^+ uptake in the intestine [11, 34, 48]. Together with NHE3, the SLC26A3 CBE (or down-regulated in adenoma), maintains the absorption of NaCl in the colon. Mutation of this transporter results in congenital chloride-losing diarrhoea [18], moreover, similar conditions develop in SLC26A3-deficient mice [35]. The fact that impaired activities of these transporters were observed in

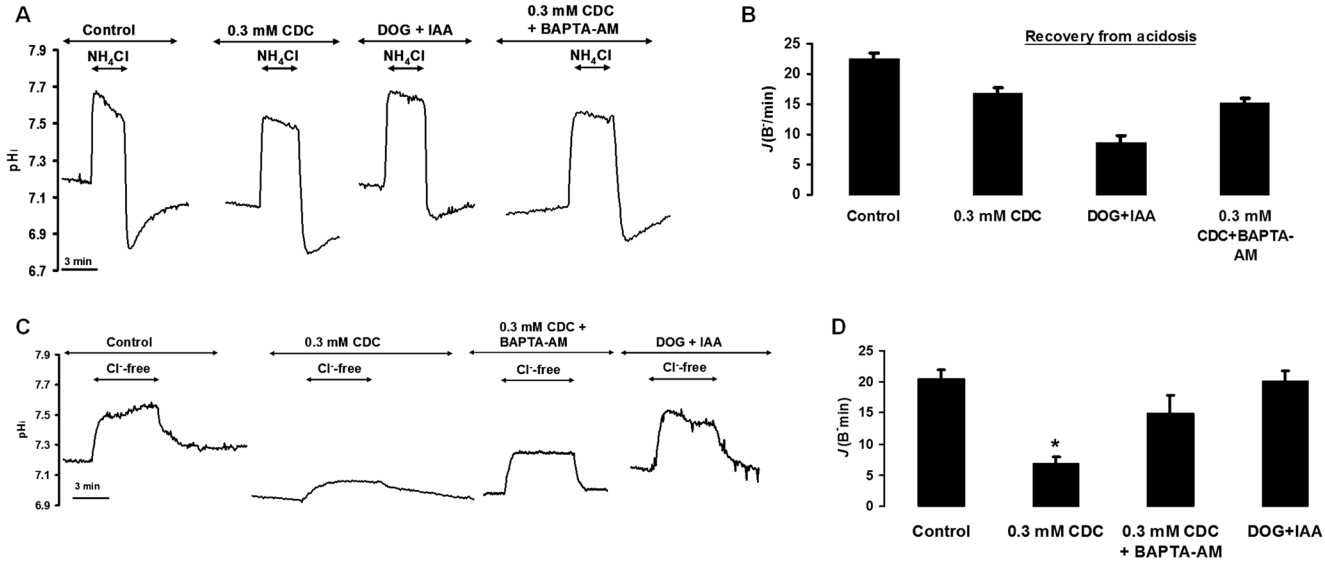

Fig. 8 A 0.3 mM CDC induced $(ATP)_i$-dependent inhibition of NHEs and Ca^{2+}-dependent decrease in the activity of CBE in isolated human colonic epithelial cells. **a** Representative pH_i curves showing the effect of 0.3 mM CDC, $(ATP)_i$ depletion or pretreatment with the $[Ca^{2+}]_i$ chelator BAPTA-AM on the initial rate of pH_i recovery from an acid load induced by the removal of 20 mM NH_4Cl. **b** Summary data of the initial rate of pH_i recovery from an acid load in HCO_3^--containing solution. The depletion of $(ATP)_i$, mimicked, but the prevention of Ca^{2+} elevation did not change the effect of CDC on the NHE activities. **c** Representative pH_i curves demonstrating the effect of 0.3 mM CDC, $(ATP)_i$ depletion or pretreatment with the $[Ca^{2+}]_i$ chelator BAPTA-AM on the removal of extracellular Cl^-. **d** Summary data of the initial rate of pH_i elevation after Cl^- withdrawal. The chelation of the $[Ca^{2+}]_i$ elevation abolished the inhibitory effect of CDC. **a** and **b** were in HEPES-, **c** and **d** were performed in HCO_3^--containing solution. Data are presented as means±SEM. n=3–6 patients/5–12 crypts/8–40 ROIs. *p<0.05 vs. control

diarrhoea-associated diseases, such as ulcerative colitis and secretory diarrhoea [8, 27, 49], further underlies the importance of the NHE3 and SLC26A3 in colonic electrolyte and water absorption.

BA can induce diarrhoea when they are present in the colon at high concentrations; therefore, we recruited ileum-resected or cholecystectomised patients and divided them into two groups depending on having (D) or not having diarrhoea (NON-D) after surgical intervention. The measurement of ion transporter activities revealed that in the D group the activities of NHE1-3 isoforms were markedly lower, compared to the control group. This inhibitory pattern is clearly different from our previous observations in ulcerative colitis patients, where the activity of NHE1 was increased, whereas the activity of NHE3 was significantly decreased in colonic epithelial cells [8]. Moreover, the activity of CBE was significantly diminished in patients in group D as well. Importantly, the function of the acid/base transporters was unaltered in colonic epithelial cells isolated from NON-D patients. These data suggest that the reduced absorptive function of the colon is probably due to the continuous presence of non-physiological concentrations of BA.

In the next step, we aimed to characterise the acute effects of BA on human colonic epithelial cells. Hamilton et al. showed that the physiological concentration of total BA—including conjugated and non-conjugated forms—in the proximal colon (cecum) reaches 1 mM [14]. In addition, in the large intestine, BAs are metabolized (mainly deconjugated) by resident bacteria [17, 20, 32] further elevating the concentration of the non-conjugated BA. Based on these observations, we used 0.1 mM CDC as low, physiological and 0.3–1 mM CDC as high, non-physiological concentrations. In our experiments, administration of CDC caused an immediate, dose-dependent and reversible decrease of the pH_i in human colonic epithelial cells. Moreover, we also provided evidence that administration of high concentration (0.3 mM) of CDC resulted in a significant inhibition of NHEs and CBE of human colonic epithelial cells, suggesting the possible toxic effects of high doses of non-conjugated BA. Using the isoform-specific NHE inhibitor HOE-642, we also showed that the functions of NHE1-3 isoforms were reduced in response to 0.3 mM CDC. Similarly, high concentration of CDC strongly inhibited the acid/base transporters of guinea pig pancreatic ductal epithelial cells [42].

To dissect the intracellular mechanisms of the inhibitory effects of BA on colonic epithelial cells, first we investigated the effects of CDC on the morphology of intracellular organelles. Previous studies demonstrated that BA can perturb intracellular organelles and induce Golgi fragmentation and disruption of the mitochondria in cultured colonic epithelial cells and in pancreatic ductal cells [4, 28, 30]. In our experiments, a 10-min exposure of the colonic epithelial cells to 0.3 mM CDC did not induce any visible alteration in the morphology of the cell compartments. Nevertheless, 1 mM CDC caused severe damage in all of the mitochondria. The mitochondria swelled up and the structure of the inner

membranes was disrupted, whereas other intracellular organelles seemed to remain intact. Although 0.3 mM CDC inhibited the activities of acid/base transporters, it did not induce alteration in the structure of intracellular organelles, therefore we investigated whether mitochondrial function is altered by BA. Administration of 0.3 mM CDC significantly but reversibly depleted the $(ATP)_i$ and decreased $(\Delta\psi)_m$ of isolated human colonic epithelial cells. The toxic effects of BAs were previously demonstrated on isolated rodent pancreatic acini [43].

Next, we investigated another potential intracellular target of BA, the Ca^{2+} signalisation, a well-known mediator of numerous cellular processes. It was shown previously that the CBE SLC26A3 and NHE3 are inhibited by the pathological increase of intracellular Ca^{2+} [6, 25]. In our experiments, CDC induced a dose-dependent sustained increase in $[Ca^{2+}]_{i,}$. The removal of Ca^{2+} from the extracellular solution significantly decreased, while preincubation of the colonic crypts with BAPTA-AM (40 μM), a fast intracellular Ca^{2+} chelator, almost completely abolished the effect of 0.3 mM CDC. If elevation of $[Ca^{2+}]_i$ occurs, the source of Ca^{2+} could be the release from the ER via IP_3R and/or RyR or Ca^{2+} entry from the extracellular space [12, 13, 31]. In our experiments, the IP_3R antagonist caffeine, but not the RyR-blocker RR or the plasma membrane Ca^{2+} channel inhibitor Gd^{3+}, reduced the CDC-induced $[Ca^{2+}]_i$ elevation. These observations suggest that BA mobilizes stored Ca^{2+} from the ER via IP_3R. However, since the inhibition of IP_3R did not completely abolish the effect of CDC, it is proposed that extracellular Ca^{2+} influx must play a role as well. This process is most probably mediated by a Gd^{3+}-insensitive Ca^{2+} channel, Na^+/Ca^{2+} exchangers or non-specific cation channels. These ion channels have large Na^+, Ca^{2+}, and/or K^+ conductance but since specific inhibitors are lacking, it is difficult to distinguish their functions. Besides, the SERCA inhibitor thapsigargin induced a further elevation of the $[Ca^{2+}]_i$ after or during CDC administration suggests that CDC does not completely empty the ER Ca^{2+} store. These observations further confirmed our hypothesis that CDC mobilizes Ca^{2+} from the ER and promotes the influx of external Ca^{2+}. The fact that the increase in $[Ca^{2+}]_i$ in response to CDC was reversible argues the possibility that it was caused by the detergent property of BA.

Finally, we examined whether there is a connection between the inhibitory effect of 0.3 mM CDC on the activities of acid/base transporters and its effects on $(ATP)_i$ or $[Ca^{2+}]_i$. We showed that the depletion of $(ATP)_i$ resulted in a similar decrease of NHE activities as it was observed following the administration of 0.3 mM CDC. In contrast, pretreatment of the colonic epithelial cells with the $[Ca^{2+}]_i$ chelator BAPTA-AM did not prevent the toxic effect of 0.3 mM CDC on the activities of NHEs. These results indicate that 0.3 mM CDC inhibits the functions of NHEs via depleting $(ATP)_i$. This is in agreement with previous observations that NHEs are ATP-dependent transporters [5, 37, 38]. Besides the Na^+ transport, the Cl^- absorptive capacity via the CBE of the colonic epithelial cells was also tested. $(ATP)_i$ depletion caused by the glycolysis inhibitors did not have any influence on the activity of CBE. However, preincubation of the colonic crypts with the $[Ca^{2+}]_i$ chelator BAPTA-AM restored the diminished activity of CBE caused by 0.3 mM CDC. This observation further supports the hypothesis that CBE is inhibited by the non-physiological elevation of $[Ca^{2+}]_i$ [25].

Taken together using isolated human colonic crypts, we showed that non-conjugated bile acids, when present in the colon at a relatively high concentration, can enter the colonic epithelial cells. Via impaired cellular ATP production and toxic $[Ca^{2+}]_i$ elevation, bile acids can decrease the activities of acid/base transporters, responsible for NaCl absorption, which can reduce fluid and electrolyte absorption in the colon promoting the development of diarrhoea. Stimulating either the sodium uptake via NHE or the chloride uptake via CBE shall offer new therapeutical approaches in the treatment of bile-induced diarrhoea.

Grant support Our research is supported by Hungarian National Development Agency grants (TÁMOP-4.2.2.A-11/1/KONV-2012-0035, TÁMOP-4.2.2-A-11/1/KONV-2012-0052, TÁMOP-4.2.2.A-11/1/KONV-2012-0073), the Hungarian Scientific Research Fund (OTKA NF105758, NF100677, K109756, PD105948) and the Hungarian Academy of Sciences (BO/00531/11/5, BO/00632/14/5). This research was also supported by the European Union and the State of Hungary, co-financed by the European Social Fund in the framework of TÁMOP 4.2.4.A/2-11-1-2012-0001 and TÁMOP-4.2.4.A2- 710-SZJÖ-TOK-13-0017 'National Excellence Program' and MTA-SZTE Momentum Grant (LP2014-10/2014).

References

1. Arlow FL, Dekovich AA, Priest RJ, Beher WT (1987) Bile acid-mediated postcholecystectomy diarrhea. Arch Intern Med 147(7): 1327–1329
2. Bachmann O, Riederer B, Rossmann H, Groos S, Schultheis PJ, Shull GE, Gregor M, Manns MP, Seidler U (2004) The Na^+/H^+ exchanger isoform 2 is the predominant NHE isoform in murine colonic crypts and its lack causes NHE3 upregulation. Am J Physiol Gastrointest Liver Physiol 287(1):G125–G133
3. Borghede MK, Schlutter JM, Agnholt JS, Christensen LA, Gormsen LC, Dahlerup JF (2011) Bile acid malabsorption investigated by selenium-75-homocholic acid taurine ((75)SeHCAT) scans: causes and treatment responses to cholestyramine in 298 patients with chronic watery diarrhoea. Eur J Int Med 22(6):e137–e140
4. Byrne AM, Foran E, Sharma R, Davies A, Mahon C, O'Sullivan J, O'Donoghue D, Kelleher D (2010) Long A bile acids modulate the Golgi membrane fission process via a protein kinase Ceta and protein kinase D-dependent pathway in colonic epithelial cells. Carcinogenesis 31(4):737–744
5. Cabado AG, Yu FH, Kapus A, Lukacs G, Grinstein S, Orlowski J (1996) Distinct structural domains confer cAMP sensitivity and ATP

dependence to the Na^+/H^+ exchanger NHE3 isoform. J Biol Chem 271(7):3590–3599
6. Cinar A, Chen M, Riederer B, Bachmann O, Wiemann M, Manns M, Kocher O, Seidler U (2007) NHE3 inhibition by cAMP and Ca^{2+} is abolished in PDZ-domain protein PDZK1-deficient murine enterocytes. J Physiol 581(Pt 3):1235–1246
7. Criddle DN, Murphy J, Fistetto G, Barrow S, Tepikin AV, Neoptolemos JP, Sutton R, Petersen OH (2006) Fatty acid ethyl esters cause pancreatic calcium toxicity via inositol trisphosphate receptors and loss of ATP synthesis. Gastroenterology 130(3):781–793
8. Farkas K, Yeruva S, Rakonczay Z Jr, Ludolph L, Molnar T, Nagy F, Szepes Z, Schnur A, Wittmann T, Hubricht J, Riederer B, Venglovecz V, Lazar G, Kiraly M, Zsembery A, Varga G, Seidler U, Hegyi P (2011) New therapeutic targets in ulcerative colitis: the importance of ion transporters in the human colon. Inflamm Bowel Dis 17(4):884–898
9. Ford GA, Preece JD, Davies IH, Wilkinson SP (1992) Use of the SeHCAT test in the investigation of diarrhoea. Postgrad Med J 68(798):272–276
10. Fromm H, Malavolti M (1986) Bile acid-induced diarrhoea. Clin Gastroenterol 15(3):567–582
11. Gawenis LR, Stien X, Shull GE, Schultheis PJ, Woo AL, Walker NM, Clarke LL (2002) Intestinal NaCl transport in NHE2 and NHE3 knockout mice. Am J Physiol Gastrointest Liver Physiol 282(5): G776–G784
12. Gerasimenko JV, Flowerdew SE, Voronina SG, Sukhomlin TK, Tepikin AV, Petersen OH, Gerasimenko OV (2006) Bile acids induce Ca2+ release from both the endoplasmic reticulum and acidic intracellular calcium stores through activation of inositol trisphosphate receptors and ryanodine receptors. J Biol Chem 281(52):40154–40163
13. Gerasimenko JV, Sherwood M, Tepikin AV, Petersen OH, Gerasimenko OV (2006) NAADP, cADPR and IP_3 all release Ca^{2+} from the endoplasmic reticulum and an acidic store in the secretory granule area. J Cell Sci 119(Pt 2):226–238
14. Hamilton JP, Xie G, Raufman JP, Hogan S, Griffin TL, Packard CA, Chatfield DA, Hagey LR, Steinbach JH, Hofmann AF (2007) Human cecal bile acids: concentration and spectrum. Am J Physiol Gastrointest Liver Physiol 293(1):G256–G263
15. Hegyi P, Gray MA, Argent BE (2003) Substance P inhibits bicarbonate secretion from guinea pig pancreatic ducts by modulating an anion exchanger. Am J Physiol Cell Physiol 285(2):C268–C276
16. Hegyi P, Rakonczay Z Jr, Gray MA, Argent BE (2004) Measurement of intracellular pH in pancreatic duct cells: a new method for calibrating the fluorescence data. Pancreas 28(4):427–434
17. Hofmann AF (2009) The enterohepatic circulation of bile acids in mammals: form and functions. Front Biosci (Landmark Ed) 14: 2584–2598
18. Hoglund P, Haila S, Scherer SW, Tsui LC, Green ED, Weissenbach J, Holmberg C, de la Chapelle A, Kere J (1996) Positional candidate genes for congenital chloride diarrhea suggested by high-resolution physical mapping in chromosome region 7q31. Genome Res 6(3): 202–210
19. Hoogerwerf WA, Tsao SC, Devuyst O, Levine SA, Yun CH, Yip JW, Cohen ME, Wilson PD, Lazenby AJ, Tse CM, Donowitz M (1996) NHE2 and NHE3 are human and rabbit intestinal brush-border proteins. Am J Physiol 270(1 Pt 1):G29–G41
20. Hylemon PB, Zhou H, Pandak WM, Ren S, Gil G, Dent P (2009) Bile acids as regulatory molecules. J Lipid Res 50(8): 1509–1520
21. Inoue M, Fujishiro N, Imanaga I, Sakamoto Y (2002) Role of ATP decrease in secretion induced by mitochondrial dysfunction in guinea-pig adrenal chromaffin cells. J Physiol 539(Pt 1):145–155
22. Keely SJ (2010) Missing link identified: GpBAR1 is a neuronal bile acid receptor. Neurogastroenterol Motil 22(7):711–717
23. Kiela PR, Xu H, Ghishan FK (2006) Apical Na^+/H^+ exchangers in the mammalian gastrointestinal tract. J Physiol Pharmacol 57(Suppl 7):51–79
24. Kunzelmann K, Mall M (2002) Electrolyte transport in the mammalian colon: mechanisms and implications for disease. Physiol Rev 82(1):245–289
25. Lamprecht G, Hsieh CJ, Lissner S, Nold L, Heil A, Gaco V, Schafer J, Turner JR, Gregor M (2009) Intestinal anion exchanger downregulated in adenoma (DRA) is inhibited by intracellular calcium. J Biol Chem 284(29):19744–19753
26. Leyssens A, Nowicky AV, Patterson L, Crompton M, Duchen MR (1996) The relationship between mitochondrial state, ATP hydrolysis, [Mg2+]i and [Ca2+]i studied in isolated rat cardiomyocytes. J Physiol 496(Pt 1):111–128
27. Makela S, Kere J, Holmberg C, Hoglund P (2002) SLC26A3 mutations in congenital chloride diarrhea. Hum Mutat 20(6):425–438
28. Maleth J, Venglovecz V, Razga Z, Tiszlavicz L, Rakonczay Z Jr, Hegyi P (2011) Non-conjugated chenodeoxycholate induces severe mitochondrial damage and inhibits bicarbonate transport in pancreatic duct cells. Gut 60(1):136–138
29. Musch MW, Arvans DL, Wu GD, Chang EB (2009) Functional coupling of the downregulated in adenoma Cl-/base exchanger DRA and the apical Na+/H + exchangers NHE2 and NHE3. Am J Physiol Gastrointest Liver Physiol 296(2):G202–G210
30. Payne CM, Crowley-Weber CL, Dvorak K, Bernstein C, Bernstein H, Holubec H, Crowley C, Garewal H (2005) Mitochondrial perturbation attenuates bile acid-induced cytotoxicity. Cell Biol Toxicol 21(5–6):215–231
31. Petersen OH, Tepikin AV (2008) Polarized calcium signaling in exocrine gland cells. Annu Rev Physiol 70:273–299
32. Philipp B (2011) Bacterial degradation of bile salts. Appl Microbiol Biotechnol 89(4):903–915
33. Rossel P, Sortsoe Jensen H, Qvist P, Arveschoug A (1999) Prognosis of adult-onset idiopathic bile acid malabsorption. Scand J Gastroenterol 34(6):587–590
34. Schultheis PJ, Clarke LL, Meneton P, Miller ML, Soleimani M, Gawenis LR, Riddle TM, Duffy JJ, Doetschman T, Wang T, Giebisch G, Aronson PS, Lorenz JN, Shull GE (1998) Renal and intestinal absorptive defects in mice lacking the NHE3 Na^+/H^+ exchanger. Nat Genet 19(3):282–285
35. Schweinfest CW, Spyropoulos DD, Henderson KW, Kim JH, Chapman JM, Barone S, Worrell RT, Wang Z, Soleimani M (2006) slc26a3 (dra)-deficient mice display chloride-losing diarrhea, enhanced colonic proliferation, and distinct up-regulation of ion transporters in the colon. J Biol Chem 281(49):37962–37971
36. Sciarretta G, Furno A, Mazzoni M, Malaguti P (1992) Postcholecystectomy diarrhea: evidence of bile acid malabsorption assessed by SeHCAT test. Am J Gastroenterol 87(12):1852–1854
37. Shimada-Shimizu N, Hisamitsu T, Nakamura TY, Wakabayashi S (2013) Evidence that Na^+/H^+ exchanger 1 is an ATP-binding protein. Febs J 280(6):1430–1442
38. Shiue H, Musch MW, Wang Y, Chang EB, Turner JR (2005) Akt2 phosphorylates ezrin to trigger NHE3 translocation and activation. J Biol Chem 280(2):1688–1695
39. Smith MJ, Cherian P, Raju GS, Dawson BF, Mahon S, Bardhan KD (2000) Bile acid malabsorption in persistent diarrhoea. J R Coll Physicians Lond 34(5):448–451
40. Surawicz CM (2010) Mechanisms of diarrhea. Curr Gastroenterol Rep 12(4):236–241
41. Thomas JA, Buchsbaum RN, Zimniak A, Racker E (1979) Intracellular pH measurements in Ehrlich ascites tumor cells utilizing spectroscopic probes generated in situ. Biochemistry 18(11):2210–2218
42. Venglovecz V, Rakonczay Z Jr, Ozsvari B, Takacs T, Lonovics J, Varro A, Gray MA, Argent BE, Hegyi P (2008) Effects of bile acids on pancreatic ductal bicarbonate secretion in guinea pig. Gut 57(8): 1102–1112

43. Voronina SG, Barrow SL, Gerasimenko OV, Petersen OH, Tepikin AV (2004) Effects of secretagogues and bile acids on mitochondrial membrane potential of pancreatic acinar cells: comparison of different modes of evaluating DeltaPsim. J Biol Chem 279(26):27327–27338
44. Walker NM, Simpson JE, Yen PF, Gill RK, Rigsby EV, Brazill JM, Dudeja PK, Schweinfest CW, Clarke LL (2008) Down-regulated in adenoma Cl^-/HCO_3^- exchanger couples with Na/H exchanger 3 for NaCl absorption in murine small intestine. Gastroenterology 135(5): 1645–653 e1643
45. Walters JR, Pattni SS (2010) Managing bile acid diarrhoea. Ther Adv Gastroenterol 3(6):349–357
46. Weintraub WH, Machen TE (1989) pH regulation in hepatoma cells: roles for Na-H exchange, Cl-HCO3 exchange, and Na-HCO3 cotransport. Am J Physiol 257(3 Pt 1):G317–G327
47. Wilcox C, Turner J, Green J (2014) Systematic review: the management of chronic diarrhoea due to bile acid malabsorption. Aliment Pharmacol Ther 39(9):923–939. doi:10.1111/apt.12684
48. Xu H, Zhang B, Li J, Wang C, Chen H, Ghishan FK (2012) Impaired mucin synthesis and bicarbonate secretion in the colon of NHE8 knockout mice. Am J Physiol Gastrointest Liver Physiol 303(3): G335–G343
49. Yeruva S, Farkas K, Hubricht J, Rode K, Riederer B, Bachmann O, Cinar A, Rakonczay Z, Molnar T, Nagy F, Wedemeyer J, Manns M, Raddatz D, Musch MW, Chang EB, Hegyi P, Seidler U (2010) Preserved Na(+)/H(+) exchanger isoform 3 expression and localization, but decreased NHE3 function indicate regulatory sodium transport defect in ulcerative colitis. Inflamm Bowel Dis 16(7):1149–1161